2012

Molecular Characterisation of the Interaction of Microbes with the Insulin Pathway

Nisr, Raid Bahr

Molecular Characterisation of the Interaction of Microbes with the Insulin Pathway

By

Raid Bahr Nisr

A thesis submitted to the University of Plymouth

In partial fulfilment for the degree of

Doctor of Philosophy

School of Biomedical and Biological Sciences

Faculty of Sciences

This project funded by Ministry of Higher Education

Baghdad, Iraq

January 2012

Molecular Characterisation of the Interaction of

Microbes with the Insulin Pathway

Abstract

Exposure to microorganisms is considered an environmental factor which can contribute to diabetes mellitus via cytotoxicity or autoimmune responses against pancreatic cells. Firstly, the effects on rat insulinoma pancreatic β-cell line of secondary metabolites pyrrolnitrin (*Burkholderia* spp), phenazine compounds (*Pseudomonas aeruginosa* and *Burkholderia* spp) were investigated. Both compounds separately showed significant cytotoxicity after 24 h and at concentrations of 10 & 100 ng/ml potentiated insulin gene transcription, Ca^{2+} content and glucose-stimulated insulin secretion (GSIS). Furthermore, the outward membrane current was inhibited by phenazine (100 ng/ml) or pyrrolnitrin (10 or 100 ng/ml).

Secondly, the capacity of 45 microbial species to bind insulin was screened in order to assess how common insulin binding was amongst microorganisms *Burkholderia multivorans*, *B. cenocepacia* and *Aeromonas salmonicida* bound insulin. A genomic library of *B. multivorans* was constructed in λ Zap Express and screened successfully for insulin binding recombinants. Recombinant phagemids p1 & p2 were excised, p1, encoded an insulin binding protein (IBP1 30 kDa) with homology to the iron complex siderophore receptor. For p2, two IBPs were detected at 20 & 30 kDa (IBP2 & IBP3), representing an intracellular and outer membrane peptide transporter. Comparison of IBP1 and human insulin receptor (HIR) produced 6 linear epitopes, and for IBP2 & IBP3 produced 3 epitopes.

Thirdly, glutamic acid decarboxylase GAD65 is a major pancreatic autoantigen contributing to autoimmune diabetes. To assess the likelihood that microorganisms possess epitopes that mimic regions on GAD, 45 microbial species were tested for homology. This was facilitated by purifying recombinant GAD protein which was used to produce GAD antiserum. Four *E. coli* cross-reacting proteins were identified using mass spectrometry, outer-membrane protein A, formate dehydrogenase, superoxide dismutase and DNA starvation protein. Epitopes occurred at the C-terminal region of GAD65 (residues 419–565), a region previously reported to be targeted by autoantibodies.

This study suggests that pyrrolnitrin and phenazine are cytotoxic to pancreatic β-cells and *B. multivorans* IBPs linear epitopes may be diabetogenic, particularly in patients with cystic fibrosis related diabetes (CFRD) who suffer a long term infections with *Pseudomonas* and *Burkholderia* species. Furthermore, microbial GAD epitopes could potentially induce an autoimmune response leading to diabetes.

List of Contents

Chapter 1

Introduction and Literature Review 1

1.1 Introduction 2

1.2 Literature review 5
1.2.1 Insulin 5
1.2.2 The Insulin receptor & biology of receptors mediating cell signaling 7
1.2.3 Insulin receptor 9
1.2.4 Glucose sensing and insulin synthesizing mechanism in β-cells 9
1.2.4.1 Glucose transportation and glycolysis modeling in β -cells 11
1.2.4.2 Mitochondrial metabolism and ATP generation 12
1.2.4.3 Long chain acyl coA (LC-CoA) & NADPH 13
1.2.5 Functional alterations of β-cell mediating glucose metabolism 15
1.2.5.1 Cell membrane electro-activity 15
1.2.5.2 K_{ATP} sensitive channels 16
1.2.5.3 Voltage –dependent calcium channels (VDCCs) 18
1.2.5.4 Insulin granule dynamics and exocytosis 19
1.2.5.5 Mobilization of insulin granules and exocytosis of insulin 21
1.2.6 Insulin gene structure and regulation 22
1.2.6.1 Transcription factors 23
1.2.7 Pathogenesis of diabetes mellitus 27
1.2.8 Interaction of microbes with β-cell and insulin pathway 30
1.2.8.1 Cytotoxicity of β-cell by microbial secondary metabolites 30
1.2.8.2 Modulation of insulin secretion by microbial toxins 32
1.2.8.3 Microbial proteins modulating β-cell intracellular cAMP 32
1.2.8.4 Microbial secondary metabolites modulating β-cell K_{ATP} channels 34
1.2.8.5 Direct β –cell damage by viral cytolysis 34
1.2.9 Microorganisms contributing to β-cell damage via autoimmunity 35
1.2.9.1 Autoimmune diseases - genetic and environmental factors 35
1.2.9.2 Factors contributing to diabetogenic autoimmune responses 36
1.2.9.3 Microbial infection as environmental factors in T1D 39
1.2.9.4 Molecular mimicry theory of epitopes 40
1.2.10 Molecular mimicry protein theory 42
1.2.10.1 Glutamic acid decarboxylase targeting 44
1.2.10.2 Islet Antigen-2 (IA-2) targeting 45
1.2.10.3 Insulin - like substances in microbes 45
1.2.10.4 Heat Shock Proteins (HSP) 46
1.2.10.5 Insulin receptors on microorganisms 47
1.2.11 T-cells mediated autoimmunity of diabetes type 1 48

1.3 Cystic Fibrosis and diabetes and infections 51

1.4 Conclusions 53

1.5 Aims & Objectives 54

Chapter 2

General Materials and Methods 55

2.1 Reagents and media 56

2.2 Microbiology 56
2.2.1 Microorganisms 56
2.2.2 Laboratory culture and storage of bacteria 58

2.3 Mammalian cell culture 59
2.3.1 Rat insulinoma (INS-1) cells 59
2.3.2 Chinese Hamster Ovary Cells (CHO) 59
2.3.3 Storage of mammalian cells 60
2.3.4 Cloning vectors 60
2.3.4.1 Bacteriophage lambda (λ) express (Stratgene, Wilmington,USA) 60
2.3.4.2 Plasmid pGEM-T Easy vector 61
2.3.4.3 Plasmid pFN22A HaloTag cMVd1 Flexi vector 64

2.4 Protein analysis 66
2.4.1 Extraction of microbial soluble proteins 66
2.4.2 Protein quantification 66
2.4.3 SDS-PAGE 67
2.4.4 Protein Blotting 69

2.5 Nucleic acid analysis 69
2.5.1 Purification of genomic DNA from Gram negative bacteria 69
2.5.2 DNA precipitation 70
2.5.3 Preparation of plasmid DNA 70
2.5.4 Plasmid preparation using Plasmid Miniprep Kit (PLN70, Sigma, UK) 71
2.5.5 Determination nucleic acids quality and quantity 71
2.5.6 DNA agarose gel electrophoresis 72
2.5.7 Elution of PCR products from agarose gels 72
2.5.8 DNA digestion by restriction endonuclease enzymes 73

2.6 Assaying gene expression using RT-PCR & qRT-PCR 73
2.6.1 Extraction of total RNA from mammalian cells 74
2.6.2 Preparing total cDNA using reverse transcriptase 74
2.6.3 Conventional PCR amplification 75
2.6.3.1 Design of primers 75
2.6.3.2 PCR amplification 75

2.7 Quantifying gene expression by absolute qRT-PCR 76
2.7.1 PCR amplification using GoTaq DNA polymerase 77
2.7.2 Ligation of PCR products into pGEMT-Easy plasmid 78
2.7.3 Transformation into *E. coli JM109* coupled with blue white screening 78
2.7.4 Checking recombinant pGEMT-Easy plasmid 79
2.7.5 Assay for mammalian expression 80
2.7.6 qRT-PCR Data normalization 80
2.7.7 Statistical analysis 80

Chapter 3

Effects of the microbial secondary metabolites pyrrolnitrin, phenazine and patulin on INS-1 rat pancreatic β-cells 81

3.1 Introduction 82

3.2 Materials and Methods 86
3.2.1 Microbial secondary metabolites preparation 86
3.2.2 Cell culture 86
3.2.3 Pancreatic β-Cell cytotoxicity 86
3.2.3.1 Cytotoxic effects of secondary compounds on INS-1 cells 86
3.2.3.2 Cytotoxic effects of BMS & PAS on INS-1 cells 87
3.2.4 Effects of secondary compounds on insulin secretion 87
3.2.4.1 INS-1 insulin secretion stimulation 87
3.2.4.2 Effects of microbial compounds on insulin secretion after 2 h 88
3.2.4.3 Effect of sublethal concentrations on insulin secretion 89
3.2.4.4 Radioimmunoassay (RIA) 89
3.2.4.5 Standard curve preparation samples for RIA 90
3.2.4.6 RIA data analysis 90
3.2.5 Effects of microbial compounds on insulin gene expression 90
3.2.5.1 Assay insulin gene expression using RT-PCR 90
3.2.5.2 Assay insulin gene expression using absolute qRT-PCR 91
3.2.5.3 Preparation clone standard curve for absolute qRT-PCR 91
3.2.5.4 Assay insulin gene expression and machine setting 93
3.2.5.5 qRT-PCR DATA normalization 93
3.2.6 Measurement of INS-1 intracellular Ca^{2+} concentration 93
3.2.7 Patch-clamp electrophysiology of INS-1 cells 94
3.2.8 Statistical analysis 95

3.3 Results 96
3.3.1 Cytotoxic effects of microbial compounds on INS-1 cells 96
3.3.2 Cytotoxic effects of *B. multivorans* and *Ps. aeruginosa* supernatants (BMS & PAS) to INS-1 99
3.3.3 Effects of microbial compounds on insulin secretion by INS-1 cells after 2 h of exposure 101
3.3.4 Effects of microbial compounds on insulin secretion by INS-1 cells after 24 h of exposure 103
3.3.5 Effect of microbial compounds on insulin gene expression 106
3.3.5.1 Amplification and cloning of insulin and β-actin amplicons 106
3.3.5.2 Insulin gene expression using absolute qRT-PCR 108
3.3.6 Measurement of intracellular Ca^{2+} levels in INS-1 cells 112
3.3.7 Patch-clamp electrophysiology of INS-1 cells 112

3.4 Discussion 115

Chapter 4

Effect of phenazine and pyrrolnitrin on gene expression of insulin and some GSIS mediating signals 122

4.1 Introduction 123

4.2 Materials & Methods 125
4.2.1 Effect of pyrrolnitrin and phenazine on insulin gene expression 125
4.2.2 Effect of pyrrolnitrin and phenazine on transcription factors genes 125
4.2.3 Quantifying mRNA of GK, GT-2, CamK4 and CamKK1 genes 128
4.2.4 Normalization of qRT-PCR Data 128
4.2.5 Amplification of amplicons using RT-PCR 129

4.3 Results 130
4.3.1 Quantifying mRNA expression of insulin gene transcription 130
4.3.2 Quantifying transcription factor gene expression 133
4.3.3 Quantification of GK, GT-2, CamK4 and CamKK1 gene expression 136

4.4 Discussion 140

Chapter 5

Screening microorganisms for binding of insulin and construction of a *Burkholderia multivorans* genomic library 147

5.1 Introduction 148

5.2 Materials and Methods 150
5.2.1 Insulin ligand binding assay with whole microbe cells 150
5.2.2 Quantification of insulin bound to *B. multivorans* and *A. salmonicida* 151
5.2.3 Extraction and solubilisation of total protein 151
5.2.3.1 Solubilisation of bacterial proteins for SDS-PAGE 152
5.2.3.2 Solubilisation proteins using TritonX 100 & low concentration of SDS 152
5.2.3.3 Solubilisation of proteins using SDS and lysozyme 152
5.2.3.4 Extraction using sonication, low SDS and lysozyme 153
5.2.4 SDS-PAGE coupled western ligand blotting 153
5.2.5 Construction of *B. multivorans* genomic DNA library 154
5.2.5.1 Extraction of genomic DNA of *B. multivorans* 154
5.2.5.2 Partial digestion of genomic DNA using *Sau3A* 154
5.2.5.3 Ligation of *B. multivorans* DNA with λ Zap express arms 155
5.2.5.4 *In vitro* packaging ligated DNA using Gigapack III Gold System 155
5.2.6 Assaying bacteriophage 156
5.2.6.1 Preparation of host bacteria 156
5.2.6.2 Phage Assay 156
5.2.6.3 Blue- white screening for recombinants 157
5.2.6.4 Amplifying the Zap genomic library 157
5.2.6.5 Screening genomic library for insulin binding 158
5.2.6.6 Secondary screening of insulin binding plaques 160
5.2.6.7 *In vivo* excision of insulin binding positive phagemids form λ Zap 160
5.2.6.8 Extraction and digestion of recombinant phagemids 162

5.3 Results 163
5.3.1 Insulin binding assay with whole cell microbes 163
5.3.2 Quantification of insulin binding 165
5.3.3 Western ligand blotting of insulin binding protein 167
5.3.4 Construction *B. multivorans* genomic library 169
5.3.4.1 Ligation of *B. multivorans* DNA into predigested λ Zap arms 169
5.3.4.2 Titration of gene bank and screening for recombinants 169
5.3.4.3 Screening *B. multivorans* genomic library for insulin binding activity 171
5.3.4.4 *In vivo* excision of positive insulin binding recombinant phagemids 171

5.4 Discussion 174

Chapter 6

Expression recombinant phagemids p1 & p2, sequencing and sequence analysis 181

6.1 Introduction 182

6.2 Materials and Methods 183
6.2.1 Expressing recombinant phagemids in *E. coli* 183
6.2.2 Southern Blotting 183
6.2.2.1 Digoxigenin-Labelling of the DNA Template 184
6.2.2.2 Hybridization 184
6.2.3 Sequencing the recombinant phagemids p1 and p2 186
6.2.4 Sequence analysis 186
6.2.4.1 ORF gene motifs and predicted amino acid sequence 186
6.2.4.2 Sequence identification by Blast –n & p 187
6.2.4.3 Phylogenetic tree and evaluation relationship 187
6.2.4.4 IBP topology prediction 187
6.2.4.5 Molecular mimicries and linear epitopes prediction 187

6.3 Results 188
6.3.1 Expressing recombinant phagemids in *E. coli* 188
6.3.2 Southern Blotting 188
6.3.3 Sequence analysis of p1 & p2 inserts 189
6.3.3.1 ORF analysis and predicted amino acid sequences for p1 189
6.3.3.2 ORFs analysis and predicted amino acid sequences for p2 194
6.3.4 Identification of ORFs encoding protein receptors 197
6.3.5 Topology prediction of IBPs sequences 200
6.3.6 Molecular mimicries and linear epitopes prediction 202

6.4 Discussion 205

Chapter 7

Molecular cloning of β-cell antigen glutamic acid decarboxylase (GAD65) using Halo tag technology, expression & purification 214

7.1 Introduction 215

7.2 Materials and Methods.....216
7.2.1 Cell culture.....216
7.2.2 Molecular cloning of GAD65 gene 218
7.2.2.1 Synthesizing total cDNA of INS-1 cells 218
7.2.2.2 Amplification of GAD65 gene and optimisation of PCR condition 219
7.2.2.3 Cloning the GAD65 products into Halo tag Flexi vector pFN22A 220
7.2.2.4 Restriction digestion of GAD65 PCR product and pFN22A vector.....220
7.2.2.5 Ligation of GAD65 PCR product into the pFN22A 220
7.2.3 Screening transformants for recombinant plasmids 221
7.2.3.1 Screening *E. coli* transformants for GAD65 recombinants.....221
7.2.3.2 Screening recombinant plasmids using restriction enzymes.....221
7.2.3.3 Screening recombinant plasmids using PCR 222
7.2.3.4 Preliminary checking of the GAD65 sequence by *Bgl II* digestion.....222
7.2.3.5 Sequencing & sequence analysis of GAD65 recombinant plasmids...223
7.2.4 Expression and purification of Halo-tag GAD65.....223
7.2.4.1 Expression and extraction of engineered GAD65 from *E. coli JM109*.223
7.2.4.2 CHO transfection optimisation 224
7.2.4.3 RT-PCR for GAD65 gene expression in CHO.....225
7.2.4.4 Purification of GAD65 Halo Tag 226
7.2.4.5 Cleavage of GAD65 Protein from the Halo tag 226
7.2.5 Characterization of the purified GAD65 protein.....227
7.2.5.1 SDS PAGE electrophoresis 227
7.2.5.2 GAD65 protein Dot Blot.....227
7.2.5.3 Quantification and concentration of the GAD65 protein 228
7.2.6 GAD65 antiserum production and titration 229

7.3 Results.....230
7.3.1 Cloning the GAD65 reading frame 230
7.3.1.1 Amplification of the GAD65 reading Frame.....230
7.3.1.2 Cloning the amplicon of GAD65.....230
7.3.1.3 Restriction digestion of recombinant plasmids 232
7.3.1.4 Preliminary checking of the GAD65 inserts.....232
7.3.2 GAD65 sequencing and sequence analysis.....235
7.3.3 Selection of recombinant plasmids for expression 235
7.3.4 Production and purification of GAD65 protein 238
7.3.4.1 Expressing of recombinant GAD65 protein.....238
7.3.4.2 GAD65 gene expression.....238
7.3.4.3 Extraction & purification of GAD65 protein.....239
7.3.5 Titration of anti GAD65 antiserum.....242

7.4 Discussion.....243

Chapter 8

Molecular mimicries epitopes between pancreatic antigen GAD65 and *E. coli* proteins.....247

8.1 Introduction 248
8.1.1 Western blotting coupled proteomic technique 249
8.1.2 The Proteomic Technique of Mass spectrometry.....250

8.2 Materials and Methods.....251
8.2.1 Microorganism culture.....251
8.2.2 Extraction of total proteins.....251
8.2.3 Screening microbial proteins using GAD65 antiserum by dot blot 251
8.2.4 Western blotting 252
8.2.5 Localization of the GAD65 cross reactive protein on SDS-PAGE gel 253
8.2.6 Identification *E. coli* protein bands using mass spectrometry.....253
8.2.7 Molecular mimicries prediction between GAD65 and *E. coli* proteins 254

8.3 Results.....255
8.3.1 Screening microorganisms using GAD65 antiserum.....255
8.3.2 Western Blotting.....257
8.3.3 MS/MS Data of *E coli* proteins 260
8.3.4 Protein Identities 260
8.3.5 *E. coli* protein OmpA (bands 1 & 2) show linear epitopes on GAD65 ...264
8.3.6 *E. coli* protein FD (band 3) shows linear epitopes on GAD65 265
8.3.7 *E. coli* protein SD (band4) shows linear epitopes on GAD65.....267
8.3.8 *E. coli* DspP (band5) shows linear epitopes on GAD65 269

8.4 Discussion.....271

Chapter 9

General Discussion 281

Appendix 1

Media preparation and formulation of reagents.....321

Appendix 2

Data relevant for this study.....332

Appendix 3

Publications of this study 347

List of Figures

Chapter 1

Figure 1.1: Schematic graph illustrating the role of insulin in glucose uptake 6
Figure 1.2: Schematic model of Human insulin receptor complex 10
Figure 1.3: Mitochondrial glucose metabolism of β-cells 14
Figure 1.4: Schematic diagram to represent the K_{ATP} channel topology 17
Figure 1.5: Schematic diagram of β-cell granule pools 20
Figure 1.6: Schematic model illustrating insulin gene promoter 25
Figure 1.7: Schematic diagram illustrating factors triggering theT1D 38
Figure 1.8: T-cell autoimmunity mechanism of diabetes type 1 50

Chapter 2

Figure 2.1: Schematic model of λ ZAP expression vector 62
Figure 2.2: Schematic map of plasmid pGEM-T easy cloning vector 63
Figure 2.3: pFN22A HaloTag cMVd1 Flexi vector map 65

Chapter 3

Figure 3.1: Chemical structure of the microbial secondary metabolites 85
Figure 3.2: Cytotoxicity of pyrrolnitrin to INS-1 cells 97
Figure 3.3: Cytotoxicity of phenazine to INS-1 cells 97
Figure 3.4: Cytotoxicity of patulin to INS-1 cells 98
Figure 3.5**:** Cytotoxicity of BMS & PAS on INS-1 cells 100
Figure 3.6: Effects of pyrrolnitrin, phenazine & patulin on GSIS at after 2h 102
Figure 3.7: Effects of exposure of INS-1 cells to pyrrolnitrin on GSIS at 2h 104
Figure 3.8: Effects of exposure of INS-1 cells to phenazine on GSIS at 24h 104
Figure 3.9: Effects of exposure of INS-1 cells to patulin on GSIS 105
Figure 3.10: Amplification & cloning of insulin & β-actin amplicon 107
Figure 3.11: Insulin gene expression after exposure to pyrrolnitrin 109
Figure 3.12: Insulin gene expression after exposure to phenazine 110
Figure 3.13: Insulin gene expression after exposure to patulin 111
Figure 3.14: Pyrrolnitrin or phenazine increase the intracellular Ca^{2}+ 113
Figure 3.15: Electrophysiology of INS-1 cells using patch clamp technique 114

Chapter 4

Figure 4.1: Effect of pyrrolnitrin & phenazine on Insulin gene expression 131
Figure 4:2: Amplification & cloning of PCR products 132
Figure 4.3: Effect of phenazine on PDX-1, MafA & NeuroD genes 134
Figure 4.4: Effect of pyrrolnitrin on PDX-1, MafA & NeuroD genes 135
Figure 4.5: Gel based RT-PCR of GK, GT, CamK4 & CamKK1 genes 137
Figure 4.6: Effect of phenazine on GK, GT, CamKK1 & CamK4 genes 138
Figure 4.7: Effect of pyrrolnitrin on GK, GT, CamKK1 & CamK4 genes 139
Figure 4.8: Graph illustrates the effect of phenazine & pyrrolnitrin on GSIS 146

Chapter 5

Figure 5.1: Insulin binds to *A.salmonicida & B. multivorans* 164
Figure 5.2: Quantification of insulin bound to *B. multivorans* 166
Figure 5.3: Western ligand & blotting of total protein of *B. multivorans* 168
Figure 5.4: The digestion of *B. multivorans* genomic DNA by *Sau3A* RE 170
Figure 5.5: Ligation of the *B. multivorans* digested DNA within λ Zap 170
Figure 5.6: Blue white Screening of *B multivorans* genomic library 172
Figure 5.7: Screening of λ Zap gene library for insulin binding 172
Figure 5.8: Agarose gel electrophoresis of recombinant phagemids 173

Chapter 6

Figure 6.1: IBP(s) detected by western ligand blotting 190
Figure 6.2: Southern blot of genomic DNA of *B. multivorans* 190
Figure 6.3: ORF analysis of inserted DNA of phagemids p1 & p2 191
Figure 6.4: Nucleotide sequence of putative ORF1 & 2 encoded by p1 192
Figure 6.5: Nucleotide sequence of putative ORF3 encoded by p1 193
Figure 6.6: Nucleotide sequence of putative ORF1& 2 encoded by p2 195
Figure 6.7: Nucleotide sequence of putative ORF3 & 4 encoded by p2 196
Figure 6.8: Phylogram tree based on nucleotide sequence of p1-ORF3 198
Figure 6.9: Phylogram tree based on nucleotide sequence of p2-ORF1 199
Figure 6.10: Transmembrane helices prediction of putative IBPs 201
Figure 6.11: Sequence homology between IBP(s) & HIR 203
Figure 6.12: Diagram showing biosynthesis of Ornibactin of *B. multivorans* 208
Figure 6.13: Graph showing the peptide transportation into the bacteria 211

Chapter 7

Figure 7.1: Flow chart illustrates the steps for cloning the GAD65 gene 217
Figure 7.2: Amplification of the GAD65 reading frame by RT-PCR 231
Figure 7.3: Preliminary identification of GAD65 encoding region from pG1 233
Figure 7.4: Excision of inserts from recombinant plasmid pG1-pG5 234
Figure 7.5: Schematic map of recombinant pG1 plasmid sequences 236
Figure 7.6: The GAD65 sequence cloned into recombinant plasmid pG1 237
Figure 7.7: Dot blot of GAD65 protein expression in transfected CHO cells 240
Figure 7.8: RT-PCR of GAD65 gene expression in transfected CHO cells 240
Figure 7.9: SDS-PAGE of recombinant purified GAD65 kDa 241
Figure 7.10: Dot blot of GAD65 produced by CHO 241
Figure 7.11: Titration of the GAD65 antiserum against the purified GAD65 242

Chapter 8

Figure 8.1: Cross reaction between microbial proteins & GAD antisera 256
Figure 8.2: Immune blotting of microbial protein samples 258
Figure 8.3: Western blotting of *E. coli* protein with GAD65 antiserum 259
Figure 8.4: Full length sequences of *E. coli* proteins identified by MS/MS 263
Figure 8.5: Sequence homology between GAD65 & protein bands 1, 2 & 3 266
Figure 8.6: Sequence homology between GAD65 & protein of band 4 268
Figure 8.7: Sequence homology between GAD65 & protein of band 5 270
Figure 8.8: Sequence homology between GAD65 & E .coli proteins shows the homology between one single epitope 280

List of Tables

Table 1.1: The cross reactivity between β-cell antigens & microbial epitopes 41
Table 1.2: Targets of the autoimmune response in T1D 43
Table 2.1: Micro strains used & optimum growth conditions 57
Table 2.2: *E coli* K12 strains used in gene manipulation experiments 58
Table 3.1: Primer sequences used to amplify insulin & β-actin gene 92
Table 4.1: Primers used to amplify insulin gene transcription factors 126
Table 6.1: Epitopes of IBP(s) & affinity for binding on HLA molecules 204
Table 8.1: The MS/MS data represents the peptide mass of *E.coli* protein 262
Table 8.2: The homology between *E coli* protein epitopes & GAD65 279

Acknowledgements

I would like to express my sincere gratitude to my Supervisor Dr Martyn L.Gilpin and my second supervisor Dr John Moody for their continuous support of my Ph.D. study and research, for their patience, enthusiasm, and encouragement. Their guidance helped me in all the time of research and writing of this thesis.

Besides my supervisors, I would like to thank Prof Noel Morgan (Peninsula Medical and Dentistry School/ University of Plymouth) for providing the INS-1 cells and assistance with the insulin secretion assay at the medical School. I would like also to thank Dr Simon Fox for all his help.

My sincere deep thanks also go to Ms Lynne Cooper for her invaluable comments and advice during my lab work.

Many thanks extended to Mr Matthew Emery, Miss Sarah Jamieson, Mrs Christine Boxley, Mr Andrew Atfield, Mrs Angela Harrop, Dr Michele Kiernan, and Mr Peter Russell. I am also grateful to all the staff of the School of Biomedical and Biological Sciences at University of Plymouth.

Last but not the least; I would like to thank my family Wasan, Yousif and Ibrahim for their patience and support during the years of study.

Author Declaration

At no time during the registration for the degree of Ph.D has the author been registered for any other University award, without prior agreement of the Graduate Committee.

Word count of the main body of the thesis without references: 62,032

Signed……..…….

Date……

Training Courses & Workshops

School of Biomedical & Biological Sciences, University of Plymouth, UK.

- BioL5124, 2008/2009 .
- Infection and immunity2408, 2009/2010.
- Microbial diseases and biotechnology3310, 2009/2010.
- General Teaching Associates Course (GTA), 2010/2011.
- Multiplexing & Luminex Technology /One day workshop, 14 /9/2010.
- Olympus Microscopy Workshop Agenda, 24-26/5/2011, arranged by Olympus Company, Lab 301 Davy Building.
- Ettan 2-D DIGE Course, 6-8/03/2012, arranged by GE healthcare /Davy 211, 212.

Workshops attended in the UK

- Agilent Microarray & Sequencing Roadshow: 8/6/2010 arranged by Agilent technologies, Novotel St Pancras /London, UK.
- Browsing genes & genomes with ensemble 11- 13 /11/2009 arranged by the European Bioinformatics Institute and Wellcome Trust Sanger Institute, University of Cambridge. Cambridge, UK.

Presentation and Conferences Attended

- British Society of Immunology (BSI) Congress, 5 – 8/12/2011, Arena and Convention Centre in Liverpool, UK, **Poster**, (Chapter 7 & 8).
- Society of Applied Microbiology Summer Conference, 4-7/7/2011, Dublin /Ireland, **Poster awarded second best poster prize,** (Chapter 5 & 6).
- 4th International Congress on Prediabetes and the Metabolic Syndrome, 6-9/4/2011/ Madrid, Spain, **Poster,** (Chapter 3).
- Annual Research Day, 5/4/2011, Centre for Research in Translation Biomedicine of University of Plymouth/UK, **Poster,** (Chapter 4).
- University of Plymouth, 14/10/2010, **Oral presentation,** (Chapter 5 & 6).
- Annual Drug Discovery conference, 1-2/7/2010, Ricoh Arena /Coventry /UK, **Poster,** (Chapter 3).
- University of Plymouth, 22/3/2009 /, **Oral presentation,** (Chapter 1).
  South West and South Wales Microbiology Forum, 24/9/2009, Peter Chalk Centre / University of Exeter /UK, **poster**, (Chapter 3).

Peer Reviewed Publications

Raid B. Nisr, A. John Moody and Martyn L. Gilpin (2012). Screening microorganisms for insulin binding reveals binding by *Burkholderia multivorans* and *Burkholderia cenocepacia* and novel attachment of insulin to *Aeromonas salmonicida* via the A-layer. FEMS Microbiology Letter 328:93-9 (Chapter 5).

Raid B. Nisr, Mark A. Russell, Abdesslam Chrachri, A. John Moody & Martyn L. Gilpin (2011). Effects of the microbial secondary metabolites pyrrolnitrin, phenazine and patulin on INS-1 rat pancreatic b-cells. FEMS Immunology and Medical Microbiology 63, 217–227 (Chapter 3 & 4).

Raid B.Nisr, Martyn L. Gilpin, and A, John Moody. (2011). Effect of phenazine on pancreatic β-cell viability and insulin secretion and gene expression. Journal of Diabetes 3, 1, p 188 (Abstract / Chapter 3).

Raid B.Nisr. Martyn L. Gilpin, and A, John Moody. Molecular mimicries of linear epitopes between pancreatic glutamic acid decarboxylase (GAD65) and proteins from *E. coli*. Immunology, 134 (Suppl 1), p 140 (Abstract / Chapter 7 & 8).

Raid B.Nisr, Martyn L. Gilpin, and A, John Moody. Molecular mimicry between *Burkholderia multivorans* insulin binding proteins (IBPs) and human insulin receptor epitopes (HIR) (Chapter 6), submitted.

Raid B.Nisr, Martyn L. Gilpin, and A. John Moody. Effects of the microbial secondary metabolites phenazine and pyrrolnitrin on expression of insulin gene and some GSIS mediating signals in rat INS-1 cells (Chapter 4), submitted.

Raid B.Nisr, Martyn L. Gilpin, and A, John Moody. Molecular mimicries of linear epitopes between pancreatic glutamic acid decarboxylase (GAD65) and proteins from *E. coli* (Chapter 7 & 8), In preparation.

Previous Publications

Raid B. Nisr. (2006). Study of the ability of *Acinetobacter* spp RB8 in utilization some aromatic hydrocarbons compounds and role of its plasmid, *Iraqi J Sci, 44*.

Raid B. Nisr., Smaira, Y. Yousif., and Wasan A. Ali (2005). Utilization of certain aliphatic hydrocarbons by *Acinetobacter* spp. isolated from local soil, *Biotech Research*, 1.

Raid B. Nisr., M H, Aljelawii., and Norria. A. Ali (2004). The role of *Pseudomonas aeruginosa* RB19 plasmid in utilization of hydrocarbon compounds, *J Al-Nahrain* Sci,7.

Raid B. Nisr, M H, Aljelawii, and Norria. A, Ali. (2002). Isolation & identification of curd oil & hydrocarbon utilizing bacteria, *Iraqi J Sci*, B43.

List of Abbreviations 1

β-cells	Beta Pancreatic Cell
HIR	Human Insulin Receptor
T1D	Type 1 Diabetes
T2D	Type 2 Diabetes
APC	Antigen Presenting Cells
GT-2	Glucose Transporter -2
GPCR	G Protein Coupled Receptor
VDCC	Voltage –Dependent Ca^{2+} Channels
GAD	Glutamic Acid Decarboxylase
SUR1	Sulfonylurea Receptor
Kir6.1	K^+ inward rectifier
IA-2	Islet Antigen -2
GK	Glucose kinase
PTP	Protein Tyrosine Phosphatase
GSIS	Glucose Stimulation Insulin Secretion
MODY	Maturity Onset Diabetes of the Young
NOD	Non Obese Diabetes Mouse
T-cell	T-lymphocytes
MHC	Major Histocompatibility Complex
RT	Room Temperature
IBP	Insulin Binding protein
MBW	Molecular Biology Grade Water
µg	Microgram
Dig	Digoxigenin
BN-PAGE	Blue Native Polyacrylamide Gel Electrophoresis
kDa	kilo Dalton
CF	Cystic Fibrosis
Bcc	*Burkholderia cepacia* complex
BCESM	*Burkholderia cepacia* Epidemic Strain Markers

List of Abbreviations 2

kbp	kilo base pair
ORF	Open Reading Frame
SD	Shine Delgarno Sequence
PP1	Serine /Threonine Phosphates 1
ABC	ATP Binding Cassette Transporters
POT	Proton dependent Oligopeptide Transporter
CBV	Coxsackie B Virus
B-cell	B-lymphocytes
HSP60	Heat Shock Protein 60
LADA	Latent Autoimmune Diabetes in Adult
MS	Mass Spectrometry
CFRD	Cystic Fibrosis Related Diabetes
IBP(s)	Insulin Binding Proteins
CamK4	Calcium/calmodulin-dependent protein Kinase 4
CamKK1	Calcium/calmodulin-dependent protein Kinase Kinase1
PFU	Plaque Forming Units
EBI	European Bioinformatics Institute
TR	Transfection Reagent
ROS	Reactive Oxygen Species
OmpA	Outer membrane protein A
FD	Format Dehydrogenase
PIP	Phage Integrase Protein
SD	Superoxide Dismutase
DspP	DNA starvation protection Protein

Chapter 1

Introduction and Literature Review

1.1 Introduction

Insulin is a hormone that regulates glucose uptake and energy synthesis of mammalian cells (Johnston and Van Horn, 2011). Since 1970 many studies have shown interactions between insulin and microorganisms. Investigations in the field of comparative biochemistry in the last two decades have demonstrated that insulin and insulin-like peptides are also present in some prokaryotes (LeRoith *et al.*, 1981) and unicellular eukaryotes such as the protozoa and yeast, besides those already identified in vertebrates (Silva *et al.*, 2002). Furthermore, studies seeking insulin binding to microorganisms have verified the presence of insulin receptors or protein-like human insulin receptor (HIR) on various microorganisms such as fungi, protozoa (Dietz *et al.*, 1989) and bacteria (Jeromson *et al.*, 1999). Recently, investigators in microbiology have reported the cytotoxicity of some microbial components to insulin producing cells i.e. pancreatic beta cells (pancreatic β-cells). Many of these components are secondary metabolites produced by soil bacteria such as *Streptomyces* and some of them are primary metabolites e.g. collagenase produced by e.g. *Clostridium sp.* These could destroy some β-cells and reduce insulin production (Myers *et al.*, 2002). There are many ways by which the human body may be exposed to these toxic components, apart from contaminated food and water (Hettiarachchi *et al.*, 2006). Moreover, studies have also shown modulation of the insulin pathway by microbial components, particularly toxins (primary and secondary metabolites) affecting specific key signals of the β-cells, severing insulin synthesis (Demain, 1999). The most important signals altered by microbial components are phosphorylation (Müller-Wieland *et al.*, 1991), glucose metabolism (Bkaily *et al.*, 1998) and insulin binding (Salituro *et al.*, 2001). It has been confirmed that the microbes and their

components can be considered as environmental factors contributing the development of diabetes mellitus (Williams and Pickup, 2004), however, diabetes is not a single disease but a group of clinical disorders or forms which is characterized recently by chronic hyperglycemia (CDCP, 2011). Traditionally, two main types of diabetes, Type 1 Diabetes (TID) which occurs in individuals who have genetic disorders of certain genes leading to an autoimmune response against the pancreatic auotoantigenes in addition to some environmental factors (Maclaren and Atkinson, 1997; MacFarlane *et al.*, 2003), and Type2 diabetes (T2D) the more prevalence type of diabetes which results from metabolic disorders such as obesity and cellular resistance to the insulin effect and it appears to be more common amongst particular ethnic groups than others (Kazlauskaite and Fogelfeld, 2003) .

A new category of diabetes, Gestational Diabetes Mellitus (GDM) is a disorder in which pregnant women exhibit high blood glucose levels during pregnancy without previously being diagnosed with diabetes (McCance and Huether, 2002).

However, recently the terms of diabetes have included new forms of diabetes such as a diabetes which results from the destruction of β-cells by toxins or chemicals or viral infection and diabetes associated with genetic defects in β-cells in insulin gene such as Maturity Onset Diabetes of the young (MODY), and a form that results from production of antibodies against the insulin receptor (MacFarlane *et al.*, 2003). Exposure to certain microorganisms appears to be a major environmental factor in T1D causing autoimmunity by molecular mimicries (MacFarlane *et al.*, 2003). Studies in the field of infectious immunity showed autoimmune responses against β-cells can be caused by microbial

infections and by viral agents destroying β-cells completely and causing T1D (Maclaren and Atkinson, 1997; MacFarlane *et al.*, 2003). However, these studies suggest an autoimmune response against β-cell autoantigens could be initiated after regular immune responses against microorganisms which have proteins with homology to β-cell components and cause a diabetogenic autoimmune response (Davies, 1997). However, No direct role has been found for microorganisms in triggering T2D or progression. However, microbial infection is one of the major secondary complications that occur in T2D patients whose immune system is compromised because of the elevation of glucose concentration in the blood. Different types of infection have been specifically associated with T2D, such as urinary tract infection (Hammar *et al.*, 2010), skin infections and foot ulcers (Tiwari *et al.*, 2012).

The microbes which reached the blood stream during infection and microbes which are ingested in contaminated food may present antigens which lead to a diabetogenic response (Vaarala, 2000; Vercelli, 2006). The autoimmune disease can be initiated and accelerated by microbial infection leading to a breakdown in self-tolerance which causes a destructive autoimmune response via activation of antigen presenting cells (APC) and subsequently production of autoantigens. On the other hand infection may have a therapeutic application achieved by immune-suppression or the remodelling the anti-inflammatory cytokines status with activation induced cell death of auto-reactive T-cells (Fujinami *et al.*, 2006). Recent studies have shown a new beneficial effect achieved by microbes used as probiotics in regulating the diabetic inflammation response initiated by gut microbiota (Delzenne and Cani, 2011).

1.2 Literature review

1.2.1 Insulin

Insulin is an anabolic hormone, a 51 amino acid peptide in humans, secreted from β-cells in the islet of Langerhans of the pancreas. Insulin is composed of two polypeptide chains (A & B) connected by disulfide bridge bonds and has a central role in regulating carbohydrates, fat and many other metabolic functions in the body (Betley *et al.*, 1989; Arumugam *et al.*, 2008). Insulin plays a vital role in regulating glucose uptake from the systemic circulation, stimulating specific membrane transporters to facilitate glucose transport into the cells, reducing plasma glucose concentration (Straub and Sharp, 2002). After insulin binds to its receptor many protein activation and biochemical cascades follow, including influx of glucose by a specific transporter, the glucose transporter 4 (Glut-4), into the cells and produce energy (Muretta and Mastick, 2009).

Insulin can also stimulate cells in the liver and fat tissue to convert the blood glucose into glycogen and store it in the liver and muscles (Bouskila *et al.*, 2008). When blood glucose level drop the body turns glycogen in adipose tissue into glucose via glycogenolysis, which is regulated by another pancreatic hormone produced by pancreatic alpha cells (α-cells) called glucagon (Kieffer and Francis, 1999) (Figure 1.1) .

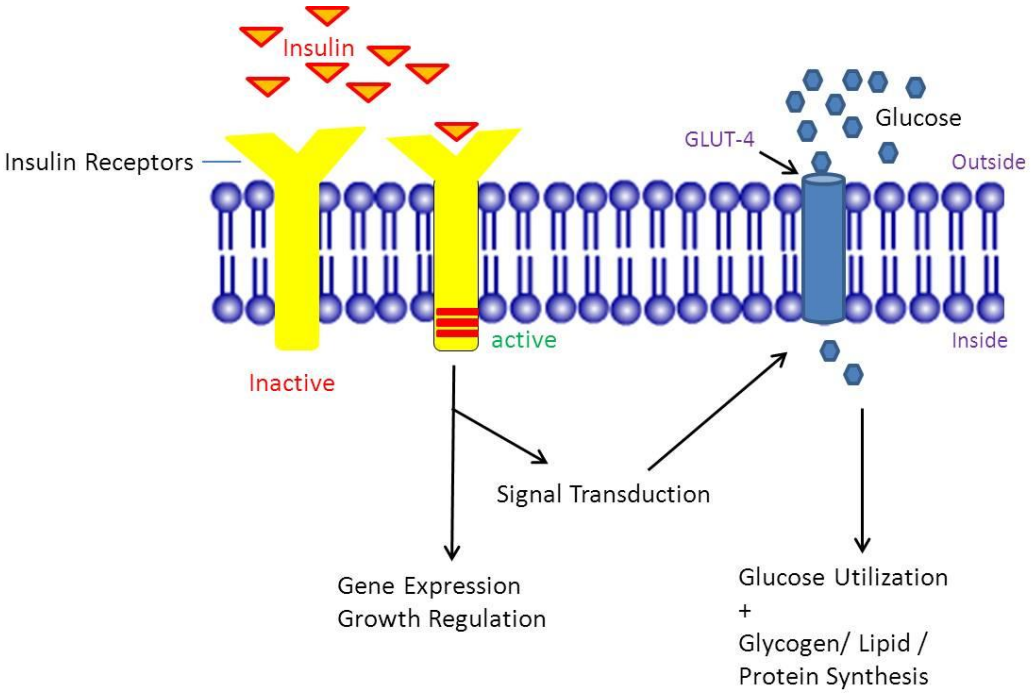

Figure 1.1 Schematic graph illustrating the role of insulin in glucose uptake. Insulin binding to its receptor induces a signal transduction pathway which allows the glucose transporter (GLUT4) to transport glucose into the cell and subsequently glucose is metabolised adapted from Beta Cell Biology Consortium (2004).

1.2.2 The Insulin receptor & biology of receptors mediating cell signaling

The cell communicates and responds via various types of receptor that react with signal molecules (specific ligands) from its environment such as nutrients or components of the vascular system (proteins, hormone, signal peptides etc.). Structurally, a receptor typically has α helix protein passing through the membrane and ligand-binding components react outside of the cell, allowing sensing of the concentration of the signal molecule even at low concentration (Pierce *et al.*, 2002). Ligand binding produces receptor conformational changes that transfer the signal through the membrane, initiating downstream biochemical cascades. There are various types of cell receptor and many extracellular signals have been detected, but the majority of receptors can be divided into four classes (Hancock, 2005). These are now described below.

G protein linked receptors

These are receptors in which the binding of ligand leads to activation of G – protein subunits, passing signals to the next component in the signal pathway. The general topology of these kinds of receptors is seven hydrophobic α-helices regions with approximately 22-24 amino acids at each span into the plasma membrane (Sheldon, 2004). In mammalian cells such receptors are normally specified in hormone binding e.g. epinephrine, serotonin, and glucagon. These receptors are great of interest to the pharmaceutical industry as targets for therapeutic interest e.g. some drugs that have action as anti-histamines (Bouskila *et al.*, 2008; Campanile and Iaccarino, 2009). Two other major signal transduction pathways regulated by the G protein-coupled receptors (GPCR) are the cyclic adenosine monophosphate (cAMP) signal pathway and phosphatidylinositol signal pathway (Brown *et al*., 2009).

Ion channel – linked receptors

These kinds of receptors are involved with neurotransmitter molecules and are classified as transmitter-gated ion channels in which the ligand binding to receptor changes the ion permeability of the plasma membrane leading to conformational changes of receptors which opens and closes an ion channel allowing efflux or influx of specific ions serving the reaction (Mercado *et al.*, 2005). In mammalian cells a clear example of such receptors are the acetylcholine receptors, composed of two identical α polypeptides which contain the acetylcholine binding sites along with three different peptides belonging to β, λ, and δ groups (Hancock, 2005).

Receptors have enzyme activity

These receptors have intrinsic enzyme activity which is characterized by the presence of a catalytic domain coupled to the receptor polypeptides (Nelson, 2008). The activity possessed by the receptor catalytic domain is controlled by a ligand binding domain. The ligand binds on the extracellular side of the membrane and the catalytic domain is on the cytoplasmic side. The catalytic activity is attributed either to a guanyl cyclase or phosphatase kinase. The receptor structure contains serine /threonine kinase activity which is diminished by serine /threonine phosphatase or they may contain receptor tyrosine kinase enzyme activity (RTK) (Sheldon, 2004; Nelson, 2008).

Tyrosine Kinase Receptors (RTK)

A class of receptor with intrinsic enzyme activity that has been studied widely, involving ligand binding, leading to activation of kinase activity of the receptor which causes phosphorylation of the receptor on its tyrosine residues (Hancock, 2005). A clear example of a tyrosine kinase enzyme receptor is the mammalian insulin receptor (IR).

1.2.3 Insulin receptor

Insulin binds with the cell membrane via heterotetrameric components making up the insulin receptor which consists of two extra cellular α subunits connected by disulfide bonds with two transmembrane β subunits whose intrinsic tyrosine kinase activity will be stimulated by autophosphorylation once insulin binds to the α subunit of the receptor (Ellis *et al.*, 1987) (Figure 1. 2).

Many studies have demonstrated the autophosphorylation and phosphorylation of intracellular substrates is essential for the signal transduction system to mediate a cellular response by the insulin receptor (Youngren, 2007). The two α subunits of insulin receptor are the ligand binding domain for the extracellular insulin, whereas, the autophosphorylation on tyrosine residues is achieved by kinase domains in the two β subunits which are in juxtaposition. The insulin receptor activation starts after insulin binding which causes structural changes of the β subunits as a result of autophosphorylation of the tyrosine residues, providing a basis for activation of the kinase and binding of downstream signalling molecules (Li and zang, 2007) .

1.2.4 Glucose sensing and insulin synthesizing mechanism in β-cells

Pancreatic β-cells act as blood glucose sensors regulating blood glucose via secretion of insulin hormone. Insulin is essential, for glucose storage regulation and prevents glycogen depletion (Li and Zhang, 2009; Tripathy and Chavez, 2010). In type 2 diabetes (T2D) β-cells become insensitive to glucose and cells become insensitive to insulin (Kahn *et al.*, 2006; Ma *et al.*, 2009).

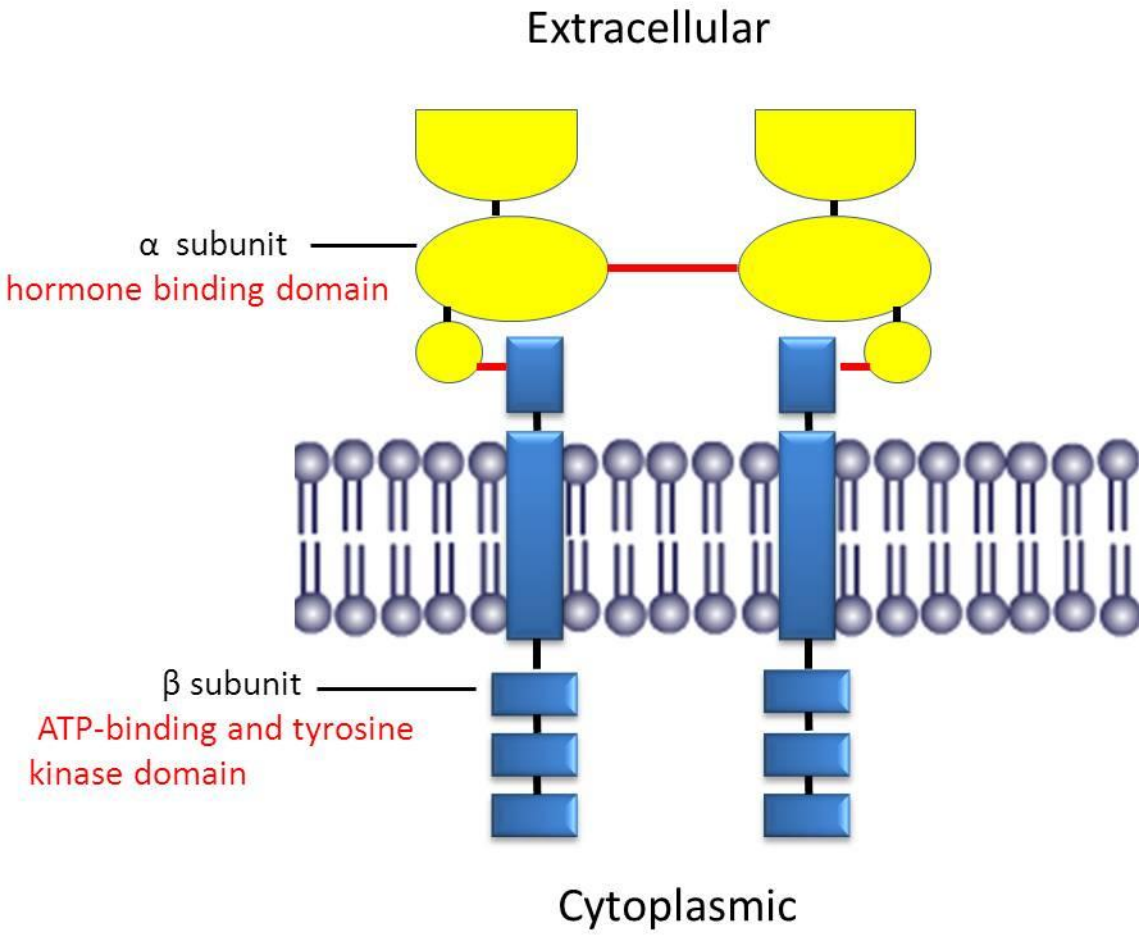

Figure 1.2: Schematic model of human insulin receptor complex. This receptor composed of two extracellular alpha subunits (yellow), both connected by disulfide bonds(red) and another disulfide bonds within two transmembrane β subunits (blue), adapted from Bowen (2004) .

Understanding glucose sensing and insulin release mechanisms of β-cells are considered a key to revealing how environmental factors contribute to dysfunction of the pancreatic islet and development of diabetes, and may facilitate developing therapeutic interventions (MacDonald *et al.*, 2005b). According to Straub and Sharp (2002) glucose sensing in β-cells occurs in two ways leading to biphasic insulin secretion. It is suggested that the glucose metabolism stimulates biphasic insulin secretion pathways (i) which is K_{ATP} channel dependent and (ii) another which is K_{ATP} channel independent, according to the signals produced from cytosolic and mitochondrial glucose metabolism respectively (Maechler *et al.*, 2006). Glucose stimulates insulin synthesis and insulin secretion in β-cells and involves following stages:-

1.2.4.1 Glucose transportation and glycolysis modeling in β -cells

Blood glucose regulation is initiated by rapid glucose uptake into β -cells, via an efficient glucose transporter-2 (GT-2) (Eisenberg *et al.*, 2005). Glucose in β-cells can enter two pathways, (i) glycolysis, where glucose 6 phosphate by hexokinase (Mercan *et al.*, 1993; Jijakli *et al.*, 1996) allowing glycolysis and pentose phosphate pathways, but in other instances some phosphorylated glucose may be converted to glycogen and stored in the liver and muscles (Pittman *et al.*, 2004). (ii) The second pathway involves metabolism of phosphorylated glucose into pyruvate, NADH and ATP to feed into the mitochondrial tricarboxylic acid (TCA) cycle (MacDonald *et al.*, 2005b).

1.2.4.2 Mitochondrial metabolism and ATP generation

The NADH and pyruvate produced by glycolysis enter mitochondrial metabolism to produce ATP. NADH can enter the mitochondria by two transporter systems, glycerol-phosphate and malate-aspartate, and these systems, play an important role as regulatory components in insulin secretion (Eto *et al.*, 1999; Rubi *et al.*, 2004).

There are two main sources of NADH, first is cytosolic and second is that liberated from the TCA cycle after mitochondrial pyruvate oxidation. Both NADH sources stimulate hyperpolarization of the mitochondrial inner membrane and increases the inner Ca^{2+} ion which provides a positive effect on ATP production by prompting dissociation of ATP synthatase inhibitor (MacDonald *et al.*, 2005a). Furthermore, the rise in mitochondrial Ca^{2+} stimulates ATP transport into the β-cell cytosol, raising the cytosolic ATP/ADP ratio (Maechler *et al.*, 2006). Approximately 98% of β-cell ATP is produced from mitochondrial oxidative metabolism (Erecinska *et al.*, 1992) and production of mitochondrial ATP is linked to regulation of insulin secretion by regulation of the ATP sensitive channel (Ashcroft, 1999; Smith *et al.*, 2007).

The insulin secretion signals are coupled with glucose metabolism in two ways. Firstly, there is the glucose induced closure of the potassium ATP (K_{ATP}) sensitive channels which increases the Ca^{2+} concentration of β -cells and triggers insulin secretion. This is the K_{ATP} channel dependent pathway which is directly linked with glucose mitochondrial metabolism and generates ATP. Secondly there is a K_{ATP} channel independent pathway thought to have an activation role for the K_{ATP} channel dependent pathway which is explained by a different hypothesis (Straub and Sharp, 2002; Doyle and Egan, 2003).

1.2.4.3 Long chain acyl coA (LC-CoA) & NADPH

Insulin secretion stimulated by glucose is correlated with increase cytosolic citrate concentration (LC-coA) which has been suggested to contribute effectively in signal modulation of insulin secretion. Part of the glucose is metabolized to citrate, which is converted to malonyl-CoA out of mitochondria and leads to inhibition of fatty acid oxidation by palmitoyltransferase1 (CPT1) and subsequently increasing cytosolic LC-CoA which initiates glucose stimulated insulin secretion (Prentki *et al.*, 1992). However, LC-CoA may be converted to diacylglycerol (DAG) and other molecules are presumed responsible for release of insulin via increases in the intracellular Ca^{2+} concentration (Konrad *et al.*, 1994; Thams and Capito, 1997).

Glucose metabolism may produce another potential mitochondrial signal molecule, NADPH that is linked with insulin secretagogues. Inhibition of NADPH synthesis reduces glucose stimulated insulin secretion (GSIS), confirming a link between GSIS and the NADP/NADPH ratios (Hedeskov *et al.*, 1987; Panten and Rustenbeck, 2008). NADPH has recently been linked with the recycle of pyruvate across the inner membrane of mitochondria (Figure 1.3) (Reinbothe *et al.*, 2009). The key pathway of pyruvate reuse and increased NADPH is the pyruvate –malate shuttle and includes producing oxaloacetate (OAA) from pyruvate using pyruvate carboxylase in TCA (Kaneto *et al.*, 2008). The OAA can be converted either to malate which can participate in numerous pathways like malate – aspartic transporter into mitochondria and the pyruvate – malate transporter from mitochondria to cytoplasm (MacDonald *et al.*, 2005a).

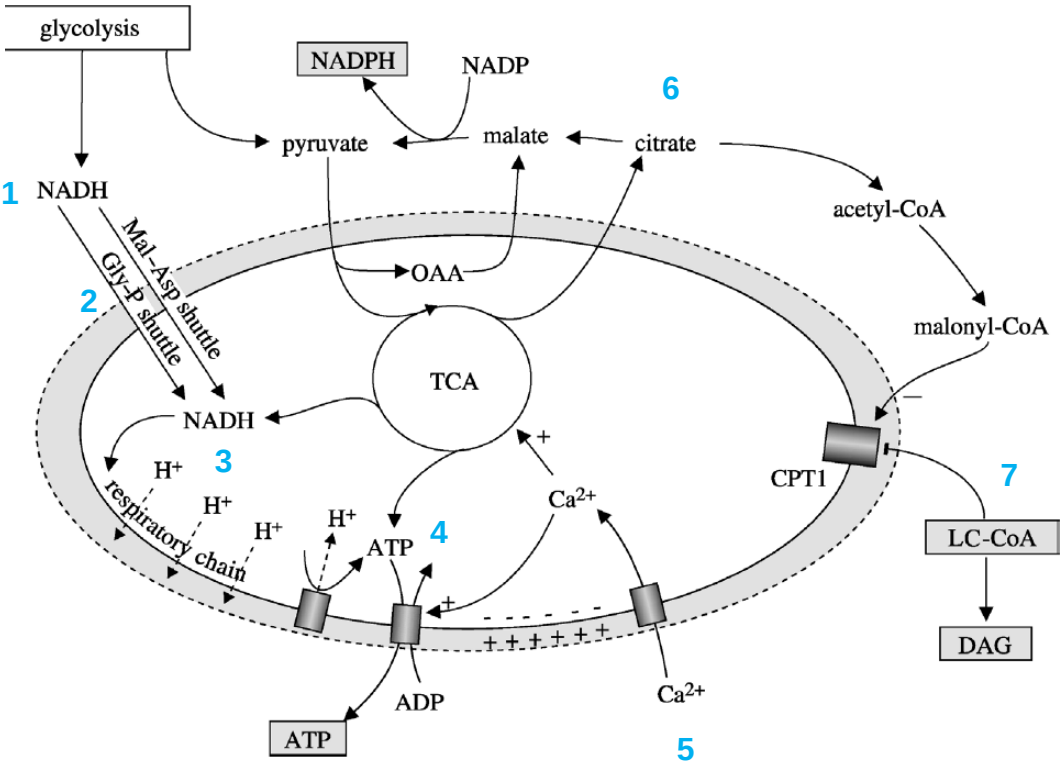

Figure 1.3: Mitochondrial glucose metabolism of β-cells and signalling contributing to insulin secretion. [1] NADH produced by glycolysis can be [2] transported into TCA cycle cross the inner membrane of mitochondria via malate–aspartate (Mal–Asp) and glycerol–phosphate (Gly–P) transporters. [3]Generation changes of H gradient in action potential of the inner membrane, [4]enhances ATP production. [5]Mitochondria inner membrane hyperpolarisation enhances drive in of Ca^{2+} and stimulates export of ATP. [6]Production acetyl-CoA and then malonyl-CoA results from citrate exported be TCA, [7]malonyl-CoA closes the LC-CoA transporters and increase in cytosolic LC-CoA and potentially causes diacylglycerol (DAG) accumulation, adapted from MacDonald *et al* (2005a).

1.2.5 Functional alterations of β-cell mediating glucose metabolism

During insulin exocytosis, β-cells undergo physiological and metabolic alteration to produce signals regulating insulin synthesis, some of which are electrical alterations involving ion channel modulation and dynamic changes of β-cells organelles (Straub and Sharp, 2002; MacDonald *et al.*, 2005b). Amongst these alterations is mediated insulin exocytosis:-

1.2.5.1 Cell membrane electro-activity

Glucose metabolism is linked tightly with insulin secretion and mediated by electrical excitability in β-cells (Pittman *et al.*, 2004). It is characterized as a mechanical coupling of glucose metabolism involving a large number of ion channels, pumps and transporters, contributing to the intracellular Ca^{2+} concentration and or other ions concentrations to form membrane potentials of (VM) -70 mV at glucose concentration between 3-5 mM. Glucose stimulates regulating membrane depolarization of β-cells by reducing the resting K^{+} concentration and initiates an electrical activity, characterized by slow wave depolarization affecting the potential factors that control opening and closing channels and regulating ion movement from and to the β-cell (Dufer *et al.*, 2007; Lim *et al.*, 2009). The β-cell membrane potentials opening and shutting K_{ATP} channels lead to changes in cell membrane polarization. This depolarization initiates action of other potential factors increasing extracellular Ca^{2+} influx via voltage –dependent Ca^{2+} channels (VDCC) leading to exocytosis of insulin, opening of voltage –dependent K^{+} channels, and terminating membrane depolarization which reduces Ca^{2+} influx and consequently insulin secretion (Gray *et al.*, 2006; Li and Zhang, 2009).

1.2.5.2 K_{ATP} sensitive channels

Ion channels are pores in amongst macromolecules in cell membranes, e.g. transporting potassium ions K^+ into the cell by passive transport, the potassium channels are the most diverse sub-group amongst ion channels existing in excitable and non - excitable cells (Mannhold, 2004). One of the more important channels in β-cells is the K_{ATP} sensitive potassium channel which is a member of the inward rectifier family, identified in different tissues including muscle cells and pancreatic β-cell and various neurons (Mannhold, 2004; Kornreich, 2007). The K_{ATP} channels are regulated by cell metabolism and provide an electrical activity to cells. In the case of the pancreatic β-cell, the channel K_{ATP} is considered one of the insulin secretion modulators (Straub and Sharp, 2002).

K_{ATP} channels are octomeric complexes composed of two different protein subunits in β-cells, there are four pore forming K^+ inward rectifier channel subunits (kir6) (passes positive charge into the cell) encoded by two different genes (Kir6.1 and 2) and two trans-membrane segments M1 and M2. Furthermore, the K_{ATP} channels have four regulatory sulfonylurea receptor subunits (SUR1) one of the ATP-binding cassette family with a total of 17 trans-membrane sectors and two cytoplasmic nucleotide binding domains (NBD) (Wheeler *et al.*, 2008; Amin *et al.*, 2010) (Figure 1.4). Glucose and ATP are considered to be implicated in the initiation of β-cell depolarization. It is clearly demonstrated that ATP or ATP-Mg^{2+} inhibit the K^+ channels activity at the Kir6.2 subunit in which the depolarization is associated. Induction of depolarization increasing Ca^{2+} influx and subsequently insulin secretion (Ashcroft, 1999).

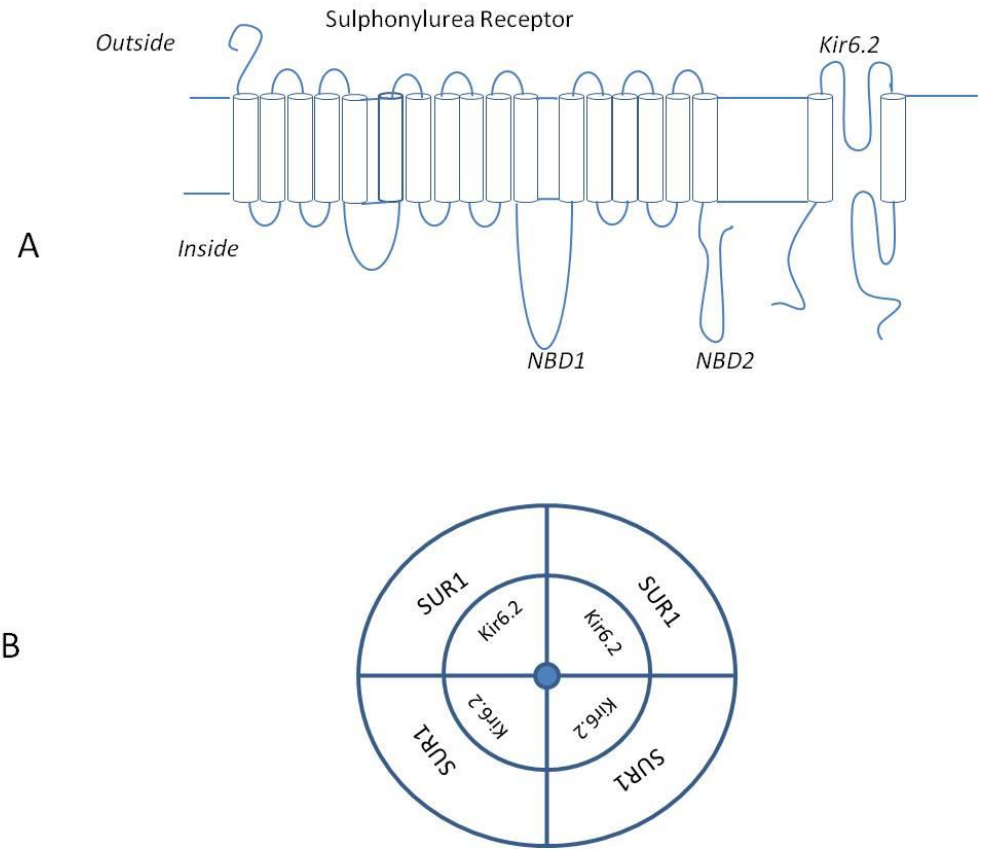

Figure 1.4: Schematic diagram showing the K_{ATP} channel topology of the β-cells which is composed of two protein complexes Kir6.2 and SUR. (A) Made up of two transmembrane Kir6.2 subunits multiple SUR transmembrane domains and a nucleotide binding domain (NBD). (B) The Optometric K_{ATP} channel complex with 4 subunits of each Kir6.2 and SUR, adapted from Mannhold (2004).

Alternative studies suggest that ATP inhibits the K_{ATP} by binding with the nucleotide binding domains NBDs (Figure 1.4) that stimulate insulin secretion even if glucose is absent. From this view point many anti-diabetic drugs have been devised to inhibit the K channels e.g. sulfonylurea compounds, and others enhance release of insulin by direct interaction with SUR1 e.g. tolbutamide and glibenclamide which are K_{ATP} inhibitors and increase the intracellular Ca^{2+} and thus insulin secretion (Ashcroft, 2000; Ashcroft and Gribble, 2000).

1.2.5.3 Voltage –dependent calcium channels (VDCCs)

The insulin secretion is coupled with increasing of intracellular Ca^{2+} concentration, which is carried by voltage –gate channels in the plasma membrane (Li and Zhang, 2009). The regulation of Ca^{2+} channels is depended on the membrane electro - activity that results from opening and closing K_{ATP} channels. At the membrane potential of -80mV, K_{ATP} channels are closed in non-stimulated β-cells (Karnieli and Armoni, 2008). However, when the Ca^{2+} channels are stimulated this leads to depolarization of the β-cell and opening of particular Ca^{2+} channels that are totally dependent on electrical activation of the β-cell and hence are known as VDCCs (Satin *et al.*, 1995; Bhattacharjee *et al.*, 1997). Ca^{2+} ions could also be released from the intracellular store in β-cells in addition to the influx of Ca^{2+} that results from depolarization and the latter may contribute in releasing the intracellular Ca^{2+} by a mechanism called Ca^{2+} – induced Ca^{2+} release (Graves and Hinkle, 2003) and prolong insulin secretion and increase insulin secretion via protein kinase C (PKC) activation. Many physiological events may increase the intracellular Ca^{2+} concentration such as accumulation of LC-CoAs that are stimulated by fatty acid palmitate and redox regulation of the Ca^{2+} channels (Fridlyand *et al.*, 2003).

1.2.5.4 Insulin granule dynamics and exocytosis

Insulin secretion, predominantly stimulated by glucose metabolism, electrical activity in β-cells and VDDC activation increases Ca^{2+} concentration and thus convey the insulin granule to exocytosis sites leading to the release of mature insulin into the blood stream (Misler *et al.*, 2009). Furthermore, insulin granules are secretory vesicles which require various functional pools (Seino *et al.*, 2009). Generally insulin granules are produced as two pool types; a docked and reserve pool. However, the docked pools are present in different functional stages based on the competency to secrete. Some are primed pools that are divided into two groups (i) immediately releasable pool (IRP) and (ii) readily releasable pool (RRP) (Gerber and Sudhof, 2002; Hou *et al.*, 2009) (Figure 1.5). The initial phase of exocytotic response can be amplified by increasing intracellular Ca^{2+} leading to insulin exocytosis from docked vesicles. The second phase is depolarization, in which vesicle mobilization fuels secretagogues. Signals generated by glucose metabolism are essential for encouraging mobilization, priming insulin granules from reserve pools and amplifying and maintaining insulin secretion (Straub and Sharp, 2002; MacDonald *et al.*, 2005b).

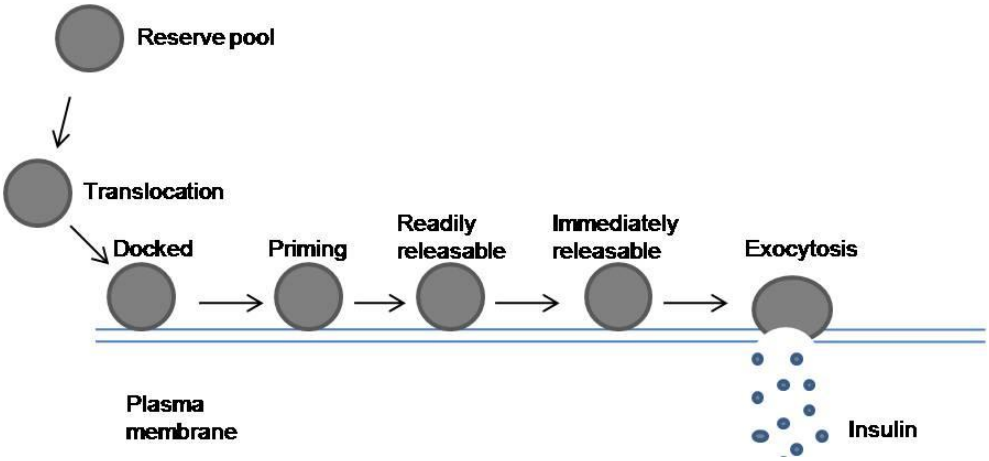

Figure 1.5: Schematic diagram of β-cell granule pools. Insulin granules exocytosis starts from reverse pool to exocytosis and insulin secretion. The process includes granules translocation from reverse site to docking, priming to releasable stage (ready and immediate) and exocytosis, adapted from Straub and Sharp (2002).

1.2.5.5 Mobilization of insulin granules and exocytosis of insulin

Insulin granules undergo enormous mobilization within the β-cells mediating the insulin secretion process by moving the granules to the cell membrane for pre-secretion perpetration (Bruns and Jahn, 2002). It is thought glucose stimulation increases the number of insulin granules connected to the plasma membrane by stimulating insulin granules movement, in addition to ATP and agents that raise the cellular cAMP (Rorsman and Renstrom, 2003; Seino *et al.*, 2009). The movement of the cytoplasmic vesicles is likely to occur along microtubules achieved by ATP-utilizing motor protein of the classical motor proteins found in various eukaryotic cells (Semiz *et al.*, 2003).

The mechanism of insulin exocytosis has been studied extensively Insulin exocytosis is mediated by merging of insulin vesicles with the plasma membrane due to a soluble N-ethylmaleimide-sensitive factor (NSF) coupled with attachment protein receptor (SNARE) proteins (Hou *et al.*, 2009). Amongst these proteins is a membrane protein named synaptosomal –associated protein25 (SNAP-25) which facilitates a specific membrane fusion by forming a complex bringing insulin vesicle to the vesicles associated membrane protein (VAMP) and plasma membrane together (Vikman *et al.*, 2009; Wang and Thurmond, 2009). These synaptotagmin components are thought to be Ca^{2+} sensors for exocytosis and SNARE proteins have various ways of interacting with VDCC that mediate a strong coupling with Ca^{2+} entry events and exocytosis of vesicles (Misler *et al.*, 2009).

The first motivation of docked insulin granules exocytosis prior to Ca^{2+} is triggered by ATP-dependent chemical modification from ready to release granules in which the competent granules are submitted for insulin release stage. Furthermore, Renstrorm *et al.,* (2002) suggested acidification results

from ATPase activity which also contributes to granule priming. The ATP /ADP ratio undergoes changes and modulates the size of the readily releasable pool (RRP) which is chemically stimulated for release by accelerating vesicle processing steps between docking, membrane fusion and granule ready for release and eventually exocytosis (MacDonald *et al.*, 2005b).

1.2.6 Insulin gene structure and regulation

Insulin plays a crucial major role in maintaining glucose levels in mammals and other organisms. Insulin is encoded by a gene located on chromosome 11 p15.5 in humans (Ohneda *et al.*, 2000; Hay and Docherty, 2006), but rat and mice have two non-allelic insulin genes (Soares *et al.*, 1985).

Structurally the human insulin gene is composed of three exons and two introns. The upstream 400 bp 5' flanking sequence has been targeted by studies to understand insulin gene expression and regulation as it contains the insulin gene promoter and the binding sites for proteins contributing to insulin transcription such as transcription factors, DNA structural protein and RNA polymerase complex (Steiner *et al.*, 1985; Ohneda *et al.*, 2000). The linear structure of the human insulin gene promoter shows three major DNA elements A3, E1 and C1 which contribute to the glucose responsive insulin transcription pathway and shows homology to the insulin promoters in other mammals (Hay and Docherty, 2006).

Glucose is the main modulator for regulating insulin biosynthesis gene expression and insulin secretion. Furthermore, glucose controls insulin mRNA stability and splicing actions via three main transcription factors (PDX-1, Beta2/NeuroD1 and MafA) regulated by signals produced from glucose metabolism (Evans-Molina *et al.*, 2007; Andrali *et al.*, 2008).

1.2.6.1 Transcription factors

Glucose metabolism in β-cells generates a discrete signal or signals that are widespread within different cell types. However, major signals that are affecting insulin secretion such as glucose metabolism signals and intracellular Ca^{2+}, can regulate insulin gene transcription, via various types of transcription factor (Docherty and Clark, 1994; Leibiger *et al.*, 2002). There are three major transcription factors that can regulate insulin gene expression in relation to the glucose metabolism:-

Pancreatic duodenal homeobox (PDX-1)

Transcription factor PDX-1 is the most important insulin transcriptional factor expressed in β-cells and is a key regulator of differentiation and development of the pancreatic progenitor cells into β-cells (Wilson *et al.*, 2003; Cerf *et al.*, 2005). PDX-1 belongs to the Para HOX gene group existing prior to the major Hox cluster of homeodomain protein that is expressed in different tissue (Keller *et al.*, 2007). The structural feature of PDX-1 is a highly conserved homeodomain with α helix domain type helix –trans-helix motif at amino acid 61. Another helix, representing the DNA –binding domain onto a N-terminal conserved sequence for transactivation lies at residues 32-38 and 60-73, PDX-1 binding occurs at region A1 at -83/-75 bp from the insulin gene promoter and second binding sequences occur on A3 at -216/-207 bp. These are critical sites for the control of transcription by PDX-1 (Le Lay and Stein, 2006) (Figure 1.6).

PDX-1 is glucose responsive, regulating insulin gene expression in differentiated β-cells. In addition, secondary activation can be achieved by the transcription factors NeuroD1, Hnf-1 and Hnf-3B. Moreover, PDX-1 regulates transcription of the insulin gene in β-cells, and somatostatin in α pancreatic

cells, together with transcription factors Nkx6.1, GT-2, and GK (Watada *et al.*, 1996). There is a strong correlation between insulin gene transcription by PDX-1 and glucose metabolism (Shushan *et al.*, 1999) via a pathway involved with phosphatidylinositol 3-kinase which stimulates PDX-1 translocation from the cytoplasm into the nucleus (Buteau *et al.*, 1999). Recent studies have shown PDX-1, GK, and pre-pro-insulin gene expression, is increased after inhibiting GSIS by inactivating insulin like growth factor receptor suggesting a regulatory role of insulin receptor for insulin gene expression and insulin secretion via regulation PDX-1 factors (Cerf *et al.*, 2005). Furthermore, PDX-1 regulates GT-2 gene expression suggesting a vital role for PDX-1 in glucose uptake and insulin sensitivity and may contribute to the development of type 2 diabetes (Walker, 2004).

Neurogenic differentiation 1 (Neurd1/Beta2)

Neurd1 is an element of the NeuroD family of basic helix –loop –helix (bHLH) transcription factors which can be split into three groups according to their DNA binding properties (Naya *et al*., 1995). Class A members bind to the DNA via heterodimers or homodimer and are ubiquitously expressed; group B NeuroD1protein forms heterodimers with bHLH proteins and is involved in controlling insulin gene expression (Naya *et al.*, 1995; Poulin *et al.*, 1997). NeuroD1 activates transcription after binding to the sequence E element on the insulin gene and is a protein encoded in β-cells, through which mutations can cause a special type of diabetes called maturity onset diabetes of the young MODY6 in humans and contributes to diabetes type I and type II diabetes mellitus (Gu *et al.*, 2010).

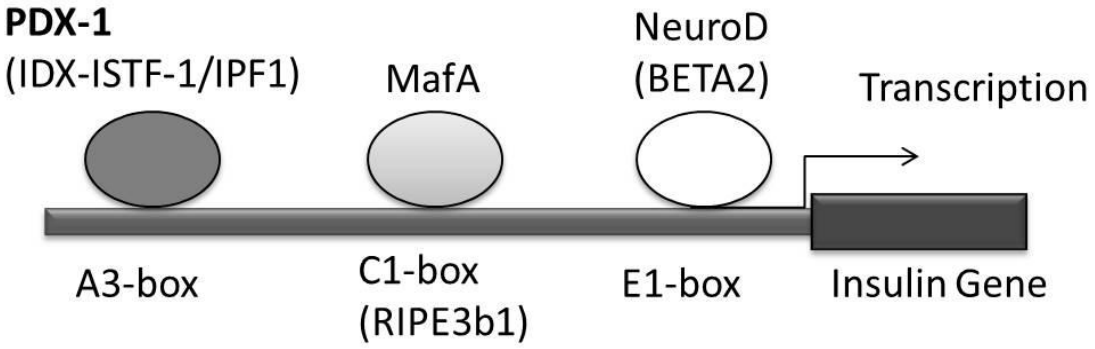

Figure 1.6: Schematic model illustrating insulin gene promoter and transcription factors PDX-1, MafA and NeuroD with transcription factors binding boxes A3, C1 and E1, adapted from Kaneto *et al* (2005).

Musculoaponeurotic fibrosarcoma homolog A (MafA)

Maf is a member of the leucine zipper family of transcription factors and is divided into groups depending on their molecular size (large and small maf). MafA has been identified as a large maf member and is an important factor in eye lens development (Olbrot *et al.*, 2002). Whereas, MafB is linked to expression of the hormone glucagon in pancreatic α-cells. MafA was initially detected in β-cells as a third regulatory element in β-cell differentiation, but is also known now to be involved in activation of transcription of the insulin gene linked with glucose metabolism (Kaneto *et al.*, 2008).

The insulin genes of various species such as human, mouse and rat contain a conserved Maf recognition element (MARE) in their promoters. MARE sequences overlap with the RIPE3b1 element (Maf), the third regulatory element, which has been shown to play a critical role in insulin gene expression and glucose-regulated expression (Kataoka *et al.*, 2004). Zhang *et al* (2005) reported “MafA deficient mice display intolerance to glucose and develop diabetes mellitus”. Moreover, insulin production stimulated by factors such as glucose, arginine and KCl was affected by MafA deficiency in addition to inhibition of insulin 1,2 and PDX-1, Beta2 and GT-2 expression. However, it has been shown recently that MafA contributing to -insulin production appears not to be mediated by other islet-enriched transcription factors such as PDX-1 , Nkx2.2, Pax4 and Isl1 (Artner *et al.*, 2008).

1.2.7 Pathogenesis of diabetes mellitus

Diabetes mellitus is a disease related to increase in the blood glucose level greater than 126 mg /d1 has characterizing hyperglycemia, however the reasons for this occurring is related to different genetic and environmental factors and can result in physiological complications. Aetiologically, forms of diabetes are classified according to the causative factors which are genetic, environmental and metabolic factors disrupting the maintenance of the normal glucose level. Amongst diabetes mellitus forms:-

I. T1D accounts for approximately 10 % of all diabetes mellitus in the western world effecting children (3-11 years) and some adults before the age of 30 years (McCance and Huether, 2002). Some studies compare the incidence and prevalence of T1D in particular countries such as Finland compared with the low occurrence in countries such as Japan. It is thought that T1D results from the interaction between environmental factors such as drugs, chemicals, nutritional intake and viral infection, leading to β-cell death and genetic factors (Genetic disorders of HLA genes) (Notkins and Lernmark, 2001). This interaction mediates autoimmune responses against one or more β-cell autoantigens such as GAD65, and IAA producing autoimmune destruction by autoantibodies or migration of cytotoxic T-cells to the pancreas (Docherty *et al*., 2010). Thus, many researchers suggest that T1D to be results from overlapping between environmental factors and genetic factors in susceptible individuals (Biros *et al*., 2005).

II. T2D is much more common than T1D, affecting about 25 % of the world's population. In the USA about 8.3 % of the population have T2D (CDCP, 2011) accounting for 90% of diabetes cases. However, in some countries like those in the Middle East susceptibility to T2D can reach up to 29 %

(Harati *et al.*, 2009). T2D results from a combination of three different factors; insulin resistance, excessive blood glucose, and progressive insulin deficiency (Kazlauskaite and Fogelfeld, 2003). Insulin resistance results from obesity and presents in 60% to 80% of T2D individuals. When insulin resistance occurs, a higher level of insulin secretion is required to maintain its biological activity. Insulin deficiency occurs when the amount of insulin producing by β-cells into the bloodstream decreases (Williams and Pickup, 2004). Hepatic glucose production can occur in which the glucagon hormone secreted from pancreatic alpha-cells, stimulates the glycogenolysis and gluconeogenesis leading to abnormal glucose production by tissues such as the liver and muscles, which raises the blood glucose level (CDCP, 2011). The genetics of this disease is still not understood.

III. Gestational Diabetes Mellitus (GDM) is a type of diabetes that affects women during pregnancy causing high levels of glucose in the blood. The prevalence of GDM is reported as 2%- 5% in England and Wales and has been increasing in recent years. It is estimated that gestational diabetes may affect up to 14 in every 100 pregnant women (Buchanan and Xiang, 2005; Chu *et al.*, 2012). Most diabetic women giving birth in England and Wales have gestational diabetes, but some have type 1 or type 2 diabetes. However, during pregnancy, some women have slightly higher than normal levels of glucose in their blood and their body cannot produce enough insulin to transport it all into the cells (Diabetes UK, 2012) and it is also thought to happen when the insulin receptors and cell signalling pathway behind the insulin receptor do not function properly which may be due to pregnancy related factors (Shao *et al.*, 2000).

IV. Maturity onset diabetes of the young (MODY) is a form of diabetes which is different from both Type 1 and Type 2 diabetes, and runs strongly in families (Fajans *et al.*, 2001). MODY is very rare compared with Type 1 and Type 2 diabetes – experts estimate that only 1-2% of people with diabetes causing moderate hyperglycemia (CDCP, 2011). It is caused by a mutation (or change) in a single gene. A mutation in genes such as Glucokinase (Osbak *et al.*, 2009), insulin gene transcription factors (Gu *et al.*, 2010) and hepatocyte nuclear factor 4 alpha (HNF α) (Saif-Ali *et al.*, 2012) have been reported to cause MODY.

V. Neonatal Diabetes Mellitus (NDM) is a form of diabetes that is diagnosed under the age of six months occurring at the rate of only one in 100,000 to 500,000 live births (NDIC, 2012). Neonatal diabetes is very rare, currently there are less than 100 babies diagnosed with it in the UK (Diabetes UK, 2012). It's a different type of diabetes than the more common Type 1 diabetes as it's not an autoimmune condition (where the body has destroyed its insulin producing cells) (McCance and Huether, 2002). Neonatal diabetes is caused by a change in a gene of the GSIS which affects insulin production or the number of β-cells (Aguilar-Bryan and Bryan, 2008).

Some other forms of diabetes have been reported to be new types of the disease, however some of them either do not have a clear pathogenesis pathway or their causes not well characterized such as diabetes created by initiating insulin receptor antibody (Dietz *et al*., 1989) or factor contributing early apoptosis of β-cells (McCance and Huether, 2002).

1.2.8 Interaction of microbes with β-cell and insulin pathway

Various hypotheses and mechanisms have been suggested with regards to the role of microorganisms and microbial components in β -cell pathogenesis. This may be by causing direct damage or by remodelling the host immune status and subsequently causing protective or destructive effects to the β –cell. Generally these effects can be classified into three categories:-

Cytotoxicity of Microbial Toxins. Some primary and secondary metabolites are thought to cause β -cell apoptosis or necrosis, and / or modulate the insulin secretion pathway and even interact with downstream regulation of the insulin gene (Hettiarachchi *et al.*, 2006; Virtanen *et al.*, 2008).

Cytolysis by Viral Infections. Pancreatic β-cells cytolysis is produced by several viral infections, notably with the enteroviruses which are thought to play a vital role in the development of diabetes type 1 (Richer and Horwitz, 2009; Stene *et al.*, 2010).

Autoimmunity Damage. These can result from an autoimmune response caused by an initial immune response against microorganisms which presents antigens with molecular mimicry to the host component. This can result in destruction of β-cells, leading to loss of insulin production (Alberti and Zimmet, 1998; Williams and Pickup, 2004) .

1.2.8.1 Cytotoxicity of β-cell by microbial secondary metabolites

With regard to diabetes studies that consider microorganisms as environmental factors being linked to the development of the disease, the traditional concept is that microbial as well as chemical, dietary factors and food may trigger autoimmune responses against β-pancreatic cell (Ju¨rgen Schrezenmeir, 2000; Biros *et al.*, 2005). However, new research in the field of toxicology has

described some dietary toxins which contaminate food and water, such as nitrates, nitrose, methyl mercury, arsenic and persistent organic pollutants. These compounds may contribute to β-cell degeneration and destroy insulin production leading to T1D (Sharp, 2009).

In addition, to these compounds there are a wide range of microbial secondary metabolites which have been shown to cause destruction of β-cells and subsequently diabetes type1 (MacFarlane *et al.*, 2003). The genus *Streptomyces* is a group of soil bacteria classified as aggressive phytopathogenic. These bacteria can infect tuberous vegetables especially potatoes and beet (Myers *et al.*, 2002). *Streptomyces* as a group produce more than 50,000 secondary compounds. Some of these compounds are antibiotics used in medicine and agriculture but some of them such as bafiolomycin, cancanomycin and streptozotocin cause β-cell destruction (Myers *et al*., 2003). Many of these toxins can be found in infected vegetables and fruits, and are found in water (Myers *et al.*, 2003). Therefore, such microbial toxins could reach the human body via contaminated food or infection with toxin–producing microorganisms. Bafilomycin A1 and cancanomycin are vacuolar proton-translocating inhibitors (vATPase) which cause glucose intolerance and pancreatic islet disruption and β-cell damage in mice (Hettiarachchi *et al.*, 2004). This suggests that such compounds should be regarded as possible diabetogenic environmental factors that contaminate the human diet (Myers *et al.*, 2001). Moreover, vATPase inhibitor producing bacteria can cause deep infection, extending 5-10 millimetres into the flesh of vegetables (Myers *et al.*, 2002; Hettiarachchi *et al.*, 2006). Intake of such vegetables may lead to an earlier progression of β-cell insufficiency and insulin deficiency in people at risk of diabetes.

1.2.8.2 Modulation of insulin secretion by microbial toxins

In addition to the cytotoxicity of some microbial toxins to β-cells, some compounds interact specifically with insulin pathway. For example Streptozotocine secondary metabolite produced by *Streptomyces achromogenes* is an aggressive diabetogenic compound used to induce diabetes type 1 in laboratory animal models (Singaram *et al.*, 1979; Baydas *et al.*, 2005). Furthermore, studies have linked the toxicity of Streptozotocine to pancreatic β-cells to nitric oxide that may be liberated from compounds having nitros group in their structure (Turk *et al.*, 1993). Streptozotocine is highly toxic and carcinogenic as it has a glucose pyranoside in its structure, facilitating its uptake by β-cells via its glucose transport (GT-2). The toxicity of streptozotocine is also attributed to its ability to cause DNA alkylation causing inhibition of insulin biosynthesis and secretion by depletion of ATP which is a key regulator of insulin secretion causing serious consequences such as β-cell necrosis and type1 diabetes (Elsner *et al.*, 2000). However, Koulmanda *et al* (2003) have shown an anti-diabetic effect is achieved when using low concentrations of streptozotocine which prevent the diabetogenic autoimmune response progression in NOD mice via neutralizing T lymphocytes cells (T-cells) mediated immune response that results from genetic predisposition factors.

1.2.8.3 Microbial proteins modulating β-cell intracellular cAMP

Toxin proteins produced by some microorganisms cause serious diseases e.g. Cholera toxin produced by *Vibrio cholera,* an 84 kDa protein causing movement of ions from the tissues to the gut lumen by stimulating adenylate cyclase in the intestine and other cell types, like fat cells, liver, leukocytes. In β-cells, adenylate cyclase stimulation increases the intracellular cAMP concentration a key signal molecule enhancing insulin secretion (Wollheim *et al.*, 1974).

Furthermore, increase in intracellular cAMP can also stimulate insulin gene transcription by signals regulated by the cAMP levels (Idevall-Hagren *et al.*, 2010).

A similar effect was also discovered with pertussis toxin, a protein exotoxin produced by *Bordetella pertussis,* a pathogen causing whooping cough. The toxin can bind to a wide spectrum of cell membrane receptors, as well as the G -protein coupled receptor G-PCR that regulates the intracellular signals in many pathways (Carbonetti, 2010). Pertussis toxin can modify the heterotrimeric G complex by catalyzing ADP-ribosylation of the α subunits of G proteins and consequently impeding the G proteins from interacting with its receptor and disrupting the intracellular signal (Burns, 1988). Inhibition of G protein keeps the GDP-bound site inactive and subsequently inhibits adenyl cyclase activity, which increases intracellular cAMP concentration and eventually insulin secretion (Hesketh and Campbell, 1987; Khalaf and Taylor, 1988; Carbonetti, 2010). The pertussis toxin has a regulatory effect on the insulin pathway and could also inhibit tyrosine autophosphorylation of the insulin receptors (Müller-Wieland *et al.*, 1991). This is the key regulator of many signals and functions controlling the insulin secretion pathway and metabolic activities and protein synthesis of the β-cells that is initiated by insulin binding (Hesketh and Campbell, 1987; Peschke, 2008).

1.2.8.4 Microbial secondary metabolites modulating β-cell K_{ATP} channels

Amongst the secondary metabolites produced by microorganisms are the antibiotics that are used as treatments against microbial infections (Doyle and Egan, 2003). Some of these compounds stimulate insulin secretion as a result of inhibiting the pancreatic K_{ATP} channels and depolarization of the cell membrane. For example, the antifungal clotrimazole can cause hypoglycemia in patients after administration (Chan *et al.*, 1997) and sulfonamide drugs such as tolbutamide have been used to treat patients with type II diabetes (Ashcroft, 1999).

It was found that the sulfonamide compounds and other compounds having imidazoline in their structure can inhibit the K_{ATP} channel via binding to the SUR1 receptor and inhibiting cell membrane current, which induces Ca^{2+} uptake via CCVD and hence insulin secretion (Mourtada *et al*., 1997). Quinolone antibiotics have recently been shown to increase insulin secretion via a similar interaction with the SUR1 of K_{ATP} (Maeda *et al*., 1996; Zünkler and Wos, 2003).

1.2.8.5 Direct β –cell damage by viral cytolysis

Recently, several viruses have been shown to infect pancreatic cells particularly the β –cells, and some of them can directly cause β -cell cytolysis e.g. Encephalomyocarditis (EMC) virus induces diabetes (Lammi *et al.*, 2005). Many enteroviruses are reported to cause cytolytic infection of β-cells. Moreover, enterovirus infection is thought to result in a destructive autoimmune response initiated by the viral infection, causing T1D in early childhood (Richer and Horwitz, 2009). Furthermore, human Coxsackie B virus (CBV) can also cause β -cell death and is linked with nitric oxide (NO) production from immune

processing during infection (Hans *et al.*, 2002). The Coxsackie B4 virus (CB4V) infection has been shown to produce tissue damage liberating β–cell autoantigens into the bloodstream and raising the possibility of the antigens to be presented by antigen presenting cells (APC) to auto-reactive T-cells and humoral immune responses, triggering T1D (Horwitz *et al.*, 2002).

1.2.9 Microorganisms contributing to β-cell damage via autoimmunity

1.2.9.1 Autoimmune diseases - genetic and environmental factors

Autoimmune disease is caused by activation of T-cell or B-lymphocytes (B-cell) or both against self-antigens causing damage and dysfunction of the target, which can be either systemic as in the case of Systematic Lupus Erythematosus (SLE) or organ specific as is seen with T1D (Mackay *et al*., 2001; Tanaka *et al*., 2010). Autoimmune responses are attributed to various factors that are classified generally as environmental factors and genetic predisposition, causing humoral and/or T-cell autoimmune response against self-tissue (Leech, 1998; Albert and Inman, 1999).

Several pathological complications are thought to occur, initiating events, leading to breakdown of self-tolerance and pathological immune response in which the autoantigens will be represented as foreign antigens creating autoimmune disease (Chan *et al.*, 1997). Antigens are normally recognized by the major-histocompatibility-complex (MHC) molecules on the surface of an APC, or the infected cells and are able to recognize a broad range of foreign antigens as the recognition process is very flexible. The immune system normally recognizes and ignores the body's own cells and does not normally overreact to non-threatening substances in the environment by a mechanism known as immune tolerance (Pihoker *et al*., 2005). Sometimes the T-cell

receptor can cross-react with autoantigens, however, protection events, preventing autoimmunity is achieved through the negative selection of self-reactive T-cells in the thymus, resulting in their apoptosis (Barkai-Golan and Paster, 2008; Zirbes and Milla, 2009). However, genetic predisposition has been linked extensively with serious immune diseases such as genetic disorders of the MHC genes which can fail in its protection selectivity mechanism and present “self-antigens” as foreign antigens leading to an autoimmune response (Fujinami *et al.*, 2006; Zirbes and Milla, 2009). In addition to genetic factors there are other kinds of autoimmune responses initiated by environmental factors such as food, bacteria and chemicals via molecular mimicry mechanisms. A sequence similarity between infectious agents and human autoantigens (self-proteins) which cross react with T or B lymphocytes, may then induce a pathogenic immune response that leads to tissue damage and disease (Davies, 1997). For example rheumatic fever instigated by group A streptococcal antigens on the M surface protein produces cross-reacting antibody to the human heart tissue (Mackay *et al*., 2001). In addition, to many enteric bacteria like *Klebsiella, Shigella* and *Streptococcus possess* an antigen containing 6 amino acids (GLn, Thr, Asp, Arg, Glu and Asp) which causes a pathogenic reactive of arthritis (Gilliland, 1989). There are a wide range of viruses and bacteria that are linked with autoimmune disease (Goldberg and Krause, 2009) in which the autoimmune response is against the β-cells such as Coxsackie virus, equine herpes virus type 1, homophiles influenza virus, and rota virus VP7 (Judkowski *et al*., 2004).

1.2.9.2 Factors contributing to diabetogenic autoimmune responses

Insulin deficiency disorder is one of the symptoms that shows β-cells decline in diabetes mellitus, a syndrome that includes abnormal accumulation of glucose

in the blood as a result of loss of insulin secretion (Alberti and Zimmet, 1998). There are two main types of diabetes. Type 1diabetes in which and the patients lose β-cells and insulin production and are totally dependent on exogenous insulin hormone administrated as a drug, and diabetes type 2 in which the body's cells no longer respond to the insulin (Notkins and Lernmark, 2001). Both genetic and environmental factors are involved in developing diabetes. From a genetic point of view T1D is associated with risk genes or disorders on human leukocyte antigen (HLA) genes of MHC genes on human chromosome 21, which has been identified as a critically susceptible locus for many human diseases including T1D (Notkins and Lernmark, 2001). The studies done on this region show that genetic disorders of these genes could create a susceptibility to develop T1D and genetic engineering experiments on mice have led to the identification of at least 25 genes that can contribute to autoimmune diabetes (Biros *et al*., 2005). However, genetic disorders of HLA-DQ2 and HLA-DQ8 genes are responsible for 70% of T1D cases amongst newly diagnosed patients (Lernmark, 2011). The genes encode cytokines, antigen co-receptor, antigen signalling cascade, and co-stimulatory molecules involved in the pathway that promotes apoptosis (Docherty *et al*., 2010). Furthermore, T1D has been identified with certain ethnic groups more than others according to genetic criteria (Biros *et al*., 2005). The autoimmune response against β-cells is classified as the main causative reason for T1D, but recently, in addition to genetic susceptibility and autoimmunity, the destruction of pancreatic beta cells (β-cells) and consequent development of T1D has also been linked with exposure to environmental factors, which may contribute up to 50% of the risk of developing this type of diabetes (Hans *et al*., 2002). Studies on genetic similarity of populations living in different conditions strongly suggested the

importance of environmental triggers of T1D and the most important factors that are thought to be T1D inducers are infection (e.g. viral infection), diet (i.e. the early presence or lack of particular food during childhood), and some inorganic compounds (e.g. arsenate) ions (Peng and Hagopian, 2006; Richer and Horwitz, 2009). New theories about overlapping between genetic predisposition and environmental factors in developing T1D hypothesize that T1D is a genetic disorder occurring on the HLA genes at positions 0501-0201 and 0301-0302 contributing an autoimmune response against particular β-cell antigens such as islet antigens (IAA) and glutamic acid decarboxylase (GAD). However, the autoimmune response can be triggered by virus, diet, bacteria, toxins and vaccines, in addition to accelerators promoting immune response and subsequently T1D (Lernmark, 2011) (Figure 1.7).

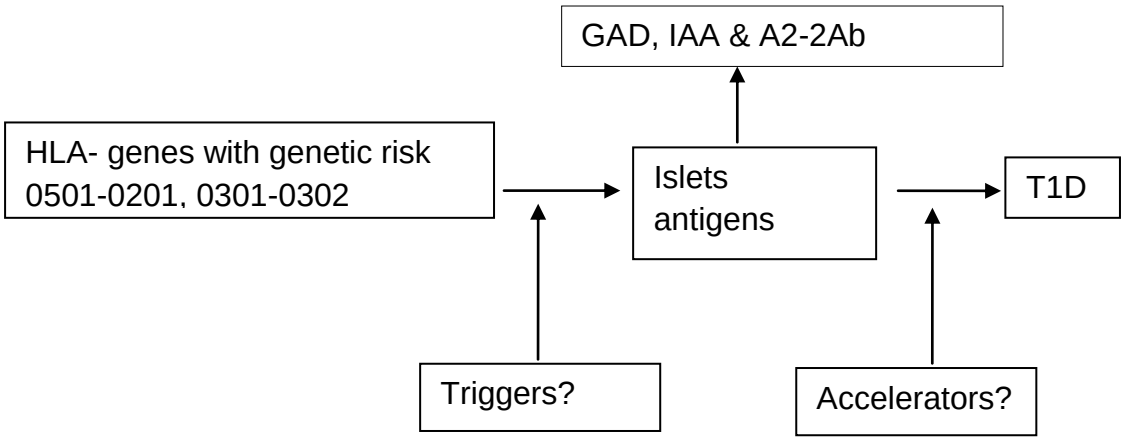

Figure 1.7: Schematic diagram illustrating the interaction between genetic predisposition of HLA gene and environmental factors (microbial infection, chemicals, food) in T1D, adapted from Lernmark (2011).

1.2.9.3 Microbial infection as environmental factors in T1D

Exposure to microorganisms appears to be one of the most important environmental factors and may contribute via different mechanisms to the development of T1D. Microbial antigens can potentially initiate auto-reactivity through molecular mimicry polyclonal activation or the release of previously sequestered antigens (Zhao *et al.*, 1998). For example, in diabetes peptides derived from the β-cell antigen Glutamic acid decarboxylase (GAD) share mimicry with peptides from Coxsackie virus P2-C protein and during infection the latter activates lymphocytes to the infection and produces autoantibodies that persist even after eradication of the infectious agents (Kukreja and Maclaren, 2000). Polyclonal activation of autoreactive lymphocytes by microbial infection can also cause increase incidence of the autoimmune disease in rodents exposed to microbial pathogens and microbes that kill cells can cause inflammation and release of sequestered antigens for autoimmunity (Mackay *et al.*, 2001).

Furthermore, several experimental studies performed on non-obese diabetic (NOD) mice (Type 1 diabetes model mouse) suggest an alternative way to present the microbial antigens is through the gut immune system and subsequently creates an immune response against β-cells (Vaarala, 2000), in addition to stimulating the β-cell autoimmunity on the basis of molecular mimicry by enterovirus infection (Stene *et al.*, 2010), some studies have demonstrated that the viral infection also could change the gut permeability and cause alterations in the mucosal immunity of dietary proteins, therefore, enteroviral infection and utilization of food with microbial contaminates might draw a link between the gut immune system and the pathogenesis of the auto immune T1D (MacFarlane *et al.*, 2003; Williams and Pickup, 2004).

1.2.9.4 Molecular mimicry theory of epitopes

The basic principles of β -cell immunological destruction initiated by microbial components has been built on the molecular mimicry concept of the similarity in amino acid sequences between microbial proteins and β-cell autoantigens. Molecular mimicry (epitope mimicry) is a widely adopted term for this mechanism which induces autoimmune disease (Fujinami *et al.*, 2006).

The theory of a mimicry mechanism in β-cell destruction may be due to an infectious agent having similar component amino acid sequences which may be as little as 10-20 or even less amino acids able to stimulate activity of (T-cell + cluster of differentiation CD4 or CD8) to produce specific antibody against the β-cell as well as the infection agent (MacFarlane *et al.*, 2003).

The role of epitopes in the development T1D has been demonstrated between GAD and tyrosine phosphatase with Coxsackie virus proteins by inducing T-cell against β-cell autoantigens. The cross reactivity between β-cell autoantigens and unknown microbial epitopes are thought to be widely involved in the development of T1D in experimental NOD mice. Table 1.1 shows microbial epitopes that have a possible role as T-cell ligands involved in the activation of diabetogenic T-cells similar to that occurring in diabetes type 1 (Judkowski *et al*., 2004). Children recently diagnosed with T1D may have autoantibody to a 17 amino acid domain of bovine serum albumin of cow's milk which can then initiate a destructive autoimmune response against β-cells through molecular mimicry with islet antigens (Alberti and Zimmet, 1998) .

Table 1.1: The Cross reactivity between β-cell autoantigens and microbial epitopes (Judkowski *et al*., 2004)

Microorganisms	**Protein**	**Sequence**
Bacterial		
Pseudomonas species	Ferrodoxin reductase component	Ac-L G V P M W V K M D-NH_2
Escherichia coli K-12	Bifunctional penicillin binding protein1C	Ac-G D Q PL W L R M D-NH_2
Burkholderia sp. Strain RP007	Hydratase/aldolase PhnE	Ac-L G V P M W S R M E-NH_2
Neissieria meningitidis	Putative phage viron protein	Ac-L V H P V W G R M H-NH_2
Methanotroph species	Methane monooxygenase α-subunit	Ac- T I G P LW K G M K-NH_2
Synechocystis species	Exopolyphosphatase gb	Ac-L S L P I W P E M E-NH_2
Methanotroph speices	Methane monooxygenase α-subunit	Ac-A I G P L W K G M K-NH_2
Alcaligenes faecalis	Phenanthrene degradative gene cluster	Ac-V G R P M W L A M D-NH_2
Synechocystis sp .PCC6803	Polyphosphate kinase	Ac-K V P P L W I L M L-NH_2
Campylobacter jejuni	Lipopolysaccharide biosynthesis protein wlak	Ac-E T R P L W K A M H-NH_2
Acinetobacter species	Terminal alkane hydroxylase	Ac-M I P P L W K F M M-NH_2
Herpetosiphon aurantiacus	Methyl transferase	Ac-A I Q P A W V I M E-NH_2
Mycobacterium tuberculosis	Hypothetical protein Rv0235c	Ac-S F V P L W A T M L-NH_2
Mycobacterium tuberculosis	Hypothetical protein Rv3629c	Ac-R M S P F W Q R M F-NH_2
Streptomyces coelicolor A3(2)	Anthranilate synthase	Ac-S L A P F W L R M Q-NH_2
Bacillus firmus	msyB gene	Ac-L F S P F W G R M A-NH_2
Escherichia coli	URF	Ac-L T G P D W L R M G-NH_2
Synechocystis sp.PCC680	Cytochrome c oxidase subunit I	Ac-S A T P N W M R M F-NH_2
Escherichia coli	49 kDa protein	Ac-K T J P H W Y R M I-NH_2
Mycobacterium tuberculosis	Propable oxidoreductase	Ac-K PT P G W Q R M V-NH_2
Viral		
Equine herpes virus type 1	Glycoprotein 14	Ac-K E R P L W N E M V-NH_2
Kaposi's sarcoma- virus	Glycoprotein M	Ac-M P K P L W D A M Q-NH_2
Human herpes simplex virus	Tegument protein	Ac-M T A P S W A R W E-NH_2
Mycobacteriophage 15	Predicated 8.2 kDa protein	Ac-M W L P V W V I M A-NH_2
Reovirus type 1	Sigma-1 protein	Ac-D E H P L W R Q M L-NH_2
Senadi virus	C protein	Ac-A T L P A W I K M P-NH_2
Clover yellow vein virus	Polyprotein	Ac-Y K E P K W F V M E-NH_2
Porcine adenovirus type 3	Hexon protein(virion component ii)	Ac-S M M P Q W S Y M H-NH_2
Human adenovirus type 34	Hexon protein	Ac-SM LP Q W S Y M H-NH_2

1.2.10 Molecular mimicry protein theory

T1D is an autoimmune disease characterized by the specific destruction of β-cells due to circulating autoantibody (Abs) directed against one or more islet–cells autoantigens such as GAD65, insulin (Siljander *et al*., 2009) and islet autoantigens IA-2 (also known as islet Ab512) (Maioli *et al*., 2004). The β-pancreatic cell has many potential autoantigens, however, some of these antigens appear to be targeted specifically in a diabetogenic autoimmune response by the immune system of individuals at risk to T1D, notably GAD65 and insulin (Maclaren, 1993; MacFarlane *et al.*, 2003) (see Table-1.2). It has been hypothesised recently that some microbes possess β-cell antigen isoforms, furthermore, proteins performing a particular function share amino acids sequences homology to some β-cell pancreatic autoantigens which have similar function, for example, GAD from *E. coli* has been suggested to bring about a diabetogenic autoimmune response against human β-cell GAD65 (Mulder, 2005) and heat shock protein-60 (HSP60) in *Pseudomonas aeruginosa* and human HSP60 pancreatic β-cell antigen (Jensen *et al*., 2001). With this is in mind studies have reported a possible link between microbial proteins ingested in contaminated food or from infection and an autoimmune response (Vaarala, 2000; Mshvildadze and Neu, 2010).

Table 1.2: Islet cell autoantigens of insulin dependent diabetes mellitus (Maclaren, 1993; MacFarlane *et al.*, 2003).

Autoantigenes	**Antibody**	**T-cell Responses**
Insulin	+	+
ICA105 (IA-2)	+	?
GAD65/67	+	+
CarboxypeptidaseH	+	+
Periphrin	+	+
HSP60	+	+
P69	+	+
ICA512	+	?
52 KDa Ag	+	+
Gangliosides	+	?
Imogen	?	+

1.2.10.1 Glutamic acid decarboxylase targeting

GAD is an enzyme that catalyses the decarboxylation of glutamate to amino butyric acid (GABA) and CO_2. There are two isoforms of GAD, GAD65 and GAD67 kDa expressed in neurons and β- cells (Notkins and Lernmark, 2001). The GAD in β-cell is anchored in the membrane and both GAD 65 and 67 and insulin are extensively targeted by the immune response in autoimmune T1D amongst others β-cells antigens (Fenalti and Rowley, 2008).

Patients with T1D possess antibodies to multiple islet cell antigens including the GAD65 isoform of GAD. GAD65 autoantibodies are also found in patients with type 2 diabetes (Fenalti and Rowley, 2008). These GADAb positive T2D patients are diagnosed as having latent autoimmune diabetes in adult (LADA) specific epitopes, LADA represents an early stage of T1D (Maioli *et al*., 2004) . T1D may be mediated by T-cell activation, and it is believed that GAD is relevant, since autoantibodies and cell mediated responses to GAD are strongly correlated with the disease progression (Zechel *et al.*, 1998; Fenalti and Rowley, 2008). The protein P2C of Coxsackie enterovirus B4 has a sequence similar to GAD amino acids 247-279 and this virus sequence is associated with cases of acute T1D by induction of immunological cross reactivity with β-pancreatic cell GAD65 (Oldstone, 1998). Furthermore, a new study has demonstrated that protein P2C shares a six amino acid homology (PEVKEK) with the GAD65 protein and T –cell and antibody cross reactivity is with these peptides (Roep *et al.*, 2002; Porte *et al.*, 2003). Mudler (2005) suggested that GAD from *E coli , Streptococcus* and *Lactobacillus* especially, which can be found in raw meat and fish, may trigger T1D when forms of GAD from the bacteria is released by host enzyme and is absorbed in to the blood producing an inflammatory response leading to β-cell destruction.

1.2.10.2 Islet Antigen-2 (IA-2) targeting

IA-2 also known as ICA512, is a group of antigens in the islet cell which can be attacked by antibody leading to β-cell destruction (Damanhouri *et al*., 2005). The major autoantigen involved (106 kDa with 979 amino acids) is a protein tyrosine phosphatase (PTP) an unusual transmembrane protein expressed in neuro and endocrine tissue and it is found in both α & β –pancreatic cells (Stayoussef *et al.*, 2011; Tridgell *et al.*, 2011). The PTP family of enzymes are critical and specific regulators of cellular processes, all PTP possess one or two conserved catalytic domains. The highly conserved active site within each domain contains an essential cysteine residue that functions a transient phosphate acceptor during de-phosphorylation (Bonifacio *et al*., 1998). Phogrin IA-2B, a strongly correlated protein represents another autoantigen in T1D (Notkins and Lernmark, 2001). It carries the same amino acid sequences of IA-2 with substitution in its catalytic domain (Cui *et al*., 1996). Many studies suggest IA-2B may be more strongly expressed in β-cell than IA-2, however, Biros *et al* (2005) explained that IA-2 and IA-2B have many epitopes associated with development of T1D through cross reaction with microbial molecular mimicry or microbial antigens such as cross reactive immune dominant peptides with C-virus, hemophilus influenza virus and rota virus VP7 with IA-2.

1.2.10.3 Insulin - like substances in microbes

Insulin and pro-insulin are major autoantigens in β- cells where preproinsulin is primarily synthesised and expressed as a 110 amino acid precursor from which 86 amino acid yield as proinsulin polypeptide after cleavage of the 24 amino acid core sequences. Upon translocation into the cytoplasm, proinsulin converts to insulin and C-peptide by pheromone convertase cleavage at dibasic residues and later are removed by carboxypeptidase (H) (Narendran *et al*., 2003). Insulin

and insulin-like peptides have been identified in different types of microorganisms. Since the 1980's some studies refer to the presence of Insulin related molecules in monera and protistia with the same features and functions of animal insulin. Furthermore, Insulin-like molecules have been discovered in bacteria such as *E coli* (LeRoith *et al*., 1981). The purified insulin-like material from *E coli* k12 which overlaps elution position of unlabelled and I^{125} labelled procaine insulin was recovered as a peak by gel filtration column (Leroith *et al*., 1985). The insulin-like components purified by HPLC have cross reactivity with insulin antibody and show similar biological functionality to mammalian insulin. Similar studies demonstrated the occurrence of proinsulin and insulin like antigens in extracts of *Cyanobacterium spirulina*, *Saccharomyces cerevisiae*, *Neurospora crassa*, *Aspergillus fumigatus* and some plants by utilizing modified ELISA and western blotting (Collier *et al.*, 1987; Souza and López, 2004).

1.2.10.4 Heat Shock Proteins (HSP)

HSPs are a group of proteins which are expressed when cells are exposed to elevated temperature or other stresses. The function of HSPs is similar in all living organisms from bacteria to human. HSPs are named according to their molecular weight such as HSP60, 70, 90 kDa. Microbial HSP(s) have been associated with some immune diseases (MacFarlane *et al.*, 2003). HSP of β-cell is considered one of the autoantigens that is frequently targeted by antibodies in some patients with autoimmune T1D (Horváth *et al.*, 2002; Abulafia-Lapid *et al.*, 2003). In terms of molecular mimicries *Mycobacterium tuberculosis* HSP65 has an important function in diabetogenses in NOD mice by T-cells responding to the HSP65 antigen and cross reacting with β-cell HSP60 (Elias *et al.*, 1990). The bacterial HSP60 from *Pseudomonas aeruginosa* which is often isolated from cystic fibrosis patients stimulates a humoral response and

cross reacting antibodies to β-cell HSP60 and may cause diabetes type 1 in NOD mice, raising the possibility that HSP60 autoimmunity may be involved in cystic fibrosis related diabetes too (Jensen *et al*., 2001).

1.2.10.5 Insulin receptors on microorganisms

Agglutination and insulin binding studies have suggested the presence of insulin receptors (IR) not only on mammalian and other animal cells but also on a spectrum of microorganisms (Souza and López, 2004). The first finding was with *N. crassa* showing the existence of insulin binding sites with high affinity on the fungal cell surface (Fawell *et al.*, 1988).

The studies performed on *N. crassa* and *Saccharomyces cerevisiae* showed that the receptors included a membrane binding protein and a juxtmembrane domain with auto phosphorylation capacity which occurs on a serine residue in a *S. cerevisiae* and a tyrosine residue in *N. crassa,* suggesting that these receptors could be a tyrosine kinase (Angermayr *et al.*, 2000; Souza and López, 2004). However, the fungal receptor protein has no protein kinase activity against itself or against substrates such as casein histone H2, in spite of the capacity of human insulin to bind with these receptors and enhance production of glucose metabolites including CO_2, ethanol, and glycogen. Consequently, the studies suggest that the receptor mediating-insulin binding induces downstream metabolic pathways (Kole *et al*., 1991).

Other studies have shown the presence of similar receptors on bacterial cells such as *Streptococcus sp* and *Burkholderia sp*. *B. pseudomallei* has a specific and saturable insulin binding capacity of approximately 5000 molecules of insulin (Woods *et al*., 1993; Jeromson *et al*., 1999). Kanai *et al* (1996) speculated that the *B. pseudomallei* insulin receptor is either for phospholipase

or protein tyrosine phosphatase, suggesting a signal transfer system regulated by the insulin receptor (Kole *et al*., 1991).

Interestingly, immunological studies have indicated that the insulin binding structures in *Streptococcus sp* and *Candida spp.* share antigenic epitopes and react with antibodies to insulin and insulin receptors purified from human cells (Dietz *et al*., 1989). This fact could explain the development of autoimmune diabetes after infection on the basis of anti-insulin or insulin receptor autoimmunity being induced by microbial surface components.

1.2.11 T-cells mediated autoimmunity of diabetes type 1

The development of T1D is commonly dependent on the β-cell destruction rate by the autoimmune response (Williams and Pickup, 2004). The autoimmune response in T1D includes both T-cell mediated (Th1) and humoral immune response mediated (Th2). According to this concept, an inflammatory immune response resulting from a microbial infection causes breakdown of the host immune tolerance leading to presentation of self-antigens through MHC class II of the antigen presenting cells to T-cells helper (CD4) which induce B-cell lymphocytes and T-cell and their cytokines products such as Interlekin2 (IL-2) Interferon gamma (INFγ) (MacFarlane *et al.*, 2003) (Figure 1.7)

The immune response targets β-cell antigens and is involved with direct binding of CD8 cytotoxic T-cell to β-cell, the T-cells can cross react specifically with β-cell antigens presented by β-cell MHC I molecules leading to cytotoxic T-cell activation and then kill the β-cell via different mechanisms like (Fas/Fasl) mediated mechanism, secretion of cytotoxic molecules, granzymes and perforin as well as β-cell destruction by pro-inflammatory cytokines mediators (IL1,TNFα,TNFβ,INFγ) and free radicals oxidants O_2 ,H_2O_2 and NO produced by

T-cell (CD4,CD8) and macrophages activated by cytokines which leads to β-cell apoptosis and T1D (Rabinovitch and Suarez-Pinzon, 1998).

The macrophages also present the microbial antigens e.g. virus proteins to CD4 lymphocytes, which turn activate B cells to produce antiviral antibodies in both models macrophages present autoantigens from the virus thus leading to the development of lymphocytes and autoantibody that react with β-cell (Atkinson and Maclaren, 1994).

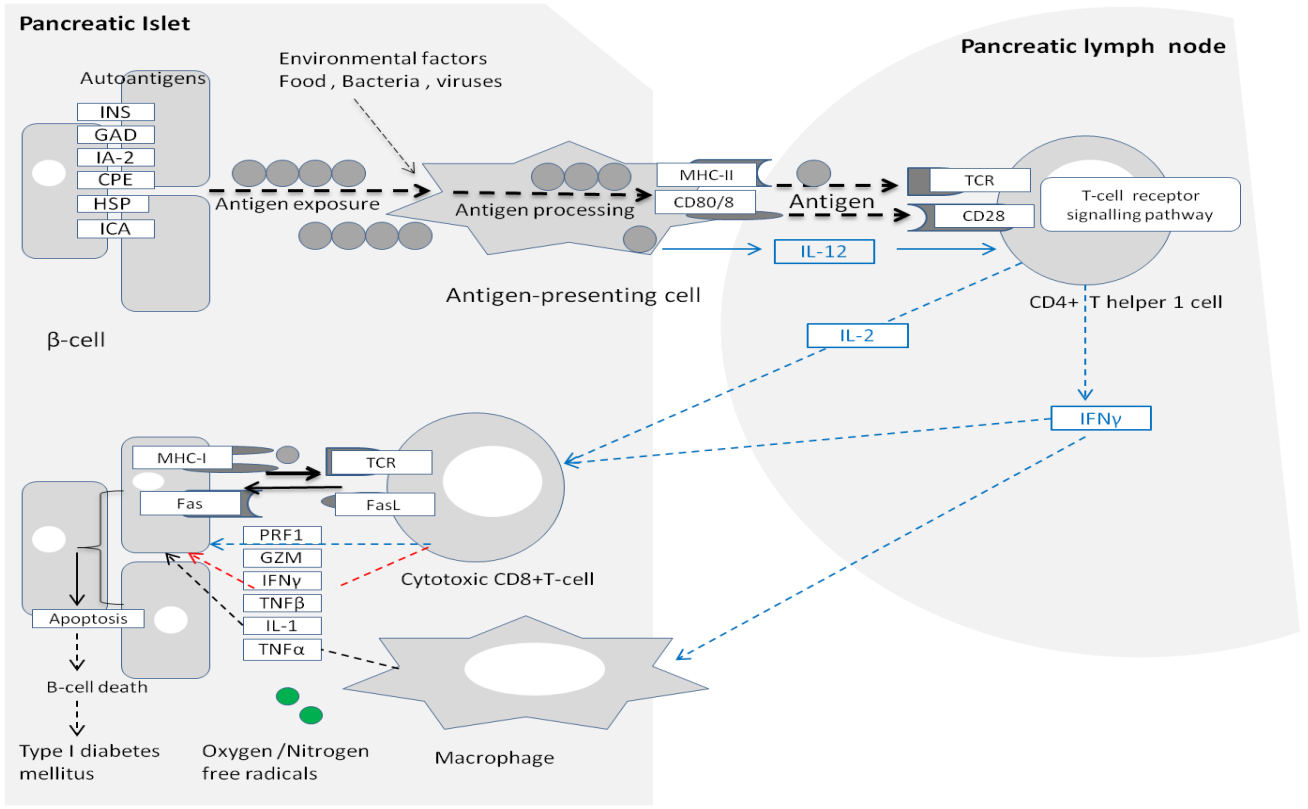

Figure 1.8: T-cell autoimmunity mechanism of diabetes type 1. Environmental factors (food, bacteria and virus antigens) can break the immune tolerance and lead to the pancreatic autoantigens presentation by the APC to the T-cell CD4 or CD8 causing β-cell death via macrophage pathway or cytotoxic T-cell pathway respectively, adapted from Bioinformatics resource centre (2008).

1.3 Cystic Fibrosis and diabetes and infections

Cystic Fibrosis (CF) is an inherited disease with higher incidence in Caucasians compared to other ethnic groups. It results from mutation in the cystic fibrosis transmembrane conductor regulation genes causing dysfunction in halide and pseudohalide transport (Farra *et al.*, 2010). Individuals with cystic fibrosis are diagnosed with many disorders including chronic respiratory infections and pancreatic insufficiency. An important complication associated with CF is diabetes; both type 1 and type 2, usually referred to as CF-related diabetes (CFRD) (Zirbes and Milla, 2009). Pancreatic insufficiency occurs early in life in approximately 85-90% of individuals diagnosed with CF and it is thought that CFRD results from pancreatic fibrosis and fat infiltration (Skretas and Georgiou, 2008). However, the pathogenesis of CFRD is unclear (Hardin *et al.*, 2001; Hadjiliadis *et al.*, 2005).

Burkholderia spp. and the fluorescent group of *Pseudomonas spp*. have emerged in the last two decades as the main opportunistic pathogens in CF and immune-compromised patients (Mc Manus *et al*., 2003; Allice *et al*., 2006). These bacteria are often found to be multi-drug resistant (Kuti *et al*., 2004; LiPuma *et al.*, 2009) and form biofilms (Moskowitz *et al*., 2010) in infected lungs causing acute lung disease with high mortality in CF patients. Moreover, they produce virulence factors that contribute to the pathophysiology of CF, including phenazine, which is produced by both types of organism (Kanthakumar *et al*., 1993; Hwang *et al*., 2002), and pyrrolnitrin, which is produced by a wide range of *Burkholderia* species (Hwang *et al*., 2002).

Furthermore, *Burkholderia* species were formally classified as members of the *Pseudomonas* genus. Some phenotypically and genotypically *Burkholderia*

species of a group called the *Burkholderia cepacia* complex (BCC) which is composed of at least 10 closely related subspecies (Baldwin *et al*., 2005). The term of genomovar had perversely been used to distinguish species in the BCC, These genomovars have been classified recently as species so that genomovar I refers to *Burkholderia cepacia* and *B. multivorans* (formally genomovar II), *B. cenocepacia* (genomovar III), *B. stabilis* (genomovar IV), *B. vietnamiensis* (genomovar V), *B. dolosa* (genomovar VI) *B ambifaria* (genomovar VII), *B. anthina* (genomovar VIII), *B. pyrrocinia* (genomovar IX) and *B. ubonensis* (genomovar X) (Mahenthiralingam *et al*., 2002; Coutinho, 2007). All genomovars have been detected in chronic infection of CF patients and the literature has also showed insulin receptors or insulin binding proteins (IBPs) are presented in *B. cepacia* (Jeromson *et al*., 1999) suggesting possible molecular mimicries with HIR may exist.

1.4 Conclusions

The interaction of insulin hormone and microorganisms can be demonstrated via insulin binding to specific receptors or binding proteins on microbial cell envelopes. These receptors may be members of a signal transduction system such as tyrosine kinase or tyrosine phosphatase or hormone binding proteins. Examples are found in bacteria such as *B. pseudomallei* and *Streptococcus and* the fungus *N. crassa* and yeast such as *S. cerevisiae*.

Microorganisms can interact with insulin producing β-cells causing damage or modify insulin synthesis (transcription and secretion).

Some microbial toxins or secondary metabolites inhibit insulin production because the cytotoxicity of these components to insulin producing β-cell. Examples are the streptozocine antibiotic and macrolide compounds produced by *Streptomyces* and collagenase enzyme produced by *Clostridium histolyticum* bacteria. Other microbial compounds can enhance insulin secretion like cholera toxin and some imidazoline compounds.

Some microbial components (insulin isoform, insulin receptors) as well as some microbial polypeptides can induce an autoimmune response (Humoral or T-cell reactivity) against insulin receptors, insulin or against the major β-cell autoantigens such as GAD, PTP, insulin, and HSP on the basis of molecular mimicry of epitopes (10-20 aa) between those proteins leading diabetogenic autoimmune response (destruction or apoptosis) against β-cell autoantigens or HIR.

1.5 Aims & Objectives

The current study aimed to characterize the interaction between the insulin pathway and microorganisms by:-

I. Studying the effect of secondary metabolites produced by bacterial species which infect CF patients, on pancreatic β-cells and insulin production. In this study, the cytotoxic effects of two bacterial secondary metabolites on the β-cell line, INS-1, were examined. The effects of sub-lethal and cytotoxic concentrations of these compounds on insulin secretion and gene transcription were also investigated.

II. Screening for insulin binding to microbes, in particular *Burkholderia spp*, using insulin peroxidase microcentrifuge tube assay. Any insulin binding proteins recognized will be characterised using a ligand blot assay and their gene(s) cloned and sequence followed by sequence analysis for molecular mimicry between insulin binding protein of microbes and the HIR.

III. Using GAD antiserum to screen for bacterial components that cross react and identify such proteins by mass spectrometry and use the sequences of these microbial proteins to search for epitopes that show molecular mimicry with pancreatic GAD.

Chapter 2
General Materials and Methods

2.1 Reagents and media

Formulation and preparation of laboratory reagents and growth media are shown in (Appendix 1). All laboratory chemicals, unless stated otherwise, were obtained from Sigma-Aldrich (Poole, UK), Stratagene (Wilmington, USA), or Qiagen (West Sussex, UK), Cell culture reagents and plastic-wares were from Lonza (Slough, UK) and Sterilin Limited (Newport, UK). Promega (Southampton, UK), Applied Biosystems (Fisher Biosciences, Warrington, UK). Reagents and equipment requiring sterilization were sterilized by autoclaving (121 °C, 15 min, pressure 15 lbs/in^2), whereas, regents containing heat sensitive compounds were sterilized using filtration through either 0.2 or 0.45 µm filters (Sartorius, Ltd).

2.2 Microbiology

2.2.1 Microorganisms

All microorganisms used in this study were categorized 1 or 2 according to the Advisory Committee on Dangerous Pathogens (ACDP). A total of 45 microbial species were used in this study and are listed in Table 2.1. Microorganisms were obtained from the School of Biomedical and Biological Sciences / University of Plymouth liquid nitrogen culture collection except *Burkholderia cepacia* strains were supplied by Dr. M L. Gilpin. *E coli K12* strains used in gene manipulation experiments in this study are shown in (Table 2.2).

All microorganisms were grown according to the optimum oxygen requirement temperature and incubation time for each species, and used to screening for insulin binding and extracting protein samples for SDS-PAGE, western blotting, dot blotting and mass spectrometry identification. Strains of *E. coli K12* were used for gene manipulation, plasmid maintaining and protein expression.

Table 2.1: Microorganism strains used due this study and some optimum growth conditions.

Bacteria	**O_2 requirement**	**Growth temp °C**	**Growth medium**
Acetobacter aceti 39	Aerobic (Aero)	30	Luria Bertani (LB)
Acinetobacter spp. SDF11742	Aero	37	LB
Aeromonas hydrophila 47	Aero	25	LB
Aeromonas salmonicida CM30	Aero	25	LB
Agrobacterium rhizogenes 15834	Aero	25	LB
Alcaligenes viscosus 45	Aero	25	LB
Bacillus subtilis EMG51	Aero	37	LB
Bacteroides fragilis NCTC 9343	Anaerobic	37	BBE
Brevibacterium linens 99	Aero	25	LB
B. cenocepacia CF	Aero	37	LB
B. cocovenenans	Aero	37	LB
B. multivorans CF	Aero	37	LB
B. thailandensis	Aero	37	LB
Cellulomonase flavigena 53	Aero	30	LB
Chromobacterium violaceum CUQ5	Aero	25	LB
Citrobacter freundii 17B	Aero	37	LB
Clostridium perfringens Type A	Anaerobic	37	LB
Corynebacterium aquaticum 3283	Aero	30	LB
Erwinia carotovora 48	Aero	30	LB
E. coli EMG1	Aero	37	LB
Hafnia alvei UTI	Aero	30	LB
Klebsiella aerogenes 17A	Aero	37	LB
Lactobacillus casei shirota	Microaerophlic	37	LB
Listeria monocytogenes 117	Aero	37	LB
Microbacterium lacticum 36A	Aero	30	LB
Micrococcus luteus 1270	Aero	30	LB
Mycobacterium phlei 52	Aero	37	LB
Nocardia cellulans 61	Aero	25/5days	LB
Ps aeruginosa ATCC 27853	Aero	37	LB
Ps fluorescens 11712	Aero	37	LB
Ps putida 12593	Aero	37	LB
Proteus vulgaris 8	Aero	37	LB
*Rhizobium sp.*97	Aero	30	LB
Rhodococcus equi 120	Aero	30	LB
Salmonella typhimurium TA97A	Aero	37	LB
Sarcina lutea ATCC 9341	Anaerobic	37	LB
Serratia marcescens 410	Aero	37	LB
Staphylococcus aureus S6	Aero	37	LB
Streptococcus pyogenes Group A	Aero	37	LB
Vibrio anguillarum CM19	Aero	30	LB
Yersinia ruckeri RS6	Aero	30	LB
Yeasts			
S. cerevisiae S28	Aero	25	Malt extract
S. carlsbergensis 171	Aero	25	Malt extract
Schizosaccharomyces octosporus 47B	Aero	25	Malt extract
Schizosaccharomyces pombe 188	Aero	25	Malt extract
Zygosaccharomyces rouxii 40	Aero	25	Malt extract

Table 2.2: *E coli* K12 strains used in gene manipulation experiments in this study**.**

Strain	Supplier	Genotype
XL1-Blue MRF´	Stratagene	Δ(*mcrA*)*183* Δ(*mcrCB-hsdSMR-mrr*)*173 endA1 supE44 thi-1recA1 gyrA96 relA1 lac* [F´ *proAB lacI*q*Z*Δ*M15* Tn*10* (Tetr)].
XLOLR	Stratagene	Δ(*mcrA*)*183* Δ(*mcrCB-hsdSMR-mrr*)*173 endA1 thi-1 recA1gyrA96 relA1 lac* [F´ *proAB lacI*q*Z*Δ*M15* Tn*10* (Tetr)] Su–(non-suppressing) λ r (lambda resistant).
JMM109	Promega	endA1, recA1, gyrA96, thi, hsdR17 (rk–, mk+), relA1, supE44, Δ (lac-proAB), [F´ traD36, proAB, laqIqZΔM15].

2.2.2 Laboratory culture and storage of bacteria

All cultures were grown in LB medium (Appendix 1) except *Bacteroides* was grown in Bacteroides Bile Esculin broth (BBE) and yeast strains were grown in malt extract medium. *E. coli* strains that bore plasmids were cultured using LB supplemented with appropriate antibiotic (s). Microorganisms were streaked on agar media to check for purity and subsequently single colonies were used to inoculate broth media. Cultures were incubated overnight unless otherwise stated according to optimum condition and growth time. Volumes of cultures (0.5 ml) were mixed with 0.5 ml of sterile glycerol, cryoprotectant and stored at -20 °C. Agar cultures were stored at 4 °C and sub cultured every 3-4 weeks.

2.3 Mammalian cell culture

2.3.1 Rat insulinoma (INS-1) cells

Insulinoma clone pancreatic beta cells INS-1 (Asfari *et al*., 1992) were kindly gifted from Professor Noel Morgan (Peninsula School of Medicine and Dentistry, University of Plymouth). Cells were (passages 12-35) cultured in RPMI -1640 containing supplements (Appendix 1). The cells were grown as a monolayer and examined by inverted microscope (Olympus CK40, UK) and sub-cultured routinely at 80% confluence by pouring off the depleted medium and washing the cells using Dulbecco's Phosphate-Buffered Saline (DPBS) twice and trypsinized by adding 2-3 ml of trypsin (0.25%) / versene (EDTA 200 mg/ml) for 1 min, the excess trypsin was removed and the cells were gently agitated until detached. Fresh medium 10 ml was used to suspend cells in 75 cm^2 tissue culture flasks by pipetting them thoroughly and carefully to get a homogeneous suspension. A haemocytometer was used for counting cells by loading a few microliters of cell suspension. The maintenance culture was passaged once every 5 days with a seeding density of 2×10^5 cell/ml and the number of cells/ cm^2 needed were determined (Wood *et al.*, 2004). Seeded flasks were incubated at 37 °C, with 5% CO_2 in a humidified atmosphere.

(No of cell/ml=No. of cells in large square of haemocytometer x 10^4)

2.3.2 Chinese Hamster Ovary Cells (CHO)

The CHO cell line was used in transfection experiments, and was obtained from the School of Biomedical and Biological Sciences, University of Plymouth liquid nitrogen culture collection. Cells were passage (16-24) in Hams F12 medium containing 0.146 gm/L glutamine and glucose 11 mM and 10% fetal bovine serum (FBS). The routine culture and passage procedure was performed as

previously mentioned for INS-1 cells (2.3.1) but the seeding density was 5×10^4 cell/cm^2 and incubated securely closed in on normal incubator at 37 °C with humidified atmosphere.

2.3.3 Storage of mammalian cells

Cells were grown to 80% confluence in order to prepare stocks for long term storage. Cells were cultured (2.3.1 & 2.3.2) in 75 cm^2 tissue culture flasks, trypsinized and harvested by centrifugation at 50 × *g* for 10 min, the supernatant was aspirated and the pellet was resuspended gently by pipetting in 10 ml of storage medium contains 20% FBS & 10% and dimethyl sulfoxide (DMSO). Aliquots of 1ml suspension were placed in 2 ml vials and incubated at -80°C overnight in insulated boxes. Afterwards, vials were removed from the insulated box and returned to - 80 °C for long store.

2.3.4 Cloning vectors

2.3.4.1 Bacteriophage lambda (λ) express (Stratgene, Wilmington,USA)

Cloning vector λ Zap, derived from bacteriophage λ was used to construct gene libraries for eukaryotic and prokaryotic organisms and express recombinant proteins. The Zap express was provided as arms pre-digested with *BamHI* and pre-treated with alkaline phosphatase with a total size of 38.9 kbp, thus λ cloning vector has 12 unique cloning sites with DNA capacity to be cloned from 0-12 kbp in length and recombinant phages can be recognized by blue-white screening as the foreign DNA will fuse to the beta glactosidase gene. Inserts can be excised out of the phage to form Kanamycin –resistant pBK-CMV phagemid vector after co-infecting *E coli* XL1-Blue recombinants with helper phage provided by in the kit (Figure 2.1).

This phagemid contains forward and reverse T7 and T3 primers respectively, facilitating sequencing the inserted DNA and sequence analysis. This type of vector also facilitates production of recombinant proteins extracellular through infection *E coli* to produce plaques. These can then be screened with antibody or via protein- protein interaction assay.

λ Zap express genomic libraries produced were amplified and chloroform 0.3% (v/v) was added and the amplified library was stored at 4 °C. Other aliquots of the amplified library were stored in 7% (v/v) DMSO in polypropylene falcon tubes at -80 °C. Excised filamentous pBK-CMV recombinants were stored in falcon polypropylene at 4 °C for 1-2 months and recombinant phagemids were used to transfect *E. coli.* Recombinant *E. coli* was stored as described in section 2.2 and recombinant phagemids extracted and stored at -20 °C for long term storage.

2.3.4.2 Plasmid pGEM-T Easy vector

This vector was provided as a 3 kbp linearized plasmid with single 3` terminal thymidine overhang on both ends to prevent the plasmid re-annealing and provide compatible overhangs for PCR products with A-overhangs. This plasmid contains an ampicillin resistance gene for use as a selectable marker in addition the lacZ gene that fused once the plasmids' T-overhangs within PCR product. The pGEM-T easy plasmid also includes a multi cloning site for easy excision of any cloned inserts and T7 and SP6 promoter for transcription and sequencing (Figure 2.2).

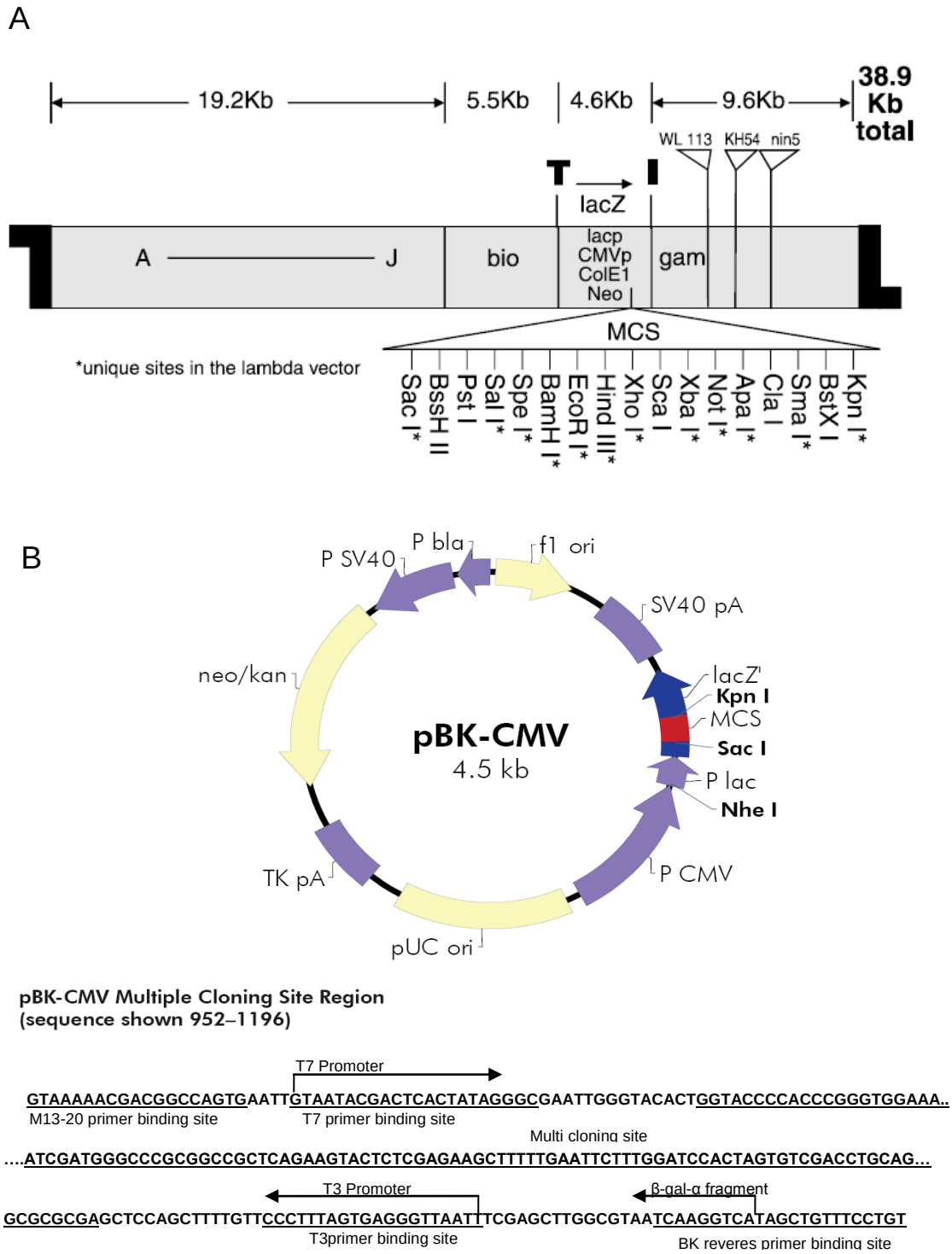

Figure 2.1: Schematic model of expression vector λ ZAP (A) and internal phagemid vector pBK-CMV (B) with multiple cloning sites, lac-z gene T7 and T3 promoters (Reproduced with permission from Stratagene, USA).

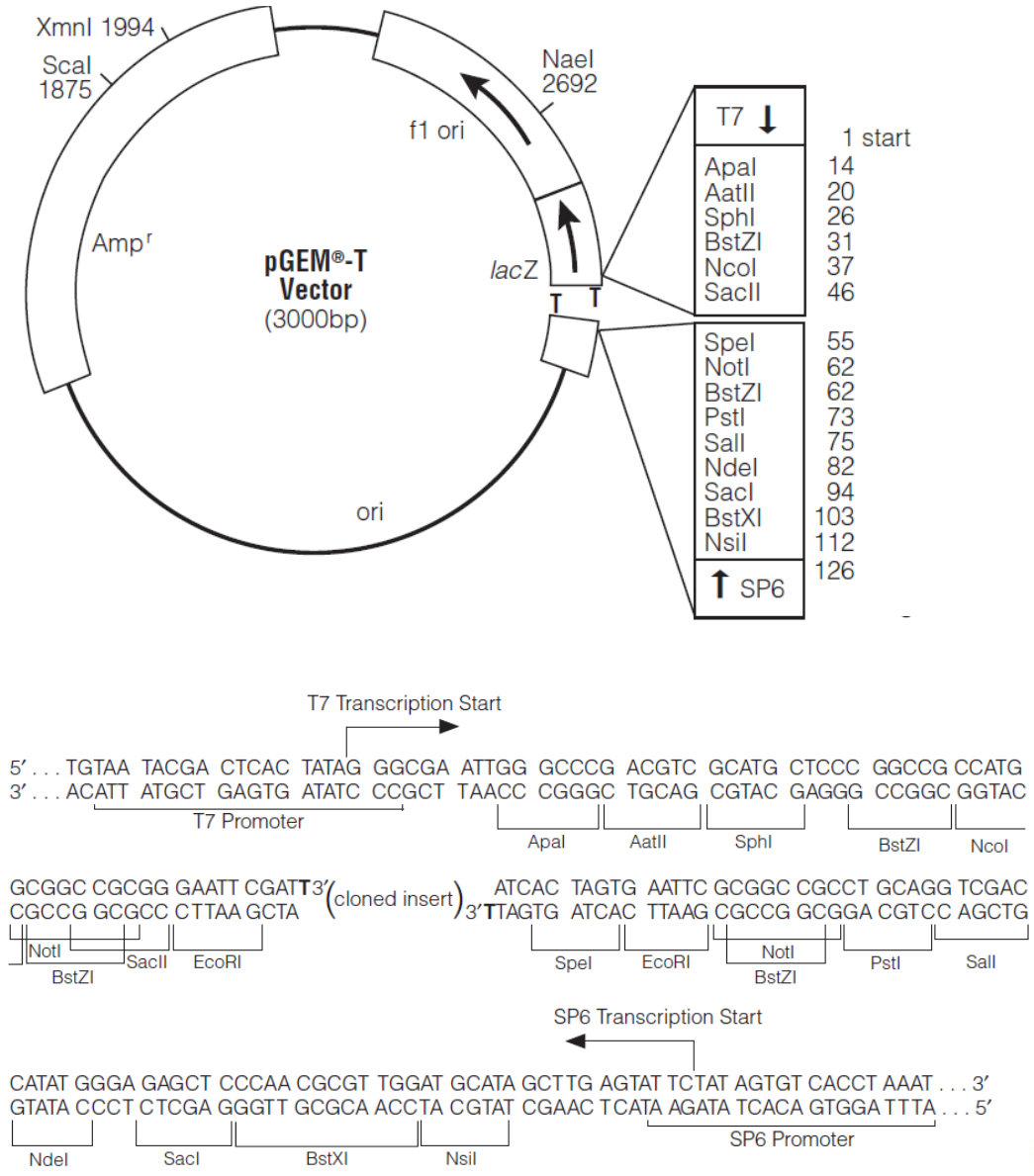

Figure 2.2: Schematic map of plasmid pGEM-T easy cloning vector and relevant sequence points T7 and SP6 RNA polymerase promoter, multiple cloning region 10–113, lacZ start codon 165, β-lactamase coding region 1322–2182 and phage f1 region 2365–2820 (Reproduced with permission from Promega, UK).

2.3.4.3 Plasmid pFN22A HaloTag cMVd1 Flexi vector

The pFN22A plasmid cloning vector (4188 bp) is designed to produce recombinant proteins appended to the halotag sequence to the amino terminus. The reading frame for protein of interest is combined with the halo tag code to produce a fusion protein and provides constitutive expression of the fusion protein in mammalian cells using a modified human cytomegalovirus (CMV) promoter, in addition to the T7 promoter for expression into *E coli.* The halo-tag region forms a covalent bound halotag ligand enabling immobilization of expressed protein as the protein to be produced will be a fusion protein combined with the halotag sequence. Furthermore, a tobacco etch virus (TEV) protease site is included for cleavage of the expressed protein from the halo-tag ligand. The pFN22A plasmid is fused with a toxic barnase gene which is replaced by the target open reading frame of the gene to be cloned. Unique restriction sites *SgfI* and *PmeI* flanking the barnase gene are ready for cloning with DNA fragments carrying similar sticky ends.

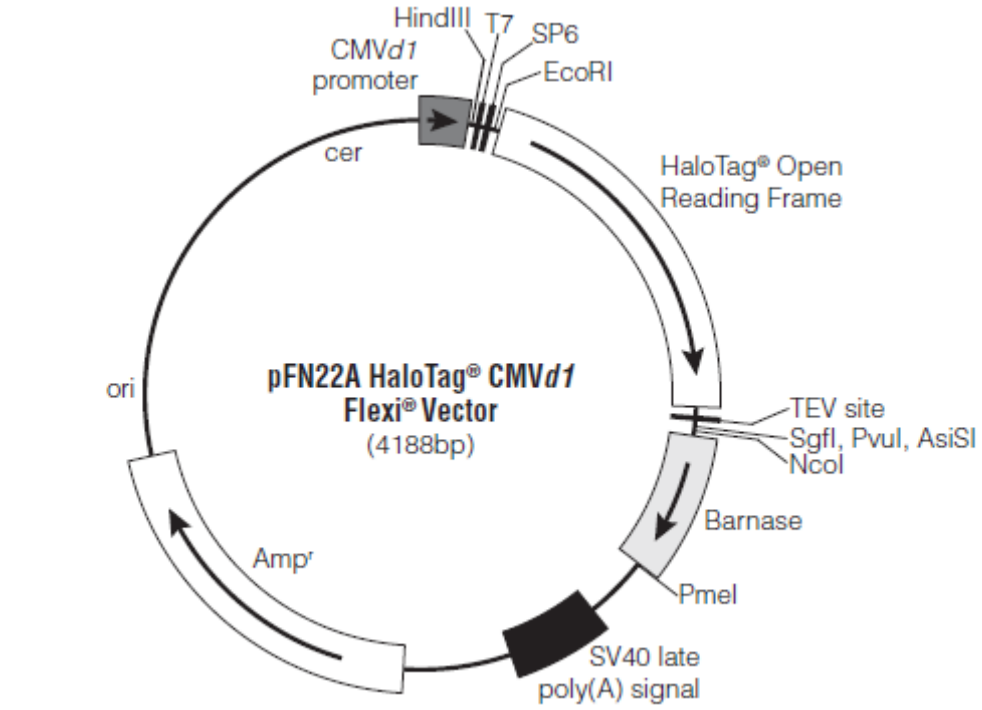

HindIII *EcoRI*

5'…AGAAGCTTAATACGACTCACTATAGGGTACGATTTAGGTGACACTATAGAATAAGGAGAATTCATC

T7 RNA polymerase promoter — SP6 RNA polymerase promoter

SgfI

ATGGCAGAAATTTCCGGCGAGCCAACCACTGAGGATCTGTACTTTCAGAGCGATAACGCGATCGCCATGG

HaloTag N-terminus — TEV protease recognition sequences

Figure.2.3: pFN22A HaloTag CMVd1 Flexi vector circle map and sequence reference points. Following features are present in the vector based on nucleotide sequence, CMVd1 enhancer/promoter 1–17, T7 and SP6 RNA polymerase promoter 132–151 and 156–175 respectively, halo tag protein coding sequence 191–1081, TEV site 1094–1114, SgfI site 1121–1128, barnase coding region 1152–1487, PmeI site 1489–1496, SV40 late polyadenylation signal 1648–1869, ampicillin resistance 2130–2990, Col E1-derived plasmid origin of replication 3145–3181, cer site (site for *E. coli* XerCD recombinase) 3852–4137 (Reproduced with permission from Promega, UK).

2.4 Protein analysis

2.4.1 Extraction of microbial soluble proteins

A single colony of fresh culture of each bacterium was used to inoculate 10 ml volumes of LB and incubated overnight at optimal temperature with or without shaking (120 rpm). The culture (0.5ml) was used to inoculate 50 ml of fresh LB medium and incubated overnight as before. The bacteria were collected by centrifugation at 4000 × *g* for 20 min at 4 °C and suspended in 5 ml protein extraction buffer (Appendix 1) containing 100 µg/ml of lysozyme, 5 µg/ml DNase I and 0.5 ml of protease inhibitor cocktail (P8340, Sigma Poole, UK) and incubated at 55 °C in a water bath for 15 min. Yeast strains, *Nocardia*, and *Mycobacterium* were lysed by an extraction buffer containing chromopeptidase (20ng/ml) instead of lysozyme and incubated at RT for 30 min. Cell suspensions were then transferred into conical tubes (20 ml) and placed on ice and sonicated (Microson XL2000, UK) using 5 sec bursts with 5 sec cooling time for a total of 4 min. The cell lysate was spun at 10000 × *g* for 30 min at 4 °C and the supernatant transferred to a fresh 15 ml polypropylene tube for quantification.

2.4.2 Protein quantification

Protein quantification employed the Bradford method (Bradford, 1976) modified for micro plate reader. Bovine Serum Albumin (BSA) stock solution (1 mg/ml) was prepared in molecular grade water (MBW) and used to prepare the standard protein solutions ranging from 50 to 600 µg/ml using a stock solution to a final volume of 500 µl as listed below.

Standard	Stock	ddH20 (µl)
0	0	500
50	25	475
100	50	450
200	100	400
400	200	300
600	300	200

Aliquots (10 µl) of each standard protein solution were pipetted in triplicate into a 96 well plate and unknown protein samples were prepared in the same way, in addition to the control wells which contained 10 µl of MBW. Next, 250 µl of Coomassie blue R250 reagent (Thermo Fisher, UK) was added to each well using a multi-channel micropipette and mixed by pipetting and left at RT for 5 min. The absorbance was determined in a micro plate reader (Molecular Devices, Manchester, UK) at 595 nm wave length. A standard curve was produced between absorbance value and protein concentrations and the linear equation, regression value (R) was extracted and protein concentration of each test sample was calculated.

2.4.3 SDS-PAGE

Sodium dodecyl sulphates – polyacrylamide gel electrophoresis (SDS-PAGE) are a widely used analytical technique for the separation of cellular proteins and estimate the relative molecular size. SDS-PAGE was performed using Laemmli's discontinuous buffer system (Laemmli, 1970) and a Biometra mini-gel apparatus (Biometra, GmbH, Germany). The glass plates were cleaned with decan detergent and washed with deionised water, followed by 70% ethanol and dried before used. The final concentration of the resolving gel was 10% or 12 % and for stacking gel was 5% of Acryl / Bis-Acrylmide stock

reagents and 0.2 % or 0.05% SDS (solution A, B and electrophoresis buffer) concentration.

The desired resolving gel solutions (Appendix 1) were mixed firstly followed by adding 40 µl the ammonium per sulphate (APS) and 15 µl TEMED for polymerisation. The resolving gel was poured into the preformed space between the glass plates and filled two thirds. Water saturated isobutanol (2ml) was added immediately to the resolving gel mix to keep reduced oxygen condition. The gel was left for at least 30 min at RT for polymerisation to occur. Next, the isobutanol layer was removed and the top of gel was washed 5 times with sterile molecular biology water (MBW) and the stacking gel was applied and a comb was inserted directly into the stacking gel to produce wells for loading protein samples. The gel was left for at least 30 min to set. After setting, the gel was transferred to the electrophoresis tank and fixed by clips on both sides and the electrophoresis buffer was poured into the tank to cover the top of the gel. The comb was removed carefully and each well was loaded with maximum 20 µl of protein sample. The gel was run at 80 V for 30 min until the proteins entered the stacking gel and the voltage was increased to 110 V. The gel was run until the dye front reached the bottom of the gel.

The gel was removed from the electrophoresis tank, plates were removed and the gel placed into a tray containing 50 ml of coomassie blue staining buffer (Appendix 1) with gentle shaking for to 2 h, after that the staining buffer was discarded and replaced with 100 ml of destaining solution which was replaced after 30 min with fresh 100 ml for 2 or 3 times until clear bands could be seen.

2.4.4 Protein Blotting

The proteins separated in SDS-PAGE gels were transferred to nitrocellulose membranes using an electro blotter system (Criterion blotter, BIO-RAD, UK) (Towbin *et al.*, 1979). After electrophoresis and prior to blotting, the gel was placed in 100 ml of transfer buffer for 10 min. Pieces of nitrocellulose were cut to the same size as the gel, along with two pieces of Whatman filter papers (3 MM). The blotting papers were pre-wetted for 2 sec in transfer buffer (Appendix 1) and one of them was placed onto one of the foam pads. The gel (section 2.4.3) was carefully placed onto the blotting paper followed by the pre-wetted nitrocellulose membrane, ensuring no air bubbles were trapped under the nitrocellulose membrane by using a clean glass rod and then the second blotting paper was placed on the gel with the second foam pad. The gel was electro blotted at 300 mA at RT for 1.5 hours; an ice pack was used to cool down the buffer. After blotting the membrane was washed using PBS and placed in 50 ml of blocking solution (Appendix1). The membrane was then subjected to the ligand binding protocol, or the standard western blotting technique involving primary and secondary antibody.

2.5 Nucleic acid analysis

2.5.1 Purification of genomic DNA from Gram negative bacteria

Genomic DNA was extracted from bacterial strains using DNeasy blood and tissue kit (Qiagen, UK). The protocol supplied by manufacturer recommended using 2×10^9 cells from overnight culture for extraction of total DNA from Gram negative bacteria. A maximum 2×10^9 cells in overnight broth culture were harvested in a microcentrifuge tube by centrifugation for 10 min at 5000 × *g* and

resuspended in suspension buffer and the genomic DNA was extracted and purified as described by the manufacturer.

2.5.2 DNA precipitation

In order to obtain 2µg/µl DNA final concentration, the genomic DNA was concentrated as described by Sambrook and Russell (2001). A one tenth of volume 3M sodium acetate (pH=6) was added and mixed with DNA solution, followed by 3 volumes of cold ethanol (100 %) with thorough mixing. The mixture was stored at -20 for 2 h to precipitate DNA and centrifuged at 13000 × *g* for 3 min. The supernatant was carefully removed and the pellet was washed with 200 µl of 70 % ethanol and centrifuged for 3 min at 13000 × *g*, the washing was repeated twice, the DNA pellet was left to dry for 10 min at RT and finally resuspended in 30µl of sterile MBW.

2.5.3 Preparation of plasmid DNA

Plasmid DNA was extracted from bacterial cultures as described by Birnboim & Doly (1979) cited by Sambrook & Russell (2001). Aliquots (1.5 ml) of overnight broth culture were centrifuged at 6000 × *g* for 2 min at RT. The pelleted cells were resuspended and left in 100 µl of B & D solution I (Appendix 1) at RT. The bacterial cells were lysed by adding 200 µl of freshly prepared B & D solution II (Appendix 1), the tubes contents mixed by gently inverting and left for 5 min at RT. Ice cold B & D solution III (Appendix 1) 150 µl was added and the tube's contents mixed and placed on ice for 10 min. The tubes were centrifuged of 13000 × *g* for 5 min at RT. Cell debris, denaturised proteins and chromosomal DNA are precipitated and the supernatant was transferred to a fresh microcentrifuge tube. Cold (-20 °C) absolute ethanol (1ml) was added and mixed with the DNA solution and incubated at -20 °C for 10 min. The mixture

was centrifuged at 13000 × *g* for 3 min and the supernatant removed. The plasmid pellet was left for 10 min to drain and then resuspended in 100 µl of solution B & D IV (Appendix 1). The DNA was re-precipitated by adding 300 µl of cold absolute ethanol, mixed and incubated for 10 min at -20 °C. The plasmid DNA was pelleted by centrifugation (13000 × *g*) for 5 min and the B & D IV solution step repeated again. The pelleted plasmid washed twice with 200 µl of 70 % ethanol, centrifuged at 13000 × *g* and supernatant removed and finally the plasmid pellet was left to dry followed by suspension it in 20 µl of MBW and stored at 4 °C.

2.5.4 Plasmid preparation using Plasmid Miniprep Kit (PLN70, Sigma, UK)

Aliquots (1.5 ml) of overnight broth culture were centrifuged (13000 × *g*) at RT and resuspended in 200 µl of re-suspension solution. Protocol was followed as described by manufacturer. The purified plasmid was eluted using 100 µl MBW and the eluted DNA was stored at 4 °C.

2.5.5 Determination nucleic acids quality and quantity

The concentration of the nucleic acids (DNA, RNA and cDNA) prepared in this study were measured, as well as purity, using a computerized Nano-drop spectrophotometer (Lab Tech, UK). Aliquots (2 µl) of buffer were used to calibrate the nanodrop and then 2 µl of nucleic samples were measured and the DNA/protein rate ($260_{nm}/280_{nm}$), DNA/contaminants rate ($260_{nm}/230_{nm}$) and DNA concentrations were recorded. The wave length was corrected for different types of nucleic acid (DNA, RNA, ssDNA). The DNA quantity and quality were checked further by running aliquots of the extracted DNA with known amounts of standard Bacteriophage λ DNA (1 µg, 0.5 µg, 0.25 µg, 0.125 µg 0.1 µg, 0.05 µg) into agarose gel electrophoresis. Depending on the fluorescence intensity of

intercalated ethidium bromide on the known concentrations of λ DNA standard, DNA concentration and molecular weight was assessed. The DNA was visualized and images were captured after electrophoresis using UV gel documentation system (UV tech, UK).

2.5.6 DNA agarose gel electrophoresis

In order to read the quality of DNA, agarose gel electrophoresis was used. The gels were prepared by dissolving 0.8 or 1.8 % of agarose into TBE buffer (1×) (Appendix 1) in a conical flask using a microwave oven on mid power for 2-3 min until the agarose completely dissolved. A drop of ethidium bromide standard solution 625 µg/ml (Sigma, UK) was added to 50 ml of molten agarose solution once the solution became cooler (50 °C) and mixed well to give final concentration 0.5 µg/ml of ethidium bromide. The molten agarose was poured into an end taped tray with comb inserted in order to create wells. After 30 min the set gel was placed into an electrophoresis tank (Pharmacia GNA100, UK) and submerged with 350 ml of TBE (1×). DNA samples were prepared by mixing them with DNA loading buffer (Appendix 1). The comb was removed and the samples were loaded into the gel's wells. The gel was run at 50 to 120 V until the dye front reached the end of gel and then the DNA was visualized using a UV transilluminator (390 nm) and photographed with the gel documentation system.

2.5.7 Elution of PCR products from agarose gels

The DNA bands that appeared at expected molecular size required for further analysis were excised from the gel using a clean sterile razor and extracted using a cleanup system (Promega, UK) following manufacturer's instructions to

purify them. The DNA concentration was measured by the nanodrop spectrophotometer and the quality was checked by agarose gel electrophoresis.

2.5.8 DNA digestion by restriction endonuclease enzymes

Restriction enzymes cleave both strands of double stranded DNA at specific nucleotide sequences called restriction sites. The definition of 1 unit of restriction enzyme is an amount of enzyme which cut 1µg of λ DNA in 1 hour at 37 °C in a volume of 50 µl. Digestion reactions were performed using restriction enzyme and restriction buffer recommended by the supplier in 1.5 ml microcentrifuge tubes, containing 1µl of DNA (1µg/1µl) dissolved in MBW plus 1µl of 10 x restriction buffer, 7 µl of MBW and finally 1µl of restriction enzyme (1unit/µl) and mixed thoroughly. Contents were collected by brief centrifugation and incubated at 37 °C for 3- 18 hours. Large quantities of DNA were digested by scaling up the reaction mixture ensuring that the enzyme volume was always 1:10 or less of the final volume of reaction mixture. Double enzyme digestion was carried out using recommended buffer by supplier or compromised buffers were prepared 1:1. The digested DNA was visualized using agarose gel electrophoresis with DNA size marker.

2.6 Assaying gene expression using RT-PCR & qRT-PCR

Reverse Transcriptase PCR RT-PCR and quantitative real time -PCR (qRT-PCR) techniques were used to study gene expression, techniques involve extraction total RNA, cDNA syntheses, conventional PCR amplification using specific primers and then compare the band intensity for each treatment to the control after run the PCR product into agarose gel electrophoresis.

2.6.1 Extraction of total RNA from mammalian cells

The total RNA was extracted using RNA sigma Kit (RTN70 sigma, UK). Cells were subculture in 25 cm^2 flasks (section 2.3.1) and RNA was extracted at confluency 80%, about 5×10^6 - 1×10^7 cell/ml were used to extract the total RNA. The medium was discarded and cells were washed using 3 ml of PBS twice to remove cell debris and medium residues. The attached cells were then lysed using lysis buffer containing 0.02% 2-mercaptoethanol and the RNA was extracted and purified using the manufacturer's protocol using the optional step involving DNase treatment to eliminate the chromosomal DNA from the RNA. RNA was eluted using DNase & RNase free MBW, and samples concentration and purity were measured using the nanodrop spectrophotometer (2.5.2). Aliquots of RNA were stored in 1.8 ml microcentrifuge tubes RNase, DNase free for long term at -70 °C freezers. All samples that showed more than 250 ng/µl were processed as follows:-

2.6.2 Preparing total cDNA using reverse transcriptase

The cDNA was prepared using extracted RNA (2.6.1). Microcentrifuge tubes (200 µl) RNase and DNase free were used for preparing total cDNA by using 1 µg RNA. The RNA was mixed with 1 µl of 10 mM dNTPs solution and 1 µl of 50 µM random nonamers and water was added to give a 10 µl final volume. The contents were mixed gently and briefly centrifuged to collect all components to the bottom; tubes were incubated in a thermal cycler (Applied Biosystem, UK) for 10 min at 70 °C to reduce mRNA secondary structure. After that tubes were placed on ice for 5 min and 10 µl of reverse transcription master mix containing 200 units of Moloney Murine Leukemia Virus Reverse Transcriptase (M-MLV - RT), 2 µl of 5 x reverse transcriptase buffer and 7 µl of PCR pure water were added to each tube to a final volume of 20 µl. The tubes were incubated for 10

min at RT to ensure elongation of random nonamers before being placed at 37 °C for 50 min at and then 5 min at 94 °C to stop M-MLV reverse transcriptase activity. The cDNA samples were stored at 4 °C for short term storage on -20 °C for long term storage. The synthesised cDNA samples (section 2.6.2) were then amplified using specific PCR setup and specific primers prepared for this purpose**.** The synthesised cDNA samples were then amplified using PCR amplification as follows:-

2.6.3 Conventional PCR amplification

2.6.3.1 Design of primers

The full length sequences of cDNA of the genes of interest were identified using ensemble software version 53 from the European Bioinformatics Institute (EBI). The primer blast software of the National centre of Biotechnology Institute (NCBI) was used to get an appropriate primer in terms of sequence, number of nucleotides and melting temperature. The annealing temperature of primers that used was either 60 or 65 °C, and the primers designed to produce amplicons of sizes 150-250 bp for the genes to be studied. The primers were commercially synthesised by Sigma genosys (Sigma Poole, Dorset, UK). Lyophilized primers were dissolved in appropriate volumes of MBW to prepare 100 mM and were stored at -20 °C.

2.6.3.2 PCR amplification

Amplicons of the genes of interest were amplified using total cDNA prepared in section 2.6.2 and primers (Section 2.6.3.1). DNase free PCR tubes (200 µl) were used for these experiments and reaction components were added respectively for individual reaction as follows:-

cDNA	2 µl
PCR reaction buffer (5 ×)	2.5 µl
Forward primer (10 µM)	0.5 µl
Reverse primer (10 µM)	0.5 µl
dNTPs solution (10 mM)	0.5 µl
Taq DNA polymerase (5 U)	0.25 µl
PCR water	18.75 µl
Total	25 µl

The contents were mixed thoroughly by pipetting and centrifuged briefly to collect the mixture at the bottom of the tubes. PCR controls were set using water instead of cDNA. Standard PCR reactions were performed using a MWG Thermo cycler (Primus 96 plus) under the following conditions; 94 °C for 2 min followed by 40 cycles start at 94 °C for 30 sec, 60 - 65 °C for 30 sec and 72 °C at 30 sec for individual cycle followed with hold the samples at 4 °C until collect them. The PCR products samples were mixed with loading buffer and run into 1% agarose gels in TAE buffer along with a 1 kb ladder and the DNA bands were visualized in gel documentation system using ethidium bromide and UV light and images were captured.

2.7 Quantifying gene expression by absolute qRT-PCR

The mRNA levels were measured for mammalian genes were also quantified using qRT-PCR or real time PCR. qRT-PCR absolute quantification method was used to measure the mRNA levels in each sample exposed to a certain concentration of cytotoxic agents. This method requires cloning the PCR products of certain genes into a suitable host vector (plasmid) such as pGEMT-easy vector, which has been extensively used for these purposes. A standard curve for a particular gene was achieved by preparing ten-fold serial dilution

series of the cloned plasmids, ranging from 5 X 10^2 to 5 X 10^6 copies were used to construct the standard curves. Cloning the gene amplicon produce by PCR into pGEMT-Easy vector requires:-

2.7.1 PCR amplification using GoTaq DNA polymerase

The PCR amplification of genes of interest were prepared using modified taq polymerase which lacks 5`-3` nuclease activity (GoTaq DNA polymerase) to achieve a PCR product with A-overhang in both ends facilitating cloning the amplicon into T-overhang ends of PGEM-T easy cloning vector. The PCR reaction was achieved using 200 µl PCR tubes. Products were synthesized by using the following reaction to final volume of 50 µl.

cDNA	2 µl
F/primer (10 µm)	1 µl
R/primer (10 µm)	1 µl
dNTPs (10mM)	1 µl
GoTaq DNA polymerase	0.25 µl
GoTaq buffer (5 ×)	10 µl
MGW	34.75 µl
Total	50 µl

The PCR started by denaturing at 94 °C for 2 min followed with a 30 cycle set up at 94 °C for 0.5 min, 60 or 65 °C for 0.5 min and 72 °C for 1min. The products were separated into 1.8% agarose gels and desired product were extracted from the agarose gels (section 2.5.6) and used in the cloning procedure.

2.7.2 Ligation of PCR products into pGEMT-Easy plasmid

The purified PCR products for particular genes were cloned into plasmid pGEMT-Easy using a Promega cloning system (A 1380, Promega, UK). The PCR products were ligated within pGEM-T plasmid using DNA ligase enzyme provided with the cloning system. The molar ratio for inserts was 1:1 and used to calculate the concentration of PCR products from the following equation.

$$\text{ng of insert} = \text{insert : vector ratio} \times \frac{\text{ng vector} \times \text{kbp size of inserts}}{\text{kbp size of vector}}$$

ligation was performed using 1.8 ml eppendorf tubes nuclease with 5 µl Ligation buffer (2 ×), pGEM-T easy plasmid 1µl (50 ng/ µl), 1 µl of T4 DNA ligase (3 units/ µl) mixed with 1 µl of a suitable concentration of the PCR amplicon DNA and MBW was added to a 10 µl final volume for each sample. Two types of control reaction were set for ligation; a positive control using control inserts DNA and a background control which is unlighted free insert DNA. The contents were mixed by pipetting and the tubes were incubated at 4 °C overnight.

2.7.3 Transformation into *E. coli JM109* coupled with blue white screening

The transformation protocol used frozen ready competent cells of the *E coli JM109* (Promega, UK) provided with pGEM-T easy cloning system (stored at -70 °C) according to manufacturer's instructions. The ligation mixtures for each amplicon and control samples were used for transformation. Ligation mixture (4 µl) volumes were placed into 15 ml polypropylene tubes. Uncut pGEM-T easy plasmid (0.1 ng) was also used as a positive transformation control to determine the efficiency of competent cells. Next, competent cells were removed to thaw in an ice bath for 5 min and 50 µl of these were transferred gently into tubes that containing the plasmid DNA with gently mixing and left on ice for 20 min, after that the sample was heat shocked by placing at 42 °C for 50 sec. The tubes

were then immediately returned to ice for 2 min and 950 µl of SOC medium (Appendix 1) was added to the tubes containing ligation mixture and 900 µl of SOC to the tubes with uncut plasmid. Tubes were incubated at 37 °C with shaking (120 rpm) for 1.5 h followed by plating 100 µl samples onto LB plates containing ampicillin (100 µg/ml), IPTG (0.1 mM), and (40 µg/ml) X-gal (Appendix 1).

The white colonies were considered recombinant transformants, while blue colonies lack inserts. A total of recombinant colonies (15 colonies) were streaked and checked again on X-gal /IPTG / ampicillin plates and a single colony was used to prepare stored aliquots of the recombinant *E. coli.*

2.7.4 Checking recombinant pGEMT-Easy plasmid

The recombinant pGEMT-easy plasmids DNA were excised by restriction enzymes in order to verify whether the right insert was cloned into the plasmid. The recombinant colonies were sub-cultured, in addition to colonies transformed within uncut pGEM-T plasmids in LB broth containing ampicillin and incubated overnight with shaking at 37 $^{\circ}$C. The cultures were used to extract the plasmid DNA (section 2.5.4) and 1µg of DNA was used for excision using *EcoRI* restriction enzyme and fragments were separated in an agarose gel (section 2.5.6). Recombinant plasmids (50 ng) were then subjected to further checking using PCR amplification (section 2.6.3.2). After excision and PCR amplification recombinant plasmids which produced inserts of the expected size were sequenced and plasmids possessing the right clone inserts in recombinant *E. coli* were stored as described in section 2.2.2.

2.7.5 Assay for mammalian expression

Triplicates of each sample were prepared in 48 well PCR plates. Each well contained 12.5 µl of SYBR green master mix, 0.5 µl each of forward and reverse primers (10 µM), 0.25 µl reference dye, 9.5 µl water and 2 µl cDNA. PCR reaction was achieved using the following conditions denaturant cycle at 94 °C for 2 min followed by 40 cycles, 94 °C 30 for 15 sec, annealing 60 °C for 30 sec and amplification at 72 °C for 30 sec. Followed with melting cycle 94 °C for 15 sec and 60 °C for 1 min and 94 °C for 30 sec. The products were detected using an Applied Biosystems Step One real time PCR instrument and software v2.1. The copy number data were collected and normalized using the β-actin data before statistical analysis.

2.7.6 qRT-PCR Data normalization

The data was collected for mammalian genes tested and normalised with β-actin gene expression data as the β-actin is used as a housekeeping gene in which the level of transcription level is almost do not affected by any factor. The normalization of β-actin copy number was done by dividing the mean of β-actin data copy number of individual sample into 1000000 to produce the normalization factor and after this the normalized β-actin values multiplied by test gene copy number to normalize the test gene data.

2.7.7 Statistical analysis

Unless stated otherwise, all the numerical data were analysed using SPSS version 17 statistical software, using one way analysis of variance (ANOVA) and multiple comparison post hoc tests (Fisher's LSD). Data are shown as means +/- SE and $p < 0.05$ is considered significant**.**

Chapter 3

Effects of the microbial secondary metabolites pyrrolnitrin, phenazine and patulin on INS-1 rat pancreatic β-cells

3.1 Introduction

Recently, in addition to genetic susceptibility and autoimmunity, the destruction of pancreatic beta cells (β-cells) and consequent development of Type 1 diabetes (T1D) have also been linked with exposure to environmental factors, which may contribute up to 50% of the risk of developing this type of diabetes (Hans *et al*., 2002). The most important factors that are thought to be T1D inducers are infection (e.g. viral infection), diet (i.e. the early presence or lack of particular food during childhood), and some inorganic compounds e.g. arsenate ions (Peng and Hagopian, 2006; Richer and Horwitz, 2009).

Amongst these potential environmental factors are microbial secondary metabolites that can cause β-cell dysfunction or destruction e.g. bafilomycin and concanomycin, produced by *Streptomyces* spp. (Myers *et al*., 2003) and cereulide produced by *Bacillus* spp. (Virtanen *et al*., 2008). Compounds from microbial sources show various interactions with β-cell proliferation and differentiation, in addition to interacting with the major β-cell pathways relating to insulin synthesis and secretion, and even with aspects of insulin gene regulation. Foods are thought to be the main means by which these compounds enter the human body, particularly through ingestion of naturally infected fruit and vegetables, as well as via foods that are contaminated during processing in the food industry. There is also the possibility that human exposure to such compounds may occur through infection with pathogens capable of producing these secondary compounds *in situ* (Virtanen *et al*., 2008). A wide range of microbial components could cause destruction of β-cells through a variety of mechanisms. Some of these components are vascular ATPase inhibitors such as bafilomycin and concanomycin while others are genotoxic compounds such

as streptozotocin or mitochondriotoxic compounds such as cereulide (Singaram *et al*., 1979; Virtanen *et al*., 2008). The compounds mentioned so far are secondary metabolites but primary metabolites such as the collagenase produced by *Clostridium histolyticum* could also destroy β-pancreatic cells (Moskalew *et al*., 1974). In some cases these compounds may be produced in relatively high concentration in individuals with long-term infection such as cystic fibrosis (CF) patients (Coutinho, 2007).

In this study it has been hypothesized that the microbial secondary metabolites produced by *Burkholderia* sp and *Ps. aeruginosa* during infection of CF suffers may contribute the β-cells cytotoxicity and diabetogenicity and subsequently CFRD. The effects on pancreatic β-cell viability and function of three microbial secondary metabolites pyrrolnitrin produced by *Burkholderia* spp. and *Ps. aeruginosa*; phenazine produced by *Ps. aeruginosa*; as well as patulin produced by *Penicillium* and *Aspergillus* spp. were investigated, using the rat clonal pancreatic β-cell line, INS-1, as a model. In addition, the effects of concentrated supernatants of cultures of *B. multivorans* and *Ps. aeruginosa* were also tested.

Phenazine, also called dibenzo-*p*-diazine, is a redox-active compound that increases intracellular oxidative stress. It has been confirmed that phenazine and its derivatives interact with various human cell lines causing increased production of reactive oxygen species which cause cellular damage (Hamill *et al*., 1981; Denning *et al*., 2003). Pyrrolnitrin, 3-chloro-4-(3-chloro-2-nitrophenyl)-1H-pyrrole, is a compound with antibiotic activity produced by *Burkholderia* spp. and the cytotoxicity of this compound to mammalian cell lines is not well tested. However, pyrrolnitrin has been identified as having an inhibitory effect on the

electron transfer chain in fungi and bacteria (Hwang *et al.*, 2002; Zhai *et al.*, 2003).

The food-contaminating toxin patulin was used as a model for exposure to secondary microbial metabolites via food. Patulin is a toxin produced by fungi *Penicillium* and *Aspergillus*, contaminating food products like apple and apple juice (Figure 3.1). The toxic effects of patulin have been studied extensively and result from its ability to bind covalently to essential sulfhydryl groups in proteins and amino acids with diabetogenic effect against mice diabetes model (Chan *et al.*, 2001; Silva *et al.*, 2007).

In this chapter the cytotoxic effects of the bacterial secondary metabolites, pyrrolnitrin and phenazine on the rat β-cell line, INS-1 were tested. The effect of the fungal toxin patulin, was also examined for comparative purposes. The cultured INS-1 cells were exposed to serial dilution of secondary metabolites at three time points. The effects of sub-lethal concentrations of these compounds on insulin secretion after two exposure times, 2, 24 h were also examined in order to verify the role of sublethal concentrations on the insulin secretion pathway. Furthermore, the patch clamp technique was also used to detect changes in the membrane depolarization associated with insulin secretion. Moreover, the intracellular Ca^{2+} was measured for same purpose as the intracellular Ca^{2+} is considered a main internal signal that mediates the secretion process and insulin pool modifications. Influences of secondary metabolites at sublethal concentrations on insulin gene expression were also investigated using RT-PCR and qRT-PCR to assess whether insulin gene transcription can be modulated or affected in response to toxicity by these compounds.

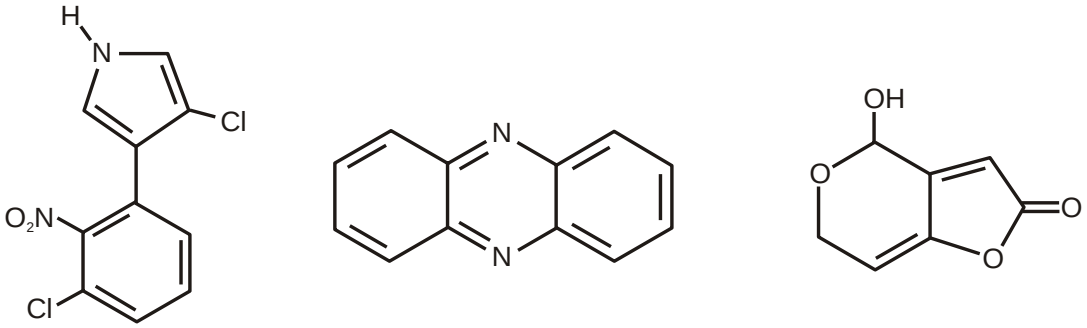

pyrrolnitrin phenazine patulin

Figure 3.1: Chemical structure of the microbial secondary metabolites: pyrrolnitrin produced by *Burkholderia spp.*; phenazine produced by *Pseudomonas* and *Burkholderia* spp.; and patulin produced by *Penicillium* and *Aspergillus* spp.

3.2 Materials and Methods

Unless stated otherwise, all experiments in this chapter were repeated at least three times.

3.2.1 Microbial secondary metabolites preparation

Purified microbial compounds (pyrrolnitrin, phenazine, and patulin, ≥ 98% purity), were obtained as powders from Sigma-Aldrich (Poole, UK). The secondary compounds pyrrolnitrin, phenazine and patulin were prepared as stock solutions at 10 mg/ml, solvents were ethanol, acetone and water, respectively. The stock solution used to prepare ten-fold dilutions 0, 1, 10, 100, 1000 and 10000 ng/µl.

3.2.2 Cell culture

Rat insulinoma cells (INS-1) cells (Asfari *et al.*, 1992) were cultured and maintain as described in Section 2.3.1. The cells were grown as monolayers, with passage number 12- 35 used for all experiments.

3.2.3 Pancreatic β-Cell cytotoxicity

The cytotoxicity of the purified phenazine, pyrrolnitrin, and patulin, and supernatants from cultures of *B. multivorans & Ps aeruginosa* (BMS & PAS, respectively) to β-cells were tested.

3.2.3.1 Cytotoxic effects of secondary compounds on INS-1 cells

The cytotoxic effects of the microbial secondary metabolites were determined using final concentrations in the range 1-10000 ng/ml. INS-1 cells were cultured in 6-well plates at a seeding density of 5×10^5 cells/cm^2 for 24 h, and then the spent medium was replaced with fresh medium containing various concentrations of the microbial compound to be tested. Triplicate INS-1 cell

samples were separately exposed to ten-fold serial dilutions of each of the test compounds (0, 1, 10, 100, 1000 and 10000 ng/ml) and incubated for up to 72 h. Two control sets of samples were prepared in the same way as the treated samples; in one set cells were exposed to the solvent (ethanol, acetone or water as appropriate, see above) at the same final concentration (0.25%) as used in the treated samples. The numbers of viable cells were determined at 2, 24 and 72 h using the trypan blue viability test which depends on the ability of viable cells to exclude trypan blue. INS-1 cell suspension (100 µl) was mixed with 100µl of 4% trypan blue for 3 min at room temperature; dead and viable cells were then counted using a haemocytometer (Wood *et al.*, 2004).

3.2.3.2 Cytotoxic effects of BMS & PAS on INS-1 cells

B. multivorans and Ps. aeruginosa were grown as described in Section 2.2.1. The cultures (10 ml) were incubated for 48 h and then centrifuged for 15 min at 6000 × *g* and the supernatants sterilized by filtration through a 0.45 µm membrane filter (Millipore, UK). Different concentrations of the supernatants (2, 4, 6 and 10 µl/ml) and LB medium (used as a control) were added to INS-1 cells cultured in 6 well plates, and the number of viable cells and percentage viability was measured as described in Section 3.2.3.1.

3.2.4 Effects of secondary compounds on insulin secretion

3.2.4.1 INS-1 insulin secretion stimulation

Insulin secretion by INS-1 cells was measured in a stimulation assay which was used to confirm that the INS-1 cells were properly responding to insulin secretion stimulation factors (2 mM, 20 mM glucose and 25 mM KCl) which are normally used as stimulators (Asfari *et al.*, 1992). INS-1 cells were splited into 24 well plates with a seeding density of 1.5×10^5 cells/well and left to attach

overnight. The medium was aspirated off and the cells washed with 500 µl Gey & Gey buffer (Appendix 1). Cells were pre-incubated with 0.5 ml of Gey & Gey A containing 2 mM glucose (Gey and Gey, 1936) for 1.5 h, after which wells were treated in one of three ways: the contents were replaced with (1) 0.3 ml of fresh Gey & Gey A or (2) with Gey & Gey B buffer containing 20 mM glucose or (3) with Gey & Gey C containing 25 mM KCl, and incubated in all cases for 1 h at 37 °C. Finally, the stimulation buffer was removed after centrifugation (10 min at 800 × *g*) and 0.25 ml of the contents of each well subjected to radioimmunoassay to measure secreted insulin.

3.2.4.2 Effects of microbial compounds on insulin secretion after 2 h

Insulin secretion by INS-1 cells was measured after exposure to 10 fold different concentrations (range 1-10000 ng/ml) of the microbial compounds pyrrolnitrin, phenazine and patulin. The INS-1 cells were seeded in 24 well plates at a density of 2×10^5 cells per well. After 2 h exposure, cells were washed with Gey & Gey buffer and resuspended in Gey & Gey buffer containing 2 mM glucose and 0.1% BSA, and the same concentration of the microbial compounds, and pre-incubated for 1.5 h at 37 °C. Next, the buffer was replaced with 2 ml Gey & Gey buffer containing 2 or 20 mM glucose and 0.1% BSA again containing the same concentration of microbial compounds, and after 1 h at 37 °C the solution was removed and centrifuged at 300 × g for 10 min. The supernatants were used for the measurement of secreted insulin by RIA as described elsewhere (Alice *et al*., 2006).

3.2.4.3 Effect of sublethal concentrations on insulin secretion

In order to investigate the effects of the microbial compounds on insulin secretion by INS-1 cells over 24 h sub-lethal concentrations (0, 1, 10 ng/ml, and the toxic concentration 100 ng/ml of the compounds phenazine and patulin; 0, 1, 10, 100, 1000, and the toxic concentration 10000 ng/ml of pyrrolnitrin) were used. After incubation for 24 h and glucose concentration 2, 20 mM the procedure described above was carried out.

3.2.4.4 Radioimmunoassay (RIA)

The samples collected in sections (3.2.4.1, 3.2.4.2 and 3.2.4.3) were subjected to RIA to measure insulin secreted by the cells after exposing them to the toxic agents. The samples were collected from the wells into 1.8 ml micro centrifuge tubes after which 50 µl sample from each well were pipetted in 3 ml tubes (used for radioimmunoassay) in duplicate. Guinea pig anti bovine insulin antibody (50 µl; Appendix 1) was added to each sample by followed by 50 µl of radio labelled I^{125} insulin ('hot' insulin; 50 pg/tube with specific activity of 100 µCi/µg) an hour after the addition of the insulin antibody. Two controls in duplicate were used, one just containing 'hot' insulin and the other containing 100 µl insulin assay buffer (IAB), representing controls for total radioactivity and non-specific binding, respectively. The contents of the tubes were mixed and stored at 4 °C overnight. Aliquots of 1 ml of 15 % polyethylene glycol 6000 containing gamma globulin antibody (1 mg/ml Appendix 1) reagents freshly prepared were added to each tube and incubated them for 1 h at room temperature. After incubation, the tubes were centrifuged at 2000 × *g* for 20 min at 4 °C; supernatants were aspirated and the amount of radioactivity was measured of each tube using a gamma counter (2470 Automatic Gamma Counter, Perkin Elmer, USA) using

Wizard 2 software. A standard curve was prepared in order to calculate the insulin content of each tube.

3.2.4.5 Standard curve preparation samples for RIA

A human insulin stock solution (8 ng/ml) prepared in IAB was used to create standard curve points corresponding to 0, 0.25, 0.5, 1, 2, 4, and 8 ng/ml. The standard samples were prepared freshly at the same time as the unknown samples; together the standard samples and unknowns were subjected to RIA processing as described in section 3.2.4.4.

3.2.4.6 RIA data analysis

The RIA data were extracted and the amount of radioactivity expressed as count per minute (CPM). The data were normalised by subtracting the mean control non-specific binding value from treatments and standard curve values. After this, the standard curve relating radioactivity and amount of insulin was prepared and fitted with a non-linear equation. From this, the amount of insulin in each sample was calculated. Data were normalised against number of INS-1 cells after toxin treatment.

3.2.5 Effects of microbial compounds on insulin gene expression

3.2.5.1 Assay insulin gene expression using RT-PCR

Reverse transcription PCR (RT-PCR) was used in order to identify the effect of these compounds on the insulin gene II transcription pathway of the INS-1 cells. INS-1 cells were cultured in 25 cm^2 flasks at 2×10^5 cells/ml and incubated for 24 h and exposed to microbial compounds (Section 3.2.3.1). Total RNA was extracted from each sample using RNA extraction Kit (2.6.1) and RNA samples (10 or 100 ng) were used to create total cDNA (Section 2.6.2). Four set of primers were used to amplify insulin gene and only one set used for β-actin

(Table 3.1). Insulin primers were assayed and one of them was selected to follow the insulin pathway. Amplification protocol achieved as previously mentioned in section 2.6.3.2 and amplified products were analysed on 1.8% agarose gels alongside with suitable molecular size ladder (Section 2.5.6) and images were captured using a Bio-Rad Gel Doc XR+ System. Band intensity was used to verify effects of the microbial secondary metabolites on insulin gene expression. Furthermore, β-actin amplification used as a control for normalization. All products sequences were justified by sequencing prior the actual RT–PCR assay.

3.2.5.2 Assay insulin gene expression using absolute qRT-PCR

qRT-PCR used as well to measure the effect of the sublethal and the lethal concentrations of the microbial compounds on insulin gene transcription. The absolute real time PCR (qRT-PCR) technique was used to measure accurately the expression of insulin subunits. Insulin and β-actin amplicons were produced using Go-Tag polymerase (Section 2.7.1) and cloned into pGEMT-easy (Sections 2.7.2 & 2.7.3) and cloned inserts were justified (Section 2.7.4).

3.2.5.3 Preparation clone standard curve for absolute qRT-PCR

The DNA concentration of recombinant pGEMT-easy produced in section 3.2.5.2 was measured using a fluorometer (Perkin-Elmer LS50B, USA) and the corresponding copy number was calculated using the following equation. The plasmid copy number was measured as copy/ng. Ten-fold serial dilution series of the cloned plasmids, ranging from 5×10^2 to 5×10^6 copies/µl, were used to construct the standard curves for both β-actin and insulin.

$$\text{Plasmid copy number} = \frac{6.02 \times 10^{23} \left(\frac{\text{copy}}{\text{mol}}\right) \times \text{DNA amount(g)}}{\text{DNA length(dp)} \times 660 \left(\frac{\frac{\text{g}}{\text{mol}}}{\text{dp}}\right)}$$

Table 3.1: Primer sequences, product size and position using to amplify insulin and β-actin gene designed by this study.

Target gene	Primers 5-3	length	Primer position	Product size (bp)
INS1-F	TCT TCT ACA CAC CCA AGT CCC G	22	186-208	103
INS1-R	AGT GCC AAG GTC TGA AGA TCC	22	289-277	
INS1m-F	GCC CTG CTC GTC CTC TGG GA	20	78-97	332
INS1m-R	CAT TGC AGA GGG GTG GGC GG	20	409-390	
INS2-F	AAA CAG CAC CTT TGT GGT TCT CA	23	78-101	115
INS2-R	GTG CCA CTT GTG GGT CCT CC	20	193-177	
INS2m-F	GAT CCG CTT CCT GCC CCT GC	20	12-31	203
INS2m-R	GGC CTC CAC CCA GCT CCA GT	20	214-195	
β-actin-F	AGG CCC AAG AGC AAG AGA G	19	251-269	332
β-actin-R	CCT CGTAGA TGG GCA CAG T	19	583-574	

3.2.5.4 Assay insulin gene expression and machine setting

Triplicates of each sample were prepared in 48 well PCR plates, each well containing 12.5 µl of SYBR green master mix, 0.5 µl each of forward and reverse primers (10µM), 0.25 µl reference dye, 9.5 µl water and 2 µl cDNA. PCR reaction achieved using following condition denaturant cycle at 94 °C for 2 min followed by 40 cycles, single cycle 94 °C 30 for 15 sec, annealing 60 °C for 30 sec and amplification at 72 °C for 30 sec. Followed with melting cycle 94 °C for 15 sec and 60 °C for 1 min and 94 °C for 30 sec the products were detected using an Applied Biosystems Step One real time PCR instrument and software v2.1. The copy number data were collected and normalized using the β-actin data before statistical analysis.

3.2.5.5 qRT-PCR DATA normalization

The Data was collected for insulin and normalised with β-actin gene expression data as the β-actin as described in section 2.6.7.

3.2.6 Measurement of INS-1 intracellular Ca^{2+} concentration

The INS-1 cells were cultured in 25 ml flasks at a density of 2×10^5 cells/ml, and after 24 h incubation at 37 °C and 5% CO_2, the cells were exposed to 0, 10 or 100 ng/ml phenazine or pyrrolnitrin, and incubated for 24 h. Next, the cells were trypsinised and centrifuged at 50 × *g* for 10 min followed by two washes with PBS containing 1 µM EDTA to remove surface Ca^{2+}. Afterwards, 1×10^6 cells were lysed using 2 ml nitric acid (0.1 M) in a fresh polypropylene tube and incubated for 1 h at 70 °C. The Ca^{2+} content was immediately measured using Inductively Coupled Plasma-Atomic Emission Spectrometry (ICP-AES) Varian 725-ES -2007 (Australia) as described by Burke and Handy (2005).

3.2.7 Patch-clamp electrophysiology of INS-1 cells

INS-1 cells were grown on circular cover slips (10 mm diameter; Nunc, UK) in 6 well plates at a seeding density of 2×10^5 cells/ml, incubated for 24 h and then exposed to the 10 or 100 ng/ml phenazine or pyrrolnitrin as described above. The cover slips were then placed on recording chambers as described by Hamill *et al.* (1981). The cells were studied using the patch clamp technique at room temperature and were perfused continuously with the external buffer (160 mM NaCl, 4.5 mM KCl, 1.8 mM $CaCl_2$, 10 mM Hepes, 1 mM $MgCl_2$ and 3 mM glucose, pH 7.2), flowing at a constant rate of 0.8 ml/min to avoid any mechanical disturbance during the experiments. The volume of the chamber was maintained at 1 ml. The whole-cell patch-clamp recording technique was used to obtain tight seal, patch-clamp recordings from individual INS1 cells. These were viewed under an inverted Zeiss microscope (Axiovert 135) with a ×60 objective lens, and equipped with a video imaging system (Hitachi). The patch pipettes were pulled using a vertical Narishige puller (PC-10) from borosilicate glass capillaries (Harvard Apparatus, 1.5 mm external diameter, 1.17 mm internal diameter) and had tip resistances of between 2 and 3 MΩ when filled with the potassium-based internal solution. Recordings were obtained by lowering a patch electrode directly onto an individual INS-1 cell while monitoring current response to 5 mV voltage pulses and then applying suction to form a 1 GΩ seal. A multiclamp 700B amplifier (Molecular Devices Inc., USA) was used for the recordings and Pclamp 9.2 software (Molecular Devices Inc., USA) for data collection, storage and analysis. Recorded signals were low-pass filtered at 5 kHz. The pipette series resistance was electronically compensated (usually to 90%); thus, voltage errors of only few millivolts occurred at peak current levels. Liquid junction potential (Vlj) between the

whole-cell pipette solution and the bath solution was calculated to be 4.8 mV using the liquid junction calculator provided by Molecular Devices and incorporated into the analysis of the current/voltage curves. The internal solution contained 120 mM KCl, 20 mM KF, 10 mM EGTA, 10 mM Hepes, 2 mM MgATP. The pH was adjusted to 7.2 with KOH. Recordings were terminated whenever a significant increase (10%) in series resistance occurred. The whole-cell capacitances of the INS 1 cells ranged from 3.0 pF to 15.0 pF, with a mean value of 8.27 ± 3.11 pF (n = 23).

3.2.8 Statistical analysis

All the data were analysed using SPSS version 17 statistical software, using one way analysis of variance (ANOVA) and multiple comparison post hoc tests (Fisher's LSD). Data are shown as means +/- SE and $P < 0.05$ is considered significant.

3.3 Results

3.3.1 Cytotoxic effects of microbial compounds on INS-1 cells

The effects of three microbial compounds, pyrrolnitrin, phenazine and patulin, on the viability of the β-pancreatic cell line, INS-1, were investigated. INS-1 cells were exposed to various concentrations of the purified microbial compounds as described in Materials & Methods. Their cytotoxicity was measured using a trypan blue exclusion test at three time points, 2, 24 and 72 h. None of the compounds showed toxicity after 2 h exposure at the concentrations tested (0-10000 ng/ml), except for the highest concentration of patulin where there was significant decrease in viability compared to the untreated control (Figure 3.4). After longer exposure, INS-1 cells showed different responses to each of these microbial compounds. At 24 h, 10000 ng/ml pyrrolnitrin was toxic to INS-1 cells, but by 72 h concentrations ≥ 100 ng/ml caused a decline in cell viability (Figure 3.2). Of the three compounds tested patulin was the most toxic; after both 24 h and 72 h exposure concentrations ≥ 10 ng/ml caused significant cell death, with complete loss of viability at 10000 ng/ml (Figure 3.4). In the case of phenazine after 24 h exposure concentrations ≥ 100 ng/ml caused a small but significant loss of viability with > 60% cell survival at 10000 ng/ml (Figure 3.3). However, after 72 h 10000 ng/ml phenazine was the only concentration where significant loss of viability was detected, indicating that the cytotoxicity of phenazine had declined between 24 and 72 h.

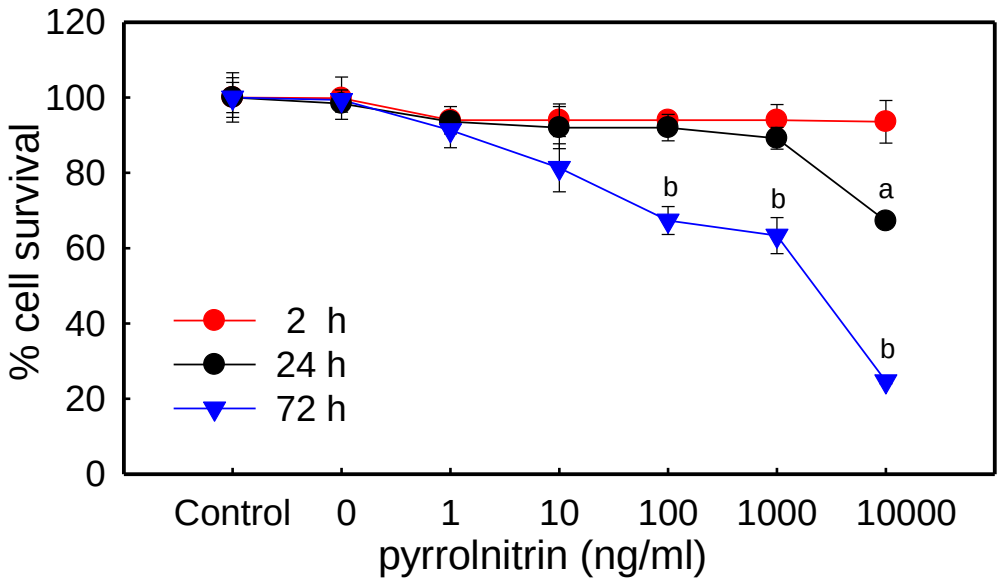

Figure 3.2: Cytotoxicity of pyrrolnitrin to INS-1 cells, at the times indicated. In each case cell survival is expressed relative to the appropriate vehicle control (ethanol) at the relevant time. The values are means ± S.E. (n = 3). The letters a and b indicate statistically significant difference (p < 0.05) relative to the appropriate control at 24 h and 72 h, respectively.

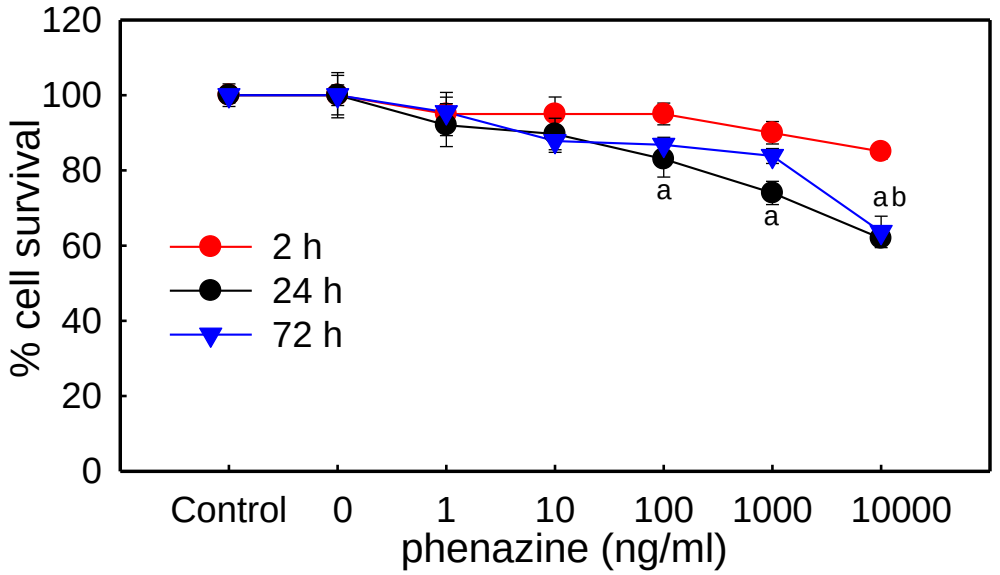

Figure 3.3: Cytotoxicity of phenazine to INS-1 cells, at the times indicated. In each case cell survival is expressed relative to the appropriate vehicle control (acetone) at the relevant time. The values are means ± S.E. (n = 3). The letters a and b indicate statistically significant difference (p < 0.05) relative to the appropriate control at 24 h and 72 h, respectively.

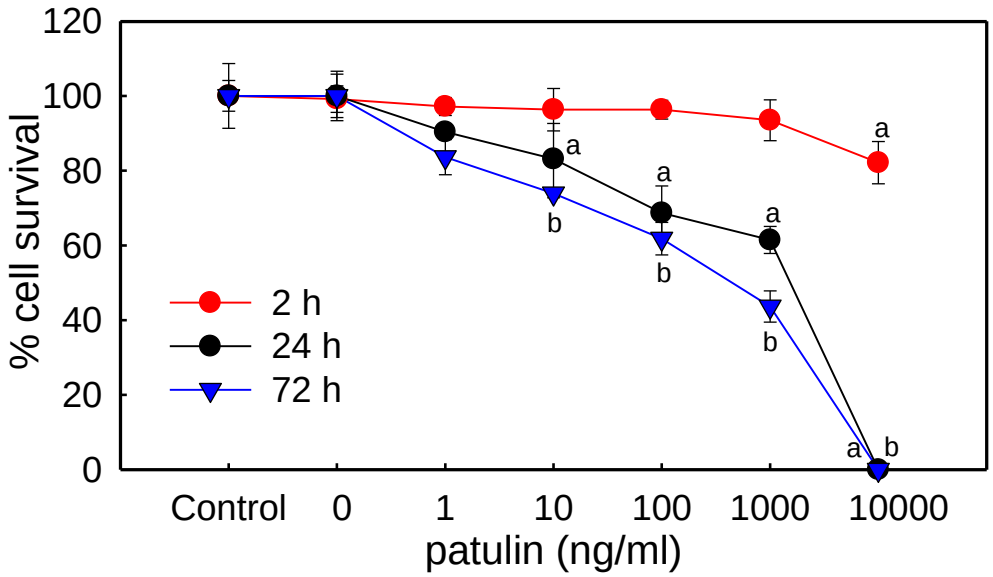

Figure 3.4: Cytotoxicity of patulin to INS-1 cells, at the times indicated. In each case cell survival is expressed relative to the appropriate vehicle control (water) at the relevant time. The values are means ± S.E. (n = 3). The letters a and b indicate statistically significant difference ($p < 0.05$) relative to the appropriate control at 24 h and 72 h, respectively.

3.3.2 Cytotoxic effects of *B. multivorans* and *Ps. aeruginosa* supernatants (BMS & PAS) to INS-1

The toxicity of supernatants from culture of both *B. multivorans* and *Ps aeruginosa* to INS-1 cells was tested. The results showed that both types of the supernatants had no significant effect on INS-1 cells viability after 2 h at any tested volume. Exposure to BMS at 6 and 10 µl/ml had a significant toxic effect on INS-1 cells after 24 and 72 h (Figure 3.5 A.), whereas, PAS at 6 and 10 µl/ml showed toxicity to INS-1 cells after 72 h, but with no toxicity after 24 h except at 10 µl/ml (Figure 3.5 B). It was also found that the toxicity of BMS was greater than that of PAS, as BMS showed maximum toxicity after 72 h producing 40% cell death compared with PAS which produced 20% cell death after 72 h.

A

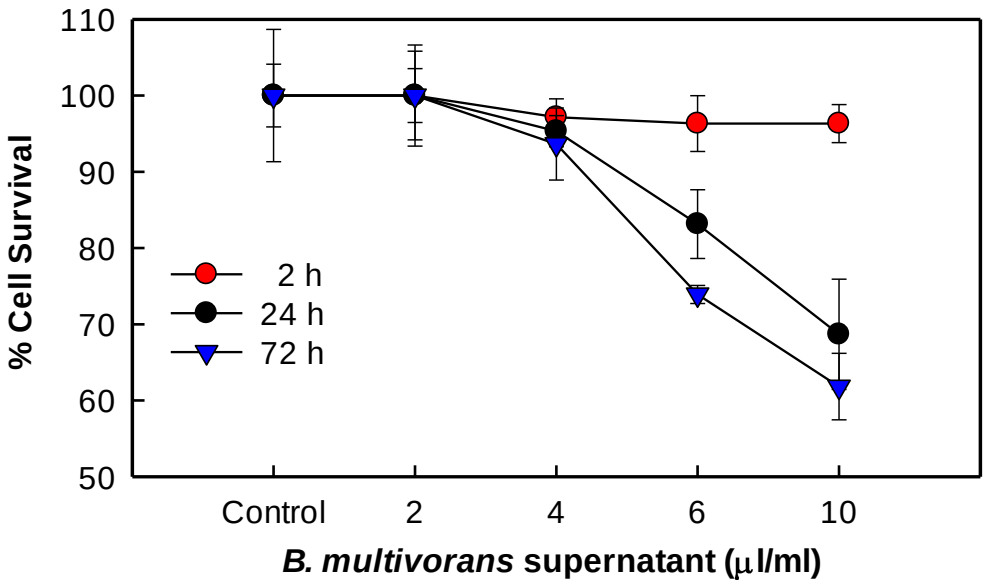

B

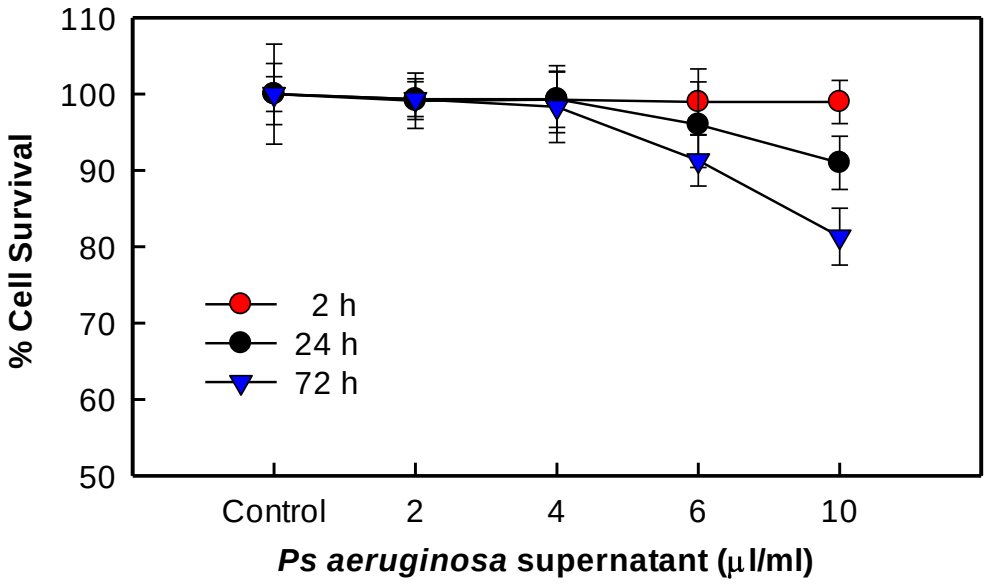

Figure 3.5: Cytotoxicity of BCS and PAS (A, B, respectively) to INS-1 cells, at the times indicated. In each case cell survival is expressed relative to the appropriate vehicle control (LB medium) at the relevant time. The values are means ± S.E. (n = 3), ***** statistically significant difference ($p < 0.05$) relative to the appropriate control at 24 h and 72 h, respectively.

3.3.3 Effects of microbial compounds on insulin secretion by INS-1 cells after 2 h of exposure

In a preliminary experiment INS-1 cells were tested for glucose stimulated insulin secretion (GSIS), i.e. that the cells responded properly to glucose increases; 0.6 ng/ml of insulin was produced by INS-1 cells after stimulation with 2 mM glucose, whereas, the secreted insulin increased to at least 2 ng/ml with 20 mM glucose, which is about 3 times compared to 2 mM glucose (Figure 3.6). Furthermore, INS-1 treated with the stimulation factor KCl also secreted insulin at about 2 ng/ml.

The effects of the microbial compounds on insulin production by INS-1 cells were also investigated as described in the materials and methods (Sections 3.2.4.). Initially, cells were exposed for 2 h to the same range of concentrations of each microbial compound as described above (Sections 3.2.4.2). The secretion of insulin was then measured after exposure of the cells to either 2 mM or 20 mM glucose for 1 h. Under these conditions the microbial compounds had no significant effect on insulin secretion compared with controls (Figure 3.6) although in all cases 20 mM significantly stimulated insulin secretion compared to 2 mM.

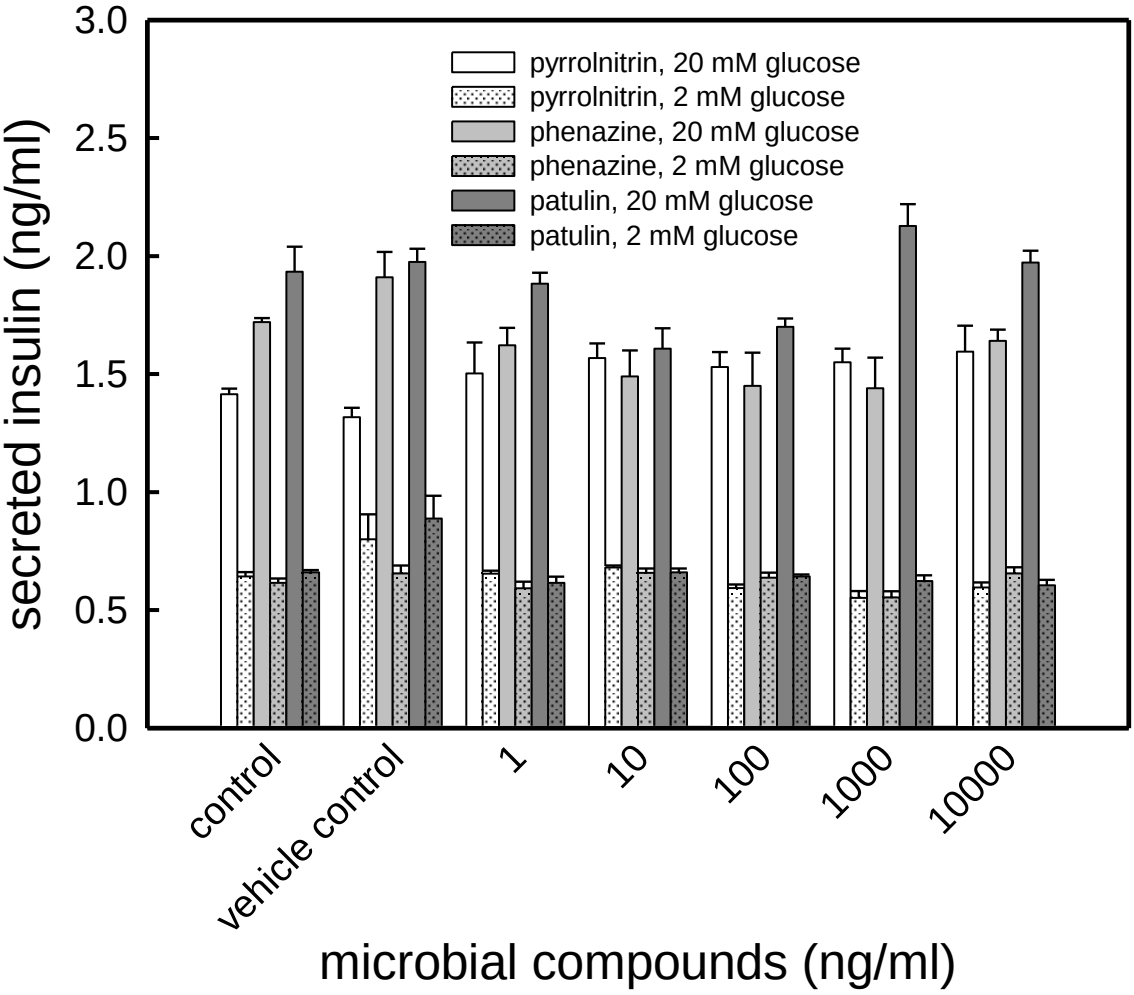

Figure 3.6: Effects of exposure of INS-1 cells for 2 h to pyrrolnitrin, phenazine or patulin on glucose-stimulated insulin secretion (stimulation with 20 mM versus 2 mM glucose, as indicated; see materials and methods (Section 3.2.4.2). The data shown are means ± S.E. (n = 4). Statistical analysis (ANOVA) showed no significant pattern of differences versus the appropriate vehicle control ($p \leq 0.05$). However, in all cases there was a significant increase in insulin secretion with 20 mM glucose compared to 2 mM glucose ($p \leq 0.05$).

3.3.4 Effects of microbial compounds on insulin secretion by INS-1 cells after 24 h of exposure

The effects of the microbial compounds on insulin production by INS-1 cells were assessed using sub-lethal concentrations of the microbial compounds at 24 h exposure time, i.e. cells were exposed for 24 h to a range of concentrations of each compound up to and including the lowest concentration that produced toxicity as described above (Section 3.2.4.3). The same glucose stimulation conditions were used.

In this case all three microbial compounds had no significant effect on INS-1 insulin secretion with a low concentration (2 mM) except for phenazine at 100 ng/ml, which caused a slight reduction in insulin secretion (Figure 3.8), but effects were seen on insulin secretion with 20 mM glucose. Pyrrolnitrin at 10 and 100 ng/ml caused a significant increase in secreted insulin but with 10000 ng/ml (a toxic concentration) there was significant inhibition of insulin secretion with 20 mM glucose (Figure 3.7). Phenazine, at 1 ng/ml, 10 ng/ml and 100 ng/ml (a toxic concentration) caused a significant increase in insulin secretion with 20 mM glucose (Figure 3.8), whereas patulin at 10 and 100 ng/ml (a toxic concentration) caused a significant reduction of insulin secretion per live cell with 20 mM glucose (Figure 3.9).

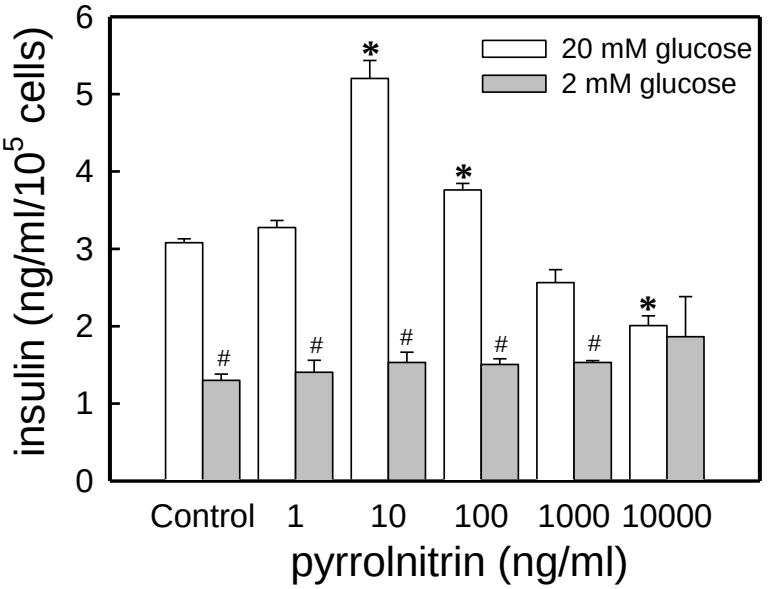

Figure 3.7: Effects of exposure of INS-1 cells for 24 h to pyrrolnitrin on GSIS (stimulation with 20 mM versus 2 mM glucose). The data shown are means ± S.E. (n = 4). * indicates significant differences ($p < 0.05$) compared to the vehicle control at that concentration of glucose. # indicates significantly lower ($p < 0.05$) insulin secretion with 2 mM glucose compared to that obtained with 20 mM glucose.

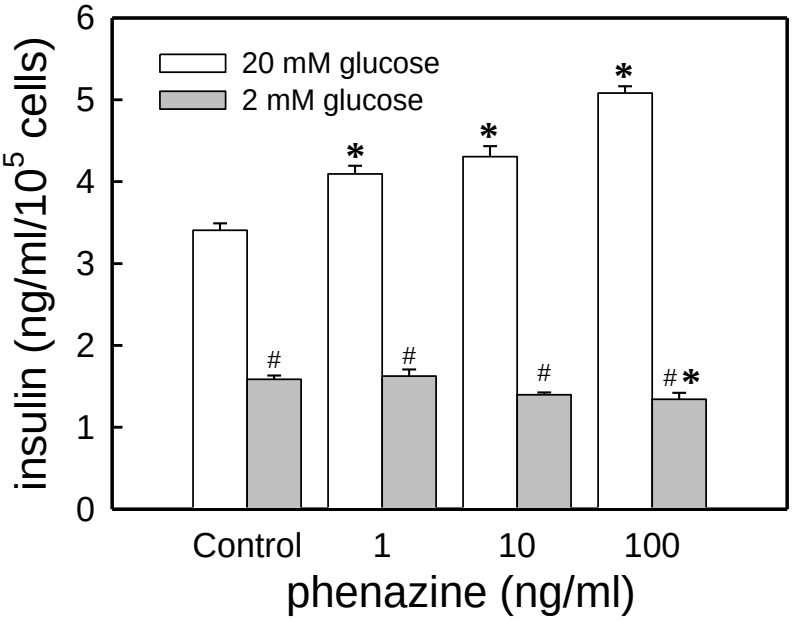

Figure 3.8: Effects of exposure of INS-1 cells for 24 h to phenazine on GSIS (stimulation with 20 mM versus 2 mM glucose). The data shown are means ± S.E. (n = 4). * indicates significant differences ($p < 0.05$) compared to the vehicle control at that concentration of glucose. # indicates significantly lower ($p < 0.05$) insulin secretion with 2 mM glucose compared to that obtained with 20 mM glucose.

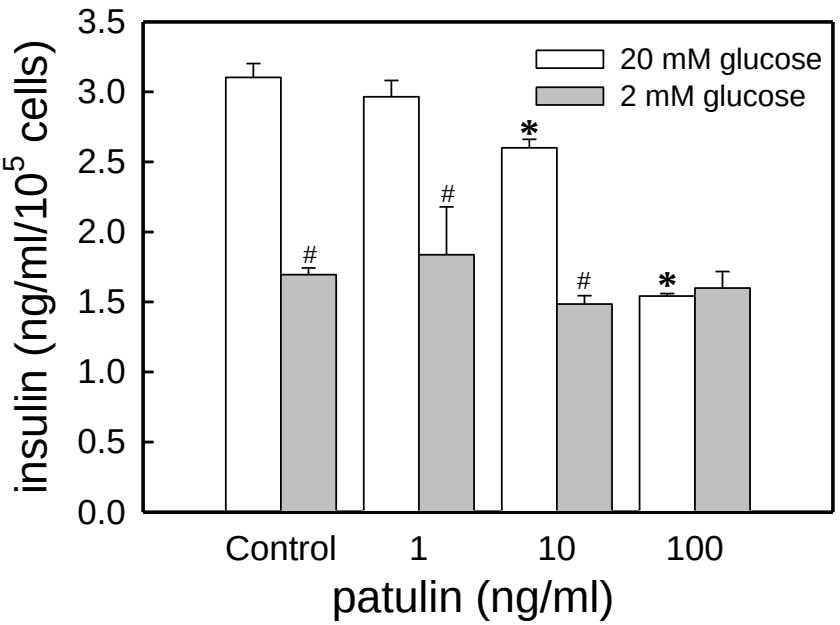

Figure 3.9: Effects of exposure of INS-1 cells for 24 h to patulin on GSIS (stimulation with 20 mM versus 2 mM glucose). The data shown are means ± S.E. (n = 4). * indicates significant differences ($p < 0.05$) compared to the vehicle control at that concentration of glucose. # indicates significantly lower ($p < 0.05$) insulin secretion with 2 mM glucose compared to that obtained with 20 mM glucose.

3.3.5 Effect of microbial compounds on insulin gene expression

3.3.5.1 Amplification and cloning of insulin and β-actin amplicons

RT-PCR was performed to measure the effects of the microbial compounds on insulin gene expression in INS-1 cells. Three of four primer sets (described in material and methods in section 3.2.5.1), Ins1, Ins-2, Ins-2m, which were designed to detect mature mRNA for the insulin gene, successfully produced amplicons at the expected sizes, 103, 115 and 203 bp, respectively, and 352 bp for β-actin (Figure 3.10 A), whereas, the primer INS-1m failed in amplification. The insulin amplicons produced by Ins-2m, and β-actin amplicon were successfully cloned into pGEMT-easy producing recombinant plasmids pM1 and pM2 (Figure 3.10 B). Excision of recombinant plasmids containing the insulin and β-actin amplicons using restriction enzymes produced inserts of the right size, 200 and 350 bp, respectively, after running on an agarose gel (Figure 3.10 B).

Recombinant plasmids with inserts have been sequenced after cloning and Blast results with the sequences clearly show that these inserts are cDNA of rat insulin II and β-actin genes (accession numbers NM 019130 and NM_031144.2, respectively) confirming that the right inserts were used in this study. The recombinant plasmid copy number was determined spectrophotometrically assuming that there is 1×10^6 insulin or β-actin gene copy/ng DNA. The plasmid stock was used to prepare a standard curve for qRT-PCR.

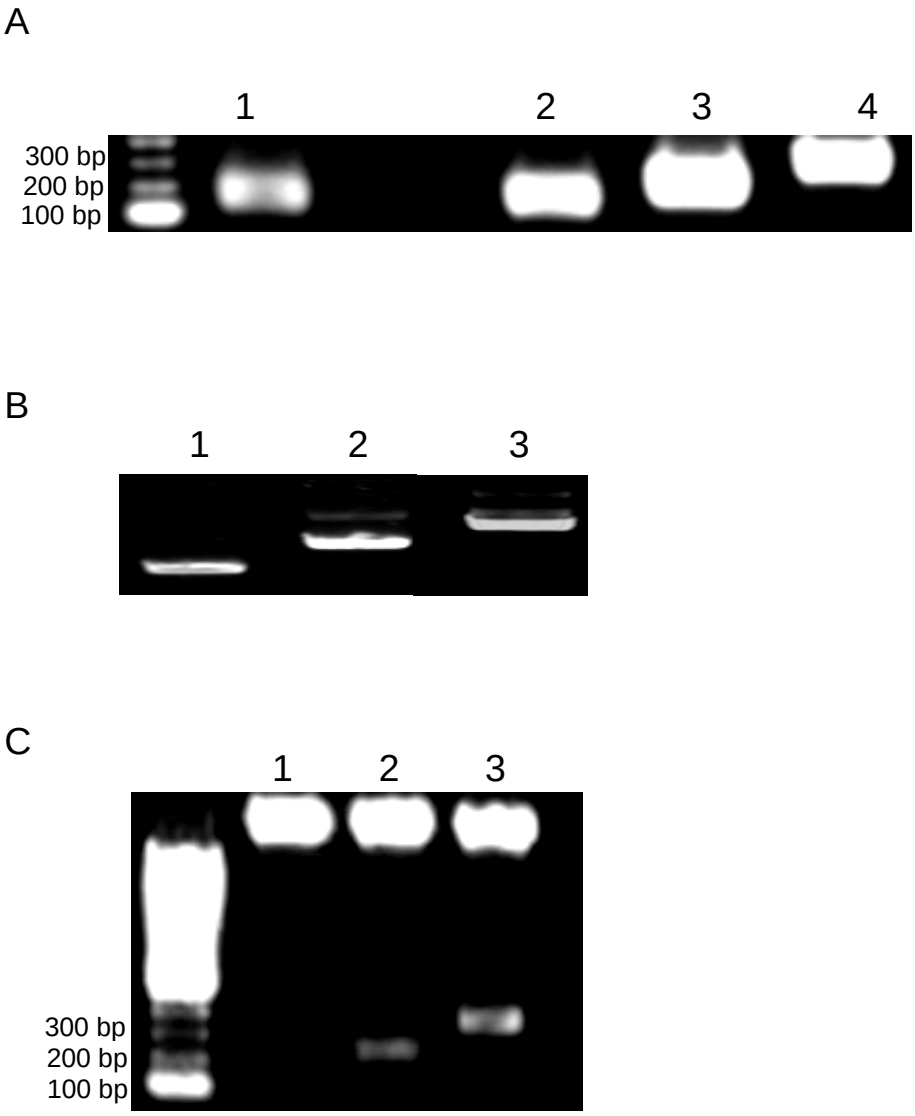

Figure 3.10: Amplification and cloning of insulin and β-actin amplicons into pGEMT plasmid: (A) RT-PCR of insulin (lanes 1, 2, 3 and 4) and β-actin (lane 5). (B) The recombinant plasmids pM1 and pM2 containing the insulin and β-actin amplicons, respectively (lanes 2 & 3) compared with non-recombinant pGEMT-easy (lane 1), (C) excision of recombinant plasmids pM1 (lane 2) and pM2 (lane 3) compared to excision of non-recombinant pGEMT-easy.

3.3.5.2 Insulin gene expression using absolute qRT-PCR

The results of RT-PCR showed bands of the expected size and the amplified insulin cDNA bands showed highest intensity after treatment with 10 or 100 ng/ml pyrrolnitrin after 24 h exposure, but only showed a faint band at the toxic concentration of 10000 ng/ml (Figure 3.11). Phenazine treatment increased the band intensity with increasing phenazine concentration even at the toxic concentration (100 ng/ml) compared to the control treatment (Figure 3.12). However, treatment of INS-1 cells with patulin had no effect on insulin mRNA levels (Figure 3.13).

The influence of these compounds on transcription was confirmed by qRT-PCR. The insulin mRNA was measured after exposure of the INS-1 cells to these compounds and the cDNA samples subjected to qRT-PCR. The melt curve analysis of insulin and β-actin products showed single peaks at the expected melting temperatures. Pyrrolnitrin in the concentration range 10-1000 ng/ml significantly up regulated insulin gene expression but a significant decrease was seen at the toxic concentration (10000 ng/ml) (Figure 3.10). In the case of phenazine, concentrations in the range 1-100 ng/ml caused an increase in transcription (Figure 3.12). The maximal increase in insulin gene transcription in each case after 24 h exposure was with 10 ng/ml pyrrolnitrin and with 100 ng/ml phenazine, respectively. Patulin showed no effect on the transcription of the insulin gene at any concentration including the toxic concentration (100 ng/ml) (Figure 3.13).

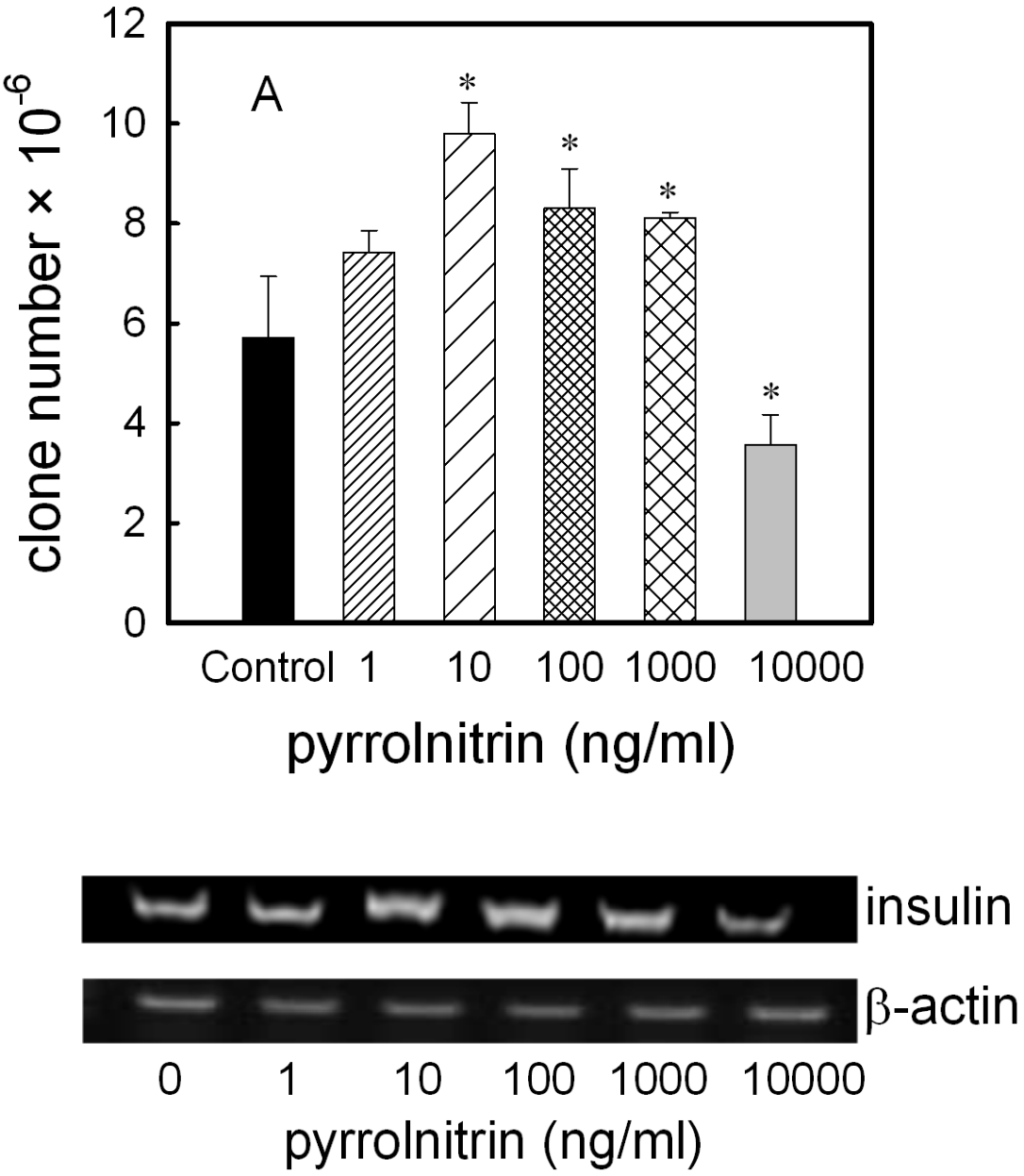

Figure 3.11: Insulin gene expression in INS-1 cells after 24 h exposure to pyrrolnitrin. (A) The number of copies of amplified cDNA of insulin gene II after reverse transcription of INS-1 RNA measured by qRT-PCR. Data shown are means ± S.E. (n = 3), normalised against β-actin as a housekeeping gene. * indicates significant differences relative to the vehicle control ($P \leqslant 0.05$). (B) gel-based RT-PCR for amplified cDNA of insulin gene II; β-actin is again used as the housekeeping gene.

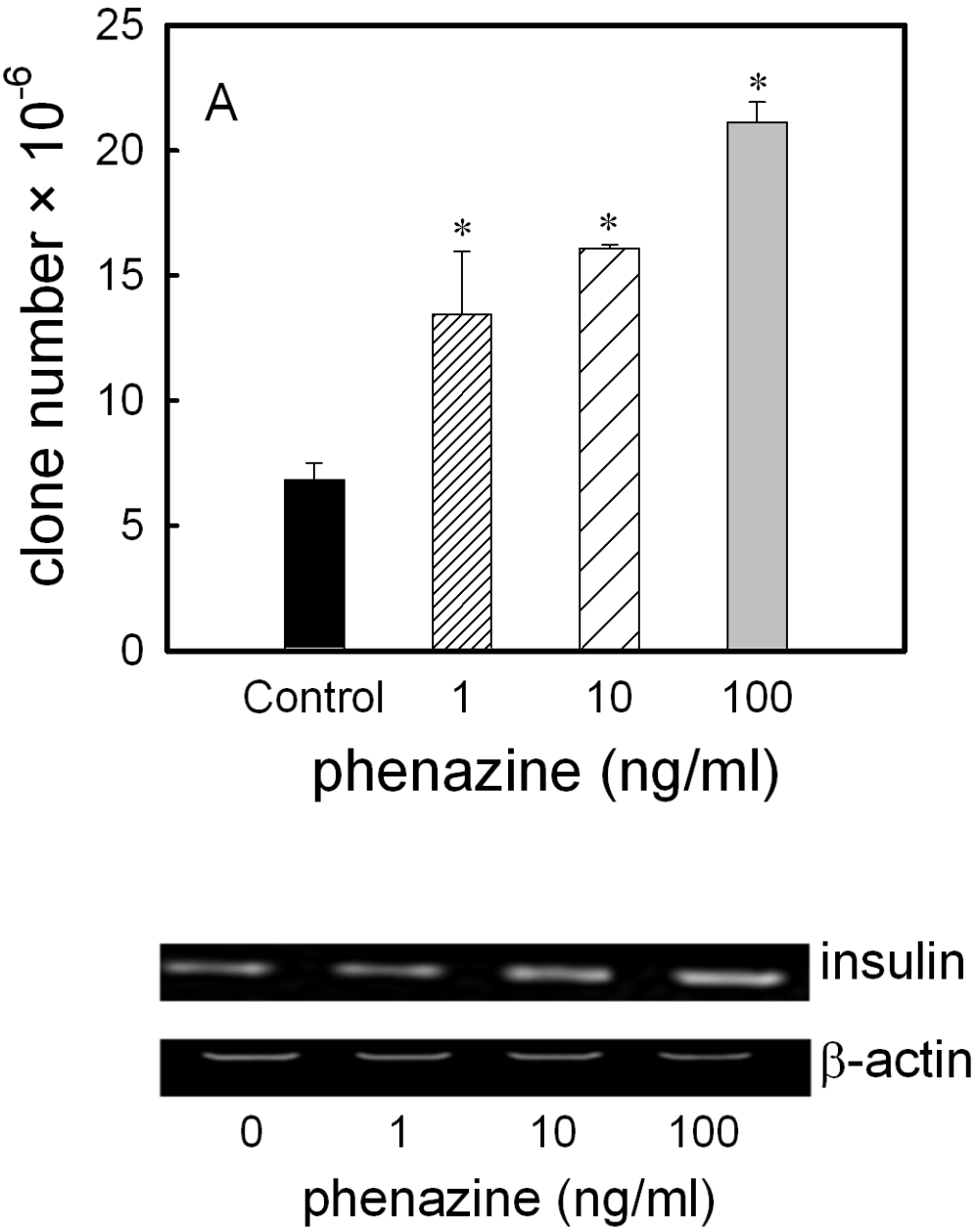

Figure 3.12: Insulin gene expression in INS-1 cells after 24 h exposure to phenazine. (A) The number of copies of amplified cDNA of insulin gene II after reverse transcription of INS-1 RNA measured by qRT-PCR. Data shown are means ± S.E. (n = 3), normalised against β-actin as a housekeeping gene. * indicates significant differences relative to the vehicle control ($P \leqslant 0.05$). (B) gel-based RT-PCR for amplified cDNA of insulin gene II; β-actin is again used as the housekeeping gene.

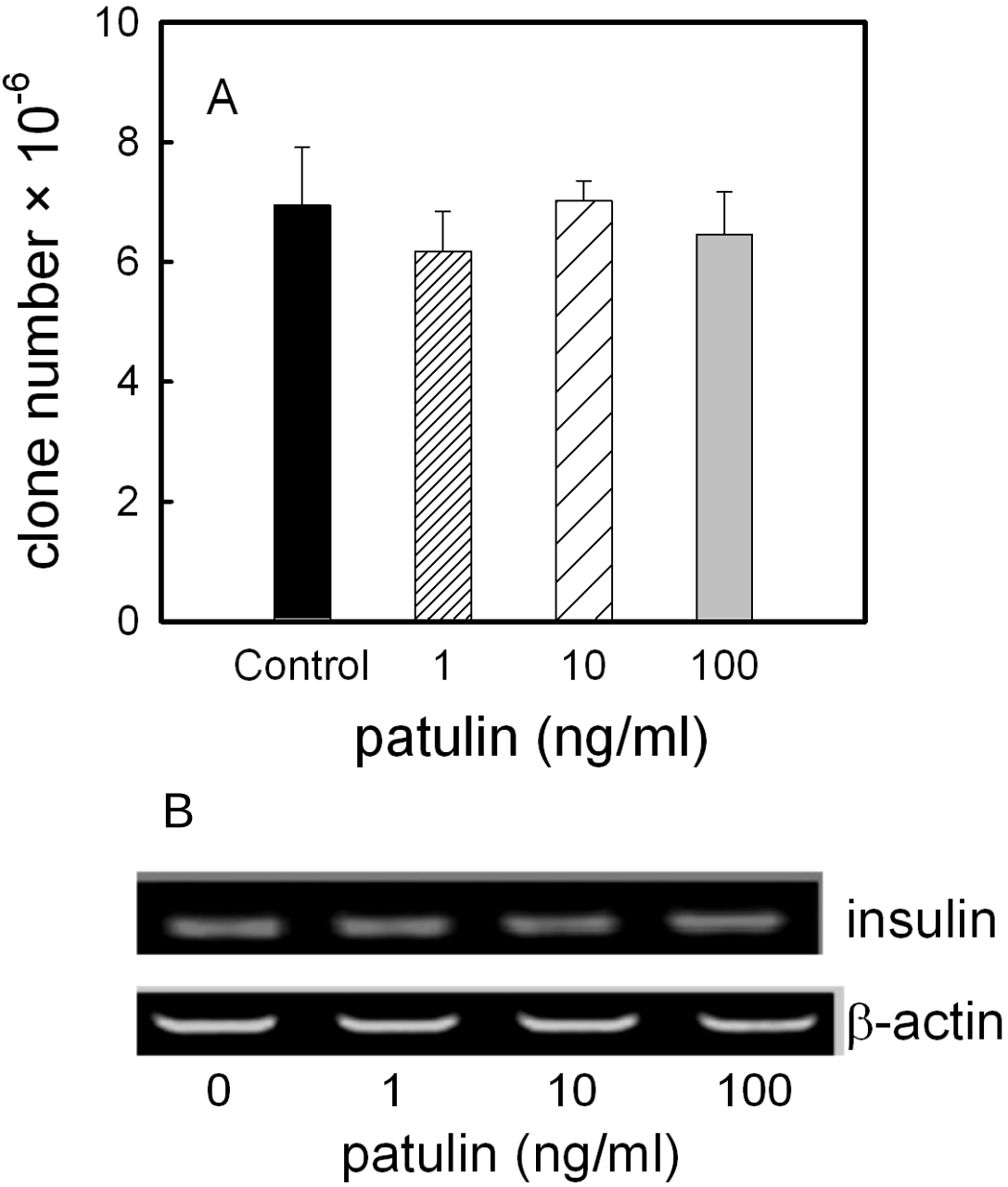

Figure 3.13: Insulin gene expression in INS-1 cells after 24 h exposure to patulin. (A) The number of copies of amplified cDNA of insulin gene II after reverse transcription of INS-1 RNA measured by qRT-PCR. Data shown are means ± S.E. (n = 3), normalised against β-actin as a housekeeping gene. * indicates significant differences relative to the vehicle control ($P \leqslant 0.05$). (B) gel-based RT-PCR for amplified cDNA of insulin gene II; β-actin is again used as the housekeeping gene.

3.3.6 Measurement of intracellular Ca^{2+} levels in INS-1 cells

Intracellular Ca^{2+} signalling pathways play a vital role in β-cell function and insulin secretion, so the Ca^{2+} content was measured to establish the effect of each of the microbial compounds under test on insulin secretion, resulting from changes in intracellular Ca^{2+} levels. Both pyrrolnitrin and phenazine induced similar and significant increases in intracellular Ca^{2+} in INS-1 cells at 10 and 100 ng/ml concentrations after 24 h exposure (Figure 3.14). The highest levels of Ca^{2+} were seen after exposure of INS-1 cells to 100 ng/ml phenazine.

3.3.7 Patch-clamp electrophysiology of INS-1 cells

At least six INS-1 cells were patch clamped after a 24 h exposure to pyrrolnitrin or phenazine (10 or 100 ng/ml) study and compared to the same number of control cells. The outward current was recorded in response to 600 ms pulses ranging from -60 to 100 mV with a 10 mV increment from a holding potential of -60 mV. The first statistically significant differences in the outward current were detected at 0 mV between control and treated cells. Pyrrolnitrin significantly reduced the outward current compared to the control (Figure 3.15 A & B). Furthermore, the membrane current inhibition was significantly higher after exposure to pyrrolnitrin using both concentrations in comparison to the control. In the case of phenazine, there was no significant difference in membrane current after exposure to 10 ng/ml, whereas, exposure to 100 ng/ml clearly induced a significant inhibition of the outward current compared to that of the control. Exposure to phenazine at 100 ng/ml produced the highest inhibition of current seen (Figure 3.15 C& D).

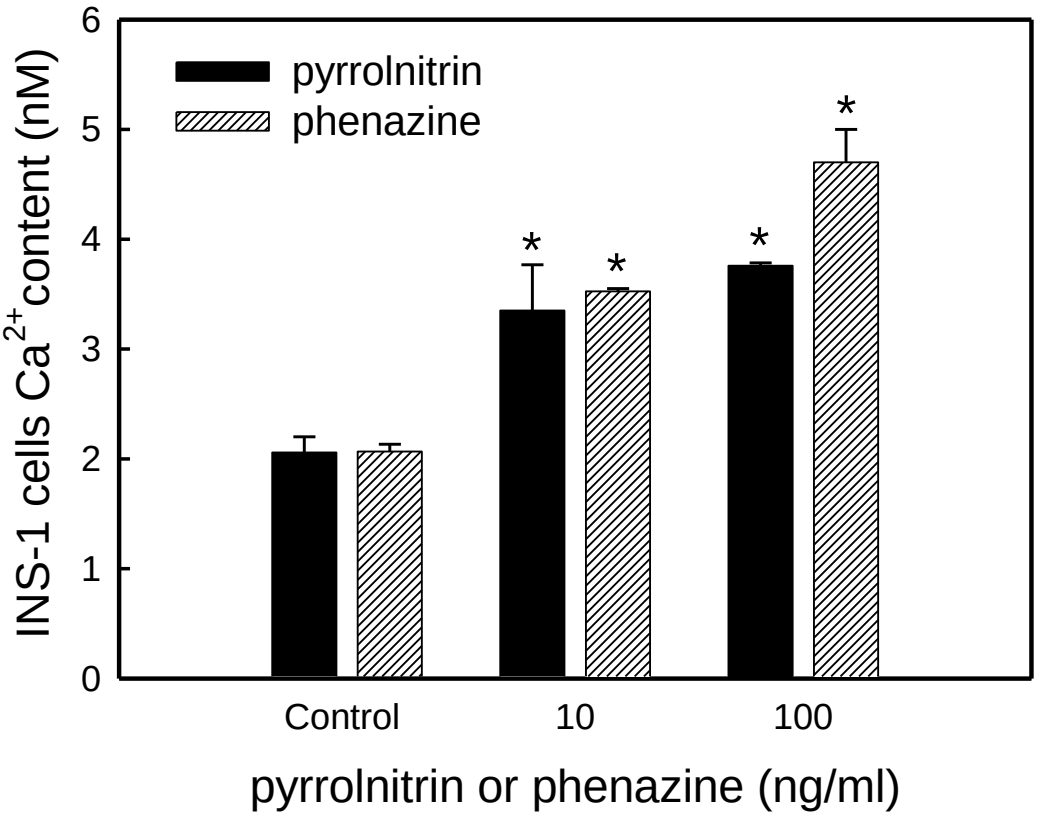

Figure 3.14: Pyrrolnitrin or phenazine increased the intracellular Ca^{2+} levels in INS-1 cells after exposure for 24 h in the presence of 11 mM glucose. The data are means ± S.E. (n = 4) * indicates significant difference compared to the vehicle control ($P \leqslant 0.05$).

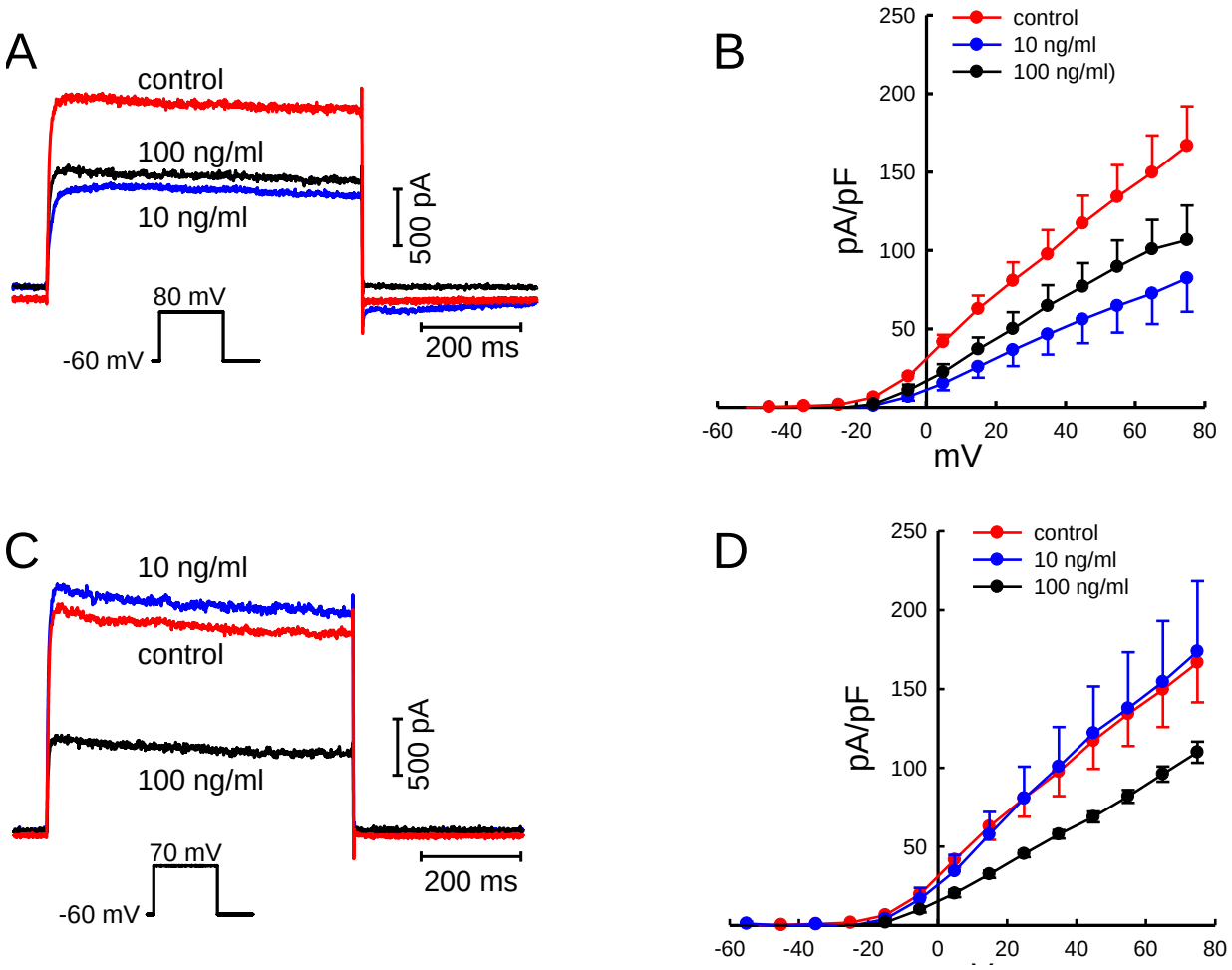

Figure 3.15: Effects of pyrrolnitrin or phenazine on membrane current of patch-clamped INS-1 cells. A & C: whole cell outward currents from representative INS-1 cells in response either to a voltage step of +80 mV from a holding potential of -60 mV (A) or to a voltage step of +70 mV from a holding potential of -60 mV (C). The INS-1 cells had been pre-exposed for 24 h to solvent (vehicle control), 10 ng/ml or 100 ng/ml (as indicated) pyrrolnitrin (A) or phenazine (C). B & D: I-V plots of the instantaneous outward currents ~ 400 ms after the start of the voltage step for the whole cell outward current after cells had been pre-exposed to solvent (vehicle control), 10 ng/ml or 100 ng/ml (as indicated) pyrrolnitrin (B) or phenazine (D). The data shown are the means for six cells.

3.4 Discussion

In this study the effects of three microbial products, pyrrolnitrin, phenazine and patulin, on INS-1 pancreatic β-cells was determined in terms of both toxicity and modulation of insulin production. The aim was to provide evidence in support of a possible link between prolonged exposure to such compounds and pancreatic β-cell death, with the possibility of individuals developing diabetes having had long-term infection with phenazine- or pyrrolnitrin-producing microorganisms such as *Pseudomonas spp.* and *Burkholderia spp*. This is of particular relevance in people suffering from cystic fibrosis (CF) who have a high rate of infection by such organisms (Govan and Deretic, 1996; Allice *et al.*, 2006). The inclusion of the fungal toxin patulin also raises the possibility of contaminated food as another source of such β pancreatic cytotoxins (Artigot *et al.*, 2009).

Patulin at 10 µg/ml was toxic to INS-1 cells within 2 h of exposure (Figure 3.4). This acute toxicity of patulin has already been demonstrated against various mammalian cells and has been attributed to its ability to inhibit RNA and protein synthesis, and also to interfere with the activity of many enzymes such as glycogen phosphorylase, glucose-6-phosphatase, hexokinase and aldolase that are considered crucial for cell survival (Wouters and Speijers, 1995). Genotoxic and neurotoxic effects of patulin have also been demonstrated (Zhou *et al.*, 2010). Patulin is widely found in normal food products such as fruit juice and cider, and particularly in products sourced from apples infected with toxin-producing fungi. The World Health Organization (WHO) and some countries have established a safety level of 50 µg/l of patulin in apple juice (CAST, 2003). A previous study showed diabetogenic effects of patulin where 10 doses of 0.1

mg injected into albino mice caused a 60% increase in blood glucose levels (Madiyalakan and Shanmugasundaram, 1978).

Phenazine showed a different pattern of toxicity at up to 10 µg/ml, it had no effect on the viability of INS-1 cells after 2 h exposure. Nevertheless, significant toxicity was seen after 24 h exposure to 0.1-10 µg/ml phenazine (Figure 3.3). Consistent with this, some phenazine derivatives are known to affect human cell proliferation. For example, pyocyanine inhibits epidermal cell growth and lymphocyte proliferation (Wilson *et al.*, 1988; Kanthakumar *et al.*, 1993), and causes neutrophil apoptosis (Allen *et al*., 2005) in addition to necrosis of respiratory epithelial cells. Another derivative, phenazine carboxylic acid, may modulate production of the cytokine IL-8 (Denning *et al.*, 2003; Look *et al.*, 2005). These effects of phenazine and its derivatives are likely to be related to their ability to catalyse superoxide production, and hence hydrogen peroxide production, via redox cycling, thus causing oxidative stress and cell injury (Ran *et al.*, 2003; Reszka *et al.*, 2004). The concentration of phenazine and its derivatives can reach 27 µg/ml in sputa from CF patients (Wilson *et al*., 1988), and hence phenazine is being considered to be an important virulence and pro-inflammatory factor which can lead to acute pneumonia in CF patients with chronically infected lungs.

Pyrrolnitrin only showed toxicity at a high concentration (10 µg/ml) after 24 h (Figure 3.2), indicative of low toxicity of this compound in comparison to patulin and phenazine. Moreover, the highest toxicity of pyrrolnitrin to INS-1 cells was only seen after 72 h. Pyrrolnitrin is known to show toxicity against microorganisms, particularly fungi and *Streptomyces* spp. (El-Banna and

Winkelmann, 1998; Hwang *et al.*, 2002), by inhibition of mitochondrial electron transfer, but little is known about the toxicity of pyrrolnitrin to mammalian cells.

The toxicity of supernatants (spent medium) from *B. multivorans and P. aeruginosa* cultures (BMS & PAS, respectively) was tested in order to assess whether there might be other toxic compounds in addition to phenazine and pyrrolnitrin. The aim of this experiment was to find compounds produced by both bacteria which could cause high toxicity at lower levels via inhibition of key *in vivo* β-cells signals, e.g. inhibition of insulin receptor, and consequently glucose metabolism and glucose uptake, leading to β-cells apoptosis. The results showed that both of BMS & PAS had toxicity at high concentrations and longer exposure times suggesting that the toxicity that results from both type of supernatants could be related to the general cytotoxic material such as lipases, proteases and ribosylating compounds. In case of BMS the toxicity was stronger than PAS probably because the nitrite and nitrate compounds that are produced extensively by *Burkholderia* spp as secondary products, such as NO_3^-, and NO_2^- (Major *et al.*, 2010) are major toxicants to pancreatic β-cells produced during the inflammatory immune responses and recently have been correlated in instigating T1D (MacFarlane *et al.*, 2003; Biros *et al.*, 2005).

As well as toxicity, these compounds have been shown for the first time to have effects on glucose-stimulated insulin secretion in INS-1 cells. Pyrrolnitrin at 10 and 100 ng/ml caused a potentiation of glucose-stimulated insulin secretion, but at 10000 ng/ml significantly inhibited it, indicating two modes of action dependent on concentration. The inhibition of secretion at this high concentration corresponds with the cytotoxicity seen after 24 h at the same concentration (Figure 3.2), and hence may just be a consequence of the

cytotoxicity, whereas, the increase in insulin secretion occurs at a concentration well below that which is cytotoxic after 24 h. Enhancement of insulin secretion is also induced by a range of pharmaceutical agents containing an imidazoline group including the α_2-adrenergic receptor antagonist efaroxan and some antibiotics, for example the antifungal agent clotrimazole (Chan *et al.*, 1997; Chan *et al.*, 2001), in addition to anti-diabetic drugs such as glibenclamide and meglitinide (Ashcroft, 1999; Mannhold, 2004). There is some structural similarity between the imidazoline group of these compounds and the pyrrole group of pyrrolnitrin. Hence, induction of insulin secretion by pyrrolnitrin might be explained by an ability of this compound to inhibit the ATP-dependent potassium channel (K_{ATP}) via its pyrrole group which may act in the same way as the imidazoline group of reagents. These bind to the Kir6.2 subunit of the K_{ATP} channel, thereby causing membrane depolarization and an influx of intracellular Ca^{2+}, which in turn increases insulin secretion (Chan *et al.*, 2001). The patch clamp results (Figure 3.15 A&C) demonstrated that pyrrolnitrin at 10 and 100 ng/ml caused significant reduction of the outward current recorded in INS-1 cells. These results support the possibility that the K_{ATP} channel and hence membrane depolarization of INS-1 cells is affected by this compound. Pyrrolnitrin at 10 ng/ml caused the highest reduction of the outward current in agreement with the secretion results (Figure 3.7).

Phenazine also increased glucose-stimulated insulin secretion in INS-1 cells with a maximum induction of secretion at 100 ng/ml (Figure 3.8). This induction by phenazine could be attributed to stimulation of glucose oxidation via the pentose phosphate pathway. The phenazine derivative, phenazine methosulphate (PMS) is known to stimulate glucose oxidation via the pentose phosphate pathway (Akpan *et al.*, 1987; Muirhead and Hothersall, 1995). It

probably catalyses the reoxidation of NADPH thereby maintaining availability of $NADP^+$, enhancing glucose metabolism and hence inducing insulin secretion. In addition, as noted above, phenazine and its derivatives, such as pyocyanine (Liu and Nizet, 2009), are capable of catalysing reactive oxygen species (ROS) production. Hence, phenazine could also be linked with insulin secretion via the enhanced production of ROS in INS-1 cells. Pi *et al*. (2007) have shown that low levels of hydrogen peroxide stimulate insulin secretion in INS-1 cells and isolated mouse islets, and that this occurred in an extracellular Ca^{2+}-dependent process. Consistent with this, it is shown here that phenazine (and also pyrrolnitrin) at 10 and 100 ng/ml caused an increase in INS-1 cell Ca^{2+} content (Figure 3.14).

In contrast to phenazine and pyrrolnitrin, the only effect of patulin on glucose-stimulated insulin secretion was inhibition (at 100 ng/ml; Figure 3.9). This effect may be linked with the ability of patulin to inhibit a wide range of enzymes, particularly enzymes that contribute to glucose metabolism, e.g. hexokinase (Madiyalakan and Shanmugasundaram, 1978). This may lead to a decline in the ATP/ADP ratio leading to hyperpolarisation of the cell membrane and inhibition of insulin secretion (Straub and Sharp, 2002). After injecting 10 rats with patulin (1 mg/kg), and noting an elevation of blood glucose levels, Devaraj *et al* (1986) suggested a diabetogenic role for patulin. Here, patulin showed toxicity and inhibited secretion at 100 ng/ml but not with lower concentrations. It is possible that at lower concentrations much of the patulin was metabolised by the cells. In support of this, it has already been shown that patulin can be metabolised in rodents (Wouters and Speijers, 1995).

Finally, both pyrrolnitrin and phenazine stimulated insulin gene II mRNA levels in INS-1 cells (Figure. 3.11 and 3.12, respectively) suggesting an additional role for these compounds in modulating insulin transcription. Pyrrolnitrin showed two effects on transcription of insulin gene II, i.e. induction at low concentrations (10 and 100 ng/ml), but inhibition at high concentration (1000 and 10000 ng/ml). This is similar to the effects of pyrrolnitrin on insulin secretion as discussed above (Figure 3.7). A similar relationship between insulin gene transcription and insulin secretion was seen with phenazine; phenazine at 10 and 100 ng/ml caused a significant increase in both (Figure 3.12 and 3.8). Together these data suggest for both pyrrolnitrin and phenazine that the up-regulation of insulin gene expression might be the result of the increase that these compounds cause in insulin secretion, since insulin is known to be a key regulator of insulin gene expression (Leibiger *et al.*, 2002). Another possible secretion-related signal that modulates insulin gene transcription is intracellular Ca^{2+}; both pyrrolnitrin and phenazine affected INS-1 cell Ca^{2+} content (Figure 3.14). For example, it has been shown (Kim *et al.*, 2002; Leibiger *et al.*, 2002) that elevation of cytoplasmic Ca^{2+} activates Ca^{2+}-dependent protein kinases and phosphatases, such as Ca^{2+}/calmodulin-dependent protein kinases (CaM kinases) and Ca^{2+}/calmodulin-dependent protein phosphatase 2B (calcineurin) both of which are involved in insulin gene transcription. It is also possible that pyrrolnitrin and/or phenazine have more direct effects on insulin transcription, i.e. not involving insulin secretion-related signals. It is known that oxidative stress can lead to depression of insulin expression via effects on the key transcription factor Pdx-1 either through enhanced degradation of Pdx-1 or through a failure of it to locate to the nucleus (Poitout *et al.*, 2006; Andrali *et al.*, 2008). On this basis, since as already noted phenazine and its derivatives enhance ROS

production, it would be expected that phenazine might cause a decrease in insulin transcription, whereas, the opposite effect was seen here. However, it may be at higher, more cytotoxic, concentrations of phenazine that a decrease in transcription would have been seen.

In conclusion, this study shows for the first time that the bacterial compounds pyrrolnitrin and phenazine, which are known antimicrobial agents, are cytotoxic to INS-1 cells, leading to the possibility that these compounds may contribute to the development of diabetes, particularly CF-related diabetes (CFRD), the assumption being that these secondary products can be transported to the pancreas via the blood from the source of their production. In contrast, at lower, sub-lethal concentrations both compounds increase both insulin secretion and insulin gene expression by INS-1 cells.

Chapter 4

Effect of phenazine and pyrrolnitrin on gene expression of insulin and some GSIS mediating signals

4.1 Introduction

Recent studies on T2D have recognized factors that are the main modulators of the insulin synthesising pathway in β-cells; glucose and GSIS pathways are major contributors in insulin gene expression and hormone exocytosis (Straub and Sharp, 2002). Disruption of the function of any elements of the GSIS pathway can actively impede insulin secretion and lead to the development of T2D. Furthermore, the regulation pattern of these markers has been used as an indicator of GSIS status (Walker, 2004). Amongst these signals which can provide a clear feedback about insulin synthesis in response to the GSIS pathway are transcription factors, especially PDX-1, MafA and NeuroD (Walker, 2004; Habener *et al.*, 2005). It has been found that PDX-1 transcription factors can regulate insulin gene expression and β-cell differentiation in response to rises in the intracellular glucose level (Keller *et al.*, 2007), whereas, the transcription factor MafA was reported to initiate insulin gene transcription in response to glucose metabolism (Zhang *et al.*, 2005). Signals like glucose kinase (GK) and glucose transporter-2 (GT-2) are majors indicators can be refer to change glucose metabolism and energy production, and compounds enhance glucose metabolism may enhance insulin gene expression (Lawrence *et al.*, 2001; MacDonald *et al.*, 2005b).

In the previous chapter it has been shown that phenazine and pyrrolnitrin increased insulin secretion, modulated membrane electrophysiology and intracellular Ca^{2+}, and insulin gene mRNA copies were significantly up regulated after treatment with phenazine and pyrrolnitrin. Therefore, the work described in this chapter was designed to confirm the effects of these compounds on insulin gene expression in INS-1 cells as well as expression of GK enzyme and GT-2.

The transcription factors PDX-1, MafA and NeuroD were measured in order to assess their contribution to insulin gene transcription in response to 24 h exposure to phenazine and pyrrolnitrin. Recently, studies have suggested that Ca^{2+}/calmodulin (CaM) – dependent protein kinase mediates insulin gene expression via a number of intracellular responses in response to increases in the intracellular Ca^{2+}. Amongst the Ca^{2+} kinase enzymes that are reported to regulate insulin gene expression are two types of kinases, calcium/calmodulin-dependent protein kinase-IV (CamK4) and its isoform calcium/calmodulin-dependent protein kinase kinase-I (CamKK1) (Yu *et al.*, 2004). We found that Ca^{2+} was increased after exposure to phenazine or pyrrolnitrin, coupled with insulin secretion, so it has been examined whether increase insulin gene expression was regulated by CamK4 and CamKK1.

Therefore, INS-1 cells were cultured and exposed to the effective concentrations (10 & 100ng/ml) of phenazine or pyrrolnitrin for 24 h and then gene expression of insulin and transcription factors (PDX-1, MafA and NeuroD) was measured using absolute qRT-PCR and RT-PCR. Transcription factor amplicons were cloned and recombinant plasmids representing individual transcription factors used to generate standard curve copy number as described in Chapter 3. CamKK1, CamK4, GK and GT-2 gene expression were measured using comparative qRT-PCR using CT values of the amplified products normalized against CT values of β-actin.

4.2 Materials & Methods

4.2.1 Effect of pyrrolnitrin and phenazine on insulin gene expression

The effects of pyrrolnitrin or phenazine (10 & 100 ng/ml) on insulin gene expression were assessed again in order to verify insulin gene up regulation after exposure to microbial secondary metabolites have been reported previously. Also gene expression of transcription factors and GSIS signal genes were measured at the same time. INS-1 cells were cultured in RPMI-1640 medium as described in Section 2.3.1 and separately exposed to concentrations of 10 or 100 ng/ml of either phenazine or pyrrolnitrin and incubated for 24 h at 37 °C and 5% CO_2 (Section 3.2.4.3). Total RNA was extracted from the INS-1 cells after at 24 h exposure (Section 2.6.1). Aliquots (1 µg) of RNA from each treated sample and control samples (vehicle + cells) were used for the synthesis of cDNA (Section 2.6.2). Insulin gene expression was measured using absolute qRT-PCR as previously mentioned (Section 3.2.5.2) using the same primer set and the data were normalized and statistically analysed as described in Sections 2.5.5 and 3.2.8.

4.2.2 Effect of pyrrolnitrin and phenazine on transcription factors genes

In addition to the insulin gene, the effects of microbial compounds on gene expression of the transcription factors PDX-1, MafA and NeuroD were also measured and cDNA prepared as in Section 4.2.1. RT-PCR and absolute qRT-PCR were used to measure transcription factor gene expression. Specific primers sets (forward & reverse) were designed (Table 4.1) as described in Section 2.6.3.1 and commercially sequenced. Using the MWG Eurofins read value service (MWG, Germany).

Target gene	Primers 5-3	length	Primer position	Product size (bp)
PdX-1-F	GAGGGGTCCGGTGCCAGAGT	20	163-182	155
PdX-1-R	GCGGGGGCACTTCGTATGGG	20	317-298	
MafA F	AGCTCCGCGGCTTCAGCAAG	20	446-465	179
MafA-R	ACGCCCCACCTCCAGCTTCA	20	624-605	
NeuroD -F	CCAGCGCTTCCTTCCCGGTG	20	629-648	215
NeuroD-R	GCCATTGATGCTGAGCGGCG	20	843-824	
GK-F	TCCTGCTACTATGAAGACCGCC	22	583-504	213
GK-R	CGCTGAGCTTTCATCCACCATC	22	795-774	
GT-2 –F	ACACCCACTCATAGTCACACC	21	194-215	155
GT-2-R	AAGCCACCCACCAAAGAACG	20	348-328	
Camk4-F	ACATTCCAAGCCCTCCAACACC	22	859-880	241
Camk4-R	GATCTGTCTTGTCCTTGCCGTC	22	1099-1078	
Camkk1	ACATCAAGCCGTCCAATCTGC	21	824 -844	201
Camkk1	TAACCCCAGTGGCCCATACATC	22	1024-1003	

Table 4.1: Forward and reverse primers used in qRT-PCR during this study to measure transcription factors and GSIS signal gene expression.

qRT-PCR was also used to verify the effects of the microbial products on transcription factor gene expression. In this case a PCR amplification was carried out using GOTaq DNA polymerase to produce transcription factors amplicons with T-overhang. The amplified products were separated using 1.8 % agarose gel electrophoresis and DNA bands with the desired molecular mass were eluted from the gel (Section 2.5.7). The transcription factor amplicons with T overhang ends were cloned into pGEMT-easy (Sections 2.7.2 and 2.7.3) and recombinant plasmids were checked using restriction enzyme excision and also by using PCR amplification followed by agarose gel electrophoresis. The recombinant plasmids were then sequenced to verify the nucleotide sequences of inserts; sequencing was obtained using the Operon Value Read service (MWG, Germany). The recombinant plasmids were then used to prepare standard curves by measuring number of copies per microlitre using a Spectrofluorometer (Perkin-Elmer LS50B , USA) and equation as described in Section 3.2.5.3 and then standard curves for each of the transcription factors were prepared in same way. Absolute qRT-PCR was used in order to identify the effect of these compounds on transcription factor copy number. Triplicates of each sample (treated & standard curve samples) were prepared in 48 well PCR plates (one plate used for each transcription factor or insulin gene). Stock master solution, enough to assess all samples, was pipetted into the wells. Each well contained 12.5 µl of SYBR green master mix, 0.5 µl each of forward and reverse primers, 0.25 µl reference dye, 9.5 µl water and 2 µl cDNA. The amplification condition was set as previously mentioned (Section 3.2.5.4) using 65 °C annealing temperature. The data were collected, normalized and statistically analysed (Sections 2.5.5 and 3.2.8.).

4.2.3 Quantifying mRNA of GK, GT-2, CamK4 and CamKK1 genes

The comparative qRT-PCR technique was used to measure mRNA levels or gene expression using cDNA samples (Section 4.2.1) to verify the effects of pyrrolnitrin or phenazine on INS-1 cells on expression of genes mediating glucose metabolism or GSIS (GK & GT-2) as well as genes which may contribute to modulation of insulin gene expression (CamK4 & CamKK1). The cDNA samples prepared in Section 4.2.1 were used to assess expression of these genes. 48 well plates were used; 6 wells were used for each sample, three of which for the target gene and the other three for the housekeeping gene (β-actin). Six samples were measured, two vehicle controls for pyrrolnitrin or phenazine were set and two concentrations each (10 & 100 ng/ml) for pyrrolnitrin or phenazine treated samples. The stock master solution, containing SYBR green dye, primers and reference dye, prepared (Section 3.2.5.3) mixed with 2 µl of cDNA prepared in Section 4.2.1 to the total volume 25 µl/well. PCR amplification conditions were as previously described (Section 3.2.5.4); the copy number data were collected and normalized using the β-actin data before statistical analysis.

4.2.4 Normalization of qRT-PCR Data

In most cases the data were normalized using the instrument software with auto-normalization. However, the data were normalized manually producing the relative quantification (RQ) values. The data was firstly normalized against the housekeeping (β-actin) gene which was achieved by subtracting the CT value of β -actin from the target gene CT value to produce the ΔCT. The ΔΔCT values of each sample were then produced by subtracting the ΔCt of the control (vehicle control) from the ΔCT value for each treatment. Afterwards, the RQ of individual

samples was then produced using the following equation (RQ= $2^{-\Delta\Delta C_T}$); data were statistically analysed (Section 3.2.8).

4.2.5 Amplification of amplicons using RT-PCR

Gel based RT-PCR was also used to assay the transcription factors, and GK, GT-2, CamK4 and CamKK1 gene expression as an additional confirmation of the qRT-PCR results and to check primer efficiency. RT-PCR was achieved using cDNA extracted from INS-1 exposed to 10 or 100 ng/ml of either pyrrolnitrin or phenazine (Section 4.2.1). Appropriate primer sets were used to amplify desired genes. Conventional PCR reaction was achieved using Red-Taq DNA polymerase. The reaction components were added respectively to final volume 25 µl for one reaction as:-

cDNA	2 µl
Forward primer (10 pM)	1 µl
Reverse primer (10 pM)	1 µl
Red-Taq polymerase (5U)	1 µl
dNTPs (10 mM)	0.5 µl
Red-Taq reaction buffer (5x)	2.5 µl
PCR water	17 µl

The mixtures were mixed thoroughly by pipetting and the standard PCR were performed using an MWG thermocycler (Primus 96 plus) under the following conditions: 94 °C for 2 min followed by 40 cycles start at 94 °C for 30 s, 60 °C or 65 for 30 s and 72 °C at 30 s for individual cycle followed with hold the samples at 4 °C until collection. The PCR products samples were run into a 1.8% agarose gel (Section 2.5.7) along with a 1 kbp ladder and then the DNA bands were visualized using UV irradiation in a gel documentation system.

4.3 Results

4.3.1 Quantifying mRNA expression of insulin gene transcription

The microbial secondary metabolites phenazine and pyrrolnitrin (10 & 100 ng/ml) have previously been shown to up regulate insulin gene II. Firstly, 10 or 100 ng/ml of each compound was used to confirm the previous insulin gene expression results. Therefore, INS-1 cells were exposed to either 10 or 100 ng/ml of phenazine or pyrrolnitrin and insulin gene expression assessed, which confirmed that both phenazine and pyrrolnitrin significantly increased insulin gene expression after 24 h exposure (Figure 4.1).

The current experiments aimed to identify which transcription factors mediated insulin gene transcription enhancement by the microbial secondary metabolites. Expression of insulin gene transcription factors was measured, and primers successfully produced amplicons of the expected molecular sizes, 155, 179 and 225 bp for PDX-1, MafA and NeuroD, respectively (Figure 4.2 A). The amplified products were extracted from the gel, and were then successfully cloned into pGEMT-easy plasmids to produce the recombinant plasmids pM3, pM4 and pM5. Restriction using *EcoRI* confirmed cloning (Figure 4.2B). PCR amplification of recombinant plasmids also produced the transcription amplicons at expected molecular size (Figure 4.2C). Sequence analyses of the recombinant plasmids have confirmed these amplicons as belonging to the insulin gene II transcription factors PDX-1, MafA and NeuroD with accession numbers NM_022852.3, XR_008949, and AF107728, respectively.

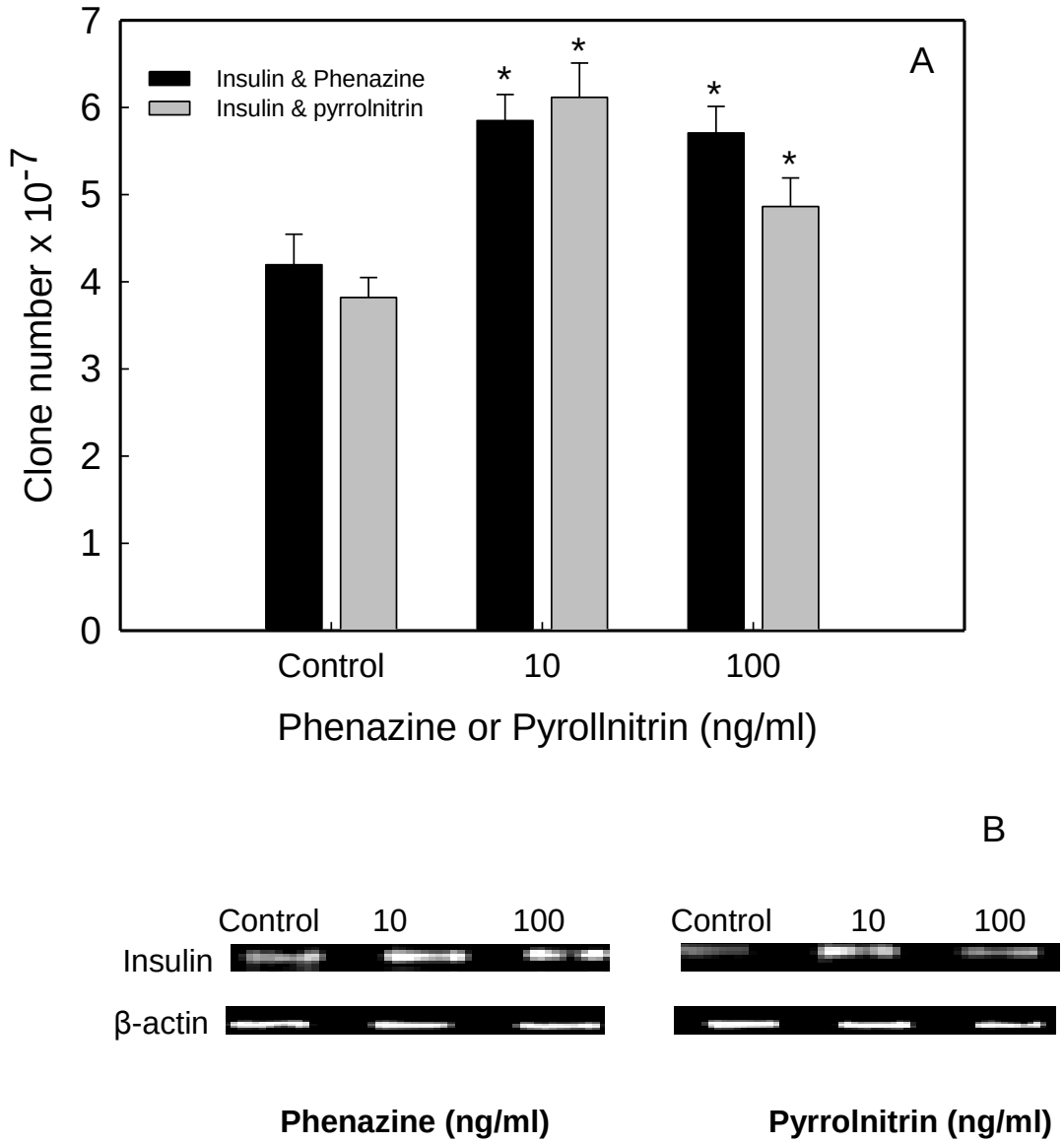

Figure 4.1: Insulin gene expression in INS-1 cells after 24 h exposure to pyrrolnitrin and phenazine: (A) the number of copies of amplified cDNA of insulin gene II after reverse transcription of INS-1 RNA measured by qRT-PCR. Data shown are means ± S.E. (n = 3), normalised against β-actin as a housekeeping gene. * indicates significant differences relative to the vehicle control ($p \leqslant 0.05$). (B) gel-based RT-PCR for amplified cDNA of insulin gene II; β-actin is again used as the housekeeping gene.

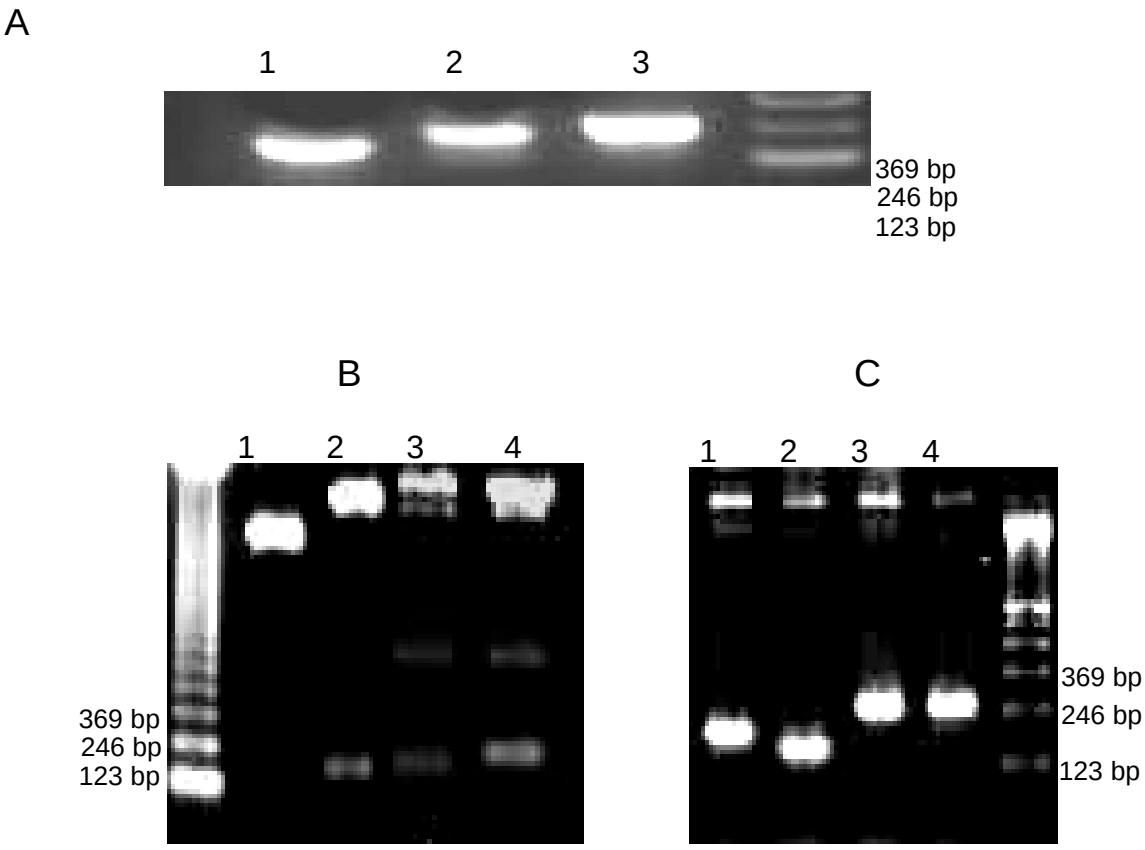

Figure 4:2: Amplification and cloning of insulin gene transcription factors in. pGEMT plasmids: (A) RT-PCR of insulin gene transcription factors PDX-1, MafA and NeuroD (lanes 1, 2 and 3, respectively); (B) excision recombinant plasmids pM3, pM4 and PM5 cloned with PDX-1, MafA and NeuroD amplicons, respectively (lanes 2, 3 and 4, respectively) after *EcoRI* digestion compared with non-recombinant pGEMT-easy (lane 1); (C) PCR amplification recombinant plasmids pM4, pM3 (lanes 1 and 2) and pM5 (lanes 3 and 4).

4.3.2 Quantifying transcription factor gene expression

The effects of phenazine and pyrrolnitrin on insulin gene transcription factors (PDX-1, MafA and NeuroD) were investigated after confirming the up-regulation of insulin gene expression by the microbial secondary metabolites using absolute qRT-PCR. This clearly showed a significant increase in MafA gene expression by INS-1 cells corresponding to the increase in phenazine concentration (10 & 100 ng/ml) after exposure for 24 h (Figure 4.2A). Similar findings were obtained by gel-based RT-PCR in which MafA expressed band intensity at 10 and 100 ng/ml was stronger than the control. In addition, at 10 ng/ml NeuroD had the strongest band intensity compared to the control and 100 ng/ml exposures (Figure 4.2B). Furthermore, phenazine (10 ng/ml) increased expression of transcription factor NeuroD, whereas, no significant effect was seen with 100 ng/ml phenazine. The results showed no significant effect on PDX-1 expression at either of the test concentrations compared to the vehicle control.

Interestingly pyrrolnitrin treatment increased expression of all three transcription factors (PDX-1, MafA and NeuroD) after 24 h incubation with 10 ng/ml, whereas, only an increase in MafA gene expression was seen in the 100 ng/ml treatment (Figure 4.4A). The results were confirmed by gel-based RT-PCR in which 10 ng/ml pyrrolnitrin increased the band intensity of all tested transcription factors compare to the control and the100 ng/ml (Figure 4.4B). No significant effect was seen at 100 ng/ml pyrrolnitrin on PDX-1 and NeuroD compared to the vehicle control (ethanol).

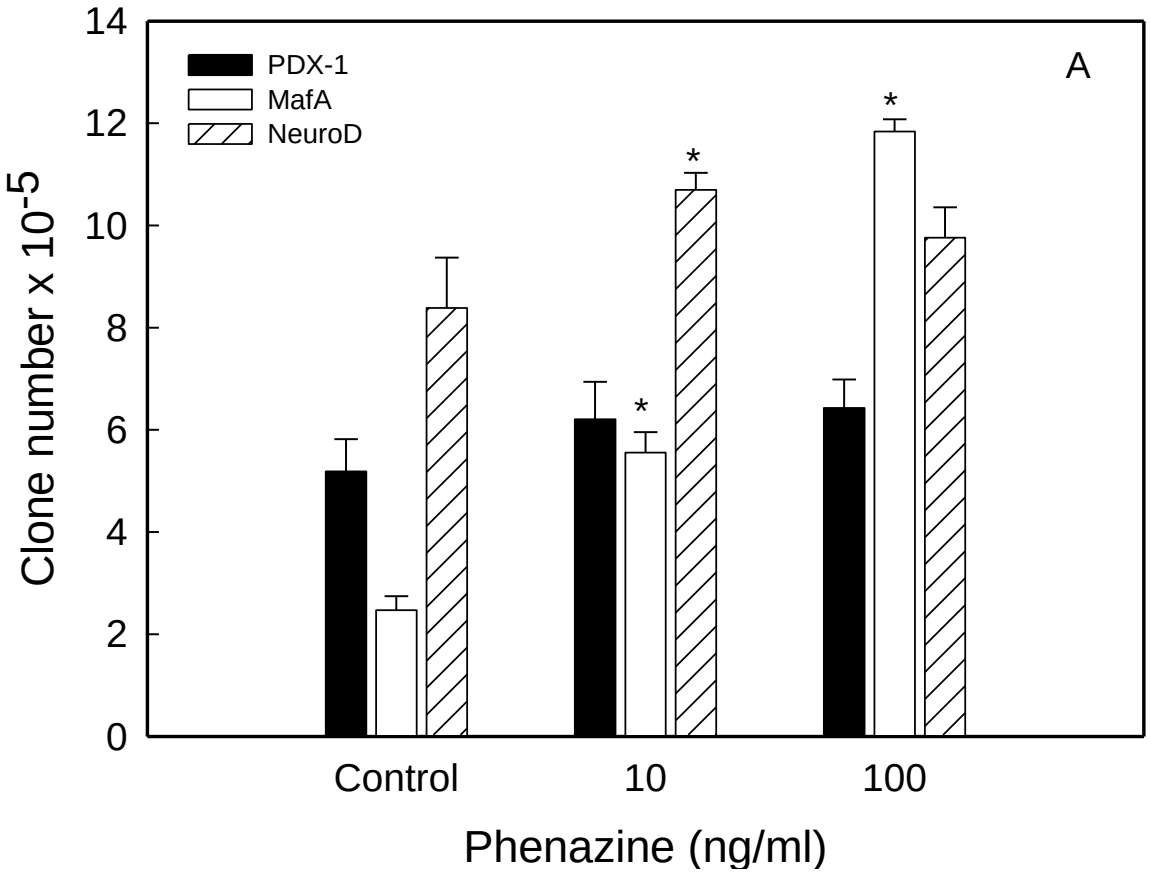

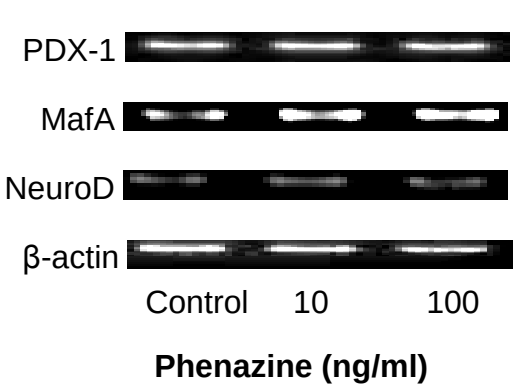

Figure 4.3: PDX-1, MafA and NeuroD gene expression in INS-1 cells after 24 h exposure to phenazine: (A) the number of copies of amplified cDNA of transcription factors after reverse transcription of INS-1 RNA measured by qRT-PCR. Data shown are means ± S.E. (n = 3), normalised against β-actin as a housekeeping gene. * indicates significant differences relative to the vehicle control ($p \leq 0.05$). (B) gel-based RT-PCR for amplified cDNA of transcription factor; β-actin is again used as the housekeeping gene.

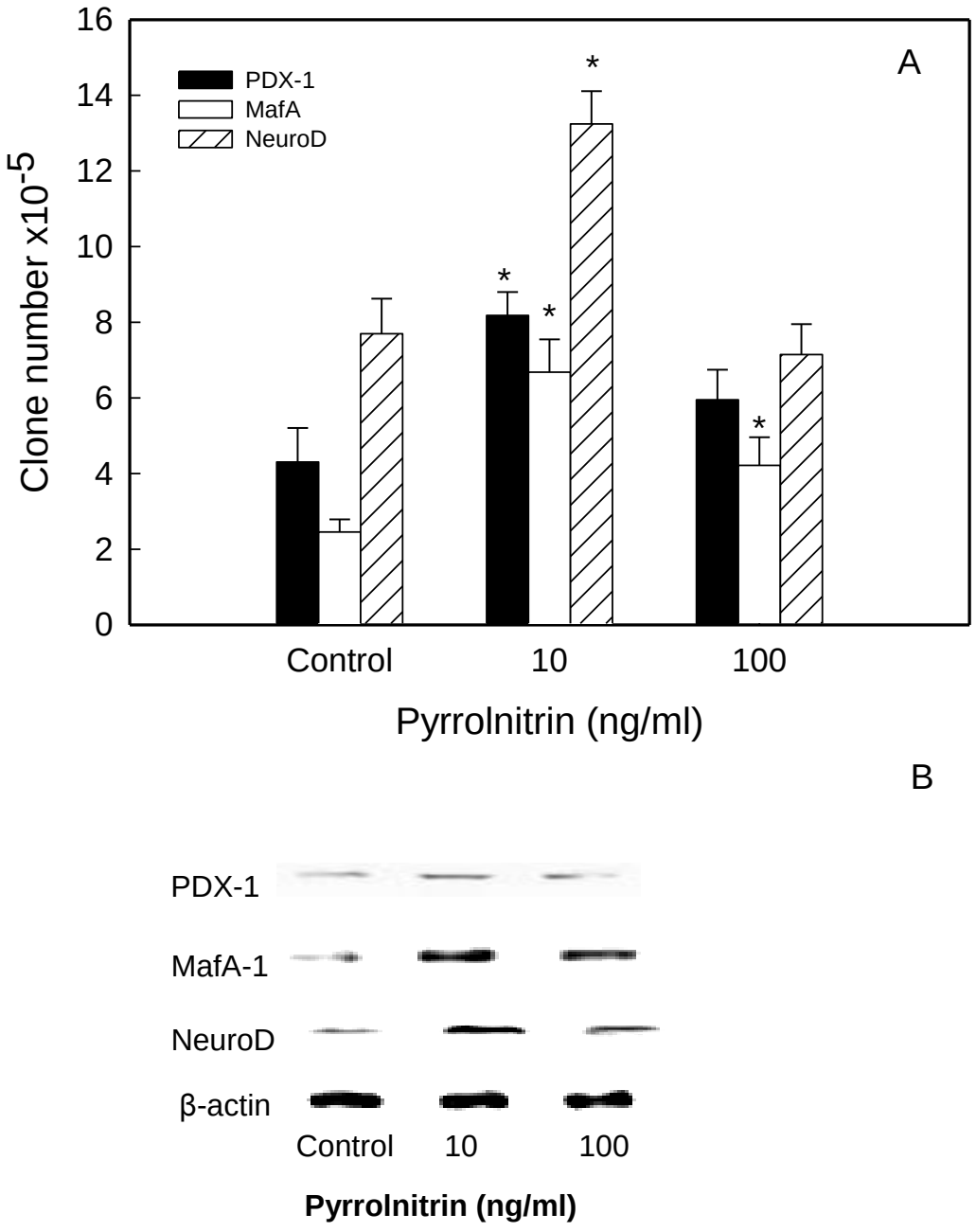

Figure 4.4: PDX-1, MafA and NeuroD gene expression in INS-1 cells after 24 h exposure to pyrrolnitrin: (A) the number of copies of amplified cDNA of transcription factor reverse transcription of INS-1 RNA measured by qRT-PCR. Data shown are means ± S.E. (n = 3), normalised against β-actin as a housekeeping gene. * indicates significant differences relative to the vehicle control ($p \leqslant 0.05$). (B) gel-based RT-PCR for amplified cDNA of transcription factor; β-actin is again used as the housekeeping gene.

4.3.3 Quantification of GK, GT-2, CamK4 and CamKK1 gene expression

The effects of phenazine and pyrrolnitrin (10 & 100 ng/ml) on the glucose phosphorylation enzyme (GK), glucose transport (GT-2), and Ca^{2+} dependent regulation of insulin gene transcription (CamKK1 & CamK4) was measured in order to identify whether these compounds interact with major GSIS signals. The results show that the designed primer for those genes successfully produced amplicons with the expected molecular sizes, 215, 155, 241 and 201 bp representing GK (M25807.1), GT-2 (NM_012879.2), CamK4 (NM_012727.3) and CamKK1 (NM_031662.2), respectively (Figure 4.5). Furthermore, sequence analysis has confirmed that amplicons belong to the targeted genes in pancreatic β-cells.

Exposure of INS-1 cells to phenazine (10 and100 ng/ml) for 24 h significantly increased GT-2, CamKK1, and CamK4 gene expression with strong significant increase was seen of GT-2 gene expression at 10 ng/ml phenazine compared to the control sample. However, significant increase in GK gene expression after 24 h exposure was seen only at 100 ng/ml with no significant effect at 10 ng/ml phenazine (Figure 4.6).

INS-1 cells incubated within pyrrolnitrin (10 or 100 ng/ml) show a different pattern to that with phenazine as GK gene expression was increased significantly at 100 ng/ml phenazine after 24 h, whereas, no significant difference was seen at 10 ng/ml (Figure 4.7). However, mRNA levels of each of GT-2, CamKK1 and CamK4 were significantly reduced to about 50% at both concentrations (10 &100 ng/ml) compared to the control.

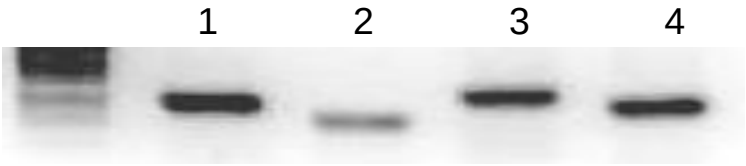

Figure 4.5: Gel-based RT-PCR of GK, GT, CamK4 and CamKK1 amplicons (lanes 1, 2, 3 and 4), respectively.

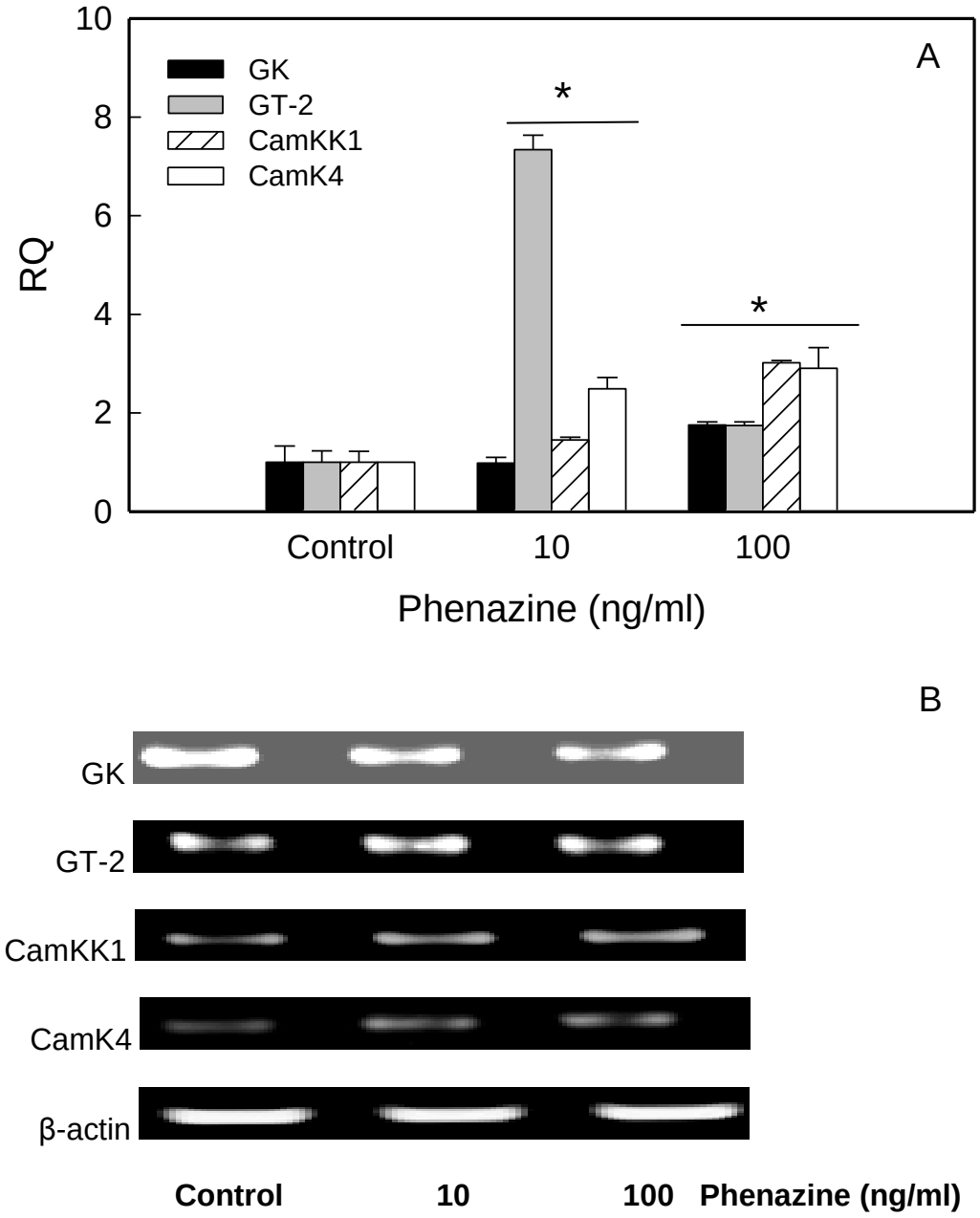

Figure 4.6: GK, GT, CamKK1 & CamK4 gene expression in INS-1 cells after 24 h exposure to phenazine: (A) shows relative quantitation of GK, GT, and CamKK1 & CamK4 amplified cDNA of INS-1 RNA measured by qRT-PCR. Data shown are means ± S.E. (n = 3), normalised against β-actin as a housekeeping gene. * indicates significant differences relative to the vehicle control ($p \leqslant 0.05$). (B) gel-based RT-PCR for amplified cDNA of transcription factor; β-actin is again used as the housekeeping gene.

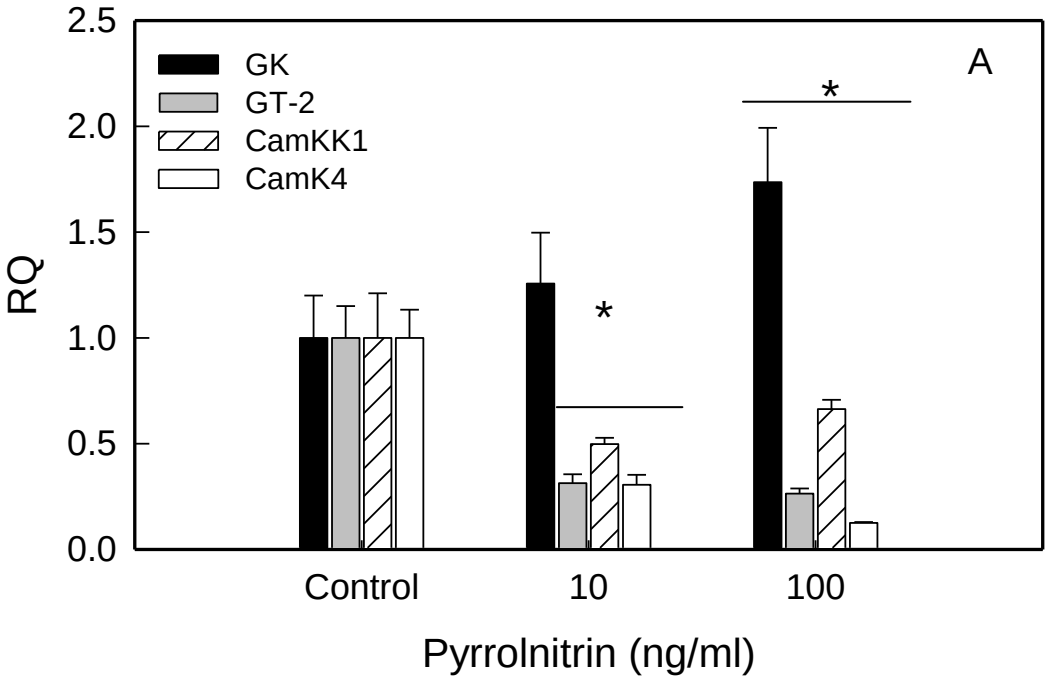

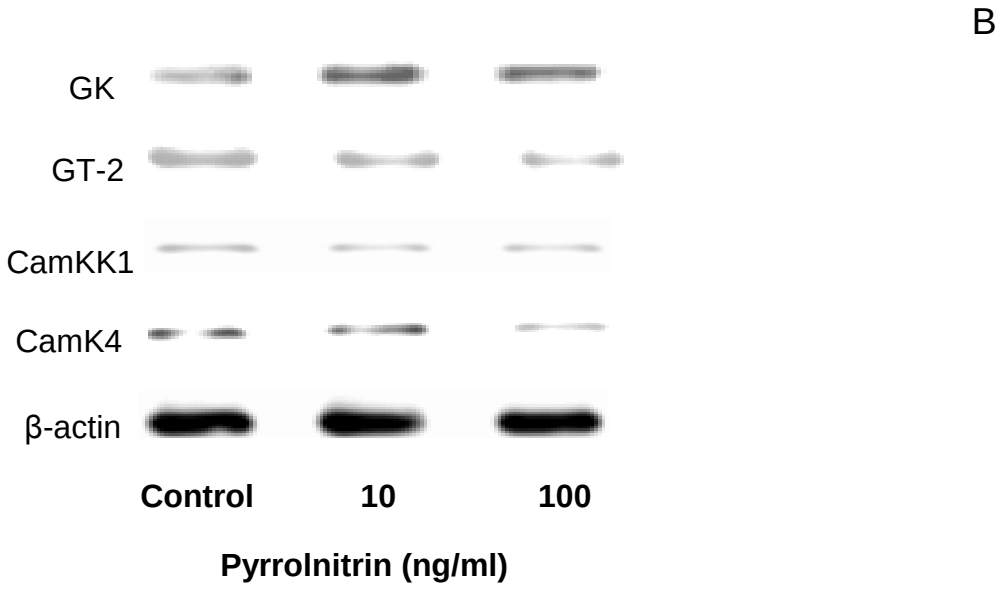

Figure 4.7: GK, GT, CamKK1 & CamK4 gene expression in INS-1 cells after 24 h exposure to pyrrolnitrin: (A) relative quantification of GK, GT, CamKK1 and CamK4 amplified cDNA of INS-1 RNA measured by qRT-PCR. Data shown are means ± S.E. (n = 3), normalised against β-actin as a housekeeping gene. * indicates significant differences relative to the vehicle control ($p \leqslant 0.05$). (B) gel-based RT-PCR for amplified cDNA of transcription factors; β-actin is again used as the housekeeping gene.

4.4 Discussion

One aim of this chapter was to confirm the effects of the microbial secondary metabolites, pyrrolnitrin and phenazine, on insulin gene expression in INS-1 cells. It has been shown previously (Chapter 3) that insulin gene expression was increased after exposure to pyrrolnitrin and phenazine at 10 and 100 ng/ml. This was confirmed again in this chapter. However, the main aim was to study the mechanisms by which these compounds affect insulin gene expression, via determination of the expression of transcription factors related to insulin gene expression. Transcription factor (PDX-1, MafA and NeuroD) expression and insulin gene are regulated via signals generated by the GSIS pathways and glucose signalling in β-cells (Kataoka *et al.*, 2002; Iype *et al.*, 2005).

Both phenazine and pyrrolnitrin stimulated insulin mRNA levels consistent with what was found in Chapter 3 which may be attributed to an enhancement of glucose oxidation producing signals that lead to increased insulin synthesis (Docherty and Clark, 1994; Poitout *et al.*, 2006). Phenazine as a redox active compound appears to modulate of insulin gene expression via glucose metabolism more than pyrrolnitrin. However, phenazine cytotoxicity to β-cells is also attributable to its redox activity as enhanced glucose metabolism leads to increased production of cytotoxic ROS, e.g. H_2O_2, which can cause necrosis of β-cells (Allen *et al*., 2005). Pyrrolnitrin also increased insulin gene expression which also could be via glucose metabolism. However, this result needs more investigation because the effect of pyrrolnitrin on mammalian cells is not well studied. The current study attributed the augmentation of insulin secretion by pyrrolnitrin to inhibition of β-cell K_{ATP} channels by the pyrrole group. However, the signals that lead to increased insulin secretion could also lead to increased insulin gene expression (Doyle and Egan, 2003).

The expression of the insulin gene under normal conditions is affected by three major transcription factors (PDX-1, MafA and NeuroD) which are regulated by changes of glucose concentration (Kataoka *et al.*, 2002; Kaneto *et al.*, 2005). The effects of phenazine and pyrrolnitrin on insulin gene transcription factors confirmed the interaction between these compounds and insulin gene expression. Phenazine at 10 ng/ml increased the expression of MafA and NeuroD, but only MafA increased at 100 ng/ml phenazine (Figure 4.3). The effect of phenazine on expression of MafA is likely to be via GSIS; studies have shown that MafA is a key modulator of GSIS (Zhang *et al.*, 2005; Artner *et al.*, 2008). It has been shown that MafA 'knockout' mice exhibit glucose intolerance and develop diabetes mellitus; the analysis of GSIS signals shows that insulin I, insulin II, GT-2, NeuroD and PDX-1, as well as other signal molecules, that regulate GSIS are all inhibited (Zhang *et al.*, 2005). Therefore, it is suggested that phenazine modulates insulin gene expression via MafA regulation. Moreover, phenazine as a redox-active compound regulates insulin secretion via enhancing ATP production and insulin receptor phosphorylation which causes glucose uptake and consequently insulin gene expression via glucose signalling (Kataoka *et al.*, 2002).

A significant increase in expression of the NeuroD transcription factor at 10 ng/ml phenazine, in addition to MafA, was also found. NeuroD is a key regulator of β-cells and insulin gene expression, as well as of differentiation of neural cells, and many studies have shown correlation between insulin transcription modulation by NeuroD and glucose uptake in response to the GSIS pathway (Kim *et al.*, 2002). It has been reported by many investigators that the regulation of NeuroD expression is controlled by MafA (Wilson *et al.*, 2003). However, no significant effect of 100 ng/ml phenazine (toxic concentration) on NeuroD gene

expression was seen, which is probably attributable to the cytotoxic or the inhibitory effect of the phenazine activity at this concentration.

Phenazine also induced significant up-regulation of glucose transporter 2 (GT-2) and glucokinase (GK) expression in INS-1 cells at both concentrations confirming the effect of phenazine on insulin gene and MafA gene expression (Figure 4.5). This data suggests that phenazine can enhance GSIS through enhancement of glucose metabolism via up regulation of glucose phosphorylation by GK, and through enhancement of glucose uptake via up regulation of GT-2 in INS-1 cells. An increase in intracellular glucose enhances insulin exocytosis, insulin gene expression, and transcription factors (Lipson *et al.*, 2006; Brunner *et al.*, 2009). Furthermore, enhancement of glucose phosphorylation by GK and subsequent glucose oxidation leads to an increase in ATP/ADP ratio, a key modulator of the membrane depolarization of β-cells that mediates insulin secretion (Straub and Sharp, 2002; MacDonald *et al.*, 2005b), which was up-regulated in INS-1 cells in response to the phenazine exposure.

This study also investigated whether changing insulin gene transcription factor expression might be accomplished by the multifunctional kinases, CamKK1 and CamK4, which belong to the calcium/calmodulin-dependent protein family, which have been recently reported to mediate insulin gene transcription (Leibiger *et al.*, 2002 ; Yu *et al.*, 2004). Again, there was good evidence to show that phenazine could modulate CamKK1 and CamKK4 gene expression (Figure 4.5) which in turn suggests that the regulation of insulin gene expression by MafA may be mediated by glucose signalling and an increase in the intracellular level of Ca^{2+}.

The effects of pyrrolnitrin were completely different from those of phenazine; exposure of INS-1 cells to pyrrolnitrin (10 ng/ml) not only increased insulin gene expression but interestingly the expression of all the transcription factors was increased in response (Figure.4.4). Whereas, MafA was the only transcription factor where there was a significant increase in expression at 100 ng/ml. The effect of pyrrolnitrin at 10 ng/ml on transcription factor expression is consistent with its effects on insulin gene expression, insulin secretion, Ca^{2+}, and electrophysiology, suggesting that pyrrolnitrin at this concentration has effects on GSIS signalling. The effect of pyrrolnitrin on PDX-1 supports the idea that pyrrolnitrin enhances GSIS, as PDX-1 is the major transcription factor that plays a role in the regulation of insulin gene expression and β-cell differentiation by GSIS (Holland *et al.*, 2005; Keller *et al.*, 2007). The results also showed enhanced MafA expression which consolidates our previous suggestion about possible GSIS modulation by pyrrolnitrin. NeuroD gene expression increased due to pyrrolnitrin exposure; it has been reported that it is possible that NeuroD regulates PDX-1 (Kim *et al.*, 2002; Wilson *et al.*, 2003). Both T1D and T2D development in human have been linked recently with the disruption of production of the insulin gene transcription factors (Walker, 2004; Luzardo and Mathews, 2010), so that research on insulin gene regulation and transcription factor expression and drugs that modulate transcription factors have been investigated often.

The current study has demonstrated the effects of pyrrolnitrin on insulin gene and transcription factor expression. Moreover; tests were made to demonstrate whether the insulin gene modulation is achieved via GSIS signals (GT-2, GK, CamKK1 and CaMK4). Interestingly, results showed different pattern to what was expected for regulation of these genes via GSIS; GT-2, CamKK1 and

CamK4 expression were significantly inhibited by pyrrolnitrin (10 & 100 ng/ml) suggesting that pyrrolnitrin has an inhibitory effect on GSIS, and maybe insulin exocytosis. In the case of GK, whose gene expression was highly up regulated after pyrrolnitrin exposure, suggesting enhanced intracellular glucose phosphorylation as was seen with phenazine. This supports the previous hypothesis that enhancement of insulin secretion by pyrrolnitrin may be attributed to its inhibitory effect on K_{ATP} channels (Macfarlane *et al.*, 2000; Yu *et al.*, 2004). However, a toxic concentrations pyrrolnitrin inhibited insulin gene transcription and secretion as previously described suggests that long-term exposure to sub-lethal concentrations could eventually inhibit insulin biosynthesis, which supports the hypothesis that pyrrolnitrin could contribute to diabetes in CF sufferers with chronic infection.

The aim of the work in this chapter was to determine effects of pyrrolnitrin and phenazine on insulin gene expression and GSIS in INS-1 cells. In conclusion, at higher concentrations, phenazine and pyrrolnitrin show cytotoxicity to INS-1 cells, whereas, sub-lethal concentrations of these compounds increased insulin secretion, i.e. they had a physiological effect on INS-1 cells. Phenazine, a redox-active compound, enhanced glucose metabolism and increased the intracellular ATP/ADP ratio, causing K_{ATP} inhibition and elevation of intracellular Ca^{2+} leading to insulin secretion. Increase in intracellular Ca^{2+} can also modulate CamKK1, CamK4 and insulin gene transcription through up regulation of MafA transcription. Moreover, redox activity has been linked with GSIS via glucose uptake through the up regulation of the GT-2, glucose metabolism via increase phosphorylation by GK and consequently intracellular ATP/ADP and insulin biosynthesis (Figure 4.8).

Pyrrolnitrin exposure at low concentration may be potentially toxic or inhibitory when either is long term exposure to sub lethal concentrations of pyrrolnitrin despite even the low concentrations. A potential application for such compounds may be by to use phenazine or phenazine like compounds in regulation of insulin secretion and gene expression experiments which may provide new information about the GSIS and regulation of the insulin gene in β-cell. However, the most interesting finding is the ability of phenazine to enhance insulin gene expression via MafA. It has been reported by many studies that the Maf family of transcription factors are the main modulators contributing to eye lens cell differentiation and proliferation. Therefore, phenazine may have a potential application in studies about eye cells. Pyrrolnitrin or compounds derived from pyrrolnitrin, (compounds with a pyrrole group) might be a source for a new generation of anti-diabetic drugs. However, the probable application for such compounds could well be to use them as laboratorial insulinotropic compounds.

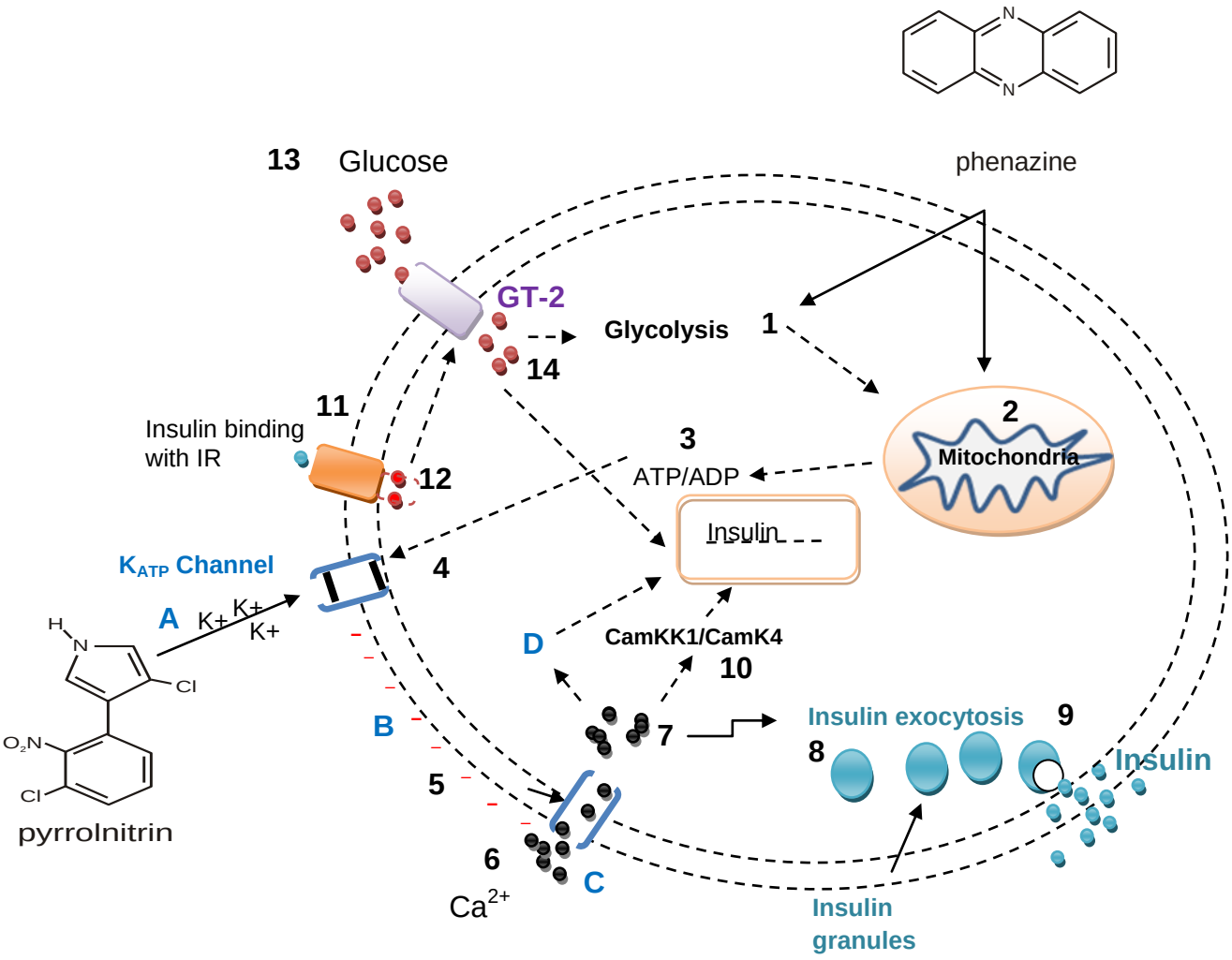

Figure 4.8: Schematic illustration of the effects of phenazine or pyrrolnitrin on GSIS and insulin secretion pathways in β-cell. Phenazine stimulates glucose oxidation via glycolysis and the TCA cycle (1, 2) and hence increases the ATP/ADP ratio (3) which blocks the K_{ATP} channel, causing depolarization of the cell membrane (4, 5) and an increase in the intracellular Ca^{2+} (6,7) thereby enhancing insulin exocytosis (via modification of insulin granule) (8.9). Increased intracellular Ca^{2+} also increases insulin gene expression via CamKK1 & CamK4 (10). Secreted insulin binds to the IR (11) enhancing phosphorylation (12) thereby up regulating signalling pathways leading to glucose uptake via GT-2 (13) and increasing intracellular glucose & insulin gene expression (14). Pyrrolnitrin may directly bind to the Kir.6.2 subunit of K_{ATP} (A) causing K^+ inhibition and depolarization of the cell membrane (B) and increase in Ca^{2+} influx and content (C) leading to increase insulin secretion (7, 8, 9) and insulin gene expression (D).

Chapter 5

Screening microorganisms for binding of insulin and construction of a *Burkholderia multivorans* genomic library

5.1 Introduction

Microorganisms and their products (protein and secondary metabolites) are considered potential environmental factors involved in causing pancreatic β-cell damage (Myers *et al*., 2003). Furthermore, it has been hypothesised recently that some microorganisms possess proteins with sequence homology to β-cell antigens, which can promote an autoimmune response against β-cells (MacFarlane *et al.*, 2003; Fujinami *et al.*, 2006). Some microbial proteins which share amino acid sequence homology to β-cell pancreatic auto-antigens may have a similar function, for example glutamic acid decarboxylase (GAD) from *E. coli* has been suggested to bring about diabetic autoimmune response against human β-cells GAD65 (Mulder, 2005), and HSP60 in *Ps. aeruginosa* and HSP60 pancreatic β-cells antigen (Jensen *et al*., 2001). Many studies have shown the presence of similar insulin receptors or insulin binding proteins (IBPs) on bacteria and other microorganisms.

In the current study it has been hypothesised that the IBP epitopes may be diabetogenic by triggering an autoimmune response against HIR on the basis of molecular mimicry, particularly in patients with CFRD who have long term infection with *Burkholderia sp*. Receptor ligand binding can be used to study the interactions of ligands (protein, substrate) with biomolecules (receptors) on the cell surface, and to form a complex to serve biological purposes *e.g.* (Downstream biochemical cascades) (Mahendrarajah *et al.*, 2011). Studying receptor ligand binding is generally performed by incubating the receptor with ligand under specific condition such as temperature, pH and ionic concentration, for a certain period of time (Wilson and Walker, 2005). Enzyme labelled and radio labelled ligand (with isotopes such as H^3, C^{14}, P^{32}, S^{35} and I^{135}) are commonly used to follow ligand binding activity.

Amongst the techniques that can be used to characterise receptor by gene cloning, which is a technique involving taking a piece of DNA from one organism and inserting into a cloning host such as bacteria (e.g. *E coli)*, mammalian cell line (e.g. CHO), or animal (transgenic animal) or plant (transgenic plant) in order to study the cloned DNA or produce encoded protein (Lodge *et al.*, 2007). This technique is achieved predominantly using particular DNA transporter molecules called cloning vectors and in many cases these vectors are plasmids, circular DNA that can autonomously replicate in host cells. Cloning involves different strategies depending on the organism that is used to clone the gene. Among these strategies is the production of gene library, a collection of genes of an organism in recombinants representing the entire genome of an organism (Sambrook and Russell, 2001). The first step is to extract the genomic DNA of the organism whose gene library is to be created and then digest the DNA partially using restriction enzymes (RE) like *Sau3A*. These fragments are then ligated into vectors pre-digested with the same restriction enzymes or isoschizomer RE (e.g. *BamHI*) (Lodge *et al.*, 2007). In the case of plasmids recombinant vectors are then introduced into the *E coli* by transformation. In the case of cosmid or bacteriophage, *in vitro* packing is used. Recombinant cells or plaques are then screened for expression of the desired gene or the gene is detected by molecular screening using specific probes (Wong, 2006).

The aim of this chapter's work was to screen the microorganisms for insulin binding components using labelled ligand (Peroxidase labelled insulin) and to quantify the amount of insulin that bound to the microbial cells using FITC labelled insulin. This chapter also started characterisation and identification of insulin binding protein's using western ligand blotting and gene cloning.

5.2 Materials and Methods

5.2.1 Insulin ligand binding assay with whole microbe cells

A total of 45 microbial species were used in this study and are listed in (Table 2.1). The peroxidase labelled insulin (Sigma, UK) was used to screen for insulin binding components on microbial cells. This assay was performed using 1.5 ml microcentrifuge tubes and 96 well plates. The microbes (bacteria, yeast strains) were produced using optimum growth conditions (Table 2.1) and each microbe culture was centrifuged in 1.5 ml microcentrifuge tubes for 3 minutes at 6500 × *g* at room temperature (RT).

The cell pellet was resuspended and washed in 500 µl of 10 mM MOPS or PBS, then re-centrifuged and resuspended in 100 µl of the same buffer and 5 µl of insulin peroxidase (1µg/µl) was added and the tubes incubated for 10 min at room temperature. Next, cells were washed in PBS three times and finally resuspended in 100 µl of MOPS and transferred into 96 well Microtiter plates. To detect the binding of insulin, 100 µl of fresh DAB/ $NiCl_2$ solution (Appendix 1) was added to each well and agitated thoroughly by pipetting and the plate was placed in the dark for a period of 10 min and photographic images were taken immediately.

The same protocol was used for FITC labelled insulin (instead of insulin peroxidase) to detect the insulin binding components on microorganisms. Samples with no insulin label were prepared for each individual species as a negative control.

5.2.2 Quantification of insulin bound to cells of *B. multivorans* and *A. salmonicida*

The bacteria were grown as described in section 2.2.1, three different dilutions were used 1:5 and 1:10 and undiluted. Aliquots of each dilution (100 µl) were plated out on triplicate LB agar plates to enumerate bacteria and some aliquots were exposed to FITC labelled insulin which was used to assess the amount of insulin binding both bacteria. The insulin binding assay was applied as mentioned above except different incubation times were used 1, 2, 5, 10, 15 and 30 min followed by washing steps (Section 5.2.1). Dilutions of FITC labelled insulin (0.125, 0.25, .0.5, 1, 2, 3 µg) were used to create a standard curve. The fluorescence signals were measured using a fluorescence multi well plate reader (Cyto Fluor II- Preseptive Biosystem – Miami, USA).

The fluorescence signal value of *A. salmonicida* (wild type, MT004) and *B. multivorans* were normalised for non-specific binding by subtracting the signal value produced within *A. hydrophila* and *Ps. aeruginosa* respectively. All values were normalised according to the concentration of FITC labelled insulin and the number of molecules bound per 10^9 cells were estimated for *A. salmonicida and B. multivorans*. The data was statically analysed as described in Section 2.2.7.

5.2.3 Extraction and solubilisation of total protein

Different protocols and procedure were followed in order to extract the IBP(s) from *B. multivorans* and *A. salmonicida* and optimise the conditions for producing active IBP(s) for western ligand blotting. The following protocols were used to prepare total bacterial lysates:-

5.2.3.1 Solubilisation of bacterial proteins for SDS-PAGE

Total soluble cell proteins were extracted from strains of *B. multivorans* and the fish pathogen *A. salmonicida* using various extraction procedures. Bacteria were grown overnight at optimum conditions (2.2.1) and 1 ml culture volume were placed in 1.5 ml microcentrifuge tubes. The cells were centrifuged for 3 min at 6500 × *g* and pellets were resuspended in 0.5 ml modified loading buffer Laemmli (1970) by reducing the SDS concentration to 0.02% instead of 0.2%. Cell pellets were also suspended in SDS loading buffer with or without 2β-mercaptoethanol (Appendix 1). Furthermore, some samples were boiled for 5 min and others were left at RT. Next, tubes were centrifuged at 6500 × *g* for 5 min and supernatants were transferred into fresh tubes and stored at 4 °C until used in SDS-PAGE electrophoresis (Section 2.4.3).

5.2.3.2 Solubilisation proteins using Triton X 100 & low concentration of SDS

Some extractions were modified using the Triton X 100 (0.1 % W/V) instead of SDS in loading buffer as the Triton X100 is a non-polar detergent and a second modification was to reduce the SDS concentration in loading buffer to 0.02% instead of 0.2%. The pellets of 1ml growth were resuspended in 1 ml of extraction buffer and left for 15 min at 50 °C after which samples were centrifuged at 6500 × *g* for 10 min and supernatants were transferred into fresh tubes and stored at 4 °C for use in SDS-PAGE electrophoresis (Section 2.4.3).

5.2.3.3 Solubilisation of proteins using SDS and lysozyme

In order to extract *B. multivorans* and *A. salmonicida* proteins two techniques were used; the first used a low concentration of SDS (0.02%) and the second used MOPS buffer containing 50 ng/ml lysozyme. Tubes were incubated for 10

min at 55 °C for lysozyme to work and centrifuged at 6500 × *g* for 5 min and the supernatant transferred to a fresh tube with 20 µl of 2 mM protease inhibitor cocktail (P8465 Sigma, UK) was added and storage was at 4 °C. A volume of protein sample and equal volume of loading buffer containing 0.02 % SDS were mixed and run into SDS-PAGE electrophoresis.

5.2.3.4 Extraction using sonication, low SDS and lysozyme

Total protein was extracted from bacteria as described in Section 2.4.1 using sonication and lysozyme and solubilized by adding low SDS (0.02 %) loading buffer and aliquots were run into SDS-PAGE.

5.2.4 SDS-PAGE coupled western ligand blotting

Western ligand blotting was used in order to assess whether the interaction of insulin with the bacterial cell surface is mediated by a specific protein component**.** Various procedures were used to separate extracted proteins in different types of gel; blue native gel electrophoresis (BN-PAGE) (Nijtmans *et al*., 2002), native agarose protein electrophoresis (Kim *et al*., 2000) for protein – protein complexes, SDS-PAGE, and native – PAGE (Laemmli, 1970). These were used in order to provide the chemo –physical conditions necessary for the components to retain capacity to bind insulin. This study used SDS-PAGE in which the SDS concentration was reduced to 0.05 % for proteins separated on polyacrylamide gels (10% or 12%) using methods described by Laemmli (1970) (Section 2.4.3).

Proteins were transferred to nitrocellulose membrane using an electroblotter system (BIO-RAD) (Towbin *et al*., 1979) at 300 mA at RT for 1.5 h. Afterwards, the membrane was washed in MOPS buffer for 5 min and blocked with a blocking buffer developed in this study. Bovine serum albumin (BSA) in 10 mM MOPS (50 ml) for 1 hour at RT. Next, the blocking buffer was replaced with 50

ml of fresh blocking solution containing insulin-peroxidase (1µg/1ml) and the membrane was incubated for 2 hours with gentle shaking at RT. Afterwards, the membrane was washed 3 times in 50 ml of MOPS buffer with gentle shaking for 10 min at RT. The blot was developed using DAB/NiCl2 enhancement.

5.2.5 Construction of *B. multivorans* genomic DNA library

5.2.5.1 Extraction of genomic DNA of *B. multivorans*

Purified genomic DNA from *B. multivorans* was produced using a Qiagen extraction kit according to the supplier's instructions (Section 2.5.1). DNA concentration was measured (Section 2.5.5) and adjusted (Section 2.5.2) to produce 1µg/µl.

5.2.5.2 Partial digestion of genomic DNA using *Sau3A*

DNA was partially digested with *Sau3A* to generate appropriate size fragments for ligation into λ zap arms, pre-digested with *BamHI.* Digestions were performed in microcentrifuge tubes (1.5 ml) using different dilutions of the *Sau3A* enzyme. *B. multivorans* genomic DNA (20 µg) dissolved in 40 µl of MBW was mixed with 10 µl of 10 x restriction buffer. Next, 5µl aliquots of DNA were dispensed into nine microcentrifuge tubes, leaving 10 µl in the original tube (tube1). MBW was added to a final volume of 10 µl in tubes 2-9 and 18 µl in tube1. *Sau3A* restriction enzyme, 2 µl containing 8 units of enzyme was added to tube1 and mixed thoroughly. Next, 10 µl from tube 1 was transferred to tube 2, and so to create 2 fold dilution series except tube 9 was left as control undigested. The tubes were incubated at 37 °C for 25 min after this the reaction was stopped by incubating the tubes at 65 °C for 5 min in order to denature the restriction enzyme. The digested & undigested DNA was analysed by running 2 µl with a standard 1 kbp DNA ladder on agarose gel electrophoresis (Section 2.5.6). Samples containing the required average size DNA fragment of 5-6 kbp

were selected for *B. multivorans* genomic library construction.

5.2.5.3 Ligation of *B. multivorans* DNA with λ Zap express arms

The *λ* Zap express vector can accommodate inserts ranging 0-12 kbp. The digested DNA 2 µl containing 0.4 µg was mixed with 1 µg dephosphorylated *λ* Zap express *BamHI* treated arms, after this 0.5 µl of 10 x of ligation buffer, 2 units of T4 DNA ligase and MBW was added to final volume of 5 µl. The ligation was mixed thoroughly and pulse-centrifuged to ensure all contents were at the bottom of tube. The ligation was incubated overnight at 4 °C and after 1µl of the mixture was analysed by agarose gel electrophoresis with undigested, digested DNA and wild type λ DNA to assess the ligation efficiency.

5.2.5.4 *In vitro* packaging ligated DNA using Gigapack III Gold System

After ligation recombinant λ phage DNA was packaged using the Stratagene Gigapack III Gold system to generate intact recombinant phage particles. A Gigapack III Gold packaging system extract was removed from – 80 °C and quickly thawed by holding the tube between fingers. The ligated DNA (4 µl) was added immediately when contents thawed. The mixture was agitated gently to avoid air bubbles being introduced and the tube spun to ensure that all contents were at the bottom of the tube. Next, the tube was incubated at room temperature (22 °C) for not more than 2 h. SM buffer (Appendix 1) (500 µl) was added to the tube together with 20 µl of chloroform and the contents mixed gently. The tube was centrifuged briefly and the phage suspension was assayed directly and stored at 4 °C.

5.2.6 Assaying bacteriophage

5.2.6.1 Preparation of host bacteria

The packaged library suspension containing recombinant phage particles was assayed on *E. coli* XL1 Blue MRF` using NYZ medium (Appendix 1). X-gal & IPTG were used to ascertain the efficiency of ligation using blue/white screening. The number of recombinant plaques was determined and the amplified library was collected and the optimum titre was determined to achieve 700 - 1000 plaques per plate.

E. coli XL1 Blue was prepared as described by the supplier (Stratagene, USA). One single colony from an overnight streak plate was transferred to 50 ml of LB broth with supplement (Appendix 1) in a conical flask. The culture was incubated with shaking (200 rpm) at 30 °C (instead of 37 °C to keep the bacteria from over growing and subsequently the number of non-viable cells reduced. The bacteria were pelleted at 1000 × *g* for 10 min and resuspended gently in 25 ml sterile $MgSO_4$ solution (Appendix 1) and used directly to perform the assay or stored at 4 °C for not more than 48 h before use.

5.2.6.2 Phage Assay

The *E. coli XL1 Blue* cultures prepared in Section 5.2.6.1 was diluted using sterile $MgSO_4$ (10 mM) solution to an OD_{600} of 0.5. After this, 200 µl aliquots of *E. coli* were used in the assay. The neat packaged phage (1µl) and serial dilutions of the packaged phage (10^{-1}, 10^{-2}, 10^{-4}, 10^{-6}, $10^{-7,}$ and 10^{-8}) were added to aliquots of the bacteria. Tubes containing phage + bacteria were incubated at 37 °C for 15 minutes to allow the phage to attach to the cells. Next, the samples were mixed with 3 ml molten, NZY top agar (46 °C) and poured on to NYZ agar plates. The plates were left to set for 10 min at RT and incubated at 37 °C

overnight. The plaques were counted and the number of plaque forming units per millilitre (pfu/ml) recorded.

5.2.6.3 Blue- white screening for recombinants

Blue-white screening depends on the insertional inactivation of the β-galactosidase gene carried on the phage vector. Recombinant phage no longer produces β-galactosidase which normally digests the synthetic sugar X-gal, so that the recombinant plaques will show no colour or a white colour. Whereas, the non-recombinant phage will produce intact β-galactosidase enzyme and consequently the plaques show a blue colour. The dilution of phage was added to 200 µl of freshly prepared *E. coli* cells at an OD_{600} of 0.5 and incubated at 37 °C for 15 min after this the contents were added to 3 ml of molten NZY top agar (46 °C) containing 15 µl of IPTG (0.5 M) and 50 µl of X-gal (250 mg/ml) sterile stock solutions (Appendix 1).

The contents were poured immediately onto NYZ agar plates and left for 10 min at room temperature to set and incubated overnight at 37 °C. The white and blue plaques were counted to assess the success of the gene bank.

5.2.6.4 Amplifying the Zap genomic library

The libraries prepared in lambda were generally amplified to prepare a large stable quantity of high titre stock. *E. coli* XL1 Blue was cultured and diluted to the appropriate cell concentration as mentioned above (Section 5.2.6.2) and aliquots of cells (1 ml) dispensed into sterile microcentrifuge tubes. Adequate tubes were prepared to plate out the whole packaged library volume. The packaged mixture was centrifuged briefly to avoid the chloroform and then dispensed into tubes of *E. coli* cells to final concentration 10^3 pfu / 200 µl cells until utilizing all the packaged library mixture. Tube contents were mixed well and incubated at 37 °C for 15 min. Each tube's contents were mixed with 3 ml

of molten NYZ top agar (46 °C) and poured onto NYZ agar plates and left to set for 10 min at RT and then incubated at 37 °C overnight to give near confluent lysis. The top soft agar layer of plates were scrubbed using a sterile spreader and removed into 50 ml polypropylene Falcon tubes with 5 ml of SM buffer to allow phage to diffuse out of the agar. Chloroform 20 µl was added to each tube to inactivate any non lysed bacteria and incubated overnight at 4 °C. After, cell debris and the agar were removed from all tubes by centrifugation for 30 min at 4000 × *g*. The clear supernatants of all tubes were carefully recovered and placed into one sterile glass bottle. Chloroform was added to 0.3 % final concentration to the library stock and the tubes were stored at 4 °C. Some aliquots of the amplified library were placed in 7% DMSO at - 80 °C for long term storage.

5.2.6.5 Screening genomic library for insulin binding

The *B. multivorans* gene library in λ Zap was screened by ligand blotting to detect recombinant phage producing a protein associated with insulin binding. Aliquots of the amplified library were diluted with SM buffer (Appendix 1). The minimum number of plaques of *B. multivorans* to be screened was determined according to the formula below (Clarke and Carbon, 1976) where N= the number of individual clones, P= probability for representing a specific gene, the f= average size of cloned fragments (kbp) and g= the size of genome (kbp).

$$N = \frac{In(1-P)}{In\,(1-f/g)}$$

According to this formula with 5-6 kbp the average size of cloned fragments, about 1500 plaques needed to be screened to find the desired recombinant. However, and in case of this study more than 30,000 plaques were screened for recombinants that contained the IBP gene by using plaque ligand blotting.

Some samples were plated out with 25 µl of IPTG solution (250 mg/ml) in the soft agar to induce the promoter of lac Z fusions. Some samples were plated without IPTG to allow non-fusion production of foreign components. Plates were left to set at RT for 10 min and incubated at 37 °C overnight.

Sterile gridlined nitrocellulose membrane (182 mm) was marked and numbered using a ballpoint pen to the centre and four quarters, transferred using two sterile forceps on to the surface of agar plates with plaques, avoiding air bubbles. The bottom of each plate was marked in the same fashion as the filter so that filters and the plate could be easy aligned after screening. The plaques were blotted onto gridlined nitrocellulose membranes for 1 h at 37 °C followed by 1 h incubation at 4 °C. The membranes were carefully transferred using forceps into petri dishes containing 20 ml of MOPS buffer and washed with gentle agitation for 10 min and the wash buffer was replaced with a fresh 20 ml of MOPS containing 3% (v/v) bovine serum albumin as blocking reagent. The membranes were gently shaken at RT for 1 hour. Next, the blocking buffer was replaced with a fresh 20 ml of same buffer containing insulin peroxidase (1µg/ml) and the membranes were gently shaken at RT for 1 h to allow binding to occur.

The binding reagent was discarded and the membranes were washed with 20 ml of MOPS buffer for 10 min with gentle shaking at room temperature for a total of three washes with the last wash using PBS. The binding activity was visualized by adding 20 ml of DAB /$NiCl_2$ prepared in PBS (Appendix 1). The membranes were placed for 15 min in the dark until positive plaques developed. The developing solution was discarded and 20 ml of tap water was added to stop the reaction and positive plaques were noted. The positive plaques were identified on the master plates using the grids on the filters. In order to pick the

positive plaques, sterile Pasteur pipettes were used to stab and remove them into 200 µl of SM buffer in 1.5 ml microcentrifuge tubes. Chloroform 20 µl was added to inactivate the remaining bacteria. The tubes were placed at 4 °C overnight to release the phage into SM buffer.

5.2.6.6 Secondary screening of insulin binding plaques

Aliquots (loop full) of positive recombinant phage solution were streaked onto NYZ agar and overlaid with soft agar (3 ml) mixed with 200 µl *E coli* host (0.5 OD) and left to set at RT for 10 min and incubated afterwards at 37 °C overnight. After incubation, plaques were blotted onto a piece of nitrocellulose membrane and the detection procedure was followed as mentioned before (Section, 5.2.7.5). The positive plaques were placed in 500 µl of SM buffer using pasture pipettes, and chloroform (20 µl) was added and the tubes were incubated at 4°C overnight to elute the phage.

5.2.6.7 *In vivo* excision of insulin binding positive phagemids form recombinant λ Zap

The *λ Zap* express vector is designed to excise recombinant pBK-CMV phagemids to facilitate further molecular analysis of cloned regions. *E coli* XL1 Blue was used as the host to perform the pBK-CMV excision. The excision depends on the co-infection of *E. coli* with the recombinant phage and a mutant helper phage that carries an amber mutation preventing phagemid replication in *E coli* XL1 Blue and this allows only the excised phage to replicate in the host. Inside the co-infected *E. coli* proteins from helper phage recognize and nicks the DNA initiator strands of recombinant phage, a new DNA synthesis begins at the site of this nick to complete the vector downstream and the DNA signal will continue through the clone inserts until the termination signal position 3` of the initiator signal the single strand DNA is recognized by gene II protein product of

the helper phage, forming circular DNA containing the insert DNA between initiation and termination.

Recombinant phage stocks were used for excising the recombinant phagemids. *E. coli* XL 1 Blue grown overnight at 30 °C in LB broth with supplements was centrifuged at 1000 × *g* for 10 min. The pellet was suspended in of $MgSO_4$ solution to an OD_{600} of 1. The recombinant phage stock was spun briefly to avoid the chloroform and 250 µl of the phage was added to 200 µl of *E. coli* in 10 ml polypropylene tubes containing 1 µl of helper phage (1×10^6 pfu) and mixed well. The tubes were placed at 37 °C for 15 min to allow the phage to attach the cells and 3 ml of LB with supplements (Appendix 1) was added to each tube and incubated at 37 °C with shaking overnight. After incubation, the tubes were placed at 65-70 °C for 20 min to lyse the bacteria.

The samples were centrifuged at 1000 × *g* for 5 min to pellet the cell debris. The supernatants containing excised phagemids packed as filamentous phage particles were transferred into fresh tubes and used to transfect the *E. coli* XLOROR. *E. coli XLROR* was grown overnight in 50 ml of LB with supplements at 30 °C, centrifuged and resuspended in $MgSO_4$ to an OD = 1. Aliquots (200 µl) were dispensed in microcentrifuge tubes then 100 µl or 10 µl of phagemid supernatant were added to the cells and the tubes were incubated at 37 °C for 15 min and 300 µl of NYZ broth was added to each tube and incubated at 37 °C for 45 min to induce and express kanamycin gene resistance carried on the phagemid prior to plating 200 µl on to Kanamycin (50 µg/ml) LB selective media and incubating overnight at 37 °C. After incubation, single colonies were streaked on Kanamycin plates to purify the clones which contained recombinant pBK-CMV double strand phagemid vector.

5.2.6.8 Extraction and digestion of recombinant phagemids

Purified phagemids were extracted using a miniprep plasmid extraction Kit (Sections 2.5.3 and 2.5.4) and 0.3 µg DNA of recombinant phagemids were digested using combinations of restriction enzymes *EcoRI* + *PstI* and *EcoRI* + *SalI* and fragments were separated by agarose gel electrophoresis (Section 2.5.6). The recombinants *E coli* XLROR were grown overnight in 50 ml LB containing kanamycin 50 µg/ml to express the cloned genes encoding insulin binding proteins (components).

5.3 Results

5.3.1 Insulin binding assay with whole cell microbes

This experiment screened various types of microorganisms Gram negative and Gram positive bacteria, yeast and Actinomyces (*Nocardia)* for insulin binding capacity. A total of 40 bacterial and 5 yeast strains were examined to determine whether they exhibited any insulin binding activity (Appendix 2). The initial assay indicated only 3 out of the 45 strains examined exhibited insulin binding activity. *B. multivorans* and *B. cenocepacia* and *A. salmonicida* wild type all showed a dark colour reaction with DAB suggesting they possessed components which bound insulin (Figure 5.1).

The fish pathogen *A. salmonicida* CM30 showed a strong reaction within 5 sec of adding the peroxidase substrate reagent, *B. multivorans* strains showed a positive result after 5 min. It was suspected that in the case of *A. salmonicida* insulin might be binding to the “A” protein of this organism, an extra protein S-layer encapsulating the bacterium. Thus a mutant of *A. salmonicida* (MT004) which lacked the A layer was subsequently tested and showed weaker and slower binding. In order to confirm this binding was with insulin and not with the conjugated peroxidase, all microorganisms that showed a positive binding activity were tested with same the peroxidase on its own and showed no reaction. All control wells (no insulin- peroxidase) showed no activity except *Ps. fluorescens* showed an activity in control and treatment wells revealing a peroxidase enzyme activity produced by this bacteria. Binding activity increased using MOPS buffer as binding buffer compared to PBS or Tris buffer.

A

B. multivorans *A. salmonicida* CM30 *A. salmonicida MT004* *E. coli EMG1*

B

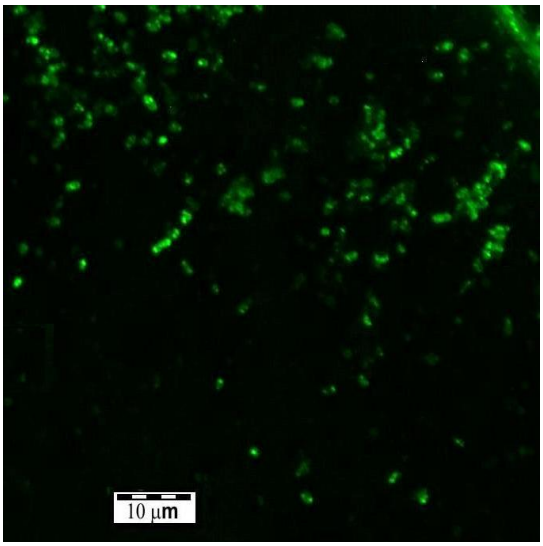

B. multivorans

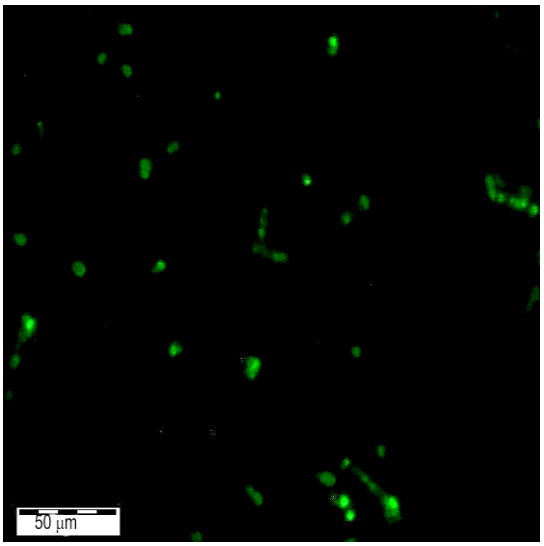

A. salmonicida MT004

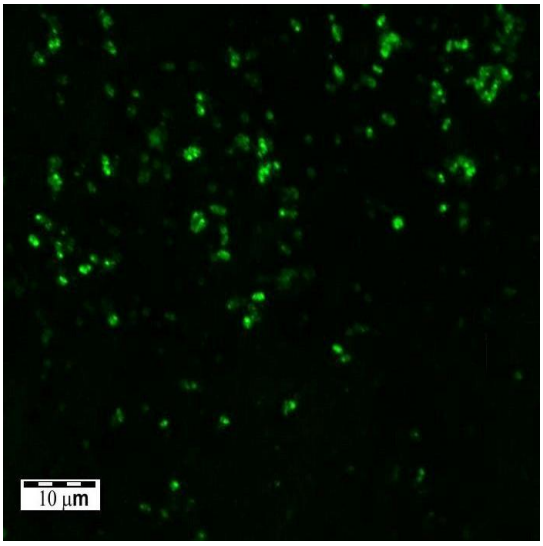

A. salmonicida CM30

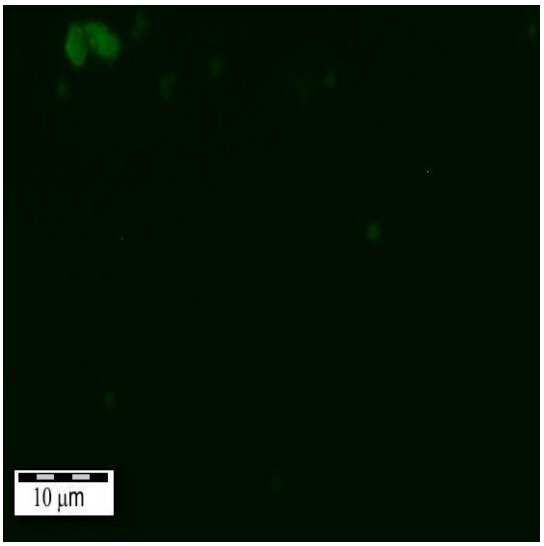

E. coli EMG1

Figure 5.1: Peroxidase-labelled insulin (A) and FITC-labelled insulin (B) bind to cell surfaces of *E. coli*, *A.salmonicida* MT004, *A.salmonicida* CM30 and *B. multivorans*.

5.3.2 Quantification of insulin binding

This test was done to quantify the amount of insulin bound to the cell surfaces of *B. multivorans* and *A. salmonicida* CM30 and the mutant MT004.

Both wild type *A. salmonicida* CM30 and *B. multivorans* showed significant insulin binding at all the time points tested, however, the amount of insulin binding to the fish pathogen *A. salmonicida* CM30 was about 105 ng/10^9 cells after 15 min incubation time which was much higher compared to 28.3 and 21.1 ng/10^9 cells binding to *B. multivorans* and the *A. salmonicida* MT004 A layer mutant, respectively (Figure 5.2). Furthermore, wild type *A. salmonicida* CM30 and *B. multivorans* showed significant binding relatively early (after 1 min) compared to the mutant *A. salmonicida* MT004 which showed significant FITC-insulin binding only after 10 min.

Insulin binding to wild type *A. salmonicida* CM30 increased steadily with time; however, *B. multivorans* showed no significant increase in insulin binding up to 5 min (13.1 ng/109 cells) but produced strong binding of 19.1 and 23.8 ng/10^9 cells after 10 and 15 min, respectively. Whereas, the mutant *A. salmonicida* MT004 showed significant binding of 15.5 and 21.1 ng/10^9 cells only after 10 and 15 min, respectively, with no significant binding at earlier times.

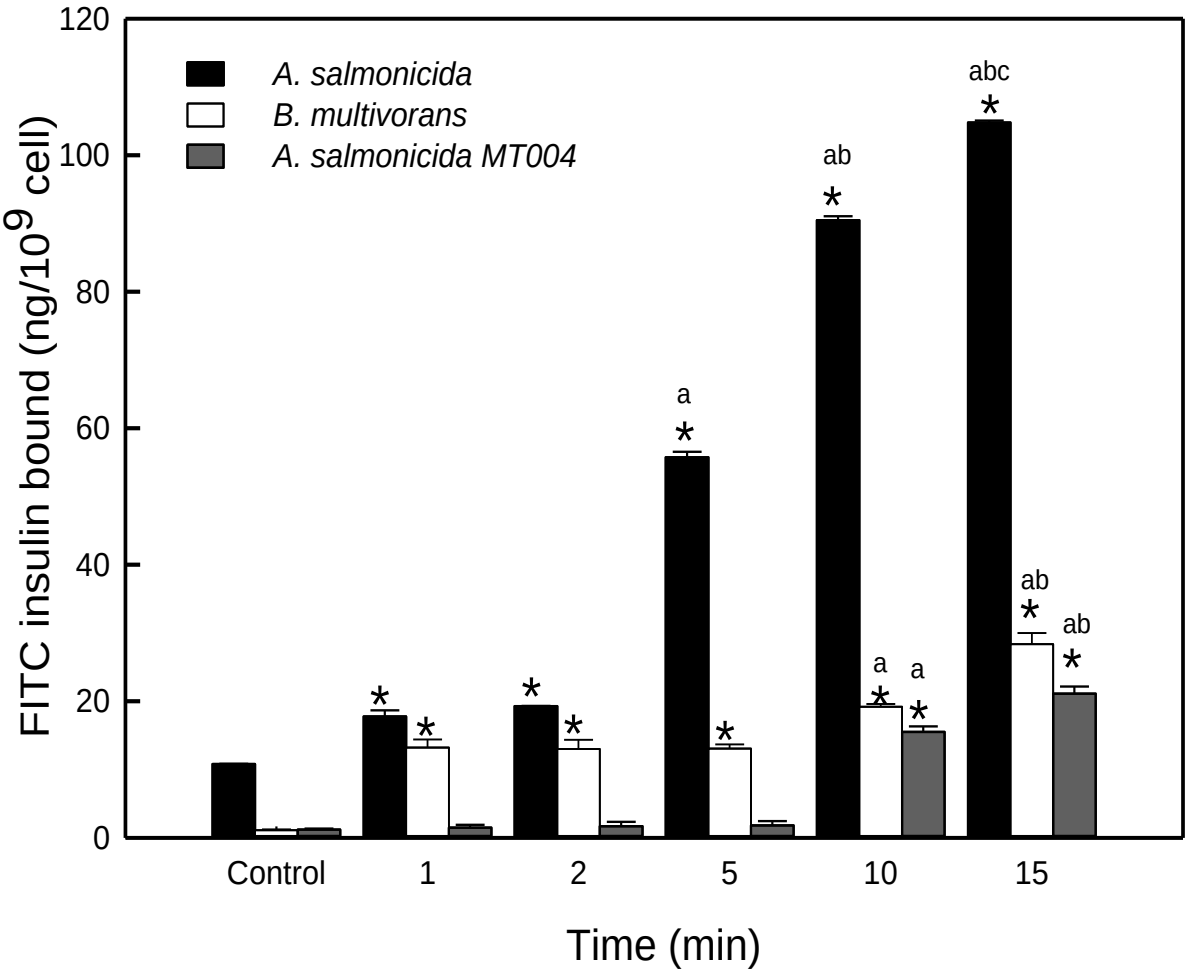

Figure 5.2: Quantification of the amount of FITC-labelled insulin bound to 10^9 cells of *A. salmonicida* (CM30 & MT004) and *B. multivorans*. The data shown are means ± S.E. (n = 4). * indicates significant differences ($p \leq 0.05$) compared to the control. a, ab and abc indicates significantly differences ($p \leq 0.05$) compare to the amount of FITC bound at earlier times for the same bacterium.

5.3.3 Western ligand blotting of insulin binding protein

Various protocols were applied during this work to separate bacterial proteins on different gels using native, SDS-PAGE (Laemmli, 1970), blue native (BN-PAGE) (Nijtmans *et al.*, 2002) and agarose gel electrophoresis (Henderson *et al.*, 2000) and both *Burkholderia* and *A. salmonicida* samples initially showed no IBP bands using standard western ligand blotting. However, a modified procedure, i.e. extraction using sonication with low SDS (0.02%) loading buffer and a low concentration of lysozyme to solubilise the whole cell lysates, showed positive results compared to the conventional boiling extraction methods. Moreover, protein separation by SDS-PAGE with 0.05% SDS instead of 0.1% significantly enhanced post blotting protein binding.

Western ligand blotting with an insulin peroxidase conjugate successfully revealed IBP bands with *Burkholderia* strains at approximately 30 and 20 kDa (Figure 5.3) but no IBPs were detected in lysates from either wild type *A. salmonicida* CM 30 or the A layer mutant MT004.

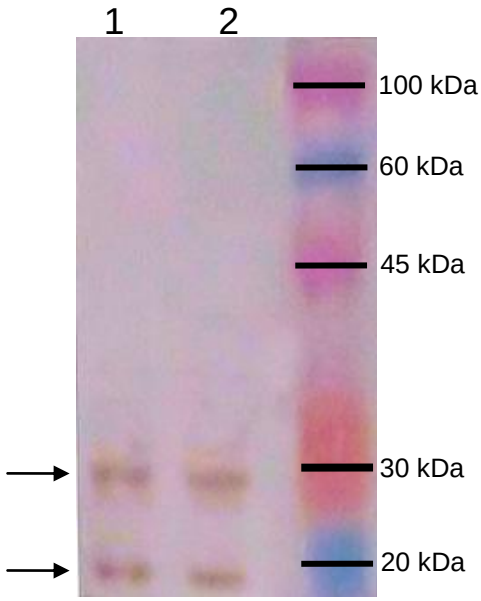

Figure 5.3: Western ligand blotting of whole cell soluble lysates of *B. multivorans* (1) and *B. cenocepacia* (2) showing binding of peroxidase labelled –insulin, to putative insulin binding proteins.

5.3.4 Construction *B. multivorans* genomic library

5.3.4.1 Ligation of *B. multivorans* DNA into predigested λ Zap arms

A genomic library of *B. multivorans* was constructed in λ Zap. The partial digestion of chromosomal DNA was achieved using serial dilutions of *Sau3A* (Section 5.2.5.2). The digested DNA was separated by agarose gel electrophoresis (Figure 5.4) alongside with 1 kbp DNA ladders and the range of fragment sizes was identified. The digestion lane 7 contained an average size of 5-6 kbp with 0.03 unit of *Sau3A.* DNA from this sample was deemed suitable for ligation within the *BamHI* sticky ends of **λ** Zap arms (Section 5.2.5.3). Subsequently, recombinant **λ** Zap with *B. multivorans* DNA inserts were generated (Figure 5.5) from ligation.

5.3.4.2 Titration of gene bank and screening for recombinants

The recombinant phage DNA was packaged into bacteriophage coats by *in vitro* packaging to produce infectious recombinant bacteriophages, representing a *B. multivorans* genomic library in λ Zap II. The library suspension titer was 5×10^6 pfu /ml. At the same time the proportion of recombinant bacteriophage in the library was estimated by plating aliquots of library suspension on the plates with X-gal and IPTG. The recombinant phage rate was around 95 % (Figure 5.6). The library was successfully amplified (Section 5.2.6.4), harvested and tittered at 2×10^{10} pfu/ml.

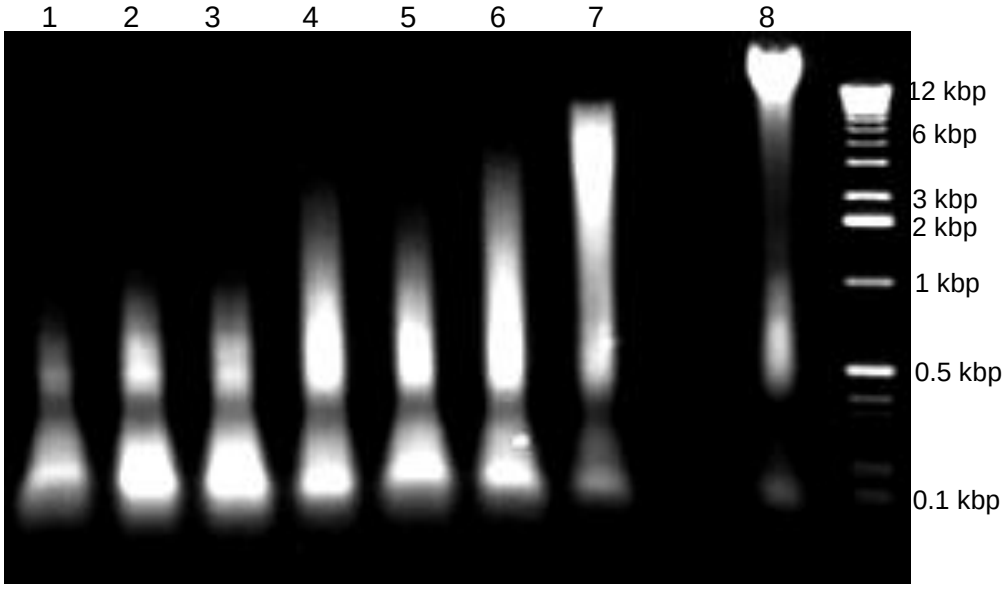

Figure 5.4: Agarose gel electrophoresis of serial *Sau3A* digests of 1µg samples of genomic DNA of *B. multivorans* using two fold dilution of enzyme (2, 1, 0.5, 0.25, 0.125 , 0.06 and - 0.03U) Lane 1-7 respectively compare to the undigested sample (control) in lane 8.

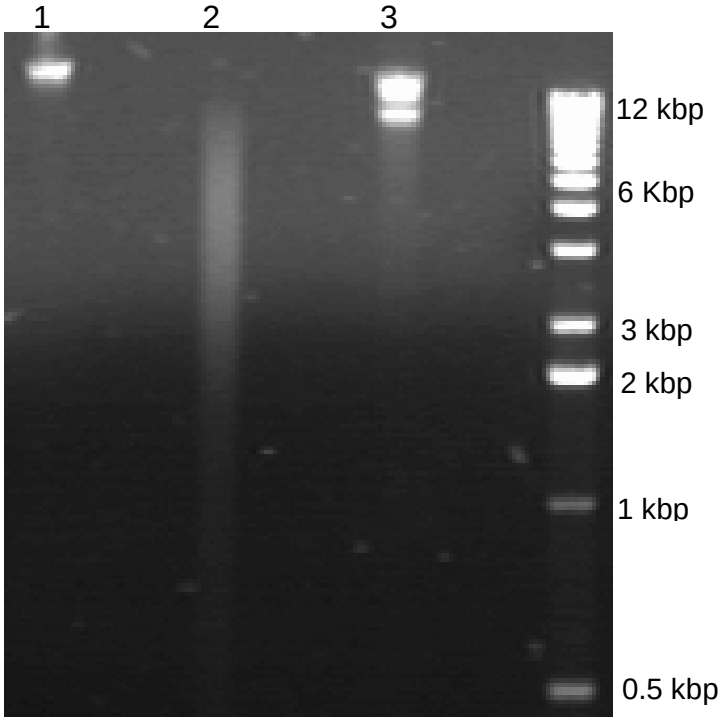

Figure 5.5: Agarose gel electrophoresis of *B. multivorans* digested genomic DNA ligated within λ Zap arms. Standard λ DNA (Lane1), *B. multivorans* genomic DNA digested with *Sau3A* (Lane2) ligation mixture (lane3), 1kbp ladder (lane 4).

5.3.4.3 Screening *B. multivorans* genomic library for insulin binding activity

A minimum of 1500 recombinant each containing an average 5-6 kbp insert were estimated to be screened to find one clone. Actually, 30000 plaques were screened for insulin binding protein. Nineteen positive plaques were identified showing insulin peroxidase activity as coloured halo or dot with DAB/$NiCl_2$ (Figure 5.7). The positive plaques recovered were rescreened again for insulin binding. Secondary screening of the positive plaques produced pure recombinants plaques. This was done by streaking positive plaques on NYZ agar and screening for IBP as before. After that only 8 clones (λ_1- λ_8) remained stable, continuing to bind insulin peroxidase.

5.3.4.4 *In vivo* excision of positive insulin binding recombinant phagemids

The positive recombinant bacteriophages were used to recover the internal recombinant phagemids pBK-CMV which carried IBP gene(s). The helper phage was used for excision of the recombinant pBK-CMV and used to transfect *E coli XLROR.* Transfectants were selected on Kanamycin plates; the internal phagemid was successfully created after helper phage co-transfection. The DNA of recombinant phagemids was separated on agarose gel electrophoresis and shown to be of a higher MW than pBR328 and non-recombinant phagemids (Figure 5.8 A). Electrophoresis of digested DNA fragments of recombinant phagemids showed two patterns of inserts, phagemid p1 (6 examples) and p2 (two). Digests were produced using combinations of restriction enzymes *EcoRI +PstI* and *EcoRI +SalI*, respectively. The p1 insert totalled 2.6 kbp consisting of 3 DNA bands 1.6, 0.8 and 0.2 kbp and the p2 showed 1 band of insert about 2.9 kbp total size (Figure 5.8 B).

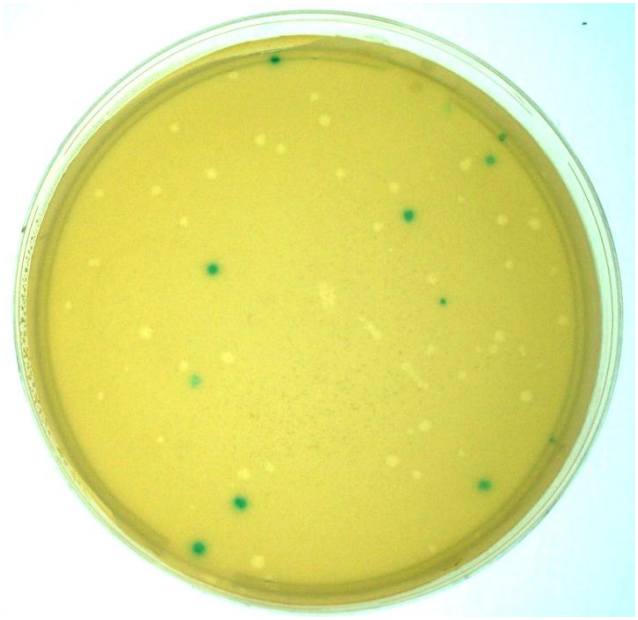

Figure 5.6: Blue white Screening of *B. multivorans* genomic library generated in λ zap vector.

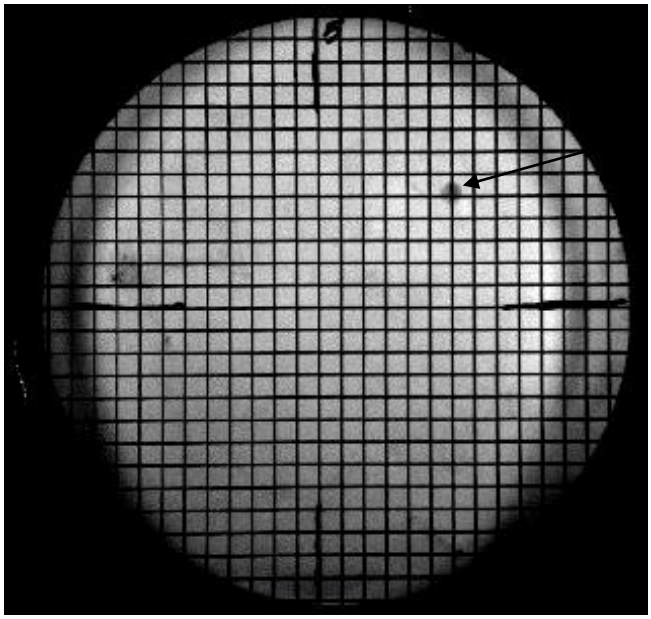

Figure 5.7: Screening of λ Zap *B. multivorans* gene library for insulin binding. The plaques were blotted onto a membrane, blocked and screened for binding of insulin peroxidase. The arrow refers to a positive binding of the peroxidase labelled insulin to a recombinant plaque producing the IBP.

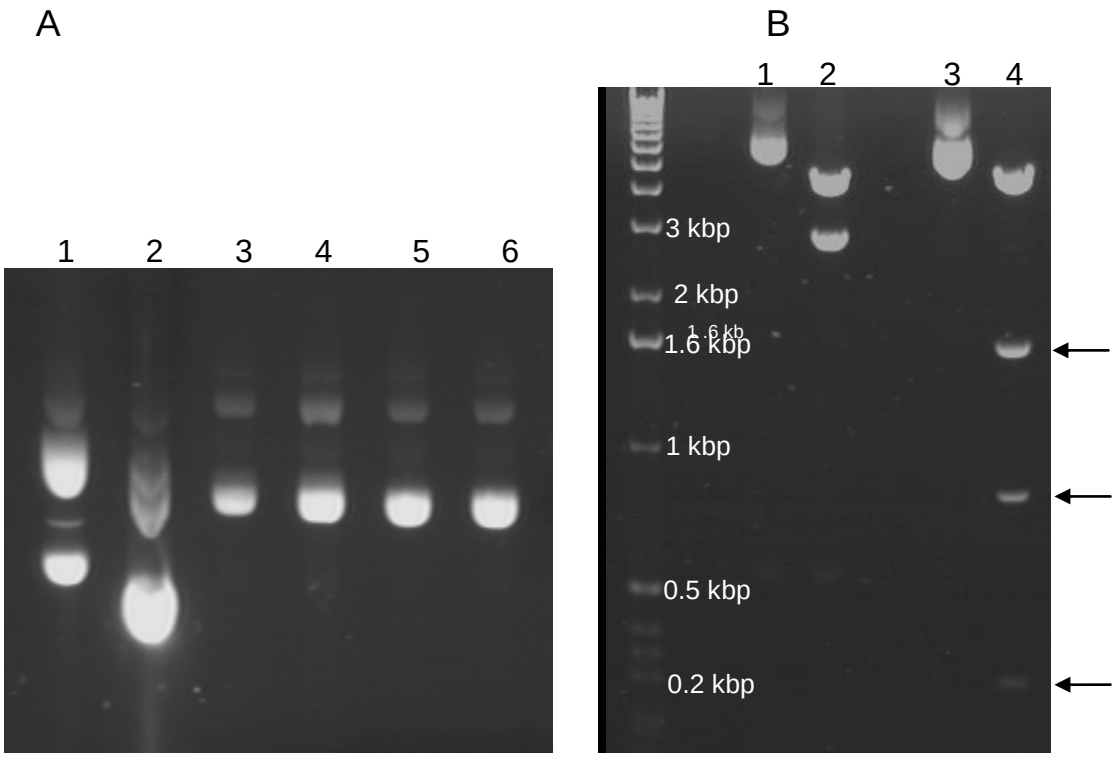

Figure 5.8: (A) Agarose gel electrophoresis of recombinant phagemids (lane 3,4,5,6 compared to non-recombinant pBK-CMV, lane 2, and pBR328 plasmid lane 1. (B) Digest of phagemids p2 (2) & p1 (4) digested by *EcoRI +SalI* and *EcoRI +PstI* respectively compared with undigested phagemids p2 & p1 (lane1 & 3 respectively).

5.4 Discussion

The current study screened 45 types of microbial species for the presence of cell surface components capable of binding with insulin hormone. The results showed strong binding activity with peroxidase labelled insulin for the fish pathogen *A. salmonicida* CM30 and opportunistic human pathogenic bacteria *B. multivorans* and *B. cenocepacia*. These positive strains showed no binding activity with just the peroxidase enzyme revealing the binding sites on these bacterial strains are binding sites for insulin and not for the peroxidase component. Hormone binding proteins or insulin binding proteins have been previously found among various types of microorganisms; bacteria, fungus and protozoa (Souza and López, 2004). Also it has been reported that some hormone-like and hormone binding proteins are produced by higher microorganisms such as fungi, including yeast, which can modulate intracellular signalling systems, cell proliferation, differentiation and other functional responses (Lenard, 1992).

Insulin binding with some fungi like *Neurospora* and yeast like *Schizosachoramyces sp* and even protozoa have shown physiological responses which provided evidence about signalling including regulation of the glucose downstream metabolic pathway (Souza and López, 2004). These insulin binding proteins and functional responses are thus clearer in eukaryotic microbes such as yeast but less clear in prokaryotic single cell microbes. The insulin ligand binding assay revealed that *B. multivorans* and *B. cenocepacia* both bound insulin. The genus *Burkholderia* is made up of Gram negative protobacteria with over 40 species occupying a wide range of ecological habitats such as water and the rhizosphere. Members of the *Burkholderia* genus can cause serious human, animal and plant diseases. However, some

have been used to enhance plant growth and bioremediation (Jones *et al.*, 2001; Stoyanova *et al.*, 2007). The *Burkholderia cepacia* complex (BCC) have emerged as a serious threat to CF patients causing pulmonary infection and necrotizing pneumonia leading to lung morbidity and mortality (Whitby *et al*., 2000), BCC bacteria produce a number of virulence factors. Including lipopolysaccharides (LPS), is a strong endotoxin which contributes to the inflammatory nature of BCC infection of CF patients (Kenna *et al*., 2003). Furthermore, BCC produce a number of extracellular products including haemolysin, protease, lipases, ATP hydrolysing enzyme like Azurin (Punj *et al*., 2003) and antimicrobial secondary metabolites (Li *et al.*, 2008). BCC acquire iron by producing a number of iron binding siderophores, salisalic acid, ornibactin and pyochelin which are important virulence factors in initialization of colonisation (Peckham *et al.*, 1996; Thomas, 2006). BCC members have multiple drug resistance and combinations of 3 or more types of antibiotics are used in order to treat BCC infections, immunomodulatory agents such as methyl prednisolone, immunoglobulin and cyclosporine are also used to treat infection (Burnie *et al.*, 1995; Jones *et al.*, 2001; Moore and Elborn, 2003).

All *Burkholderia* genomovars have been identified in CF patients; however, *B. cenocepacia and B. multivorans* are the most commonly found being isolated from around 90% of CF patients. These genomovars often transfer among patients and even infect normal individuals in some cases and are known as the epidemic strains (Mahenthiralingam *et al*., 2002).

Wood *et al* (1993) demonstrated for the first time insulin binding on the *B. pseudomallei* cell surface and estimated that there were 5000 insulin binding sites per cell, *B. cepacia* was reported to bind insulin (Kanai *et al*., 1996). Furthermore, another study noted increase in the *B. cepacia* growth rate after

the culture was incubated with insulin hormone for 24 h suggesting the bacteria can use insulin as a growth substrate (Jeromson *et al*., 1999). It was demonstrated that the commercial insulin markedly inhibits the growth of *P. pseudomallei* in vitro and in vivo (Woods *et al.*, 1993), however, Simpson & Wuthiekanun, (2000) suggested that the preservative m-cresol in insulin commercial preparation caused inhibition of *B. pseudomallei* growth and not insulin. Moreover, the insulin receptors on *B. pseudomallei* and *B. cepacia* were suggested to be part of a signal transfer system such as for phospholipase or protein tyrosine phosphatase (Kanai *et al*., 1996).

The current study shows a strong binding of insulin peroxidase and FITC insulin to wild type of *A. salmonicida* CM30 compared to the binding seen with an A-layer mutant and *B. multivorans*. A study of the insulin binding protein of *N. crassa* showed that the protein was a signal transduction member interfering with glucose metabolism and 10^3 insulin binding sites were estimated per cell (Kole *et al*., 1991).

The present study indicated for the first time an insulin binding activity within *A. salmonicida,* revealing a novel insulin binding protein. Wild type *A. salmonicida* produced strong binding with insulin but the *A. salmonicida a* mutant MT004 which lacks the A-layer protein envelope, produced much lower insulin binding. The A-layer of *A. salmonicida* plays an important role in pathogenicity, facilitating resistance to phagocytosis and bacteriophage infection (Kaplin *et al.*, 1996; Nikoskelainen *et al.*, 2005).

A mutant lacking the A-layer is non-virulent *A. salmonicida* (Ellis, 1988; Marsden *et al.*, 1996; Fast *et al.*, 2009) and it was reported that the A-layer could be used as a vaccine and plays a protective role in fish against *A. salmonicida* infection (Arnesen *et al.*, 2010).

Other binding studies indicate the ability of *A. salmonicida* to bind specifically some conserved proteins like collagen types I and IV and estimated that high amounts of radiolabelled collagen bound, and that collagen binding was fast and saturable with high affinity and irreversible (Trust *et al.*, 1993). Fibronectin and laminin are basement membrane large extracellular glycoproteins and play a crucial biological role in cell adhesion and cell-cell contact in mammalian cells and have been reported to bind tightly to the *A. salmonicida* A-layer. However, neither *A. salmonicida* A-layer mutants nor *A. hydrophila* bind either of those proteins (Doig *et al.*, 1992).

It has also been shown that the A-layer plays an important role in an iron chelating – process via direct binding to the hydrophobic iron structure in a siderophore-independent *A. salmonicida* species. However, A-layer is the major siderophore receptor or chelator in siderophore dependent species in which siderophore like anguibactin, aerobactin, enterobactin, and hydroxamate siderophores mediate iron uptake mechanisms (Hirst *et al.*, 1991; Fernandez *et al.*, 1998). In addition to the A-layer contribution in siderophore binding, it was discovered that the *A. salmonicida* can bind porphyrin, the haemin protein to sequester iron which is correlated with many virulence factors like some protease and haemolysin etc. (Kay *et al.*, 1985).

SDS-PAGE and western ligand blotting were used in order to identify the insulin binding proteins. Various types of electrophoresis and blotting strategies were used in order to promote successful insulin binding. Many procedures were used to extract a solubilised active IBP(s). Low concentration of lysozyme in protein extraction, and low SDS used for cell wall lysis and in loading buffer and electrophoresis buffer showed positive results for insulin binding with *B. multivorans* & *B. cenocepacia*.

Furthermore, modification of SDS-PAGE and blotting conditions were useful to minimise ligand binding inhibition by SDS, by reducing SDS concentration of resolving and stacking gel as well as in the electrophoresis buffer.

Protein blotting conditions were also altered using 300 mA for 90 min instead of 40 mA for 24 h. Furthermore, the blocking solution of BSA dissolved in MOPS buffer instead of casein prepared in PBS buffer improved binding.

Western ligand blotting for insulin binding proteins of *B. multivorans* & *B. cenocepacia* revealed 2 positive protein bands at about 30 and 20 kDa in each species of *Burkholderia* tested, and may represent active monomer proteins from a diametric protein complex, or alternatively, these proteins may be an insulin degrading enzymes which attacks the beta chain of insulin in mammalian cells (Wang *et al.*, 2006). Similar enzymes have been discovered in microorganisms to utilize insulin and other oligo peptides (Kole *et al*., 1991). Some other microorganisms like *N. crassa* have been shown to possess two IBPs, at 55 kDa and 110 kDa (Kole *et al*., 1991) and the protozoa *Tetrahymena pyriformis* also has two IBPs at 30 & 50 kDa (Christopher and Sundermann, 1996) .

Once IBPs were recognised, steps were taken to identify sequences responsible for IBP(s) in *B. multivorans* by creating a genomic library. The gene bank (or genomic library) is a powerful strategy to identify genes for unknown proteins with functional activity, moreover, gene cloning is increasingly being used for ligand binding studies in order to produce the native form of either the ligand or the receptors (Wilson and Walker, 2005; Lodge *et al.*, 2007).

Identifying proteins with insulin binding activity and determining its amino acid would reveal whether sequences share homology with the human insulin receptor. If so, this may initiate an autoimmune response against human insulin

receptor and subsequently be involved in development of diabetes, particularly in the case of patients with CF with chronic infection with strains belonging to the *B. cepacia* complex. A *B. multivorans* genomic library was successfully produced in λ Zap express vector to facilitate screening the library for insulin binding.

Screening for insulin binding proteins in microorganisms particularly those associated with human was a starting point for this study to look for similarity between insulin binding proteins of microorganisms and (HIR) that might have a role in causing a diabetic autoimmune response. If the IBP(s) on microorganism share mimicries within HIR, then during infection the antigen presenting cells and macrophages will process those mimicries for those invaders (microorganisms) to the immune defence system leading to an autoimmune response against the same epitopes on HIR. This study presents a possible pathogenic role for microorganisms in developing diabetes in CFRD patients as they suffer from long term infection by *B. cepacia* II (*B. multivorans),* and *B. cepacia* III (*B. cenocepacia*) (Mahenthiralingam *et al*., 2002; Coutinho, 2007). However, in the case of *A. salmonicida* it could represent a potential risk for those consuming fish meat contaminated by *A. salmonicida*. In both cases human insulin bound on *Burkholderia spp* and *A. salmonicida a* can be processed as a foreign antigen, as it is seen as part of the bacterial protein during the host immune responses and subsequently lead to an autoimmune response to self-antigens such as insulin or insulin receptor and the individual may subsequently become diabetic.

In conclusion, this study indicates insulin binding proteins on microorganisms particularly Gram negative bacteria might play a role in causing a diabetic autoimmune response. It shows for the first time insulin binding to components on the cell envelope of the fish pathogen *A. salmonicida* and the greater part of insulin binding is mediated by the A-layer, however, the current study failed to produce IBP(s) by ligand blotting. Also, it has been confirmed that insulin binding occurs on *B. multivorans* and successful ligand blotting has identified two IBP bands of 20 and 30 kDa. Construction of a gene library will facilitate characterisation of IBPs in *Burkholderia* which in turn may contribute to our understanding of the development of diabetic autoimmune response particularly in case CF-related diabetes (CFRD).

Chapter 6

Expression recombinant phagemids p1 & p2, sequencing and sequence analysis

6.1 Introduction

Diabetes can be the result of an autoimmune response against self β-cell auto antigens leading to permanent damage which causes diabetes type 1 and recently autoimmunity has been implicated in diabetes type 2. Molecular mimicries between microorganisms (bacteria, virus, etc.) and self β-cell antigens have been hypothesised to trigger a diabetogenic immune response. Furthermore, it has been found that some microorganisms do possess proteins with sequence homology to β-cell antigens which could contribute to an autoimmune response against β-cells (MacFarlane *et al.*, 2003; Fujinami *et al.*, 2006). Some microbial proteins which share amino acid sequence homology to β-cell pancreatic auto-antigens may have a similar function, heat shock protein60 (HSP60) from *Ps. aeruginosa* and HSP60 of pancreatic β-cells antigen (Jensen *et al*., 2001).

IBPs of *Burkholderia* could result in the development of diabetic autoimmune response against insulin or insulin receptor, on the basis of molecular mimicry, particularly in CFRD suffers who often have *Burkholderia* infections and develop diabetes for unclear reasons. This chapter involves searching for linear molecular mimicry between proteins in the insulin associated pathway like insulin receptors and major β- pancreatic antigens and microbial proteins.

The main aim of the work in this chapter was to identify the *B. multivorans* IBPs sequences via the cloned gene(s) encoding IBPs (Chapter 5) and then search databases for sequence homology of the translated sequences of IBP genes and protein sequences of HIR. The recombinant phagemids were used to express the IBP(s) in *E. coli*, the recombinant cells were grown and protein lysates were subjected to western ligand blotting and compared to the original

extract of *B. multivorans.* Southern blotting was used in order to confirm the origin of the DNA encoding IBP(s) was from *B. multivorans*.

In order to identify the sequences encoding IBP(s), the recombinant phagemids (p1 & p2) were sequenced and analysed to identify possible ORF(s) start and stop codons and Shine Dalgarno ribosomal RNA binding domain (SD) sequences. ORFs were analysed and translated sequences used to identify homologues protein sequences and extract properties such as MW and transmembrane proteins. Translated proteins were specifically used to search for homology with the HIR to identify any molecular mimicries or linear epitopes between IBP(s) and HIR. The affinity of these epitopes to MHC I molecules was used to identify the possibility of presentation of these epitopes for immunological processing.

6.2 Materials and Methods

6.2.1 Expressing recombinant phagemids in *E. coli*

Recombinant phagemids (p1 & p2) were grown in 50 ml LB (Section 2.2.2) containing 50 µg /ml kanamycin incubated at 37 °C overnight with shaking (120 rpm). The total protein was extracted (Section 2.4.1) from the *E. coli* recombinant and from *E. coli* non-recombinant host bacteria and *B. multivorans,* as negative and positive controls, respectively. Cell lysates were subjected to western ligand blotting to detect insulin binding proteins (IBPs) (Section 5.2.4).

6.2.2 Southern Blotting

Southern hybridisation is a technique used to locate a particular gene sequence within an entire genome and was used to confirm the origin of the insert DNA within p1 & p2 was from *B. multivorans*. The genomic DNA of *B. multivorans* was digested using *EcoR V*, denatured and transferred from a gel to a membrane. Phagemids p1 & p2 DNA were used to prepare the digoxigenin

label probes encoding IBP(s) which were used to detect the complementary sequence in the digested genomic DNA on the membrane.

6.2.2.1 Digoxigenin-Labelling of the DNA Template

The hybridisation was performed using a digoxigenin DNA labelling kit (Roche Applied Science) in which the DNA probes were generated during replication using random primed labelling which by hybridization of random oligonucleotides to the denatured DNA template. The complementary DNA strand is synthesised by Klenow enzyme using the 3' OH termini of the random oligonucleotides as primers and mixture of deoxy-riboneucleotides containing DIG-11-dUTP label for elongation. The p1 and p2 DNA was extracted and concentrated (Section 2.5.2) and used as DNA templates. DNA (500 ng) in 15 µl of MBW in a 1.5 ml microcentrifuge tube was denatured by heating in a boiling water bath for 10 min followed by quickly chilling on ice. Next, hexa-nucleotide mix (10 x) 2 µl, dNTP labell (2 µl) and Klenow enzyme (1 µl) was added, mixed, centrifuged briefly and incubated overnight at 37 °C. The same procedure was performed using pBR328 linearised by *BamHI* as a control labelling.

6.2.2.2 Hybridization

B. multivorans genomic DNA (2µg) was digested overnight using *EcoRV* restriction enzyme (Section 2.5.8) and separated on agarose gel electrophoresis (Section 2.5.6) alongside with pBR328 linearized by *BamHI*. The gel was electrophoresed for 3 h at 120 V until the front bromophenol blue dye reached to 2 cm to the end of the gel. The agarose gel was depurinated by submerging in 0.2 N HCl with gently shaking for 15 min followed by placing the gel in denaturation solution (Appendix 1) for 45 min with gentle shaking in order

to denature the double stranded DNA fragments. The denaturation solution was replaced with neutralization solution (Appendix 1) for 30 min at RT with constant agitation after this the neutralization solution was replaced with fresh amount of the same solution and left with shaking for 15 min.

The DNA was transferred using the southern blotting capillary transfer system (Scot, UK). The apparatus was washed with MBW and filled with 2 litre of 10 × SSC buffer (Appendix 1). A filter paper wick was wetted and placed on the surface of blotting base and the agarose gel was placed in the centre of wick and aluminium foil was placed around the gel to cover the wick area around the gel to prevent short –circulating during transfer. A piece of positively charge nylon membrane, cut to the size of the gel and wetted with water and then with 10 x SSC buffer was placed on the gel surface, a glass rod was passed over the membrane to remove air bubbles between the membrane and the gel. Two Whatman 3 mm filter papers (same size as membrane) were wetted in 10 x SSC and placed on the nylon membrane. Paper towels, 10 cm^2 high were placed on the top of the filter papers and a 0.5 Kg weight was placed on top and left for 20 h to allow capillary transfer of the DNA to the nylon membrane. The membrane was removed carefully from the gel using forceps and placed on the transilluminator with wave length adjusted to 254 nm for 5 min for binding the DNA to the membrane by UV cross linking. The membrane was rinsed with MBW and left to air dry. The membrane was marked and cut into strips for use with different probes. The membrane stripes were pre-hybridized by immersing them in 30 ml of pre-hybridisation buffer (Appendix 1) at 68 $^{\circ}C$ for 2 hours in a hybridisation oven. The pre-hybridisation solution was replaced with fresh amount of pre-hybridisation solution containing DNA probes 25 ng/ml which was pre-denatured by boiling for 5 min and placed directly in ice water bath prior to

use. The membranes were left overnight for hybridisation and were washed twice for 5 min in 30 ml of stringency buffer I (Appendix 1) with constant agitation at RT, and washed twice for 15 min in 30 ml of stringency buffer II (Appendix 1) at 65 °C. The membranes were prepared for detection by rinsing for 5 min in 30 ml maleic acid buffer (Appendix 1) and then immersed in 50 ml blocking solution (Appendix 1) for 30 min at RT with gentle shaking. The blocking solution was replaced with a fresh amount of blocking solution containing 1:5000 Antidigoxigenin antibody–AP to final concentration of 150 mu/ml. The membranes were washed twice with 50 ml washing buffer for 15 min and equilibrated for 5 min in 10 ml detection buffer and incubated overnight in 20 ml of detection buffer containing 40 µl/ml from NBT/BCIP stock solution. The reaction was stopped by replacing the developing solution with TE buffer and images were taken.

6.2.3 Sequencing the recombinant phagemids p1 and p2

The pBK-CMV phagemid has two binding sites for T7 and T3 primers (forward and reverse respectively) for sequencing. Recombinant phagemids samples were commercially sequenced using read value sequencing by MWG Eurofins/Germany.

6.2.4 Sequence analysis

6.2.4.1 ORF gene motifs and predicted amino acid sequence

Online sequence analysis software of the European Molecular Biology Laboratory (EMBL) was used in order to find ORFs by detecting possible ATG, TAC codons. The program also looks for stop codons TAA, TAG and TGA that terminate translation. Motifs like -10, -35 and SD sequences were also identified

using the NCBI identifier. EMBL tool was used to predict the MW of proteins encoded by the ORF(s).

6.2.4.2 Sequence identification by Blast –n & p

The ORFs sequences were used to search the Genbank database (NCBI) using the Blast-n algorithms to predict for protein encoded by the ORFs. Furthermore, Blast –p was used to look for significant similarity between proteins encoded by cloned ORFs and HIR and epitopes were predicted.

6.2.4.3 Phylogenetic tree and evaluation relationship

The tree was constructed using ClustalW2 programme online from European Bioinformatics Institute (EBI) multiple alignment of sequences from Blast-n of ORFs sequences encoding IBP(s). The phylogram showing evolutionary relationship and the degree of homology (100%) between sequences were edited to the tree.

6.2.4.4 IBP topology prediction

The online HMMTop software from ExPASy tools of the Swiss institute of Bioinformatics was used to predict the transmembrane α-helix domain into the IBPs structures.

6.2.4.5 Molecular mimicries and linear epitopes prediction

The molecular mimicries or homology between IBP (1, 2 and 3) of *B. multivorans* and HIR were predicted. The translated sequences of IBP(s) were searched against amino acid sequences of HIR accession number AAI17173 (Appendix 2) using high sensitivity software online Blast P2 from ExPASy and proteomics tools from the Swiss Bioinformatics Institute.

6.3 Results

6.3.1 Expressing recombinant phagemids in *E. coli*

The insulin binding proteins from recombinants were detected using western ligand blotting using proteins extracted and solubilised from confluent lysis of *E. coli* XL1 Blue by recombinants λ_1 & λ_2 and from recombinant *E. coli XLROLR* carrying phagemids p1 and p2. Solubilised proteins were separated by SDS-PAGE with molecular weight markers and transferred by electro blotting to a nitrocellulose membrane and subjected to western ligand blotting. Blotting revealed insulin peroxidase bands showing binding activity from of λ_1 & λ_2 samples (Figure.6 Appendix 2).

The total protein was then extracted from p1 or p2 *E. coli* recombinants as before and subjected to the western ligand blotting to detect the IBPs and the results showed p1 phagemid produced an insulin binding band of about 30 kDa, equivalent in size to one of the *B. multivorans* IBPs, revealing that p1 carries the gene for IBP1. Whereas, p2 showed two bands (IBP2 & IBP3) with MW identical to 20 & 30 kDa of IBPs in *B. multivorans* (Figure 6.1).

6.3.2 Southern Blotting

Southern hybridisation was used to verify the presence of p1 and p2 inserts DNA in the *B. multivorans* genome. Digoxigenin labelled probes of p1 and p2 were prepared and used to identify the insulin binding genes on *B. multivorans* genomic DNA completely digested by *EcoR V.* The p1 probe hybridised successfully with two bands on the genomic DNA of *B. multivorans* and was smaller in size than linearized pBR328. The p2 hybridised with one sequence of chromosomal bands. The hybridisation referred that p1 may be resulted from ligation DNA fragments belonging to different regions on the *B. multivorans*

chromosomal DNA, whereas, the p2 identified one chromosomal band demonstrating that the p2 originate to one region of chromosomal DNA of *B. multivorans* (Figure 6.2). The sequence analysis of the p1 showed an *EcoR V* digestion site producing two fragments 2063 bp and 362 pb, whereas, no *EcoRV* restriction site was detected on the p2 sequences.

6.3.3 Sequence analysis of p1 & p2 inserts

6.3.3.1 ORF analysis and predicted amino acid sequences for p1

The inserts in phagemids p1 and p2 were sequenced to identify the insulin binding protein genes and subsequently the proteins. The two inserts showed overlapping sequences and were 2600 and 2900 bp for p1 and p2 respectively. Theoretical ORFs identifier detected 3 and 4 ORFs on p1 and p2 respectively (Figure 6.3). All ORFs of p1 & p2 show high homology with sequence from *B. multivorans*.

The ORFs sequence analyses identified 3 ORFs 1, 2, and 3 on the insert of p1 (Figure 6.3). ORF1 (282 bp) sequences flanked by nucleotides 138-422 showed no clear gene motifs, apart from the start codon and stop codon (Figure 6.4). Nucleotide sequence blast showed that this sequence is related to the gene Ornibactin synthatase, part of the siderophore ornibactin pathway. The ORF2 (636 bp) occurred at sequences 420-1061 (Figure 6.4), sequence blast showed high similarity to the Acetyl coA transferase gene of *B. multivorans* members. The ORF3 of p1 flanked by nucleotides (1155 - 2054) showed -35, -10 and SD sequences accompanying start and stop codons.

The blast result for ORF3 showed a polypeptide with 299 amino acid residues and calculated MW 32.79 kDa and showed similarity with the outer membrane iron complex (Figure 6.5).

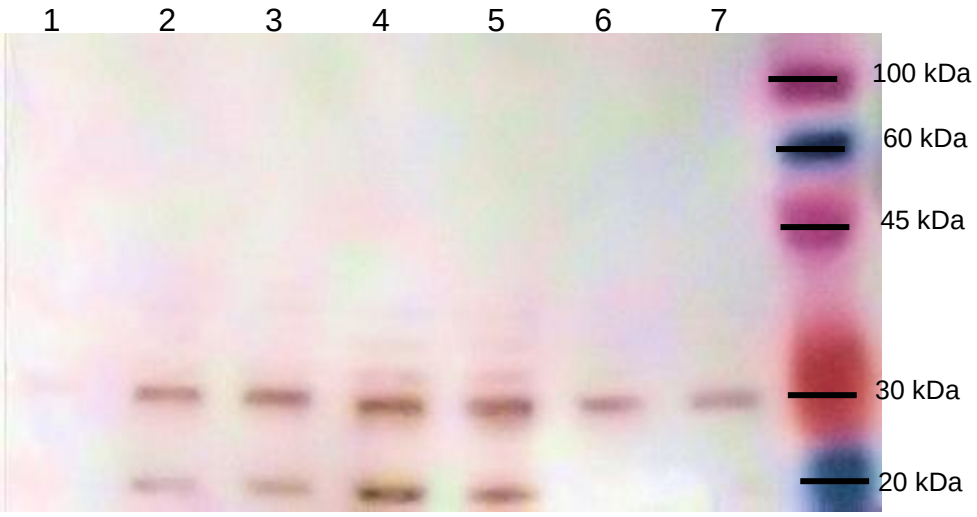

Figure 6.1: IBP produced by western ligand blotting of whole cell lyaste of *E.coli XLROR* recombinants with p1 phagemids (Lane 6, 7) recombinant with p2 (Lane 5, 4) *and B. multivorans* (3, 2) and non-recombinant *E coli* (lane1).

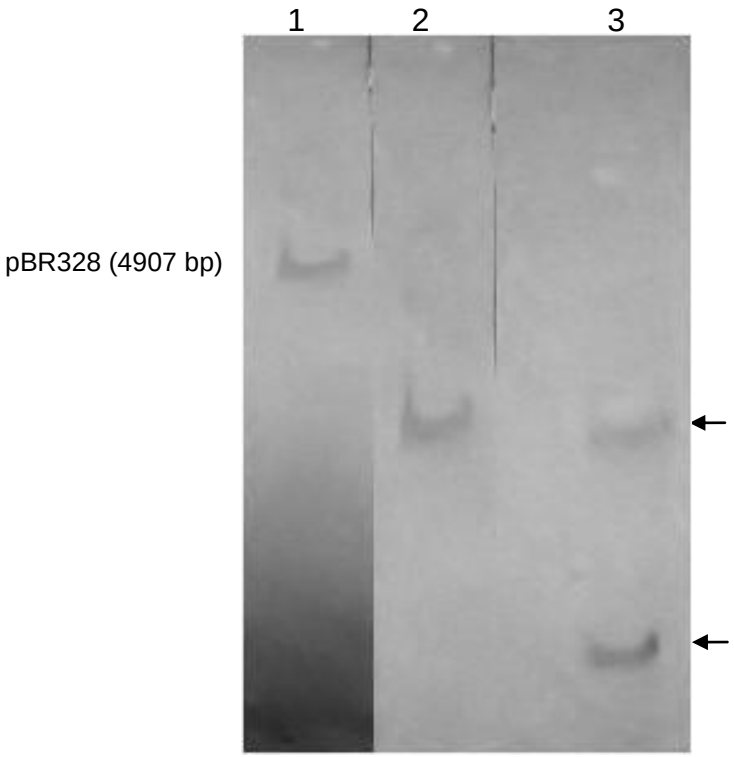

Figure 6.2: Southern blot of *EcoRV* –digested genomic DNA of *B. multivorans* using Dig- labelled p2 and p1 probes and linear (2 & 3 respectively). Lane 1 shows pBR328 Dig probe binding to itself (control).

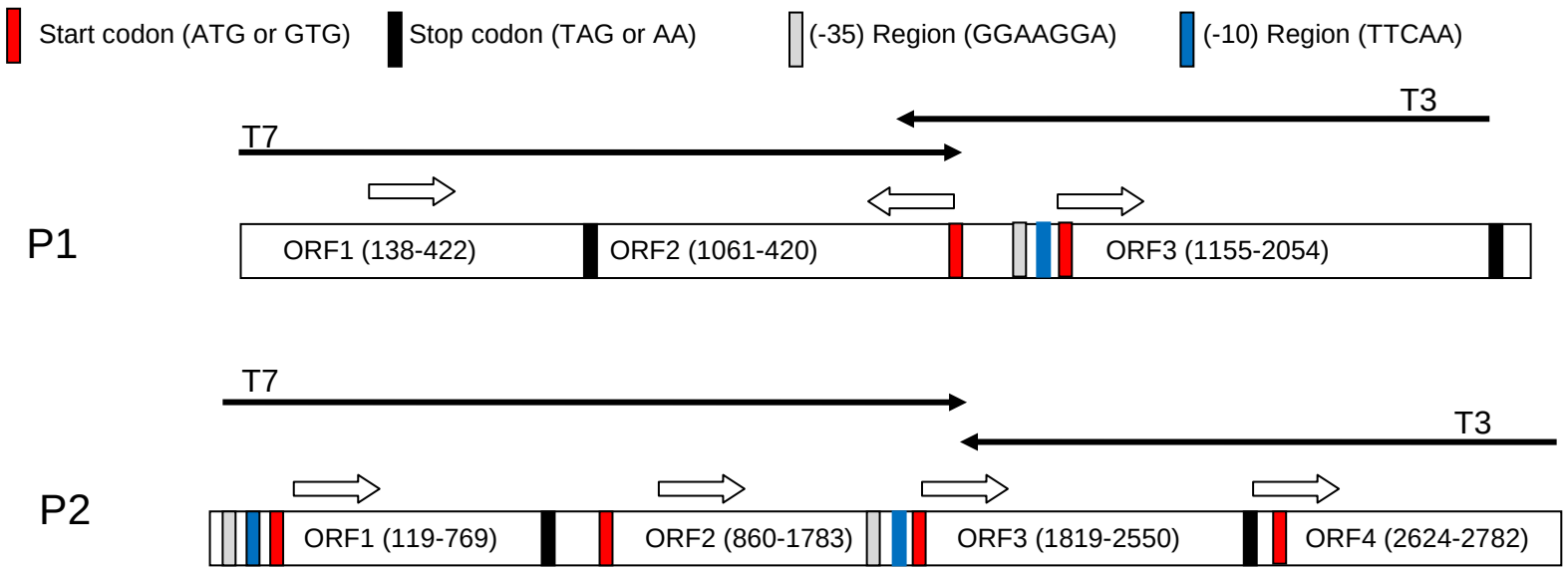

Phagemid-Insert size	ORFs	Size bp	Translation encoding sequence	No of a.a	Protein (MW)
p1-(2600)	ORF1	282	Ornibactin Synthatase	94	10 kDa
	ORF2	639	Acetyl CoA:N6-hydroxylysine acetyl transferase	213	22 kDa
	ORF3	897	Iron complex outer membrane receptor protein	299	32.79 kDa
p2-(2750)	ORF1	648	Predicted periplasmic or secreted lipoprotein	216	23 kDa
	ORF2	921	POT family proton-dependent oligopeptide transporter	307	33.6 kDa
	ORF3	729	Serine threonine phosphatase-1	243	26 kDa
	ORF4	156	No significant similarity	52	5.8 kDa

Figure 6.3: ORF analysis and gene arrangements and translation of inserted DNA of p1 and p2 recombinant phagemids using ORF finder programme online (http://www.ebi.ac.uk/Tools/sequence.html) indicating full gene in ORF3 in p1 and ORF1& 2 in p2.

P1-ORF1

61 TTTTTGAATTCTTTGCGCATCGCCAACATTCATCCGGGCATCACGGCCGACGGTTCGCCG

Start Codon /ORF1

121 TACCAGCGGCGCGGCGC**ATG**GGCGACGCTCGATGCGCTGCACGGCGCGCGCGGCGAGCGC

181 GTCGACTGGGCGACCGGCACGACGACGCCGGTCGCGCCCGTGACGATGACGGGCGCCTCG

241 TTCCACTATGTCGACAACGGCATCGATTCCGGCGAGGTGATCTGCGACGTGCTCGACACG

301 CCGATCGCGCCGGACGACACGATCCTCGAACTGCGCTGGAACAACTTCCAGCGCAGCCTG

361 TTTCCGGCGCTCGAGCGCGGGCTGCATCTCCTCGCCGATCGCCACGACGCGGGAGCACT**TGA**

Stop Codon

P1-ORF2

1061 Start Codon

atggcaccgacgctgacgcaacccgaagaagcgatcgagacggccgacggcgacgtcgccgcc

M A P T L T Q P E E A I E T A D G D V A A

998

ttgcgcgatcacggcgccgatacggcgcccgccgccgaccgcgtgctcgacgcatggcggccc

L R D H G A D T A P A A D R V L D A W R P

935

gacgatccgccgggcgcgctgctcgccgagctcgtcgcgctgttcaataccgacgcacggcgc

D D P P G A L L A E L V A L F N T D A R R

872

gatgcggcgacgatcgcgctgccgatcgcgggcaccgacccggacgccgtcgccgcgtacgtc

D A A T I A L P I A G T D P D A V A A Y V

809

gcgcgcgcggtgcgcgaaggcgtgatcgacgcggcgcaacgcgcgggcgaccgccttgacgtg

A R A V R E G V I D A A Q R A G D R L D V

746

accacgtcgcgcgcgacgttctggcagcatccgcagccctggctgaaggcgcccgcgtcgggc

T T S R A T F W Q H P Q P W L K A P A S G

683

gggatgccgctgcgctacacgatcacgaacggccaccgtcatccggtgcggccgccgacgccg

G M P L R Y T I T N G H R H P V R P P T P

620

gccggcgagatctatgcgcgctacatgccgcaggtcgggatgacgttcagcctgcgcaccgtc

A G E I Y A R Y M P Q V G M T F S L R T V

557

gacgtcgacgcgcatgcggacctcttcagcggctggatgaatctcgatcgcgtcgcgcat

D V D A H A D L F S G W M N L D R V A H

494

ttctgggatcagcgcggcacgcgcgacgagcatgccgcgtatctcgcggagcggctcgccgat

F W D Q R G T R D E H A A Y L A E R L A D

431 ccgcacatg**tag** Stop Codon

P H M *

Figure 6.4: Nucleotide sequence of putative genes encoded by ORF1& 2 of p1. Initiation and termination codons are highlighted and the green segment represents vector DNA sequence.

P1-ORF3

```
1060 CCCGATGATC TCGCGCGCCT GCAGGTCGAC ACTAGTGGAT CACGAAGGAC
                -35                          -10        SD
1111 ATTTAGGAAG GCGACGGCAA CTTCAACTAT TACCGGAAGA GAGG
     Start Codon
1155 gtggtcgctcggctatcagttcgagcacaacctgaactcgatgtg
       V  V  A  R  L  S  V  R  A  Q  P  E  L  D  V
1200 gacgttccggcagaacacgcgatggatgcatctgtcgctcgacaa
       D  V  P  A  E  H  A  M  D  A  S  V  A  R  Q
1245 cggctcggtgtggggagcgggcttcgccgacgaaacgctgaccga
       R  L  G  V  G  S  G  L  R  R  R  N  A  D  R
1290 aatcaaccgctgggccggcgtgttccagatgaactacagccgctt
       N  Q  P  L  G  R  R  V  P  D  E  L  Q  P  L
1335 cgacatcgacaacaacctcgagggccgttttgcgacgggtccgct
       R  H  R  Q  Q  P  R  G  P  F  C  D  G  S  A
1380 ccagcacacgctgctgctcggttccagtacaaccgccagacggcg
       P  A  H  A  A  A  R  F  Q  Y  N  R  Q  T  A
1425 accgatagcgaatggctcgccgccgcgccgacgctgaacctctac
       T  D  S  E  W  L  A  A  A  P  T  L  N  L  Y
1470 aacccggtgtacacgccggtcacgacggccgtgttttccgatccg
       N  P  V  Y  T  P  V  T  T  A  V  F  S  D  P
1515 gacaccacgtaccgcaccaacacgtacacgacgatgaacacgttc
       D  T  T  Y  R  T  N  T  Y  T  T  M  N  T  F
1560 ggcctgtacgcgcaggaccagatcaagtggaaccgctggacgctg
       G  L  Y  A  Q  D  Q  I  K  W  N  R  W  T  L
1605 acgctcggcggccgcgaggactgggtcaacatgcggatggacgat
       T  L  G  G  R  E  D  W  V  N  M  R  M  D  D
1650 cgcgcggccggcacgcagtcgaaggccgacgtgtcggcgtttacg
       R  A  A  G  T  Q  S  K  A  D  V  S  A  F  T
1695 ggccgcgtcggcctcacgtatcaggccggctacgggctgtcgccg
       G  R  V  G  L  T  Y  Q  A  G  Y  G  L  S  P
1740 tatatcagctattcgacgtcgttcaatccgatcatcggcgtgagc
       Y  I  S  Y  S  T  S  F  N  P  I  I  G  V  S
1885 ttgctcgacggcggggtgccgaagccgacgcgcggcagacagatc
       L  L  D  G  G  V  P  K  P  T  R  G  R  Q  I
1930 gaagcgggcctgcgctggcagccgcccggcaagaacctgatgctg
       E  A  G  L  R  W  Q  P  P  G  K  N  L  M  L
1975 aatgccgcgatctatcagatcaaccagaccaacggcgttacgccg
       N  A  A  I  Y  Q  I  N  Q  T  N  G  V  T  P
2020 gcgctgctgacgcacgatccgagcggcacgaaatccgtgcagacc
       A  L  L  T  H  D  P  S  G  T  K  S  V  Q  T
2065 ggggaagtgcgcgcgcgcgggatcgagctgagcgcaaccggcaag
       G  E  V  R  A  R  G  I  E  L  S  A  T  G  K
2110 gtcacgccgaacctgtcgctgatcgcgtcgtacgcgtatcagtga
       V  T  P  N  L  S  L  I  A  S  Y  A  Y  Q  Stop codon
```

Figure 6.5: Nucleotide sequence of putative gene encoded by ORF3 in p1. Sequence includes putative -35, -10 and SD regions are underlined in black. Initiation and termination codons are highlighted in red and the green regions represents vector DNA sequence.

6.3.3.2 ORFs analysis and predicted amino acid sequences for p2

The analyses for p2 identified 4 ORFs on of the DNA insert (Figure 6.3). ORF1 representing between bases 119-769 with SD region and clear -35, -10 regions were identified (Figure 6.6). ORF1 encodes for a 216 amino acid polypeptide with calculated MW of 23 kDa. The Blast-n result of this sequence showed that the nucleotides have 100% homology with a sequence for the periplasmic secreted lipoprotein and transporters associated protein of *B. multivorans.* ORF2 showed no accompanying -35 and -10 regions but identified start and stop codons on the sequence 860-1783 nucleotides encoding a protein with 307 residues and 33.6 kDa theoretical MW. However, the blast-n search of these ORFs nucleotides showed significant similarity with an oligopeptide transporter sequence in the Genbank database as well as the translated protein resulted from Blast-p (Figure 6.6).

ORF3 was flanked by sequences (1819-2550) with apparent -35, -10 motifs and start and stop codons, furthermore, the translated sequences produced a protein with 243 residues and ≈26 kDa MW with similarities to serine threonine phosphatase-1 in *B. multivorans* (Figure 6.7). ORF4 represented by nucleotides 2624-2782 showed, no clear motifs except start and stop codons (Figure 6.7) and the blast results revealed no significant similarity.

P2-ORF1 -35 -10 SD

71 TTCT**TTGGAC T**CGCTCGTGT **TTCAAC**TGCC GGTCAGCT**AG GAGAA**CCG

Start Codon

atgaaaaccgacaagcagttgaagcaggatgtccaggacgaactggagtcagacccgtcgatcgattcgacccgtatcggtgtcgaggtg
M K T D K Q L K Q D V Q D E L E S D P S I D S T R I G V E V

209
gctgaccggatcgtgacgctttcggggcacccgccgagctacgcggagaagctggcgatcgagcgcgcggcgaaccgcgtggccggtgtc
A D R I V T L S G H P P S Y A E K L A I E R A A N R V A G V

299
aaggcgctcgtcgtggacatgaccgtgcatctgccggacgacgacgtgcgcaccgacgaggacatcgcgaaggcggtacgctcggtgctg
K A L V V D M T V H L P D D D V R T D E D I A K A V R S V L

389
cactggacggtcggtctacatgacgacgcggtcaaggtgcaggtcgaacgcggctggatcacgttgtccggcaaggtcgactgggcatac
H W T V G L H D D A V K V Q V E R G W I T L S G K V D W A Y

479
cagagccacctggccgtgcgcgccatctcgcagatgcgcagcgtgacgggcgtgaccgaccacatcacggtacaggggacggtcggttcg
Q S H L A V R A I S Q M R S V T G V T D H I T V Q G T V G S

569
gacgacatcggcggaaacatcaaacgcgcgatcatgcgccacgcggagcgcgaggctaagcatatcgcgatcgaagtgcacgacggcacc
D D I G G N I K R A I M R H A E R E A K H I A I E V H D G T

659
gtgcggctgtccggaaaagtcggctcgttctccgaacgcaaggccgtgcgcggggccgcgtggtccgcgcgcggcgtgcgcgccgtcgtc
V R L S G K V G S F S E R K A V R G A A W S A R G V R A V V

749 gacgatctggtggtcgagtaaGGTCGGTAGCCGGATGAGCAGTCCACGGAGATCAAGGAGGGC
D D L V V E Stop codon

825 ORF2/Start Codon
AGTCAAATGACACTTTCGGGTGAACTTCACGAAGCGGACTGGTCGGTCatg**atg**cacgcacctgtt
M M H A P V

P2-ORF2

979
tcacaaacccgatcgtttacgacggtcttcctcatcgaaatgtgggagcgcttcggctactacggcatggccgcgctcctcgtcctcttc
S Q T R S F T T V F L I E M W E R F G Y Y G M A A L L V L F

1884
atggtcgacaggctcggtttcaccgacagccatgcgaacctcacgtggggtgcgttcaccgcactcgtctacgcctcgccgtcgatcggc
M V D R L G F T D S H A N L T W G A F T A L V Y A S P S I G

1264
ggctggatcggcgacaaggtgctcggcgcgcgccgcacgatgatcctcggcgcggccgtgctgtgcgccggctacctgatgctggcggtg
G W I G D K V L G A R R T M I L G A A V L C A G Y L M L A V

1354
ccgaacgacgcgctcgcctatatgtatgcgtcgctcggcgtgatcgtcgtcggcaacgggctgttcaaggccaacgcggcgaacctcgtg
P N D A L A Y M Y A S L G V I V V G N G L F K A N A A N L V

1444
cgccgcatctacgaaggcgacgacgcgcgcatcgacagcgcgttcacgatctactacatggcggtcaacatcggctcgacggtgtcgatg
R R I Y E G D D A R I D S A F T I Y Y M A V N I G S T V S M

1534
ctggcgacgccgtggatcaaggatcactggggctggcacaccgcgttcgcggtctgctgcggcggcatgctgctcgcgatcctgaacttc
L A T P W I K D H W G W H T A F A V C C G G M L L A I L N F

1624
atgctgatgcatcgcacgctggcgcacatcggctcgcagcccgacgacgagccgatccgctggaagcgcctcggggccgtcgcggcgggc
M L M H R T L A H I G S Q P D D E P I R W K R L G A V A A G

1714
ggcgtcgcgctcgcgctcgtcacgctgtacgtgctgcagcacaagcaactggcagtggcaagcgtgtggacggccgcggtcgcgattctc
G V A L A L V T L Y V L Q H K Q L A V A S V W T A A V A I L

1804
gcgatcttcgcgtacatgatcgcgaagtcggaacgctcggagcgcgccggcctgatcgccgcgctcgtgctgatcgcgcaggtgatcctg
A I F A Y M I A K S E R S E R A G L I A A L V L I A Q V I L

1894
ttcttcatcttctacgtgcagatgtcgacctcgctgacgctgttcgcgctgcgcaacgtcgatccgcgcttcatcctgttcggcacgacg
F F I F Y V Q M S T S L T L F A L R N V D P R F I L F G T T

1984 ctgtaa Stop Codon
L

Figure 6.6: Nucleotide sequence of putative gene encoded by ORF1& 2 in p2. ORF1 includes putative -35, -10 and region and SD. Initiation and termination codons are highlighted.

P2-ORF3

```
       -35                -10                SD
1780 TTGATGGTGT CTGGGCTCGA AACCGCCGCG CGGAGCGG
    Start Codon
1819 atgagcgcttccgccctcctccatcgtcatccggccaacgtcgcg
      M  S  A  S  A  L  L  H  R  H  P  A  N  V  A
1864 ggccgcgacttcgtcgtcggcgatctgcacggctgcgtcgatgcg
      G  R  D  F  V  V  G  D  L  H  G  C  V  D  A
1909 ctgcgcgcactgctgcgcgaggtgcgcttcgatccggcgcgcgac
      L  R  A  L  L  R  E  V  R  F  D  P  A  R  D
1954 cggctgttctcggtcggcgatctcgtcgaccgcgggccggcatcc
      R  L  F  S  V  G  D  L  V  D  R  G  P  A  S
1999 gaaaccgcgctcgagctgctcgatcgcccgtggtgtcacgtcgtg
      E  T  A  L  E  L  L  D  R  P  W  C  H  V  V
2044 cgcggcaatcacgaagaagtgctgagcctcgtcgcgcgcggcaag
      R  G  N  H  E  E  V  L  S  L  V  A  R  G  K
2082 ctgccggccgacgcatggcgcggcatcggcggcgactggggcgcc
      L  P  A  D  A  W  R  G  I  G  G  D  W  G  A
2134 gatctgccgcccgagcggctgcgcgcgtacgcggcgcgcgtcgac
      D  L  P  P  E  R  L  R  A  Y  A  A  R  V  D
2179 gcgctgccgctcgtgcgcgtgatcggcgaaggcgcgacgcgcttc
      A  L  P  L  V  R  V  I  G  E  G  A  T  R  F
2224 aacgtgctgcatgcggaattcttcggctcggacgccgatctagat
      N  V  L  H  A  E  F  F  G  S  D  A  D  L  D
2269 accggcgactatccgcccgacgtgcgcgagcggctgatctggggc
      T  G  D  Y  P  P  D  V  R  E  R  L  I  W  G
2314 cgcgatctcgtgcagggactcgtcgatccgggctggcaggccggc
      R  D  L  V  Q  G  L  V  D  P  G  W  Q  A  G
2359 ctctcgctgacctgcagcggccatacgccggtgcgcgtgccgcag
      L  S  L  T  C  S  G  H  T  P  V  R  V  P  Q
2404 cggatcggcgcgcaatggttcatcgatacgggtgcgttcgcaccg
      R  I  G  A  Q  W  F  I  D  T  G  A  F  A  P
2449 gccggccggctgacgctcgccgagccgcgcacgggacagacgtgg
      A  G  R  L  T  L  A  E  P  R  T  G  Q  T  W
2494 tcgatcacgcaggccgccgcacgcgaacgcggagcggccgcgtgg
      S  I  T  Q  A  A  A  R  E  R  G  A  A  A  W
          Stop Codon
2539 ccgctgccgtgaCGCCCGCACGACTGTCCGGCCGGACACCGCGACACA
      P  L  P  *                    Start Codon
2587 CATACCGCCTCGAATGCACGGGCAGCGCAACGCCCGCATGCGCACCTACC

2637 CGACCTGATTCAGCRSTCGAACACCGCGTCGATCGCGGAGCCGTTCCAGT

2687 TGTACTCGAGATACGCCGCGTGATGGCAGTCGCGCAGCAGCGTCGTGCGA
                                                Stop Codon
2737 AACGCCGCGAGGCATTCGCCGTGCGGATCGCGCACCGACGGAATAGA
```

Figure 6.7: Nucleotide sequence of putative gene encoded by ORF3 & 4 in p2. ORF3 includes putative -35, -10, region and SD are underlined. Initiation and termination codons are highlighted.

6.3.4 Identification of ORFs encoding protein receptors

The blast results of the nucleotides sequences for the ORF(s) revealed three proteins with receptor and membrane function. The current study has hypothesised that the IBPs are receptor proteins and their MW should be approximately either 20 or 30 kDa. Accordingly, three ORF(s) could possibly encode IBP(s). ORF3 of p1 revealed a protein of 32.7 kDa (IBP1) representing a TonB- siderophore receptor (accession number AP009385.1) belonging to *B. multivorans* and the Blast-p of this sequence precisely revealed that this protein is an ornibactin siderophore receptor of *B. multivorans* and is found in other species of the BCC and other *Burkholderia* sp or TonB siderophore dependent receptor with (accession number CP000868.1) of *B. multivorans* and other *Burkholderia* species (Figure.6.8).

ORFs 1, 2 in p2 have been suggested to produce possible IBP2 & 3 respectively. ORF1, predicted to produce a 23 kDa (IBP2) protein called periplasmic or secreted lipoprotein in *B. multivorans* (accession number AP009387.1) and functionally is showing homology to an amino acid or peptide transporter in the *Burkholderia* genus only (Figure 6.9 A).

The ORF2 blast results of p2 indicated that ORF2 encodes a 33.6 kDa (IBP3) protein transporter belonging to the proton amino acid, oligopeptide transporters family (POT) of *B. multivorans* (proteins with putative function of transportation of protein, oligopeptide and amino acids) in the *Burkholderia* genus (accession number AP009386) (Figure 6.9 B).

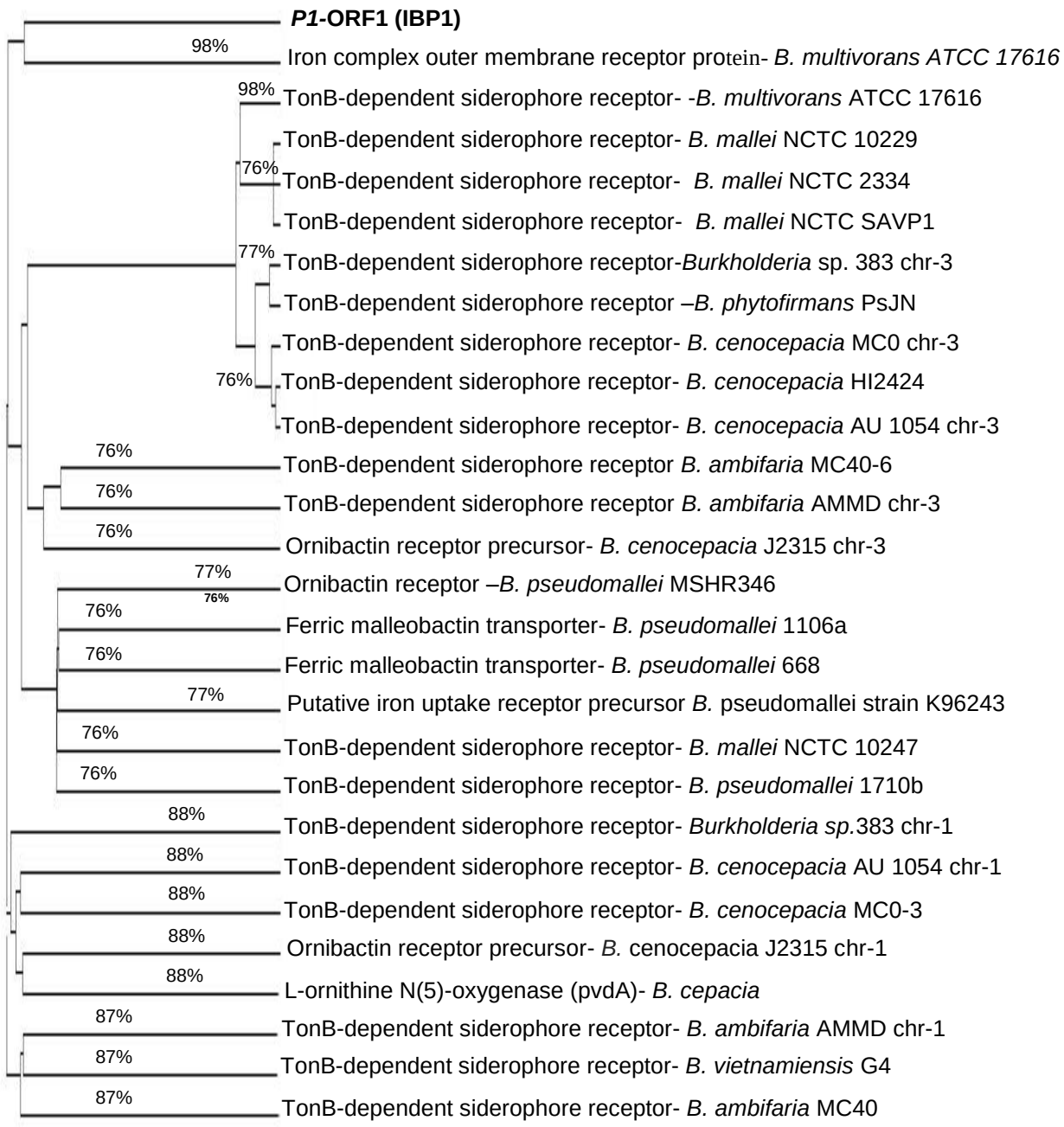

Figure 6.8: Phylogram rooted tree based on nucleotide sequence of p1-ORF3. The tree was constructed using the ClustalW2 programme multiple alignment of sequences using the Blast of ORF3 sequence. The phylogram shows evolutionary relationship and degree of homology between sequences from related bacteria.

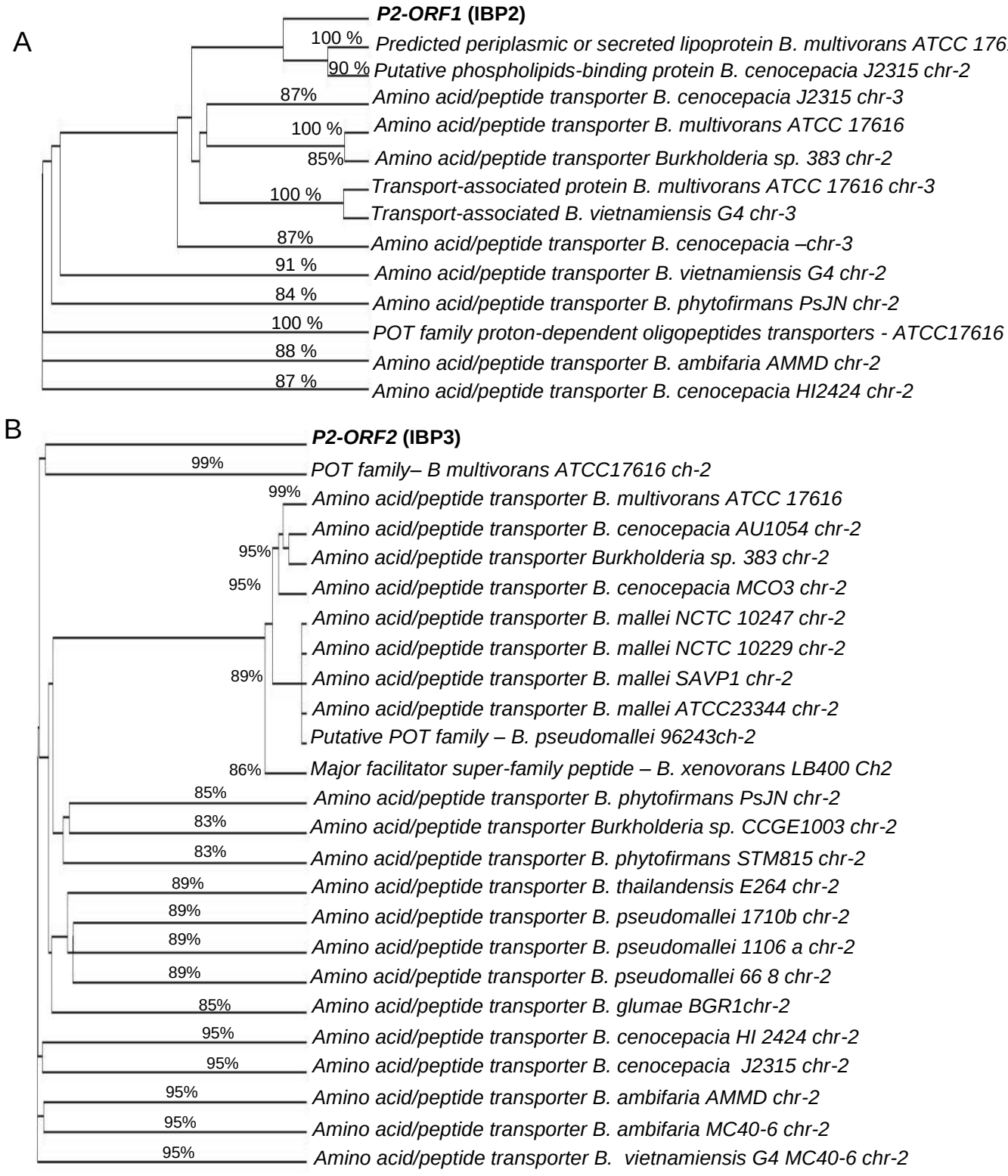

Figure 6.9: Phylogram rooted tree based on nucleotide sequence of p2-ORF1 & 2 (A & B respectively). The tree was constructed using the ClustalW2 programme multiple alignment of sequences using the Blast of ORF3 sequence. The phylogram shows evolutionary relationship and degree of homology between sequences, from related bacteria.

6.3.5 Topology prediction of IBPs sequences

The translated sequences of putative IBPs were scanned for further confirmation that they may play a role as receptors for insulin. Putative IBP(s) sequences were searched for transmembrane α helix domains using TMMTop software. The IBP1 (siderophore ornibactin receptor) 299 residues encoded by ORF3 in recombinant phagemid p1 produced one α helix domain of 23 amino acids between residues 95 -117 (Figure 6.10).

The IBP2 (periplasmic or secreted lipoprotein) is a 23 kDa protein with transportation activity and is composed of 216 residues encoded by ORF1 of p2 (Figure 6.9 A). The protein topology prediction showed a soluble protein structure with no transmembrane helices (Figure 6.10). However, in the case of IBP3 encoded by ORF3 producing a 33.6 kDa peptide transporter belonging to the oligopeptide transporters family POT of *B. multivorans,* the transmembrane test revealed 9 transmembrane α-helices domains with 19 or 20 residues occurring at residues 24-43, 52-70, 79-96, 101-118, 139-158,171-189, 210-228, 233-253 and 262-280 residues producing a typical transmembrane protein structure (Figure 6.10).

```
VVARLSVRAQ PELDVDVPAE HAMDASVARQ RLGVGSGLRR RNADRNQPLG 50
IIIIIIIIII IIIIIIIIII IIIIIIIIII IIIIIIIIII IIIIIIIIII

RRVPDELQPL RHRQQPRGPF CDGSAPAHAA ARFQYNRQTA TDSEWLAAAP 100
IIIIIIIIII IIIIIIIIII IIIIIIIIII IIIIIIIIII IIIIHHHHHH

TLNLYNPVYT PVTTAVFSDP DTTYRTNTYT TMNTFGLYAQ DQIKWNRWTL 150
HHHHHHHHHH HHHHHHHOOO OOOOOOOOOO OOOOOOOOOO OOOOOOOOOO

TLGGREDWVN MRMDDRAAGT QSKADVSAFT GRVGLTYQAG YGLSPYISYS 200
OOOOOOOOOO OOOOOOOOOO OOOOOOOOOO OOOOOOOOOO OOOOOOOOOO

TSFNPIIGVS LLDGGVPKPT RKRQIEAGLR WQPPGKNLML NAAIYQINQT 250
OOOOOOOOOO OOOOOOOOOO OOOOOOOOOO OOOOOOOOOO OOOOOOOOOO

NGVTPALLTH DPSGTKSVQT GEVRARGIEL SATGKVTPNL SLIASYAYQ 299
OOOOOOOOOO OOOOOOOOOO OOOOOOOOOO OOOOOOOOOO OOOOOOOOO
```

IBP1

```
MKTDKQLKQD VQDELESDPS IDSTRIGVEV ADRIVTLSGH PPSYAEKLAI 50
IIIIIIIIII IIIIIIIIII IIIIIIIIII IIIIIIIIII IIIIIIIIII

ERAANRVAGV KALVVDMTVH LPDDDVRTDE DIAKAVRSVL HWTVGLHDDA 100
IIIIIIIIII IIIIIIIIII IIIIIIIIII IIIIIIIIII IIIIIIIIII

VKVQVERGWI TLSGKVDWAY QSHLAVRAIS QMRSVTGVTD HITVQGTVGS 150
IIIIIIIIII IIIIIIIIII IIIIIIIIII IIIIIIIIII IIIIIIIIII

DDIGGNIKRA IMRHAEREAK HIAIEVHDGT VRLSGKVGSF SERKAVRGAA 200
IIIIIIIIII IIIIIIIIII IIIIIIIIII IIIIIIIIII IIIIIIIIII

WSARGVRAVV DDLVVE 216
IIIIIIIIII IIIIII
```

IBP2

```
MMHAPVSQTR SFTTVFLIEM WERFGYYGMA ALLVLFMVDR LGFTDSHANL 50
IIIIIIIIII IIIIIIIIII IIIHHHHHHH HHHHHHHHHH HHHOOOOOOO

TWGAFTALVY ASPSIGGWIG DKVLGARRTM ILGAAVLCAG YLMLAVPNDA 100
OHHHHHHHHH HHHHHHHHHH IIIIIIIIHH HHHHHHHHHH HHHHHHOOOO

LAYMYASLGV IVVGNGLFKA NAANLVRRIY EGDDARIDSA FTIYYMAVNI 150
HHHHHHHHHH HHHHHHHHII IIIIIIIIII IIIIIIIIHH HHHHHHHHHH

GSTVSMLATP WIKDHWGWHT AFAVCCGGML LAILNFMLMH RTLAHIGSQP 200
HHHHHHHHOO OOOOOOOOOO HHHHHHHHHH HHHHHHHHHI IIIIIIIIII

DDEPIRWKRL GAVAAGGVAL ALVTLYVLQH KQLAVASVWT AAVAILAIFA 250
iiiiiiiiiH HHHHHHHHHH HHHHHHHHOO OOHHHHHHHH HHHHHHHHHH

YMIAKSERSE RAGLIAALVL IAQVILFFIF YVQMSTSLTL FALRNVDPRF 300
HHHIIIIIII IHHHHHHHHH HHHHHHHHHH OOOOOOOOOO OOOOOOOOOO

ILFGTTL 307
OOOOOOO
```

IBP3

Figure 6.10: Transmembrane helices prediction of putative IBPs (I indicating inside, O outsides and H transmembrane) using HMMTop software (Exapsy online tools) predicted transmembrane domain sequences appear in red in IBP1 & IBP 3 and not for the soluble intracellular protein IBP2 (B).

6.3.6 Molecular mimicries and linear epitopes prediction

Searches for linear epitopes with sequence homology between HIR subunit α and putative IBPs elicited 6 significant epitopes on IBP1 (outer membrane iron complex receptor) with statistically significant similarity to the HIR occurring at residues 979-1016, 780-801, 742-750,641-646, 595-606, and 316-330, with 12, 9, 6, 4,6 and 7 identical residues and 15, 10, 9, 6, 6 and 9 positive residues respectively (Figure 6.11). The IBP2 protein (intracellular peptide transporter) produced 3 different epitopes which together cover a larger area on HIR compare to the IBP1, IBP2 epitopes occurring at residues 620-646, 558-587 and 451-474 of HIR possessing 8, 8 and 8 identical residues as well as 13, 14 and 13 positive residues respectively. The IBP3 (transmembrane peptide transporter protein) produced 2 putative epitopes occurring at residues 591-614 producing 10 identical and 15 positive residues and residues 198-202 with just 5 identical residues showing homology to HIR.

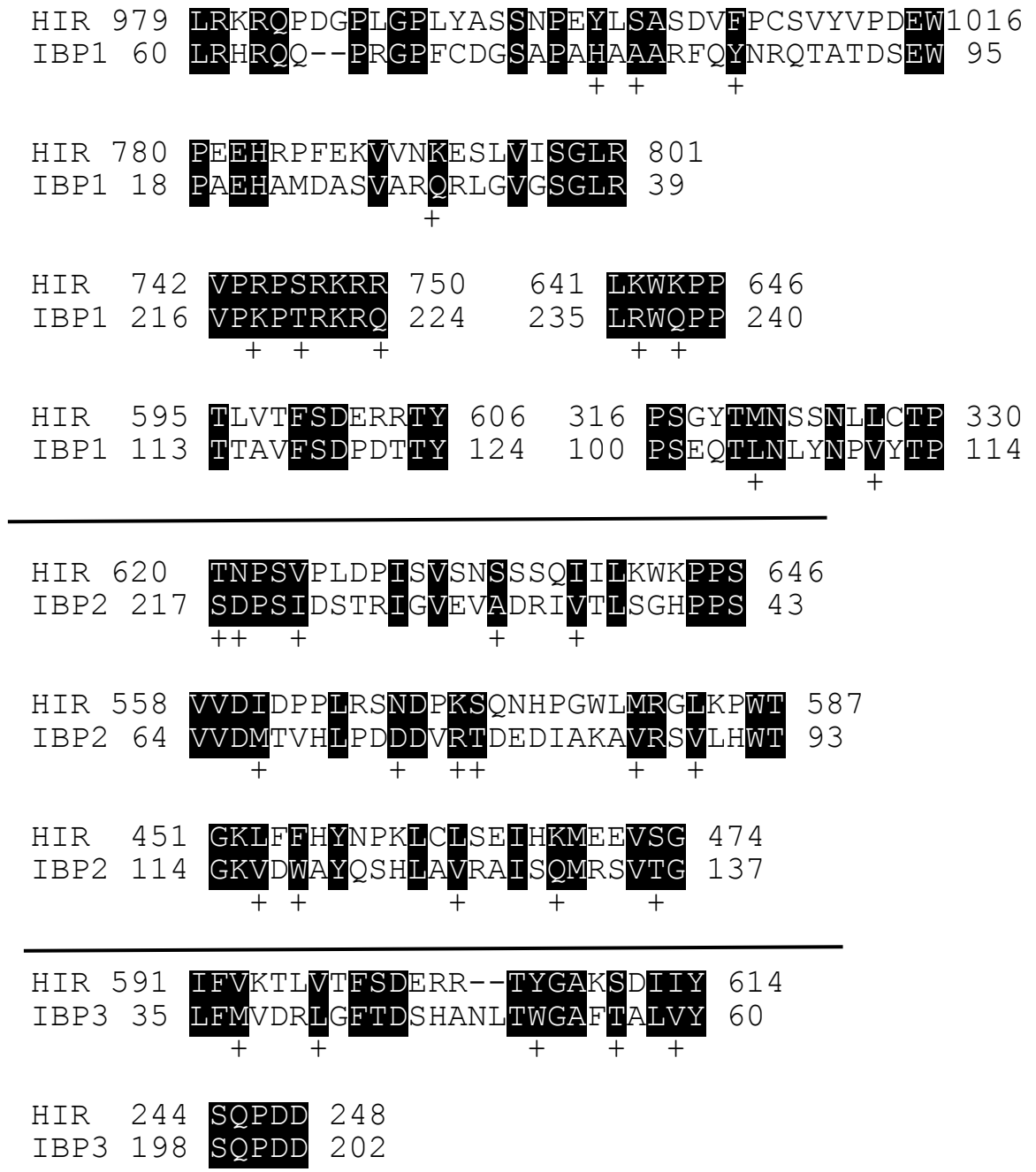

Figure 6.11: Amino acid sequence homology between IBP(s) in *B. multivorans* and HIR using Blast P2 software, + refers to the positive amino acids with same polarity.

Table 6.1: Epitopes extracted from *B. multivorans* IBP(s), sequences and position on HIR. The black highlighted letters refer to positive amino acids.

Epitopes	Position on HIR	Similarity %	Sequences
IBP1-E1	794-801	60	KESLVISGLR
IBP1-E2	742-750	100	VPRPSRKRR
IBP1-E3	641-646	100	LKWKPP
IBP1-E4	698-606	55.5	FSDERRTY
IBP2-E5	558-565	62.5	VVDIDPPL
IBP2-E6	466-474	66.66	IHKMEEVSG
IBP3-E7	605-614	80	TYGAKSDIIY
IBP3-E8	244-248	100	SQPDD

6.4 Discussion

The construction of a genomic library in this study allowed the identification of IBP genes in *Burkholderia* and the determination of their amino acids sequences. Additionally, sequence homology between the human insulin receptor and *Burkholderia* IBP(s) was also facilitated. The molecular mimicries between HIR and *Burkholderia* IBP(s) may initiate an autoimmune response against human insulin receptor or insulin hormone and subsequently initiate diabetes, particularly in the case of CF patients suffering chronic infection with *B. cepacia* complex.

The western ligand binding of solubilized proteins extracted from confluent lysates showed 3 additional proteins with molecular weight up 30 kDa or more bands particularly in p1 (Appendix 2). The insulin binding multiple bands are attributed to be chimerical proteins including peptide fractions from β-galactosidase protein as confirmed by study of *Coulton et al* (1986). Also, production of recombinant IBP is achieved by inducing the promoter of β-galactosidase possessing IBP in its sequence. Southern blotting using the p2 probe indicated one positive band on *Burkholderia* DNA referred to sequences occurred on continuous chromosomal region, whereas, the p1 probe identified two bands which probably resulted from ligation of two fragments of *B. multivorans* DNA belonging to different places on the chromosomal DNA .

Sequences determination of IBP(s) encoding genes in recombinant phagemids p1 and p2 was the major goal of this chapter's work. Expressing p1 and p2 in *E.coli* and then western ligand blotting results have clearly indicated a protein band produced by p1 (IBP1) with an apparent MW of 30 kDa. Whereas, p2 expressed a couple of IBPs (IBP2 & IBP3) with theoretical MW of 20 & 30 kDa respectively which suggested that more than one IBP in *B. multivorans.*

The recombinant phagemids were sequenced and analysed. Sequence analysis identified 3 ORFs 1, 2 and 3 in the insert of the recombinant phagemid p1, all of which are involved in the synthesis, production and binding of iron siderophore compounds. ORF1 and 2 appear to be involved in the Ornibactin siderophore pathway (synthesis and regulation). Nucleotide sequence blasts of ORF1 proved that the sequence is ornibactin synthatase (OrbF) which plays a role in the release of iron from the ornibactin structure. ORF2 encodes Acetyl CoA: N6-hydroxylysine acetyl transferase gene (OrbL) of *B. multivorans* which is functionally connected to the ornibactin synthetase (Figure 6.12 B) (Agnoli *et al*., 2006; Yuhara *et al*., 2008) controlling transcription of genes responsible for ornibactin modification (Thomas, 2006). This study suggests that ORF1 & 2 belong to genes involved in ornibactin siderophore pathway indicating putative intracellular functions without extracellular ligand binding components. Therefore, ORF1 and ORF2 are not likely to be directly involved in insulin binding at the cell membrane. The ORF3 sequence analysis determined start and stops codons, -35, -10 and SD motifs and encoded a 32.7 kDa protein (IBP1) and corresponded to the sequence of an Iron complex outer membrane receptor, or TonB siderophore dependent receptor (orbA) (Figure 6.12 B).

The Blast p result of the translated protein of this sequence showed precisely that this protein represents a receptor for ornibactin siderophore. The iron complex outer membrane receptor comprises the iron chelated onto the siderophore complex receptor (Yuhara *et al*., 2008) .

Western ligand blotting of *E. coli* recombinant with p1 produced a protein with MW approximately 30 kDa (Figure 6.1) which could represent a subunit of the ornibactin receptor (total MW of 78 kDa) (Sokol *et al*., 2000; Thomas, 2006) or could be a novel siderophore -like receptor protein. The blast results suggest

that the protein is an outer-membrane receptor protein, therefore, more likely to be one of the IBP(s). The Blast-n result also showed homology with the TonB siderophore dependent receptor which has been identified in many Gram negative bacteria to transport siderophore and Vitamin B12 from the outer membrane receptor to periplasmic space (Moeck and Coulton, 1998; Alice *et al*., 2006). The results also show the presence of a transmembrane α-helix domain (Figure 6. 10) suggesting that this protein is one of the transmembrane proteins whereas, no transmembrane α-helices were detected in the other proteins encoded by p1 ORFs.

Iron plays a crucial role in modulating many virulence factor pathways and the genus *Burkholderia* produces up to four types of siderophore; pyochelin, ornibactin, cepabactin and cepachline (Crosa, 1989; Smalley *et al*., 2001). Ornibactin harbours a tetra peptide with two hydroxate groups and a single hydroxycarboxylate group. The main structure includes C-terminal ornithine, D-aspartate with serine residue and threonine and N ornithine in addition to an acyl group that normally provides a carbon chain length of 4 or 6 or 8 which gives three types of ornibactin (Figure 6.12 A) (Stephan *et al*., 1993; Agnoli *et al*., 2006).

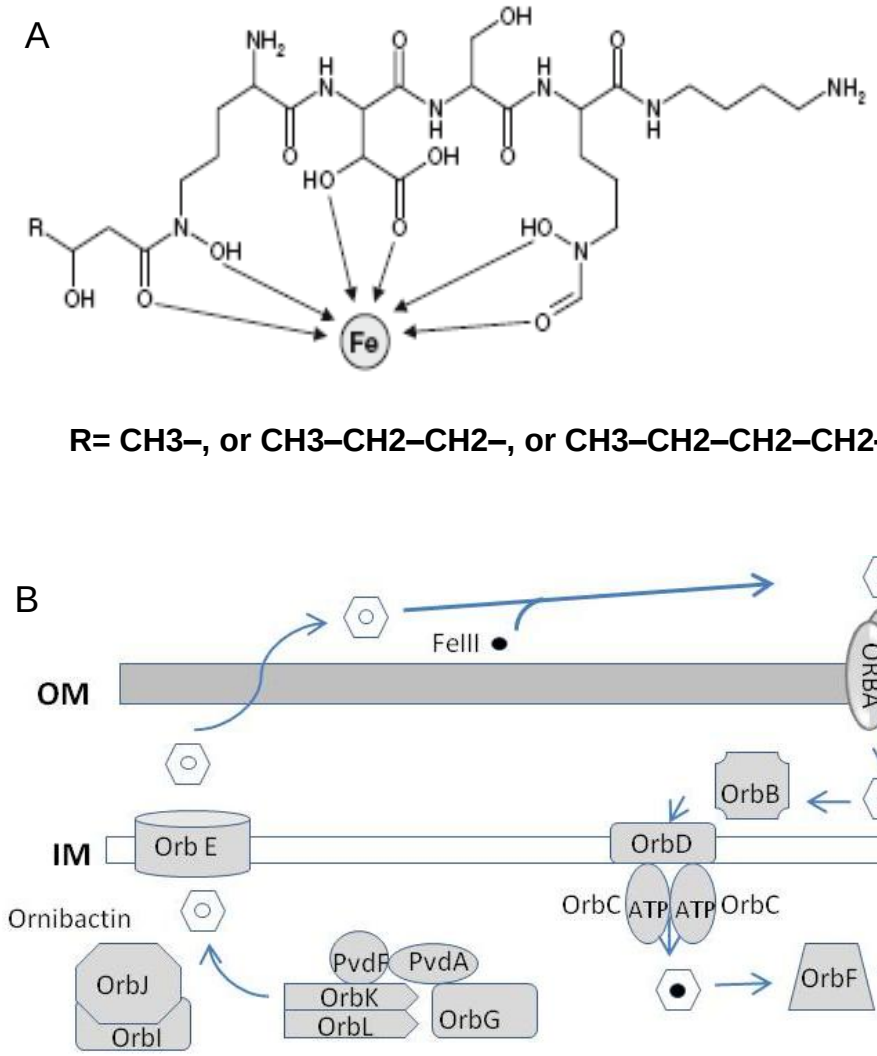

R= CH3–, or CH3–CH2–CH2–, or CH3–CH2–CH2–CH2–CH2–

Figure 6.12: Schematic diagram showing biosynthesis of Ornibactin siderophore of *B multivorans* (A) Ornibactin structure and carbon chain represented by R group. (B) Ornibactin biosynthesis and extra cellular ornibactin complex receptor ORBA that using TonB complex. Transport of ferric –ornibactin across the inner membrane (IM) requires a permease consisting of OrbB, OrbC and OrbD and the ferric ion is released by the action of OrbF. The amino acid precursors are modified by PvdA, PvdF, OrbG, OrbK and OrbL and converted into ornibactin by OrbI and OrbJ, adapted from Thomas (2006) .

ORFs analysis of the p2 insert DNA sequence presented four open reading frames 1, 2, 3 and 4, ORF1 sequence (23 kDa) showed full gene motifs. The Blast-n result of ORF1 nucleotides showed similarity with periplasmic secreted lipoprotein or transporter-associated protein of *B. multivorans* and species of the same genus only (Figure 6.9 A). The protein encoded by ORF1 presumably represents a new member of the transporter system that appeared in Gram negative bacteria which exports molecules and toxic substances across the two membranes of the cell envelope (Paulsen *et al*., 1997; Tomii and Kanehisa, 1998). Structurally, this peptide transporter system consists of four membrane associated domains, two of which are highly hydrophobic and two are located at the cytoplasmic face of the plasma membrane (Paulsen *et al.*, 1997).

In Gram negative bacteria the peptide transporter requires a substrate binding protein located in the periplasmic space or associated with the extracellular face of the plasma membrane (Steiner *et al.*, 1995; Daniel *et al.*, 2006). The blast results have shown that the protein encoded by ORF1 is IBP2 a peptide transporter with domain of proton-dependent oligopeptide transporter (POT) family the primary function of which is thought to be the transport of peptides or amino acid as nitrogen source and this peptide transporter has been involved in the recycling of cell wall peptides (Steiner *et al.*, 1995; Yen *et al.*, 2002). The α-helix transmembrane domain prediction showed no transmembrane domain (Figure 6.10) suggesting this protein is one of the soluble transporters that work intracellular which subsequently confirm the blast results indicating that this is a periplasmic transporter.

The periplasmic peptide transporter requires a membrane transporter or domain that mediates the peptide transportation from the environment outside the cells to the periplasmic and then to the cytoplasm. ORF2 encodes a 31.7 kDa protein

(IBP3), a transmembrane peptide transporter belonging to the proton amino-acid, oligopeptide transporters family of *Burkholderia* species (Figure 6.9 B). It contains a 9 α-helix domains (Figure 6.10) which can bind peptides and represents a typical transmembrane protein with a binding site. The POT transporter family is a group of ion-dependent peptide transporters derived from the ABC – transporters. This type of transporter has 2 highly hydrophobic transmembrane domains which were previously only seen in eukaryotic *Saccharomyces cerevisiae* and *Candida albicans,* but recently have been discovered in a limited number of bacterial species and other prokaryotic cells (Tomii and Kanehisa, 1998; Saier, 2000; Preveral *et al.*, 2009).

The POT transporter is relatively different from those in eukaryotic as the bacterial transporter requires a peptide binding protein located in the periplasmic space cooperatively associated with extracellular transport (Chiang *et al.*, 2004; Ronnestad *et al.*, 2007). In the case of this study the IBP3 is likely to be a transmembrane peptide transporter which binds insulin and transports it to the periplasmic space, from which the insulin will be immobilised for hydrolysis and then transportation of amino acids is achieved by another type of cytoplasmic transporter (Figure 6.13). The current theory could also explain binding of insulin to fungi and yeast including other types of microorganisms. Moreover, it has been established that *B. cepacia* can utilize insulin as carbon energy source a (Jeromson *et al.*, 1999). The Blast-n result of p2 ORF3 nucleotides showed homology with serine/ threonine protein phosphatase 1 of *B. multivorans*. The serine /threonine protein phosphatase1 (PP1) can act in opposition to serine/threonine kinase and there is no obvious role for these proteins that has been found in *Burkholderia.* However, the role of serine/threonine kinases-phosphatase has been demonstrated as part of ATP

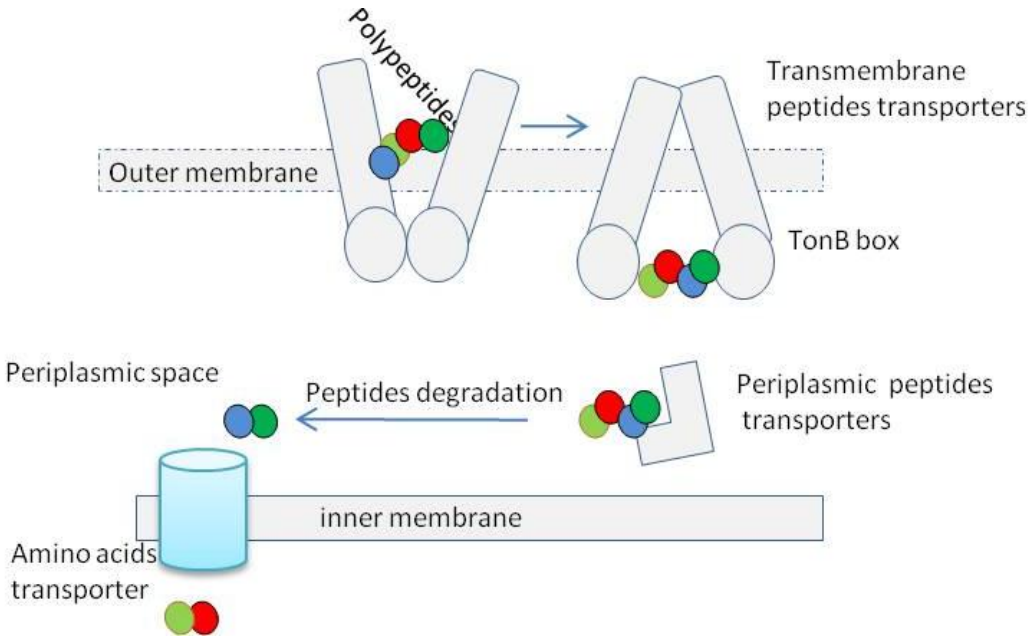

Figure 6.13: Schematic graph showing the peptide transportation across Gram negative bacteria as described by Steiner *et al* 1995. Transportation poly peptides firstly achieved by binding on to transmembrane transporter which then transport the polypeptides or oligo peptides to the periplasmic space in which the periplasmic transporter followed by peptide degradation producing amino acids or small oligo peptides ready to transport and use as energy source.

cassette binding transporter (ABC transporter) gene in which the phosphatase encoded gene is always located adjacent to the transporter protein gene prompting a possible role in membrane transporters in *Mycobacterium*. More direct evidence has been provided about the involvement of serine /threonine kinases in the pathogenicity of *M. tuberculosis* and serine/threonine kinase / phosphatase was found on *Streptococcus aglactiae* membranes and the envelope of *S. pneumonia*, (Cozzone *et al*., 2004; Cozzone, 2005).

This study suggests that the recombinant phagemid p2 carrying a transporter operon gene encoding the transmembrane transporter protein (IBP3) and periplasmic transporter protein (IBP2) controlled by a regulatory signal transduction enzyme (serine/threonine phosphatase). Thus, ORF3 is suggested to be a member of the signal transduction system which regulates a series of biological functions that are connected with cell wall receptors leading to insulin binding on the *B. multivorans* outer membrane. Furthermore, PP1 has been found in the nucleus of eukaryotic cells involved in many different cellular processes such as glycogen metabolism, calcium transport protein synthesis and intracellular transport (Stefaan and Brian, 1995). The Blast result also matches a Metallophosphoesterase or RES protein domain (accession number CP000869.1) part of a super family playing a key physiological role in the cellular pathway of signal transduction e.g. phosphoprotein phosphatase and DNA repair (DNA nuclease) (Keppetipola and Shuman, 2008). However, ORF3 is also suggested to be a member of the signal transduction system that regulates a series of biological activities connected with cell wall receptors leading to insulin binding on the *B. multivorans* cell wall.

The current study identified for the first time that insulin binds to either the transmembrane ornibactin siderophore receptor (IBP1) of *B. multivorans* or a

member of the iron uptake system and is consistent to what was found in *A. salmonicida,* in which the A-layer is also involved in siderophore intake, as well as binding insulin. Moreover, insulin binding with a transmembrane protein on *B. multivorans* may also be attributed to the transmembrane oligopeptide transporter (IBP3) activity working cooperatively within a periplasmic oligopeptide transporter protein (IBP2) to utilize the oligopeptides like insulin as amino acid or nitrogen sources.

The blast results also showed molecular mimicries shared between HIR and translated IBP(s) like IBP1-E2, IBP1-E3, IBP2-E6 and IBP3-E8 which may contribute to development of diabetic autoimmune response against HIR particularly in CF suffers with *B. multivorans* species. During infection there is also the chance to present the insulin bound on *Burkholderia* by antigen presenting cells (APC) as a foreign antigen leading to a diabetic immune response against insulin. *Burkholderia* IBP epitopes, or insulin bound to IBP's, could be presented by the MHC-II molecules of APC to the T- cell CD4 initiating the B-lymphocytes to produce antibodies, moreover *Burkholderia* can live intracellualrly inside macrophages and lung epithelial cells which will then present the IBP(s) epitopes via MHC-I to the T-cell CD8 and subsequently induce a cytotoxic T-cell leading to β-cell death.

The current study suggests binding of insulin to *B. multivorans* via the ornibactin receptor siderophore receptor can occur which may mean that extracellular siderophore can bind with HIR and subsequently impede insulin binding to its intended receptor leading to inhibition of the glucose metabolism signal which causes apoptosis or insulin resistance particularly in pancreatic β-cells.

Chapter 7

Molecular cloning of β-cell antigen glutamic acid decarboxylase (GAD65) using Halo tag technology, expression & purification

7.1 Introduction

Autoimmune disease is an immune response driven by self- components, leading to the creation of autoantibodies against self-antigens. T1D is commonly attributed to a genetic susceptibility of the HLA genes, particularly HLA-DQ2 and HLA-DQ8, which are recently reported to contribute up to 90 % of the risk of developing T1D (van Lummel *et al.*, 2011). In addition, a diabetic autoimmune response is also linked to T2D. However, the immune response initiators are still unclear (Lernmark, 2011). GAD65 auto-antibodies target epitopes, linear and conformational, distributed over the whole protein backbone, however, these epitopes or similar ones may occur in microorganisms, which raises the potential risk that these microbes could be environmental factors contributing to diabetic autoimmune responses via molecular mimicries (Judkowski *et al.*, 2004). Studies of the GAD65 autoantibodies from type1 diabetes patient's blood have purified GAD65 autoantibodies and used them for detecting sequences involved in autoimmunity.

The aim of the present study was to investigate the prevalence of molecular mimicries of the pancreatic GAD65 antigen in selected species of microorganisms, particularly bacterial species. So that a GAD65 antiserum or a GAD65 polyclonal antibody that covers the full length of the GAD65 was prepared in order to identify all possible epitopes with homology to the full length of GAD65. A search was made for microbial proteins presenting similar epitopes to GAD65 by creating GAD65 antiserum and using this antiserum to search the microorganisms for cross-reaction. Highly purified GAD65 antigen protein was prepared using Halo-tag technology, using the rat GAD65 gene cloned using PCR.

PCR cloning is a very powerful and common technique, fast and specific to the target clone gene with a particular function and for protein purification. The technique involves the use of PCR primers which recognize sequences flanking the ORF of the gene to be cloned. Those PCR primers have extra short DNA sequences with restriction enzyme sites incorporated into primer sequences (Wong, 2006). The GAD65 nucleotide reading frame sequence was inserted in frame with the halo-tag encoding sequence to produce a GAD65 –halo tag labelled protein (Promega, UK).

Firstly, total RNA extracted from pancreatic β-cells (INS-1) was used to create total cDNA. Next, the GAD65 encoding sequence was amplified using specific primers which encoding restriction sites for both sides (N & C –terminals). The GAD65 reading frame amplicon was cloned into the expression vector pFN22A incorporated within the Halo tag sequences. The halo link has a protease digestible site to liberate expressed GAD65 protein during purification steps. The recombinant plasmid was then used to express GAD65 as a fusion protein in two cell systems; *E. coli* JM109 and a mammalian cell line (CHO). The fusion protein that was expressed (GAD65-Halotag fusion protein) was purified using an affinity chromatography to liberate GAD65 protein. The purified GAD65 was utilized to produce the GAD65 antiserum which was used to screen proteins of different types of microorganism for cross reaction (Figure 7.1).

7.2 Materials and Methods

7.2.1 Cell culture

INS-1 and CHO were cultured and passage as detailed in Sections, 2.3.1 & 2.3.2 respectively.

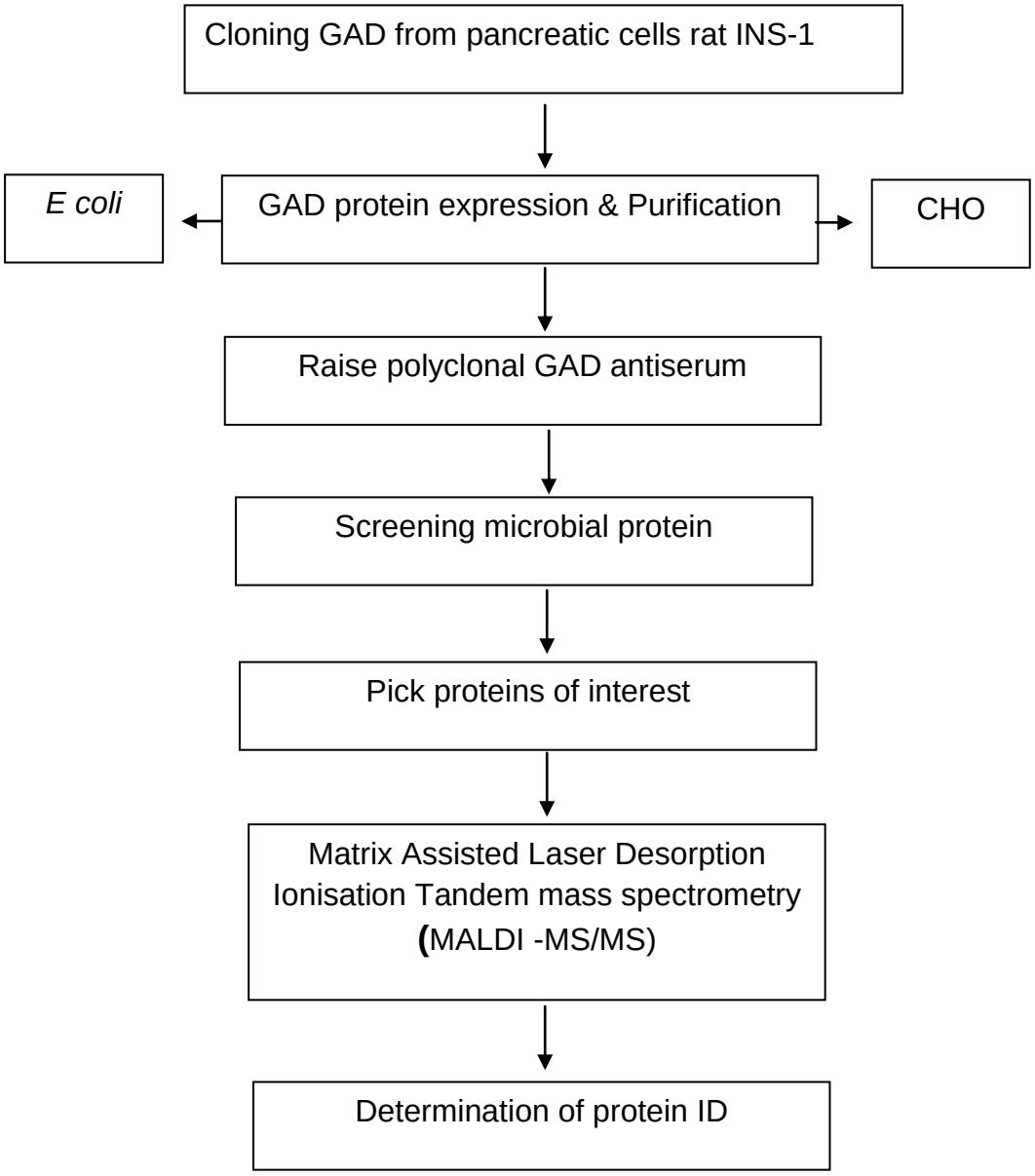

Figure 7.1: Flow chart illustrating the steps for cloning the GAD gene, production and purification of the GAD protein and raising polyclonal GAD antiserum which was used to screen microbial proteins followed by identifying the protein which can cross erect within GAD antiserum.

7.2.2 Molecular cloning of GAD65 gene

7.2.2.1 Synthesizing total cDNA of INS-1 cells

Total RNA was extracted from 10^7 cells of INS-1 as described in section 2.6.1. The RNA concentration was measured using a Nanodrop spectrophotometer (Section 2.5.5) and 4 µg of RNA was used to synthesize cDNA by mixing with 1µl of oligo-dT primers (0.5 µg/µl) in a 200 µl PCR tube (Nuclease free). Tubes were tightly closed and put in a preheated thermal cycler PCR block at 72 °C for 5 min, after which placed on ice water for 5 min, and then centrifuged at 10000 × *g* for 10 sec to collect the mixture and stored on ice until used.

Avian Myeloblastosis Virus (AMV) Reverse Transcriptase mix (200 U/µl) (Promega, UK) was prepared to synthesize the total cDNA by mixing the following components to a final volume of 15µl

GO scripts reaction buffer (5X)	4 µl
$MgCl_2$ (25 mM)	3 µl
Go Script reverse transcriptase	1 µl
dNTPs (10mM)	1 µl
MBW	6 µl

Next, 5 µl (1000 ng/µl) of the RNA mixture was mixed with 15 µl of reverse transcriptase mixture in microcentrifuge tubes (1.5 ml) (final volume 20 µl) and briefly centrifuged for a few seconds to collect the mixture to the tube bottom. Tubes were incubated in a preheated thermal cycler block for 5 min at 25 °C followed by 1 h incubation at 42 °C and 15 min at 70 °C for thermal inactivation of reverse transcription.

7.2.2.2 Amplification of GAD65 gene and optimisation of PCR condition

A pair of primers was used to clone the GAD65 gene from INS-1 cells and producing sticky ends compatible with the ends of the Flexi cloning vector pFN22A (Promega, UK). The forward and reverse primers for the GAD65 gene were designed using online software provided by promega online services http://www.promega.com/techserv/tools/FlexiVectorTool/default.aspx.The forward primer had 35 bases and a *SgfI* restriction site, 5`-GCGT GCGA TCGC CATG GCAT CTCC GGGC TCTG GCT-3`, and the reverse primer had 45 bases and a *PmeI* restriction site 5`- GCAG GTTT AAAC CAAA TCTT GTCC CAGG CGTT CGAT TTCT TCAA TG -3`. The PCR amplifications were performed using cDNA prepared previously (Section 7.2.2.1) and either 2 or 5 µl of total cDNA were mixed with 45 µl of the following master mix and MBW water added to total volume 50 µl.

cDNA	2 or 5 µl
F/primer (10 µM)	1 µl
R/primer (10 µM)	1 µl
dNTPs	1 µl
GoTaq DNA polymerase	0.25 µl
GOTaq buffer	10 µl
MBW to final volume	50 µl

The PCR was started at 94 °C for 2 min to denature the DNA followed by 30 cycles set at 94 °C for 1 min, and different annealing temperatures were used 60, 65, 67 or 69 °C for 1min followed by extension steps at 72 °C for 2 min. The products were separated in 0.8 % agarose gel electrophoresis (Section 2.5.6) and the bands that appeared at expected molecular size were excised from the gel and extracted using a clean-up system (Section 2.5.7). The purified products were used in the follow cloning protocol.

7.2.2.3 Cloning the GAD65 products into Halo tag Flexi vector pFN22A

Flexi vector pFN22A was used to facilitate production of a fusion protein containing the halo-tag protein linked to the GAD65 protein. The GAD65 amplicon produced by PCR (Section 7.2.2.2) was quantified, and its purity assessed (Section 2.5.5). The GAD65 DNA quality was confirmed by running aliquots in 0.8 % agarose gel and then stored at - 20 °C until used.

7.2.2.4 Restriction digestion of GAD65 PCR product and pFN22A vector

The purified GAD65 PCR product and pFN22A were digested using double digestion with restriction enzymes *SgfI* and *PmeI* in microcentrifuge tubes using following reaction components in a final volume of 20 µl.

Flexi Digest Buffer (5X)	4µl
GAD65 PCR Product	4µl (77 ng)
pFN22A	2µl (200 ng)
SgfI & *PmeI*	2µl (20 unit)
MBW	8µl

GAD65 and pFN22A digestion mixtures were incubated at 37 °C for 30 min, or 15 min, respectively, after which both were placed at 65 °C for 20 min to inactivate the restriction enzymes and samples were run into an agarose gel. The digested GAD65 and plasmid DNA were treated using a PCR clean up kit (Section 2.5.7), and the purified products were quantified and checked again into an agarose gel. The samples stocks were stored in ice until ligation.

7.2.2.5 Ligation of GAD65 PCR product into the pFN22A

The ligation of these components was performed in a 1.5 ml microcentrifuge tube using the following mixture to final reaction volume of 20 µl.

Ligase buffer (2X)	10µl
pFN22A	1µl (50 ng)
GAD DNA	1µl (75 ng)
T4 DNA ligase	2µl (6 unit)
MBW	6µl

Tubes were incubated at room temperature for 1 h and some were left at 4 °C overnight. Next, ligation mixtures were used to transform *E. coli JM109* competent cells (Section 2.7.3) and samples were plated on LB plates with ampicillin (100 µg/ml).

7.2.3 Screening transformants for recombinant plasmids

7.2.3.1 Screening *E. coli* transformants for GAD65 recombinants

Transformed colonies appeared on ampicillin plates after 24 h and were screened for plasmids with GAD65 inserts. Colonies were streaked onto ampicillin plates and single colonies were grown in LB broth overnight at 37 ºC. Plasmids were extracted using alkaline lysis method (Section 2.5.3) and run into 0.8 % agarose gels alongside with non-recombinant pFN22A. Recombinants showing a higher molecular weight comparable to the plasmid control were used for further analysis.

7.2.3.2 Screening recombinant plasmids using restriction enzymes

Inserts in the recombinant plasmids were excised using the restriction enzymes *SgfI* and *PmeI*. Plasmid DNA digestions were performed in 1.5 ml of microcentrifuge tubes in a final volume of 20 µl containing.

Digestion buffer (5x)	4 µl
SgfI & *PmeI* enzyme	0.5 µl (20 U/µl)
Plasmid DNA	5 µl (250 ng)
MBW	10.5 µl

Samples were mixed thoroughly by pipetting and samples were incubated at 37 °C for 2 h, followed by 65 °C for 10 min, and then chilled on ice for 5 min. Next, 5 µl of loading buffer was added and samples were loaded and run into agarose gels.

7.2.3.3 Screening recombinant plasmids using PCR

The GAD65 inserts were also checked using PCR amplification. Reactions were performed in PCR tubes (0.2 ml) using 2 µl of diluted plasmid DNA (20 ng/µl) as template and 48 µl of master mix (Section 7.2.2 2) making a final volume of 50 µl. Amplification was carried out using the following conditions; denaturing at 94 °C for 2 min followed by 30 cycles of 94 °C for 1 min, 69 °C for 2 min and 72 °C for 2 min. The products were separated by 0.8% agarose gel electrophoresis and the images were captured.

7.2.3.4 Preliminary checking of the GAD65 sequence by *Bgl II* digestion

In order to confirm whether the PCR product amplified (Section 7.2.3.3) was for the GAD65 gene sequence, the GAD65 mRNA sequence was used to determine a theoretical restriction map using the EBI software online, this predicted the number and size of fragments after digestion with restriction enzyme. Restriction analysis revealed a restriction site for the restriction enzyme by *Bgl II* cleaving the GAD65 amplified gene sequence into two fragments (1073 bp and 694 bp). The PCR amplified products resulting from amplification of GAD65 recombinant plasmid were purified using the PCR product clean-up system (Section 2.5.7). The purified DNA was digested using *Bgl II* as previously described in Section 2.5.8 and the product run into an agarose gel.

7.2.3.5 Sequencing & sequence analysis of GAD65 recombinant plasmids

The recombinant plasmids were commercially sequenced using the MWG Eurofins read value service (MWG, Germany) for sequencing using the reverse reading primer associated with the pFN22A vector, 5-CTTC CTTT CGGG CTTT GTTAG-3. The second primer (reverse) was designed in this study, 5-ACGT GAAT GCGA TGAG CCTG-3. The sequences were analysed by Blast –n and checked for ORF, stop codon, and the fusion region, confirming the amino acid sequence of the TEV protease digestible site, furthermore, the sequences were carefully checked for mutations.

7.2.4 Expression and purification of Halo-tag GAD65

The successful recombinant plasmid pG1 (pF22A-GAD65) has T7 and cMVd1 promoters allowing transcription and expression of the cloned gene in two hosts, *E. coli* and mammalian CHO, respectively. The GAD65-Halo tag protein was purified by affinity chromatography resin system (Promega, UK). In this technique the Halo tag sequence of the engineered GAD65 binds covalently and specifically to the affinity resin, allowing stringent washing for unbound protein. The GAD65 could then be released from the halo-tag protein with TEV protease. TEV protease was easily removed from the protein of interest as the TEV has a N-terminal histidine tag that binds to the His link resin and allows recovery of the purified protein.

7.2.4.1 Expression and extraction of engineered GAD65 from *E. coli JM109*

A single colony from a fresh culture of recombinant *E. coli* - pG1 was used to inoculate 10 ml volumes of LB medium containing 100 mg/ml ampicillin and 0.05% glucose, with and without rhamnose (which was used as a stimulator for the T7 promoter) and incubated overnight at 37 °C with 120 rpm shaking speed. Cultures (0.5 ml) was used to inoculate 50 ml volumes of LB medium and

incubated overnight as before. The cells were collected by centrifugation at 4000 × *g* for 20 min at 4 °C. Next, cells were suspended in 5 ml protein extraction buffer (Appendix 1) containing 100 µg/ml of lysozyme, 5µg/ml DNase I (final concentration) and 0.5 ml of protease inhibitor cocktail I (P8340, Sigma, UK), in conical tubes (20 ml) and sonicated on ice using 5 sec bursts with 5 sec cooling time for a total of 4 min. Afterwards, ATP and $MgSO_4$ were added to a final concentration of 2 mM and 10 mM, respectively, and incubation was at 37 °C for 10 min to dissociate the chaperonin proteins that bind the halo sequences during purification steps. The cell lysates were centrifuged at 10000 × *g* for 30 min at 4 °C and the supernatant transferred to a fresh 15 ml polypropylene tube and store at - 70 °C until purification.

7.2.4.2 CHO transfection optimisation

The recombinant plasmid pG1 was also used to produce the GAD65-Halo tag fusion protein in mammalian host cells, Chinese hamster ovary cell line (CHO) by transfection in order to enhance the amount protein produced as it was more efficient in the mammalian cell in comparison to the *E. coli*. The transfection protocol used the chemical transfection reagent (TR) FUGENE HD (Promega, UK).

The current study used transient transfection which allowed the highest number of transfectants to be available to produce an adequate amount of the GAD65 protein. The transfection conditions were optimised to determine the appropriate amount of the TR producing the maximum of CHO transfectants cells. Tissue culture plates (96 well) were used to plate out the CHO cells to be transfected, using the protocol for adherent cells recommended by the supplier. CHO seeding density of 2×10^4 cell/well was used and incubation was as described (Section 2.3.2) for 24 h. Next, the depleted medium was replaced with 100 µl of

fresh medium, followed by 2 µl of GAD65 recombinant plasmids pG1 DNA (200 ng/ µl). Samples with different volumes of TR in separate wells to produce TR/DNA mixtures of 6:1, 5:1, 4:1, 3:1, 2:1 and 1:1 ratios to a final volume of 10 µl in wells and incubated at room temperature for 15 min and then mixed briefly by pipetting. Alternatively, the TR/DNA mixture was added to the cells directly after removing the old medium and transfection was allowed for 10 min at RT and after that CHO growth medium was added and the plates were incubated for 48 h for expression. Total protein was extracted and subjected to dot blot to identify GAD65 expression. The TR/DNA ratio expressing the strongest reaction with GAD65 antibody was applied to large-scale production in 25 cm^2 flasks. The total protein extracted from 10^7-10^9 CHO cell, were trypsinized (Section 2.3.2) and resuspended in 2 ml of extraction buffer (Appendix 1) and subjected to sonication for 1 min as described in section 2.4.1. Afterwards, the cell lysates were mixed with 1ml of Triton –X100 (0.1%) and left on ice for 20 min and re-sonicated as before, then centrifuged for 30 min for 10000 × *g* and the supernatant (2 µl) was checked for GAD production using dot blot and positive samples were stored at -70 ºC until purification.

7.2.4.3 RT-PCR for GAD65 gene expression in CHO

The TR/DNA ratio which produced the highest protein expression was used to assess GAD65 gene expression as a further confirmation for GAD65 expression and transfection efficiency. CHO seeded in 6 well plate (10^6 cell / well) and transfection with pG1 applied using 3:1, 4:1, 5:1 or 6:1 TR/DNA mixture (Section 7.2.4.2). The total RNA was extracted and cDNA synthesised (Sections 2.6.1 & 2.6.2, respectively), PCR amplification was performed as described in 7.2.2.2.

7.2.4.4 Purification of GAD65 Halo Tag

During the purification and cleaving process the protein lysates expressed by *E. coli* or CHO were treated separately and stored in separate tubes. The halotag purification system was used to purify the recombinant GAD65 using Halo Link Resin (Promega, UK) which has high affinity to halo tag sequence which was combined to the GAD65 sequence.

Aliquots (4ml) of halo link resin were pipetted into 15 ml polypropylene tubes and centrifuged at 1000 × *g* for 5 min at RT, supernatants were discarded and resins were subjected to calibration steps. The resin equilibration was achieved by re-suspending the halo link resin in 10 ml of extraction buffer and mixing thoroughly until producing a homogenised suspension. Suspensions were spun at 1000 × *g* for 5 min and the supernatant removed. This step was repeated twice and after the third wash the resin was immediately mixed with 10 ml cell lysate of *E. coli* or CHO supernatant. Next, the lysate was resuspended by inverting the tube on a tube rotator for end over end mixing for 1 h at RT. Tubes were centrifuged as before and supernatants were transferred into fresh tubes and ATP and $MgSO_4$ $7H_2O$ were added to a final concentration of 4 mM and 20 mM, respectively. Tubes contents were mixed at RT for 30 min and the resin was then collected by centrifugation and washed 3 times with 10 ml volumes of extraction buffer as before.

7.2.4.5 Cleavage of GAD65 Protein from the Halo tag

After the third wash, the pelleted halo link resin was resuspended in 1.1 ml of TEV protease cleavage solution (Appendix 1) by pipetting until homogenised and transferred to a fresh 15 ml tube and incubated with agitation at RT for 1 h. After which, tubes were centrifuged at 3000 × *g* for 5 min and the supernatant was transferred to a fresh 15 ml tube. The resin was re-suspended again in 1 ml

of extraction buffer for the second elution and mixed well by inverting and centrifuged as step before. Supernatant was added to the first elution sample to a 2 ml final volume. In order to remove the TEV residues, 50 µl of His link resin (resin has affinity to bind the TEV protease) was mixed with the eluted supernatants and mixed thoroughly at RT for 20 min. Next, the sample was centrifuged at 1000 × *g* for 5 min at 4 °C and the supernatant was aspirated off into a fresh 1.5 ml micro centrifuge tube. Protein samples from crude cell lysates and purified protein were subjected for characterisation.

7.2.5 Characterization of the purified GAD65 protein

7.2.5.1 SDS PAGE electrophoresis

Aliquots of 12 µl of cleavage protein samples extracted from recombinant CHO and *E. coli* and were subjected to SDS-PAGE (Section 2.4.3) alongside protein standard markers (C1992, S8320 Sigma, UK) and total cell lysates for comparison.

7.2.5.2 GAD65 protein Dot Blot

Dot blots were performed using a Minifold I 96-Well Dot-Blot System (Schleicher & Schuell, Germany). Firstly the vacuum plenum was placed and then a filter support plate was placed on top followed by 10 × 12 cm of pre wetted Whatman filter paper. A piece of nitrocellulose membrane was cut to fit the 96-well block and soaked with washing buffer (Appendix 1) for 5 min. This was placed on the filter paper and the sample well plate was placed finally on top. Next, 2 µl of protein samples of transfected cell lysates and concentrated and diluted, purified GAD65 were loaded into the wells. Vacuum pressure was applied at 0.9 bars for 3 min and after the membrane was placed in 50 ml of blocking solution (Appendix 1) for 1.5 h with gentle shaking at RT.

The blocking solution was replaced with a fresh volume and the anti GAD65/67 secondary antibody developed in rabbit (G6163 Sigma, Pool, UK detecting amino acids 570-585 DIDLIEEIERLGQDL on both types of GAD65) was added at 1:10000 and the membrane was incubated for 2 h with gentle shaking at RT. After that the blocking reagent was discarded and 100 ml of washing buffer was added to wash the membrane with shaking for 10 min at RT. The wash step was repeated for a total of 3 times. Next, anti-rabbit anti IgG antibody labelled with alkaline phosphatase (Sigma, Pool, UK) was mixed with 50 ml of washing solution to final concentration of 1:30000 and added to the membrane followed by incubation at RT for 1 h with gentle shaking. The membrane was washed as before and then 20 ml of alkaline phosphatase substrate (Appendix 1) was added and left for 24 h to visualize the protein antibody binding. Finally the membrane was dried out at RT and a digital image was captured.

7.2.5.3 Quantification and concentration of the GAD65 protein

The purified GAD65 protein concentration was measured using the Bradford method (Section 2.4.2) and the protein solution was concentrated using a centrifugal filter (Millipore, UK) reservoir type YM10, to obtain an appropriate concentration (≈1 mg/ml) adequate for a mouse immunisation protocol to produce GAD65 antiserum. Filters were inserted into 2 ml vial supplied with the kit and aliquots (500 µl) of each sample were pipetted into the reservoir tubes. The tubes were centrifuged for 30 min at 13000 × *g* in microcentrifuge, after which, the reservoir was removed from the vial and placed upside down into a fresh vial and centrifuged 3 min at 1000 × *g*. The reservoir was removed and the protein concentration measured and 2 µl samples were run into SDS-PAGE and the stock was kept at -20 °C until use.

7.2.6 GAD65 antiserum production and titration

The purified protein GAD65 produced by mammalian CHO cells was used to produce the GAD65 antiserum. The antiserum was raised commercially using a Biogensis immunization protocol (Biogenesis, Germany). The GAD65 protein (1.2 mg/ml) was sent to the Biogenesis on dry ice. The immunization was performed using two mice according to a schedule over 49 days: -1st day – 1st immunisation/pre-immune serum (0.02 ml serum), 28th day -2nd immunisation , 35th day – 3rd immunisation, 42nd day-4th immunisation, 49th day –final bleed (0.5 ml serum).

After 49 days, the GAD65 antiserum was received and divided into aliquots of 50 µl stored in 200 µl microcentrifuge tubes at -20 °C. The optimum dilution of antiserum for detection purposes was determined using different dilutions of 1:500, 1000, 2000, 4000, 6000, 8000 against 5 µg samples of GAD65 protein (prepared in Section 7.2.5.2) using dot blotting (Section 7.2.5.3). The optimum concentration was the dilution which gave the strongest reaction without background or nonspecific binding. Pre-immunisation serum was used as a control to check for nonspecific binding or nonspecific antibody cross reaction.

7.3 Results

7.3.1 Cloning the GAD65 reading frame

7.3.1.1 Amplification of the GAD65 reading Frame

Total cDNA was synthesised from RNA of INS-1 cells and the full length GAD65 reading frame was successfully amplified. PCR amplification of the GAD65 reading frame sequence was optimised at different annealing temperatures 50, 60 67 & 69 °C. The first three temperatures produced have shown additional DNA bands at about 0.5 kbp, in addition to the GAD65 band which appeared at the expected size of 1755 kbp. Furthermore, high primer dimmer was seen (Figure 7 .2 A, B and C). However, PCR amplification using 5 µl cDNA and 69 °C annealing temperature produced a sharp and strong single band at the expected molecular size for the amplified GAD65 gene (Figure 7.2 D).

7.3.1.2 Cloning the amplicon of GAD65

The GAD65 PCR products amplified at 69 °C using Go tag DNA polymerase that produces an A overhang and *SgfI* and *PmeI* restriction site on both 5` and 3` ends was purified using a PCR clean up kit. The highly pure samples were digested by restriction enzymes and separated by agarose gel electrophoresis and the GAD65 band was successfully recovered from the gel and purified.

The vector pFN22A DNA was digested by *SgfI* and *PmeI* releasing the barnase gene band at 335 bp (Figure 7.3 lane 5 & 9), and the linear plasmid DNA was eluted from the gel and ligated within the GAD65 fragment to successfully produce recombinant pFN22A containing the GAD65 reading frame (instead of toxic barnase sequences), and recombinant plasmids were successfully transformed into *E. coli JM109*.

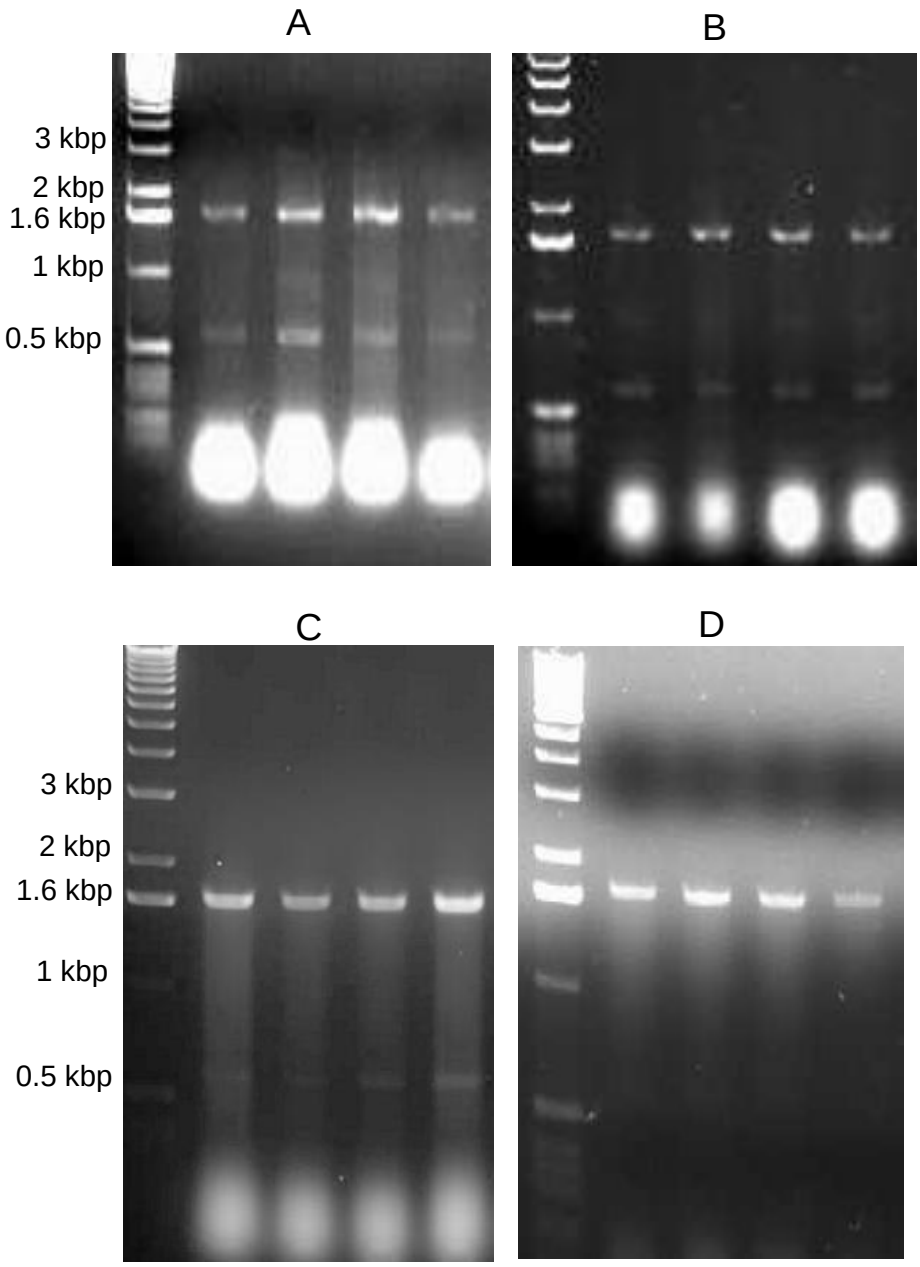

Figure 7.2: Amplification of the GAD65 reading frame by RT-PCR. Annealing temperature optimisation used 2 µl cDNA, at 60, 65 and 67 °C shown in A, B and C respectively and GAD65 amplification using 5 µl cDNA and 69 °C annealing temperature (D).

7.3.1.3 Restriction digestion of recombinant plasmids

Recombinant plasmids (pG1-pG20) were extracted from the transformants and samples were run into agarose gels. Plasmids with higher molecular weight (Appendix 2) then the vector only, were selected and digested with *SgfI* and *PmeI*. The results (Figure 7.3) show successful cloning and correct size inserts in 20 plasmids extracted from a total of 100 recombinant colonies subjected to screening. However, the majority of recombinant plasmids produced no inserts after restriction enzyme digestion examples are shown in Figure 7.4, lane 10 11, 12. Example of recombinant plasmids producing the desired insert of GAD65 at the expected molecular size about 1755 bp are shown in Figure 7.4 lanes 2, 4, 6, 7, 8.

7.3.1.4 Preliminary checking of the GAD65 inserts

The recombinant plasmids were subjected to PCR amplification for inserts representing the GAD65 encoding region, using the GAD65 primers used initially to amplify the GAD65 region from INS-1 cDNA. The amplification clearly produced a single band at the expected molecular size (1755 bp) (Figure 7.4 lane 1&2), whereas, the plasmids which showed unsuccessful cloning after digestion produced a product at 600 bp (Figure 7.3 lane 3 & 4). In addition, the GAD65 region was double checked by digestion this PCR product by restriction enzymes as the GAD65 cDNA sequences supposed to produce two bands 1073 bp and 694 bp after digestion with restriction enzyme *Bgl II* according to the cDNA restriction map of GAD65 region. The digestion of amplified DNA cloned in pG1-pG5 has shown two bands at the exact molecular size comparable to the1 kbp ladder (Figure 7.3 lane 7 & 9).

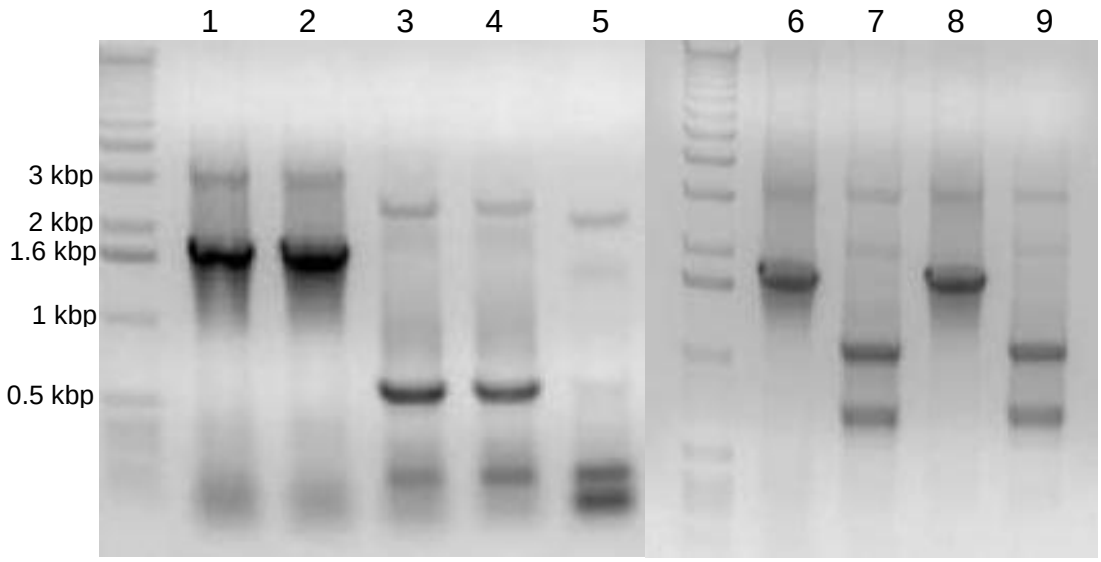

Figure 7.3: Preliminary identification of GAD65 encoding region from recombinants pG1 & pG2. Amplification GAD65 encoding region from pG1 & pG2 (lane 1 & 2) and unsuccessful cloned plasmids (lane 3 & 4) compare to the non-recombinant pFN22A (lane 5). The restriction digestion of GAD65 amplicons DNA amplified from both PG1 & 2 using *Bgl II* (lane 7, 9) producing to DNA fragments 694 & 1073 respectively.

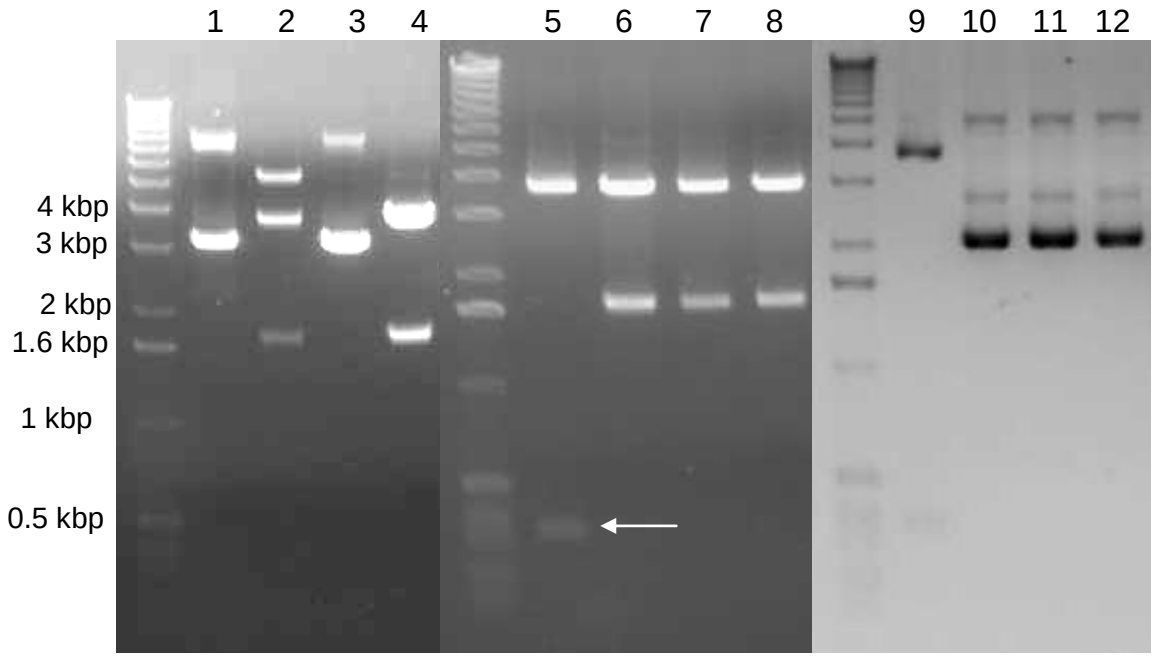

Figure 7.4: Excision of inserts from recombinant plasmid pG1-pG5 (lane 2, 4, 6, 7 & 8) with *SgfI* and *PmeI* compared with recombinant undigested (lane 1&3) and digested the pFN22A (lane 5&9) producing barnase gene. Lane 10, 11 & 12 show recombinant pFN22A with incorrect sequences or missing digestible sites.

7.3.2 GAD65 sequencing and sequence analysis

Five recombinant plasmids (pG1-pG5) were sequenced and the results clearly confirmed the GAD65 1755 bp sequence was cloned. The full length of the GAD65 encoding sequence with sequence blast produced up to 100% similarity to GAD65 antigen cDNA from rat pancreatic β-cells (Figure 7.6). The blast results of the GAD65 sequence of pG1 and pG2 showed the full length sequences without any mutations or deletions which may impede the protein expression. However, the sequence analysis of the other plasmids (pG3, pG4 & pG5) expressed alteration in nucleotide sequences, as well as some deletions, creating different GAD65 reading frames. These were not used, sequencing results of pG1 & 2 showed no alteration of the TEV protease digestible encoding sequences.

7.3.3 Selection of recombinant plasmids for expression

Two recombinant plasmids (pG1 & pG2) carrying the GAD65 region with no sequence alteration producing correct GAD65 coding region were elected for protein production (Figure 7.5 A). However, recombinant plasmids pG1 & pG2 produce full length sequences of GAD65 with no mutation or deletion (Figure 7.6) in addition to the complete sequences of the digestible TEV protease site and *SgfI & PmeI* restriction sites (Figure 7.5 B). Plasmid pG1 was used to produce the GAD65 protein in both *E. coli* and CHO.

A

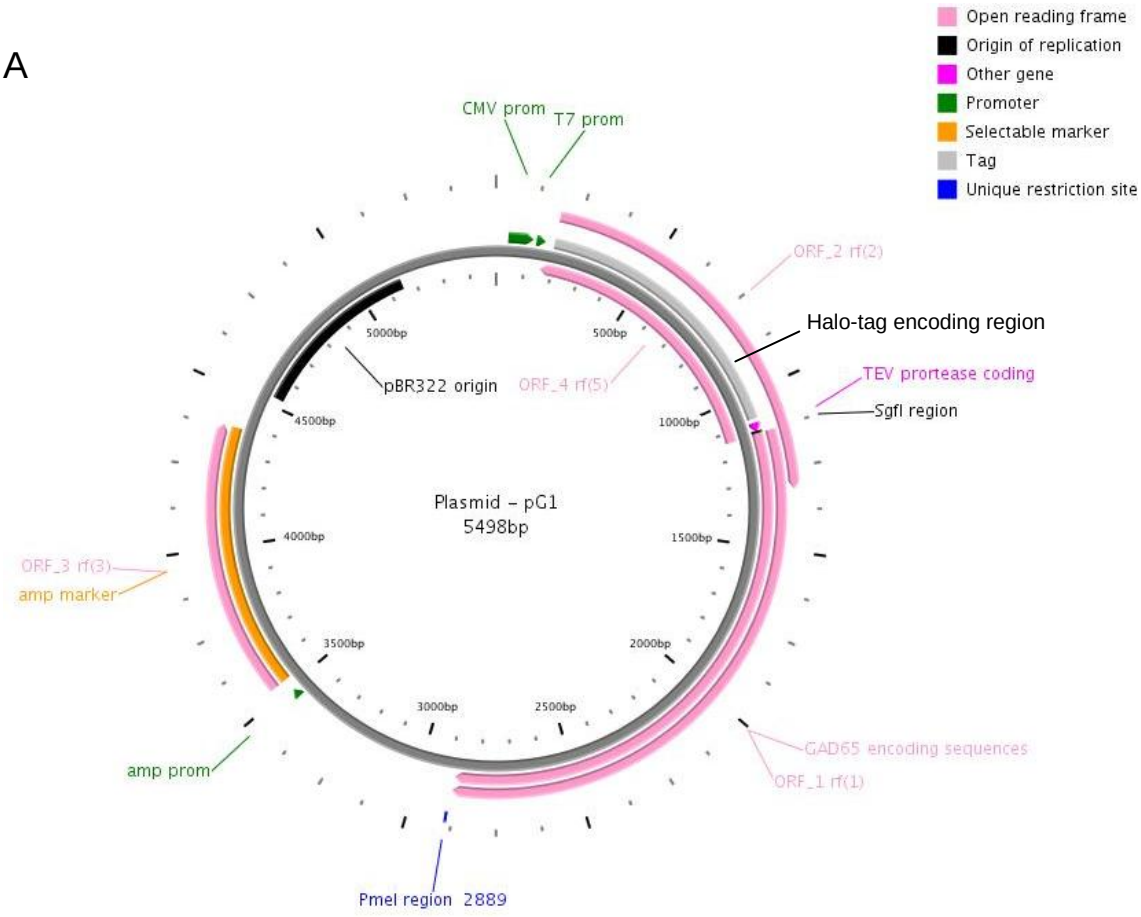

B

Halo sequences TEV site *SgfI*

5'- 1080 CGAGCCAACC ACTGAGGATC TGTACTTTCA GAGCGTGCGAT/CGCCATGGCATCTCCG-3'

M A S P

PmeI

5′- GCAGGTTT/A AAC CAA ATC TTG TCC CAG GCG TTC GAT-3'

Stop codon V L D Q G L R E I

Figure 7.5: Schematic map of recombinant pG1 plasmid sequences (A), the map shows relevant sequences after the recombination halo tag and barnase gene (which was replaced by GAD65 region), TEV protease site and unique restriction sites of *SgfI* and *PmeI* and CMV and T7 promoters. The map achieved using full sequences of pG1 plasmid by using PlasMappar version 2 (Dong *et al*., 2004). The full length sequences of restriction sites for *SgfI* & *PmeI* and TEV digestible site combined with halotag and GAD sequences (B).

```
1-ATGGCATCTCCGGGCTCTGGCTTTTGGTCCTTCGGATCTGAAGATGGCTCTGGGGATCCTGAGAAC
  1- M--A--S--P--G--S--G--F--W--S--F--G--S--E--D--G--S--G--D--P--E--N--
 67 CCGGGAACAGCGAGAGCCTGGTGCCAGGTGGCCCAAAAGTTCACGGGCGGCATCGGAAACAAGCTA
 23 -P--G--T--A--R--A--W--C--Q--V--A--Q--K--F--T--G--G--I--G--N--K--L--
132 TGCGCTCTGCTCTACGGAGACTCTGAGAAGCCAGCAGAGAGCGGCGGGAGCGTGACCTCGCGGGCC
 45 -C--A--L--L--Y--G--D--S--E--K--P--A--E--S--G--G--S--V--T--S--R--A--
198 GCCACTCGGAAGGTCGCCTGCACCTGTGACCAAAAACCCTGCAGCTGCCCCAAAGGAGATGTCAAT
 67 -A--T--R--K--V--A--C--T--C--D--Q--K--P--C--S--C--P--K--G--D--V--N--
264 TATGCACTTCTCCACGCAACAGACCTGCTGCCAGCCTGTGAAGGAGAAAGGCCCACTCTCGCATTT
89  -Y--A--L--L--H--A--T--D--L--L--P--A--C--E--G--E--R--P--T--L--A--F--
330 CTGCAAGATGTAATGAACATTTTGCTTCAGTACGTGGTGAAAAGTTTTGATAGATCAACTAAAGTG
111 -L--Q--D--V--M--N--I--L--L--Q--Y--V--V--K--S--F--D--R--S--T--K--V--
396 ATTGATTTCCATTACCCCAATGAGCTTCTTCAAGAGTATAATTGGGAATTGGCAGACCAACCGCAA
133 -I--D--F--H--Y--P--N--E--L--L--Q--E--Y--N--W--E--L--A--D--Q--P--Q--
462 AATCTGGAGGAAATTTTGACGCACTGCCAAACAACTCTAAAATATGCGATTAAAACAGGGCATCCC
155 -N--L--E--E--I--L--T--H--C--Q--T--T--L--K--Y--A--I--K--T--G--H--P--
528 CGATATTTTAATCAGCTGTCTACCGGATTGGATATGGTTGGATTAGCAGCAGATTGGTTGACATCA
177 -R--Y--F--N--Q--L--S--T--G--L--D--M--V--G--L--A--A--D--W--L--T--S--
594 ACAGCAAACACGAACATGTTTACCTATGAGATCGCCCCTGTATTTGTACTACTGGAATATGTGACA
199 -T--A--N--T--N--M--F--T--Y--E--I--A--P--V--F--V--L--L--E--Y--V--T--
660 CTAAAGAAAATGAGGGAAATCATTGGCTGGCCAGGAGGCTCTGGCGATGGAATCTTTTCTCCTGGT
221 -L--K--K--M--R--E--I--I--G--W--P--G--G--S--G--D--G--I--F--S--P--G--
726 GGTGCCATCTCCAACATGTACGCCATGCTCATTGCCCGCTATAAGATGTTTCCAGAAGTCAAGGAA
243 -G--A--I--S--N--M--Y--A--M--L--I--A--R--Y--K--M--F--P--E--V--K--E--
792 AAGGGGATGGCGGCGGTGCCCAGGCTCATCGCATTCACGTCAGAGCATAGTCACTTTTCTCTCAAG
265 -K--G--M--A--A--V--P--R--L--I--A--F--T--S--E--H--S--H--F--S--L--K--
858 AAGGGAGCTGCAGCCTTGGGGATCGGAACTGACAGCGTGATTCTGATTAAATGTGATGAGAGAGGG
287 -K--G--A--A--A--L--G--I--G--T--D--S--V--I--L--I--K--C--D--E--R--G--
924 AAAATGATCCCATCTGACCTTGAAAGAAGAATCCTTGAAGTCAAACAGAAAGGATTTGTTCCTTTC
209 -K--M--I--P--S--D--L--E--R--R--I--L--E--V--K--Q--K--G--F--V--P--F--
990 CTGGTGAGTGCCACAGCTGGAACCACTGTGTACGGGGCTTTTGATCCTCTCTTGGCTGTAGCTGAC
331 -L--V--S--A--T--A--G--T--T--V--Y--G--A--F--D--P--L--L--A--V--A--D--
1056 ATCTGCAAAAAATATAAGATCTGGATGCATGTGGATGCTGCTTGGGGTGGAGGGTTACTGATGTCT
353  -I--C--K--K--Y--K--I--W--M--H--V--D--A--A--W--G--G--G--L--L--M--S--
1122 CGGAAACACAAGTGGAAGCTGAACGGTGTGGAGAGGGCCAACTCTGTGACATGGAATCCCCACAAG
375  -R--K--H--K--W--K--L--N--G--V--E--R--A--N--S--V--T--W--N--P--H--K--
1188 ATGATGGGTGTCCCCTTGCAATGTTCGGCTCTCCTGGTCAGAGAGGAGGGACTGATGCAGAGCTGC
397  -M--M--G--V--P--L--Q--C--S--A--L--L--V--R--E--E--G--L--M--Q--S--C--
1254 AACCAGATGCATGCTTCCTACCTCTTTCAGCAAGATAAGCACTATGACCTGTCCTATGACACGGGA
419  -N--Q--M--H--A--S--Y--L--F--Q--Q--D--K--H--Y--D--L--S--Y--D--T--G--
1320 GACAAGGCCTTGCAGTGTGGACGCCACGTCGATGTCTTTAAATTATGGCTCATGTGGAGAGCAAAG
441  -D--K--A--L--Q--C--G--R--H--V--D--V--F--K--L--W--L--M--W--R--A--K-
1386 GGGACTACTGGATTTGAAGCTCACATTGATAAGTGTTTGGAGCTGGCAGAGTATTTATACAATATC
463  -G--T--T--G--F--E--A--H--I--D--K--C--L--E--L--A--E--Y--L--Y--N--I--
1452 ATTAAAAACCGAGAAGGATATGAAATGGTGTTCGATGGGAAGCCTCAGCACACAAATGTCTGCTTC
485  -I--K--N--R--E--G--Y--E--M--V--F--D--G--K--P--Q---H--T--N--V--C--F--
1518 TGGTTTGTACCTCCTAGTTTGCGAGTTCTGGAAGACAATGAAGAGAGAATGAGCCGCCTCTCAAAG
507  -W--F--V--P--P--S--L--R--V--L--E--D--N--E--E--R--M--S--R--L--S--K--
1584 GTGGCGCCAGTGATTAAAGCCAGAATGATGGAGTATGGGACCACAATGGTCAGCTACCAACCCTTA
529  -V--A--P--V--I--K--A--R--M--M--E--Y--G--T--T--M--V--S--Y--Q--P--L--
1650 GGAGATAAGGTCAACTTCTTCCGCATGGTCATCTCAAACCCTGCAGCAACTCACCAAGACATTGAC
551  -G--D--K--V--N--F--F--R--M--V--I--S--N--P--A--A--T--H--Q--D--I--D--
1716 TTCCTCATTGAAGAAATCGAACGCCTGGGACAAGATTTGTAA
573  -F--L--I--E--E--I--E--R--L--G--Q--D--L
```

Figure 7.6: the GAD65 ORF sequence cloned into recombinant plasmid pG1 expressing full length sequence 1755 bp and protein with 585 amino acids without any mutation confirming binding the GAD65 sequence.

7.3.4 Production and purification of GAD65 protein

7.3.4.1 Expressing of recombinant GAD65 protein

The recombinant plasmid pG1 encoding GAD65 was successfully transformed into competent *E. coli* JM109 and transformants were used to produce the protein intracellularly. Over expression of the GAD65 fusion protein was not toxic to the *E. coli* JM109 strain as the transformants grew, were grown properly in LB broth, with and without stimulators (rhamnose and glucose). The pG1 plasmid was successfully transferred into CHO cells by a transient transfection protocol which was applied to express the GAD65 protein into CHO.

The dot blot results showed a strong reaction of protein extracted from CHO cells treated with TR (3, 4, or 5 µl) and 200 ng plasmids as these concentrations produced strong dark blots. The CHO cells which were treated by the highest concentration of TR (6 µl) and lowest (1 or 2 µl) produced weak or no reaction (Figure 7.7). The TR/DNA complex which was added directly to the cells produced a strong reaction comparing the TR/DNA that mixed with growth medium. The dot blot of protein extracted from *E. coli* produced a strong reaction with GAD65 antibody compared to the samples extracted from transient transfection of CHO.

7.3.4.2 GAD65 gene expression

The CHO transfection efficiency was also measured by assaying GAD65 gene expression by RT-PCR. CHO transient transfection with recombinant plasmid pG1 was performed using the conditions producing strong reactions in the dot blot. Transfectants using TR/DNA 3:1, 4:1, 5:1, and 6:1 were used to assess the GAD65 gene expression. The recombinant CHO were grown in 96 well plates and subjected to the RT-PCR procedure. The results clearly shown bands of

the expected molecular size of GAD65, however, the strongest band was seen with amplified cDNA from samples treated with 1:4 µl TR/DNA (Figure 7.8).

7.3.4.3 Extraction & purification of GAD65 protein

The *E. coli* recombinant and transfected CHO cells were used to extract the engineered GAD65. *E. coli* transformants were grown and 100 ml of recombinant *E. coli* and 10^9 recombinant CHO were subjected separately to the purification procedure (7.2.4.4). The results show a recombinant protein of 97 kDa was extracted successfully from both extracts (*E. coli* and CHO). The recombinant protein was composed of 65 kDa of GAD65 and 32 kDa of halo tag protein. The captured protein was cleaved by TVE protease to produce GAD65 protein free from the halo link sequences and the results show clearly a protein with 65 kDa MW without any TVE contaminates which was removed from S-TEV resin treatment (Section 7.2.4.5). However, the GAD65 purified protein concentration which was extracted from the transiently transfected CHO cell was relatively less than the amount of protein produced by *E. coil*. The CHO cells protein yield was 400 µg/ml, whereas, from *E. coli* it was about 1mg/ml. Therefore, the yield of purified protein was increased by concentration to 1.2 mg/ml protein produced by CHO and 2.6 mg/ml of GAD65 protein produced by *E. coli.* Proteins were then subjected to the SDS-PAGE (Figure 7.9) and dot blot (Figure 7.10).

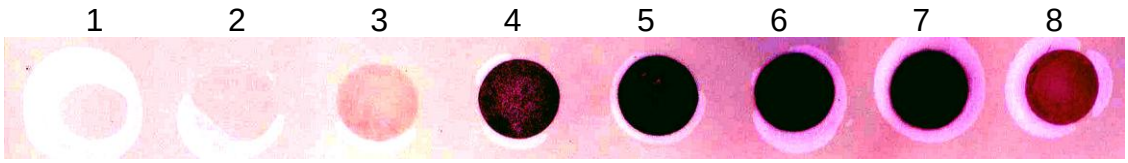

Figure 7.7: Dot blot of GAD65 protein expression showing optimization of transfection of CHO cells by pG1 recombinant plasmid screened without GAD65 antibody. Controls were CHO treated only by TR treated (1) and CHO treated by pG1 plasmid (200 ng) only (2). GAD65 protein expression from transfectants CHO (3, 4, 5, 6. 7 & 8) treated with TR/DNA 1:1, 2:1, 3:1, 4:1, 5:1 and 6:1, respectively, detected by GAD65 antibody.

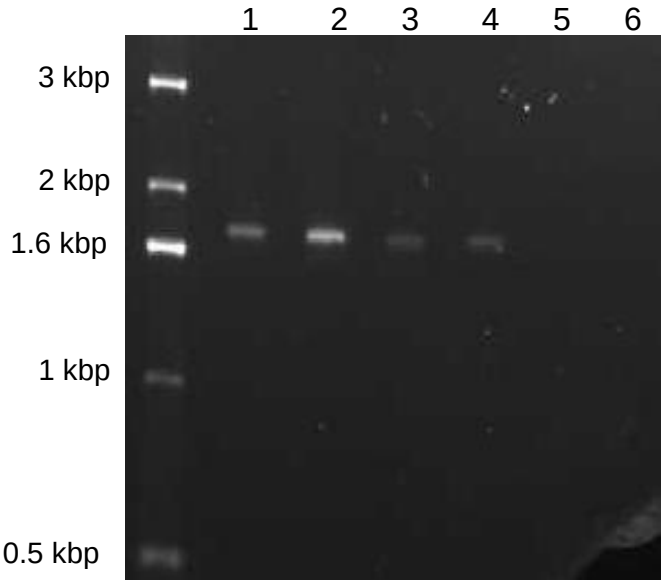

Figure 7.8: RT-PCR of GAD65 gene expression in CHO transient transfectants carrying the GAD65 recombinant plasmid pG1. The lanes representing optimization of transfection for GAD65 gene expression using 200 ng plasmid DNA and 3,4,5 and 6 µl TR were produced in lanes 1,2,3,4 respectively and lane 5, 6 represents control treated DNA and control treated 3 µl transfection reagent, respectively.

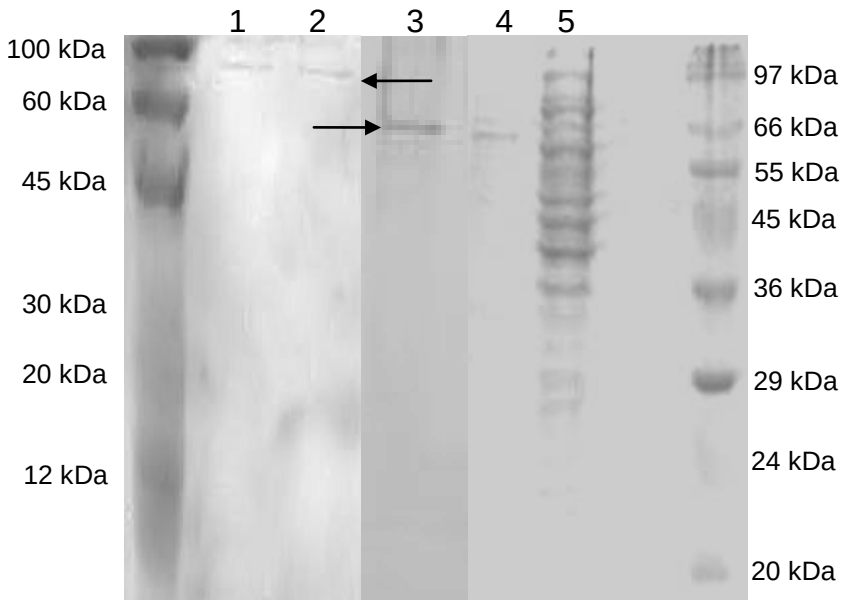

Figure 7.9: SDS-PAGE of recombinant purified engineered 97 kDa Halo Tag - GAD65 protein expressed in CHO cells and *E. coli* (lanes 1, 2 respectively), and the purified GAD65 after purification (lanes 3 & 4) total protein extracted from non-recombinant CHO (lane 5).

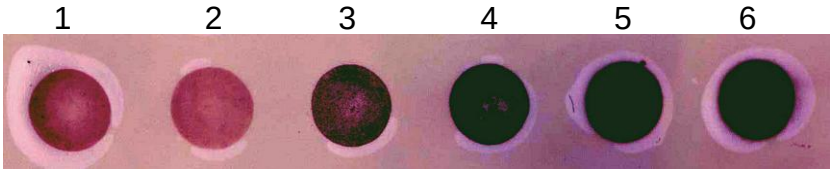

Figure 7.10: Dot blot of GAD65 produced by CHO after protein concentration steps using 5 µl protein samples.

7.3.5 Titration of anti GAD65 antiserum

The polyclonal sera were raised by Biogenes according to the immunization plan (Section 7.2.6). The serum was checked with the GAD65 protein produced by this study. GAD65 protein extracted from the INS-1 cells was used to titrate the serum producing strong reactions at dilution 1:500, 1:1000, Moderate reaction with 1:2000, 1:4000, and weak reaction at 1:6000 & 1:8000. The pre immune serum at 1:2000 dilution produced no reaction, as did the BSA protein as a negative control (Figure 7.11). Therefore, for the current study the 1:2000 dilution was used for further studies.

1:500 1:1000 1:2000 1:4000 1: 6000 1:8000

Pre-immune sera (1:2000) Control (BSA)

Figure 7:11: Titration of the GAD65 antiserum using dilutions of antisera against the purified protein GAD65 produced in this study. Controls GAD65 against pre immune sera (1:2000) and negative control for BSA.

7.4 Discussion

GAD65 is an enzyme that catalyses the conversion of glutamic acid to amino butyric acid and CO_2, GAD65 is a major autoantigen in T1D. The production and purification of this antigen has become a crucial initiative to researching the development of T1D and disease predication (Hagopian *et al.*, 1993b; Zimmet, 1996). Furthermore, GAD65 has been suggested as a therapeutic agent for T1D (Tuomilehto *et al.*, 1994).

The current study selected the GAD65 antigen amongst other pancreatic beta cell antigens to search for molecular mimicries in microorganisms (bacteria & yeast). GAD65 was chosen as it is one of the major β-cell antigens, and GAD65 antibody is found in 70-80 % of T1D patients and predominantly seen against GAD65, developing as an autoimmune response (antibodies) during early childhood stages (Atkinson *et al.*, 1990; Hagopian *et al.*, 1993a; Hagopian *et al.*, 1993b; Myers *et al.*, 2000). It was also verified that GAD65 autoimmunity mediates T2D in some cases producing latent antibodies diabetes mellitus (LADA) which has T2D symptoms leading to inhibition of insulin secretion and then develops T1D.

The GAD65 enzymes function has been reported in a wide range of bacteria like *E. coli*, (Smith *et al.*, 1992; Mulder, 2005), *Lactobacillus* (Kim *et al.*, 2007), *Bacteroides* and *Clostridium* (Jilly *et al.*, 1984) and some fungi such as yeast. Therefore, there was a possibility of molecular mimicries among the secondary structure of enzymes sharing similar function. For example, the secondary structure of GAD65 containing cofactor pyridoxal 5 phosphatase (PLP) binding domain sequence shares conformational epitopes (protein fold) with other PLP depending proteins in bacteria such as the PLP sequence of ornithine decarboxylase and aspartate aminotransferase of *Lactobacillus* (Momany *et al.*,

1995; Qu *et al.*, 1998). Sequence similarity or linear epitopes were one of the main targets of this study, trying to find sequences similar between microbial proteins and beta cell GAD65 protein. The GAD65 antibodies (anti-serum) was used as a tool to search for proteins extracted from a range of microorganisms with epitopes that could play a role as initiators in the development of an autoimmune response. Consumption of food and water containing microorganisms and infections due to pathogenic bacteria were hypothesised as the main sources of exposure.

The GAD65 antiserum (GAD65 polyclonal antibodies) was raised in this study to search for microbial proteins with GAD65 molecular mimicries. The Halo tag technology used cDNA library cloning or PCR cloning of the gene which encoded the GAD65 protein to produce the GAD65-halotag fusion protein. In the case of this study the GAD65 region was successfully amplified using primers having digestible restriction sites. The GAD65 reading frame was cloned within the halo tag of binary expression vector pFN22A. Recombinant plasmid pG1 transformed into the *E. coli* and transformation expressed a high number of transformants. However, some transformants had plasmids with no inserts or restriction digestion sites-missing plasmids post ligation (Figure 7.3 lane 10, 11 & 12). The reason for this problem was the GAD65 fragments which were eluted from the gel after digestion which were contaminated with Exo-nucleases diminishing the sticky ends of the insets and vector and creating a blunt end instead. To avoid this problem, the PCR products were re-purified using cleaning kit and checked aliquots into the agarose gel and used the rest in the digestion and ligation experiments which successfully produce highest number of recombinant plasmids.

The recombinant plasmids pG1 or pG2 successfully expressed GAD65 and showed similarity with GAD65 from pancreatic β-cells, corresponding to 95% for humans and 100% for rat GAD65 for the full length of the GAD65 sequences (1755 bp). The plasmid pG1 showed no mutation and was used to produce GAD65 protein.

Recombinant pG1 encoding full length GAD65 (65 kDa) incorporated with halo-tag protein encoding sequences (32 kDa) to produce the full length protein of GAD65-halo-tag protein (97 kDa). A two expression host system was used in this study, *E. coli* to produce the protein under the promoter T7, and CHO cells to produce protein in mammalian model under the cMVd1 promoter which is suitable for constitutive expression in mammalian cells. Transient transfection was used to express GAD65 in CHO as the plasmid pG1 has no selectable marker for selecting recombinants for permanent production. Therefore, CHO optimisation was performed for transfection ratio (DNA: TR) in order to determine the best conditions for producing a high number of transfectants and subsequently the highest protein concentration.

GAD65 produced from different types of expression host, *E. coli* and CHO, was concentrated to 2.6 and 1.2 mg/ml respectively; however, GAD65 expressed in CHO, not from *E coli*, was used to prepare the GAD antiserum. The reason for this was to avoid any proteins of *E coli* contaminating the preparation which may be introduced during purification steps, which would produce antibody against *E. coli* antigens. This could have subsequently affect the results, as the GAD65 antiserum was used to screen microbial protein samples from different type of microorganisms including *E. coli* and other related species.

The GAD65 protein in both forms 65 and 67 kDa encoding genes have been cloned previously by many studies and protein was produced extensively in

various types of microorganism especial *E. coli* (Huang *et al*., 1990; Yamashita *et al*., 1993; Park and Oh, 2007) as well as fungi and yeast like *S. cerevisiae* (Papakonstantinou *et al.*, 2000).

No complication was indicated in term of protein expression and post translational modification. The animal cells of which the monolayer adherent CHO cells are widely used to express various genes and recombinant proteins. Also, CHO has been used as animal model cells to express the cloned GAD65 gene and GAD65 cDNA to study regulation mammalian expression of pancreatic and brain GAD65 and 67 (Papouchado *et al.*, 1996; Schütt *et al.*, 1997). The studies also referred that expression GAD65 as fusion or tag protein has no effect on GAD65 enzymes catalytic activity or immune activity (Papakonstantinou *et al*., 2000). The current study has reported cloning and expression GAD65 from rat pancreatic cell INS-1 and expressing GAD65 protein into either bacterial host (*E. coli*) or mammalian model (CHO) the GAD65 produced as tag protein (GAD65 + Halo tag sequences) designed for highly purified GAD65 protein. The Halo tag GAD65 provides the ability to produce abundant of GAD65 from transfectants bacterial or mammalian compare to GAD65 purification using GAD65 antibody which has been shown a limited amount produced by this method (Papakonstantinou *et al*., 2000). During this study the GAD65 antiserum was prepared to screen the microbial proteins for GAD molecular mimicries.

The GAD65 protein, halo tag technology was efficiently used, in production GAD65 fusion protein with halo tag protein sequence. Affinity chromatography was used to prepare GAD65 free of the halo-tag. The full length of purified GAD65 antigen protein was used to develop GAD65 polyclonal antiserum.

Chapter 8

Molecular mimicries epitopes between pancreatic antigen GAD65 and *E. coli* proteins

8.1 Introduction

GAD65 is implicated in T1D formation via the development of autoimmunity against GAD65 in humans particularly in the early stages of childhood (Sabbah *et al*., 1996; Petersen *et al*., 1999; Bonifacio *et al*., 2000). Both humeral and T-cell responses are involved and studies suggest microbial infection to be the main initiator of autoimmunity (Abulafia-Lapid *et al.*, 2003; Fujinami *et al.*, 2006). It has been proposed that molecular mimicries between the infections agents (bacteria and viruses) and the β-cell auto antigens are involved (Judkowski *et al.*, 2004; Westall, 2006).

This chapter continues on from work in chapter 7 in trying to identify bacteria with GAD65 molecular mimicries. The GAD65 antiserum prepared previously was used to examine proteins extracted from various types of bacteria and yeasts using a dot blot technique. Cross reacting positive protein samples were separated by SDS-PAGE in duplicate gels, one for blotting and a second was for staining and used to identify the corresponding positive blotted bands. Western blots were screened using GAD65 antiserum. Cross reacting proteins on blots were used to detect corresponding proteins on stained gels.

These proteins were extracted from the gel and analysed by mass spectrometry (MS/MS). The MS data of each protein were used to search the MS database for exact protein identity and accession number. The full length sequences were extracted from the NCBI database and searched for similarity within GAD65 protein sequences to find the linear epitopes between these proteins and GAD65. In addition, the number of identical and positive amino acids between bacterial epitopes and GAD65 protein were recorded and used to select possible epitopes. Such proteins may be classified as environmental factors,

which possibly contribute to the development of diabetes type 1 on the basis of molecular mimicry.

8.1.1 Western blotting coupled proteomic technique

Western blotting is an analytical technique that has been used for the last three decades to recognize certain protein sequences on antigens using specific antibody. The antibodies can recognize these epitopes or components amongst mixtures of biomolecules. In addition western blotting has also been used to identify particular components of protein structure, such as recognizing post translation modifications (Gravel, 2007).

The basic principle of this technique is dependent on separating proteins by SDS-PAGE electrophoresis and then transferring these proteins to nitrocellulose membrane. Transferred protein (s) are detected by antibody and secondary antibody labelled with an enzyme and then a chromogenic substrate is used to detect enzyme activity and hence proteins of interest (Towbin *et al*., 1979).

Recently, recognition of proteins by western blotting has been enhanced by coupling blotting to 2 dimensional (2D) protein gel electrophoresis (Hu *et al*., 2010). Proteins are run firstly into a pH gradient gel until all the proteins reach their PI, at which the protein's net charged will be zero, and proteins will now be separated according to molecular weight. Pieces of gel containing separated proteins are run horizontally into 1D SDS-PAGE. Proteins appear as dots which can be electro-transferred to a membrane and then detected using chemiluminescence or enzyme labelled antibody (O'connor and Hames, 2008). The positive binding of the antibody-antigen can be quantified.

8.1.2 The Proteomic Technique of Mass spectrometry

Mass spectrometry (MS) is one of the analytical techniques which measures the mass/charge ratio of gas phases ion of protein peptide (Sparkman, 2000). The MS principle uses the ionization of chemical compounds to generate fragmented molecules, with particular charges and measures their mass-to-charge ratios. Mass spectrometry is now used in a number of fields, including biochemistry (Siuzdak, 1994), biotechnology (Dalluge, 2000), microbiology (Seng *et al.*, 2010; Welker and Moore, 2011) pharmacology and proteomics / functional genomics (White and Brown, 2004; Rudek *et al.*, 2005).

Recently, matrix assessed laser desorption / ionisation (MALDI) has been developed which uses electrospray ionization by laser. This has made it possible to ionise large thermally label biomolecules and transfer them to the GAS phase without dissociation, with the ability to analyse Mogadishu molecules. This allows determination of the composition of chemical structures, such as proteins and other compounds (Bernot, 2004). Identification of proteins or polypeptides proceeds with their extraction from a gel after 2D separation, followed by digestion with an endo-protease like trypsin, which cuts on the C-terminal side of lysine or arginine to produce a peptide fragment. The mass of each fragment is determined by “MALDI and the digested products are co-crystallized with a solid phase matrix and presented on a metal surface to a laser which adsorbs them and the mass of each peptide is given by its speed of flight towards the detector. The original proteins are identified by comparison with the MS data with protein data taken from a protein database such as NCBI and Swiss Prot, MS can easily distinguish proteins from mixtures of 3 or more from organisms (Bernot, 2004).

8.2 Materials and Methods

8.2.1 Microorganism culture

A total of 45 strains of microorganisms (Table 2.1) were grown in 10 ml aliquots of an appropriate medium as described in Section 2.2.1 with shaking at 120 RPM and cells were harvested and subjected to protein extraction.

8.2.2 Extraction of total proteins

Broth cultures were centrifuged for 3 min at 6000 × *g* and cell pellets were washed with 1ml of PBS and suspended in 2 ml of protein extraction buffer, and total protein was extracted from each culture as described in Section 2.4.1. Protein extracts were quantified by the Bradford method (Section 2.4.2).

8.2.3 Screening microbial proteins using GAD65 antiserum by dot blot

The microbial extracts were screened for immune active proteins that cross-reacted with GAD65 antiserum as described previously in chapter 7. Proteins which cross react allow detection of possible molecular mimicries between microbial proteins and GAD65 antigen. Aliquots of 3-5 µl (20 µg) of total protein extracts from each microorganism were subjected to dot blot (Section 7.2.5.3). The membrane was blocked with blocking solution and then replaced with fresh blocking solution containing GAD65 antiserum (Section 7.2.6) using a dilution of 1:2000 and incubated with gentle shaking for 1.5 h at RT. Next, the membrane was washed 3 times and then exposed to the secondary antibody with peroxidase label (1:6000) with shaking for 1h at RT followed by three washings and developed using DAB/$NiCl_2$ for 20-30 min in the dark and images were taken.

8.2.4 Western blotting

The total protein samples which showed a positive dot blot with anti-GAD65 serum were screened for specific proteins mediating the cross reaction via western blotting. All samples were prepared using 0.5 ml of bacterial lysate (20 µg/µl) mixed with 0.5 ml of SDS-PAGE loading buffer (Appendix 1) in 1.5 ml microcentrifuge tubes. Samples were placed in a boiling water bath for 5 min and then placed at 4 °C for 10 min. Next, samples were centrifuged and aliquots run into SDS-PAGE (Section 2.4.3). Resolving gel (10 %), stacking gel (5 %) and electrophoresis buffer (Appendix 1) were prepared as described by Laemmli (1970) using the original SDS concentration (0.2 %) as well as the loading buffer. Identical protein samples were run into two double gels; one was used for staining and second used for western blotting. The protein samples were loaded into the wells using different volumes of 5, 10, 15 and 20 µl alongside a protein standard marker (C1992, Sigma, UK). After electrophoresis, one gel was stained as described in Section 2.4.3 and the other gel was used to electro-blot the proteins onto a nitrocellulose membrane using the conditions described in Section 2.4.4.

The membrane was blocked in 50 ml of blocking buffer (Appendix 1) with shaking at RT for 1 h. Afterwards, the blocking buffer was replaced with fresh 30 ml of blocking buffer containing GAD65 serum (1:2000) and incubated at RT with gentle shaking for 1.5 h. The blocking buffer was discarded and the membrane was washed using 50 ml of washing buffer (Appendix 1) with shaking for 10 min at RT, repeated for a total of 3 times. Next, the washing buffer was replaced with fresh buffer (50 ml) containing anti-mouse IgG antibody peroxidase labelled (A 9917, Sigma, UK) (1:10000) and incubated at RT with gentle shaking for 1 h. The membrane was then washed as described

before and after last washing step, the washing buffer was replaced by 20 ml of developing buffer DAB $NiCl_2$ (Appendix1) and left in the dark for colour development at RT for 15 min. Afterwards, the reaction mixture was discarded, the membrane was washed with MBW and images captured. The active bands were localized on the membrane and the molecular weight of each band was estimated.

8.2.5 Localization of the GAD65 cross reactive protein on SDS-PAGE gel

The blotted developed membrane was then stained with 20 ml of ponceau S solution (Appendix1) with gentle shaking for 10 min followed with 2-3 washes with 20 ml of DW until clear distinct protein bands appeared. The protein bands were used to detect the reactive bands on the second SDS-PAGE gel (Appendix 1) using band detection software (Quantity one software Bio-Rad, UK). All bands expressing a positive immune reaction with GAD65 serum were identified and excised from gels using a sharp razor. Excised bands were placed in separate 1.5 ml microcentrifuge tubes containing 1ml MBW.

8.2.6 Identification *E. coli* protein bands using mass spectrometry

Protein bands of *E. coli* were identified using MALDI mass spectrometry (MS/MS), at the Proteomics Facility, School of Biochemistry, and University of Bristol. The protein bands were cut into $1mm^2$ pieces and digested with sequencing grade trypsin (Promega, UK) using a ProGest automated digestion system (Digilab Ltd, UK.).

Trypsin was subjected to autolysis, generating fragments that can interfere with protein sequencing, HPLC or mass spectrometry analysis of the peptides. In addition, autolysis can result in the generation of pseudotrypsin, which has been shown to exhibit an additional chymotrypsin-like specificity.

The resulting peptides were analysed by MS and mass spectra were recorded in positive ion mode on an Applied Biosystems 4700 MALDI mass spectrometer. MS spectra were recorded in reflector mode. For MS/MS analysis the top 5 most intense, non-tryptic, precursors were selected for fragmentation by collision induced dissociation. MS and MS/MS data were analysed using GPS Explorer 3.5 software (Applied Biosystems). MS/MS peaks were filtered to exclude peaks with a signal to noise ration less than 35 over a mass range of 50 Da to 20 Da below the precursor mass. The data was analysed using the MASCOT algorithm (Matrix Science) using the NCBI database. A maximum number of missed cleavages of 1 and a charge state of +1 were assumed for precursor ions. A precursor tolerance of 100 ppm and an MS/MS fragment tolerance of 0.15 Da were used in the database search. Routinely, samples were analysed with methionine oxidation considered a variable modification. Protein ID's were determined for the top 20 hits from mass data for each of 5 bands resulting from specific research on the *E. coli* database and other microorganisms to check for contamination. The protein yield or protein score of each band was determined and used as an indicator for the protein recovered from the gel and its purity. The protein accession numbers of each signal band were identified and the full length of the linear sequences was extracted, and the protein molecular weight used to search for the protein ID.

8.2.7 Molecular mimicries prediction between GAD65 and *E. coli* proteins

The immune active proteins of *E. coli* were detected using MS/MS and sequences were identified. The top 20 ID of proteins have been identified by MS data of individual band. The blast-p software from NCBI was used to search for homology between each protein and GAD65 sequences using high similarity parameters. The linear epitopes of each protein were extracted and numbers of

identical residues were identified. Also, the positive amino acids which include the identical residues plus the amino acids belonging to the same amino acid polarity group were determined.

8.3 Results

8.3.1 Screening microorganisms using GAD65 antiserum

The GAD65 antiserum prepared in Section 7.2.6 was used to screen proteins extracted from selected microorganisms using a dot blot analysis. Results showed cross-reactivity with some microbial proteins. A strong dark coloured dot blot was produced with bacterial protein samples of species belong to the *Enterobacteriaceae,* particularly *E. coli*, *Salmonella typhimurium* and *Serratia marcescens* (Figure 8.1). A weaker reaction was seen with proteins extracted from *Klebsiella aerogenes* and *Citrobacter freundii*.

The dot blot reaction colour intensity was quantified and peak densities recorded for individual microbial protein samples. The results showed a strongest reaction with *Aeromonas hydrophila* (500 peak density). The range of peak densities detected amongst the *Enterobacteriaceae* members was 320-450. There was also a strong reaction with *Vibrio anguillarum*. Weak or non-significant reactions were seen with other microorganisms except *Rhizobium spp, P. aeruginosa, and Hafnia alvei.* The yeast strains *Zygosaccharomyces rouxii*, *Schizosaccharomyces octosporus* and *Saccharomyces carlsbergensis* showed significant differences from the control and from other negative protein samples. The quantification measurements of the positive dot blots using the peak density analysis was used as an indicator of antigen antibody binding efficiency.

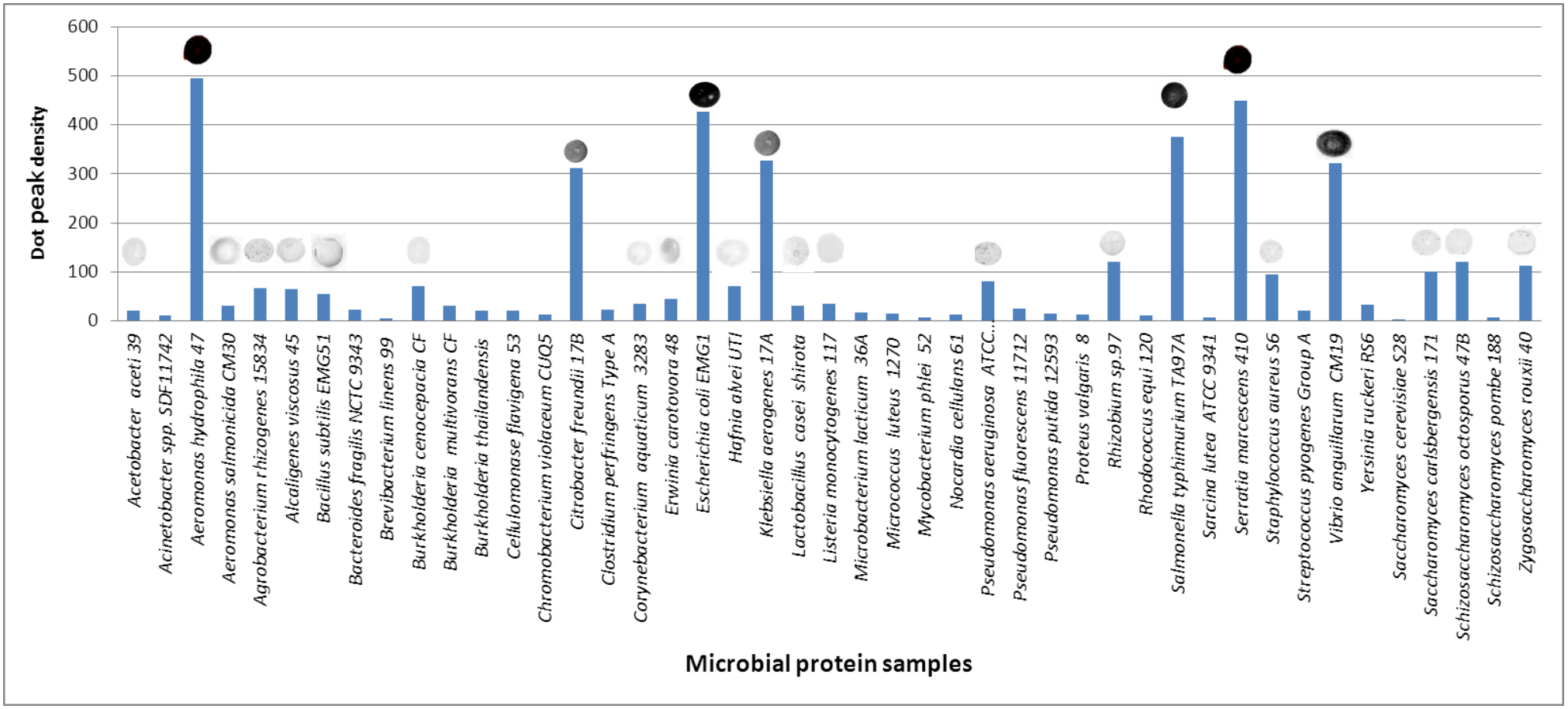

Figure 8.1: Initial screening of microbial protein samples for cross reaction against pancreatic antigen GAD65 antiserum using dot blotting. The values represent the peak density of each dot blot of microbial protein samples.

8.3.2 Western Blotting

Bacterial lysates which expressed a positive dot blot reaction against GAD65 polyclonal antiserum were subjected to western blotting to reveal proteins sharing linear epitopes within pancreatic β-cell antigen GAD65. A strong reaction was detected with protein samples extracted from some bacterial strains such as *E. coli*, *C. freundii, S. typhimurium, K. aerogenes, and S. marcescens* as well as *A. hydrophila and V. anguillarum*. The results showed strong bands of different MW position on the membrane. In the case of *E. coli*, 5 protein bands (B1-B5) were detected with molecular weights of about 55, 40, 36, 22, and 18 kDa, respectively (Figure 8.2). The *E coli* B3 band is appearing to be similar in size other *Enterobacteriaceae* protein bands and band 1 was of a similar size seen in *S. marcescens* and *S. typhimurium.* The protein samples of *A. hydrophila* produced three protein bands with MW ranged (35, 55, 60 kDa) and *V. anguillarum* produce one band of 35 kDa.

Dilutions of *E coli* protein samples were run into gels and western blotting produced consistent results, 5 immune active bands (Figure 8.3) and these immune active bands were easily detected in SDS-PAGE gels and successfully excised, and stored in MBW and prepared for MS/MS identification.

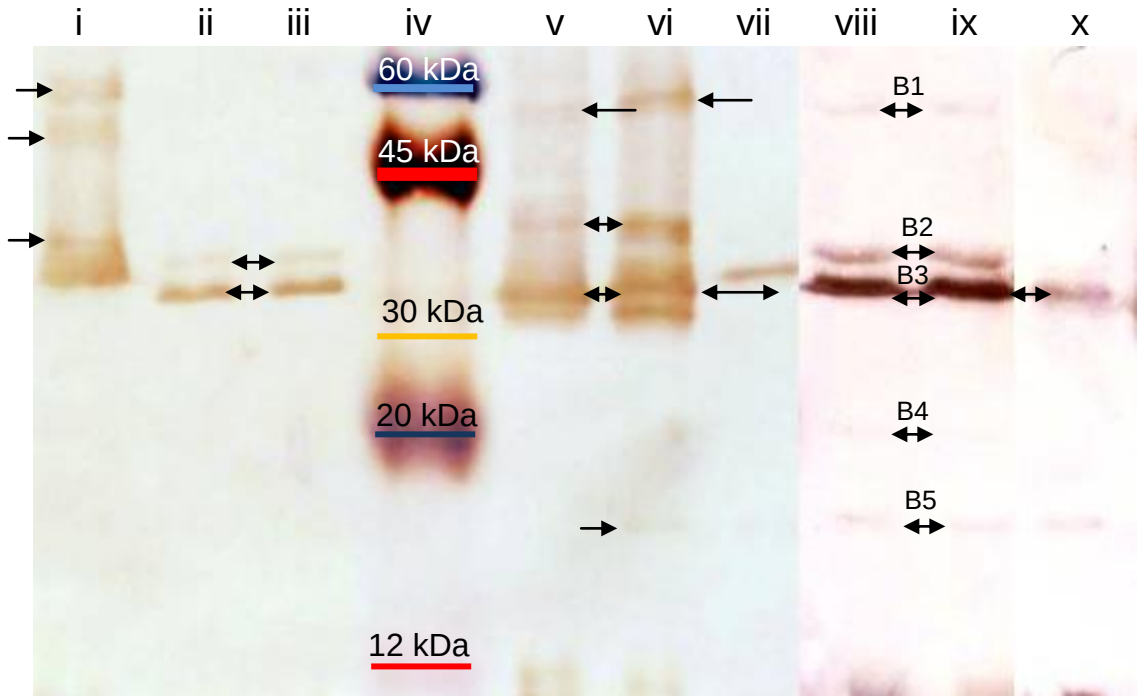

Figure 8.2: Immune blotting of protein samples extracted and screened against GAD65 antiserum. Lane i, represents *A. hydrophila*, *K. aerogenes* (Lane ii & iii), lanes v, vi and vii represent *S. typhimurium, S. marcescens* and *C. freundii* respectively. Protein samples of *E. coli* (lanes viii and ix) and *V. anguillarum* (lane x).

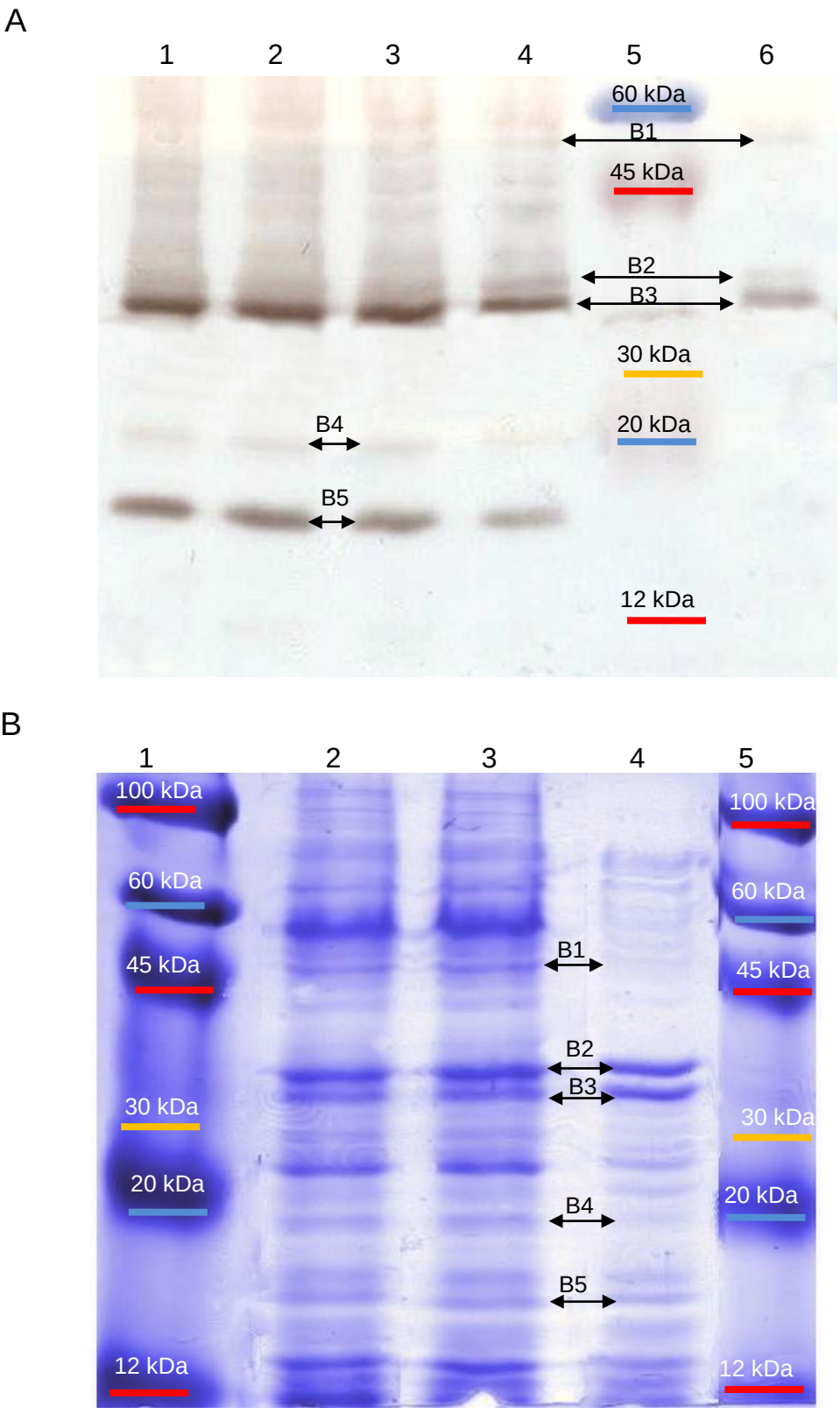

Figure 8.3: Western blotting of *E. coli* protein with GAD65 antiserum (A) using 10 µl loading sample (1,2) and 20 µl (3,4) and 1:5 diluted sample (6). Identifying the immune-active protein bands on SDS-PAGE using 10 & 20 µl of sample and 20 µl of 1:5 diluted samples (lane 2, 3, 4), respectively.

8.3.3 MS/MS Data of *E coli* proteins

Five positive protein bands presenting cross reaction with GAD65 antibody were analysed using MS/MS. One of the most important parameters that should be noted about MS/MS sequence data generated is the ion score value. This number means that the corresponding peptide was run in the MS/MS mode of the mass spec and the resulting amino acid sequence matched the identified protein, the ion score values confirm the protein identity which increases the confidence in the ID. In these searches, any protein with a score > 62 is classed as having a significant identity and obviously the higher the score above this value the more significant the identity matches. All the analysed bands have given significant identity for at least one protein fragments and some contain multiple proteins homologous. In the case of the protein bands which gave more than one significant ID fragment the protein MW determined by western blotting was used to identify the protein. In the case of this study the protein with the highest score and identical MW to a protein band found by western blotting was used to scan for GAD65 linear epitopes. However, the top 20 proteins reported by MS/MS with significant protein identity also expressed significant similarity with putative epitopes similar to the GAD65 protein.

8.3.4 Protein Identities

The ion score and the mass of each peptide resulting from the digestion of band 1 were used to search the database and both parameters revealed high significant protein identity (Table 8.1). According to the western blot, band1 was localized between 60-45 kDa MW of the protein standard markers (Figure 8.2) and the estimated MW was 47.2-50 kDa using band detecting program (Quantity one software Bio-Rad, UK). However, the blast results of mass data of fragment of this band against the *E. coli* data base showed a strong significant

ion score (200) identifying one protein, an outer membrane protein A (OmpA) (Figure 8.4) accession number (AC) gi/ 9120052 of *E. coli* strain UTI89.

The theoretical MW of band2 which was seen on western blotting was about 40 kDa and the MS/MS analysis for the first 20 proteins showed proteins with different MWs (18 - 40 kDa), 19 of which belong to different strains of *E. coli*. The results revealed a high score protein (135) OmpA which was also detected for b1 with having a MW of 40.08 kDa and the same accession number (gi/ 9120052) belonging to *E. coli* strain UTI89. The western blot also showed GAD65 antisera producing immune activity against a protein with an estimated theoretical MW of 35 kDa (b3) Identification of this protein band 3 by MS/MS showed a high protein score (200) with strong similarity to a 33.9 kDa protein from *E. coli* format dehydrogenase (FD) accession number gi/300925913 (Figure 8.4).

The results also showed a cross reacting protein at 22 kDa MW (band 4) by western blotting of *E. coli* proteins. The peptide mass analysis extracted from MS/MS for band 4 showed a high protein score (93) and significant ion score for superoxide dismutase (SD) of *E. coli* IAI39 with 21.3 kDa and protein accession number gi/218699776. Finally, the western blotting of *E. coli* proteins showed a strong reaction with band 5, with a 18 - 20 kDa estimated MW. The MS analysis of protein extracted from band 5 showed protein with high significant a protein and ion score and the top 20 protein showed that the band 5 protein was either a 18.6 kDa DNA starvation protection protein (DspP) or a 22 kDa ferritin –like domain (FLD) protein of *E. coli* protein with accession number gi /91209847 and gi/300816460, respectively and ion score 221.

Table.8.1: The MS/MS data represents the peptide mass of *E. coli* protein fragments for bands (1-5) which can react with GAD65 antiserum.

Peptides Mass	Sequences range	A. A Sequences
Band1 / Outer membrane protein A- gi/ 9120052- ion Score 200		
818.467	142-148	LGGMVWR
1214.6348	346-356	AALIDCLAPDR
1233.6295	142-152	LGGMVWRADTK
1280.6648	280-291	DGSVVVLGYTDR
1370.7394	346-357	AALIDCLAPDRR
1486.7379	106-118	MPYKGDNINGAYK
1654.8334	128-141	LGYPITDDLDIYTR
2232.1848	219-241	FGQGEAAPVVAPAPAPAPEVQTK
2600.4114	256-279	ATLKPEGQAALDQLYSQLSNLDPK
3478.8103	188-218	LEYQWTNNIGDAHTIGTRPDNGMLSLGVSYR
Band2 / Outer membrane protein A- gi/ 9120052- ion Score 135		
818.434	147-153	LGGMVWR
1214.6135	347-357	AALIDCLAPDR
1222.712	307-317	AQSVVDYLISK
1233.6038	147-157	LGGMVWRADTK
1280.6481	281-292	DGSVVVLGYTDR
1370.7003	347-358	AALIDCLAPDRR
1378.7444	306-317	RAQSVVDYLISK
2600.3621	257-280	ATLKPEGQAALDQLYSQLSNLDPK
2601.2979	164-188	NHDTGVSPVFAGGVEYAITPEIATR
Band3 / Format dehydrogenase - gi/300925913- ion Score 200		
829.5217	91-96	LEWLIR
1151.6145	190-199	ESMKTLASER
1357.7317	12-24	SATNSITPPSQVR
1456.7268	284-295	ADEEENNLHEEK
1513.7573	11-24	RSATNSITPPSQVR
1552.705	98-110	DGCMHCSDPGCLK
1664.6648	97-110	kDGCMHCSDPGCLK
Band4 / Superoxide dismutase - gi/218699776 ion Score 93		
859.4906	52-58	SLEEIIR
1294.6244	118-128	NFGSGWTWIVK
1381.6495	1-12	MSFKLPALPYAK
1630.7567	93-108	VAEAIASFGSFADFK
1694.8374	31-44	HHQTYVTNLNNLIK
2014.9225	13-30	DALAPHISAETIEYHYGK
2547.2092	169-189	NARPGYLEHFWALVNWEFVAK
3680.7427	59-92	SSEGGVFNNAAQVNHTFYWNCLAPNAGGEPTGK
3867.0647	134-168	LAIVSTSNAGTPLTTDATPLLTVDVWEHAYYIDYR
Band5 / DNA starvation protection protein - gi /91209847 ion Score 221		
915.5387	28-35	ATVELLNR
924.44	49-55	QAHWNMR
951.5353	11-18	ATNLLYTR
1020.5472	125-133	YAIVANDVR
1043.6222	27-35	KATVELLNR
1148.6332	125-134	YAIVANDVRK
1485.7032	71-83	TALIDHLDTMAER
1517.8641	36-48	QVIQFIDLSLITK
1604.7936	120-133	ELADRYAIVANDAVR
1676.7825	56-70	GANFIAVHEMLDGFR
1692.7747	56-70	GANFIAVHEMLDGFR
1768.847	154-167	DLDKFLWFIESNIE
1932.9041	135-153	AIGEAKDDDTADILTAASR
2263.0864	106-124	SYPLDIHNVQDHLKELADR
2414.3337	28-48	ATVELLNRQVIQFIDLSLITK

Band 1 - Outer membrane protein A (OmpA)

```
   1 mkdltvlsrw ryswrilddn eaqkmkktai aiavalagfa tvaqaapkdn twytgaklgw
  61 sqyhdtgfip nngpthenql gagafggyqv npyvgfemgy dwlgrmpykg dningaykaq
 121 gvqltaklgy pitddldiyt rlggmvwrad tkanvpggas fkdhdtgvsp vfaggveyai
 181 tpeiatrley qwtnnigdah tigtrpdngm lslgvsyrfg qgeaapvvap apapapevqt
 241 khftlksdvl ftfnkatlkp egqaaldqly sqlsnldpkd gsvvvlgytd rigsdaynqa
 301 lserraqsvv dyliskgipa dkisargmge snpvtgntcd nvkqraalid clapdrrvei
 361 evkgikdvvt qpqa
```

Band 2 - Outer membrane protein A (OmpA)

```
  1 msrspvkdlt vlsrwryswr ilddneaqkm kktaiaiava lagfatvaqa apkdntwytg
 61 aklgwsqyhd tgfinnngpt henqlgagaf ggyqvnpyvg femgydwlgr mpykgsveng
121 aykaqgvqlt aklgypitdd ldvytrlggm vwradtksnv ygknhdtgvs pvfaggveya
181 itpeiatrle yqwtnnigda htigtrpdng mlslgvsyrf gqgeaapvva papapapevq
241 tkhftlksdv lftfnkatlk pegqaaldql ysqlsnldpk dgsvvvlgyt drigsdaynq
301 alserraqsv vdyliskgip adkisargmg esnpvtgntc dnvkqraali dclapdrrve
361 ievkgikdvv tqpqa
```

Band 3- Format dehydrogenase (FD)

```
   1 mametqdiik rsatnsitpp sqvrdykaev aklidvstci gckacqvacs ewndirdtvg
  61 nnigvydnpn dlsakswtvm rfseveqndk lewlirkdgc mhcsdpgclk acpaegaiiq
 121 yangivdfqs eqcigcgyci agcpfdiprl npednrvykc tlcvdrvvvg qepacvktcp
 181 tgaihfgtke smktlaserv aelktrgydn aglydpagvg gthvmyvlhh adkpnlyhgl
 241 penpeisetv kfwkgiwkpl aavgfaatfa asifhyvgvg pnradeeenn lheekdeerk
```

Band 4- Superoxide dismutase SD

```
   1 msfklpalpy akDalaphis aetieyhygk hhqtyvtnln nlikgtafeg ksleeiirss
  61 eggvfnnaaq vwnhtfywnc lapnaggept gkvaeaiaas fgsfadfkaq ftdaaiknfg
 121 sgwtwlvkns dgklaivsts nagtplttda tplltvdvwe hayyidyrna rpgylehfwa
 181 lvnwefvakn laa
```

Band 5- DNA starvation / stationary phase protection protein Dps

```
  1 mstaklvksk atnllytrnd vsdsekkatv ellnrqviqf idlslitkqa hwnmrganfi
 61 avhemldgfr talidhldtm aeravqlggv algttqvins ktplksypld ihnvqdhlke
121 ladryaivan dvrkaigeak dddtadilta asrdldkflw fiesnie
```

Figure 8.4: Full length sequences of *E. coli* proteins identified from bands detected by western blotting with GAD65 antiserum and analysed by MS/MS and extracted DATA matched against the *E. coli* Genbank protein database.

8.3.5 *E. coli* Outer membrane protein A (OmpA) bands 1 & 2 show linear epitopes on GAD65

Both bands B1, B2 matched with one protein identity which was OmpA which produced homology to the C-terminal region of GAD65 between GAD65 residues 512-542 producing 10 identical and 17 positive residues (Figure 8.5).

The MS data of *E. coli* protein bands have identified proteins with identical or similar ion score in addition to the actual proteins identified by each band. These proteins expressed not just strong similarity to the protein bands but also produced similarity to the GAD65 protein. The protein of band 2 has been identified as OmpA, however, the peptides Mass data showed similarity to one of the *E. coli* elongation factor (EF) Accession number /NP 289886 which showed 2 epitopes similarity with GAD65 N-terminal sequences occurred on residues 139-153 and 104-117 respectively first one has 6 identical and 10 positive residues, whereas, the second epitopes has 5 identical and 10 positive residues. Third epitopes produce homology to GAD65 C-terminal flanked by residues 530-547 sequence with 7 identical and 10 positive residues.

8.3.6 *E. coli* protein Format Dehydrogenase (FD) band 3 shows linear epitopes on GAD65

The third protein, the beta subunit of FD produced 4 epitopes occurring at residues 317-327, 237-262, 541-565, 451-469 and having 4, 5, 7, and 6 identical and 8,10,11 and 9 positive residues respectively. The results showed a 45.25 kDa phage integrase protein (PIP) in *E. coli* E 22 with protein identification number gi/193063621, with a high ion score (120). Searching for homology between GAD65 and PIP amino acid sequences showed 4 epitopes, three of them occurred at the GAD65 C-terminus. These epitopes were at residues 419 – 452, 444 - 459, 454 - 488 and containing 12, 5 and 10 identical residues and 16, 8 and 16 positive residues, respectively. Whereas, the fourth epitope occurred at the GAD65 N-terminal sequence (residues 93-113) having 8 identical and 11 positive residues. The C- terminal epitopes shared sequence localized at the same region on GAD65 (residues 454-459) between epitope 1 and 2 and shared sequences (444-452) between epitope 1 and 3 (Figure 8.5).

The top 20 blast results of MS data of band 3 also matched with a 19.68 kDa bacteriophage baseplate protein (BB) accession number gi/284920613 and a 20.10 kDa hypothetical protein (HP) No gi/215486150 of *E coli*. The BB blast against GAD65 showed one epitope flanked by residues 105 -131 with strong similarity producing 8 identical residues and the 15 positive residues and the HP showed 4 epitopes produced 9,4,5 & 7 identical with 9,6,8 and 13 positive residues share within GAD65 sequences (Figure 8.5).

i & ii-Outer membrane protein A (OmpA-Band 1 & 2)

```
OmpA    8-SWRILDDNEAQ--KMKKTAIAIAVALAGFAT-36
GAD65 512-SLRVLEDNEERMSRLSKVAPVIKARMMEYGT-542
```

1- Elongation factor (EF)

```
EF    155-RELLSQYDFPGDDTP-169    53-APEEKARGITINTSHVEY-70
GAD65 139-NELLQEYNWELADQP-153   530-APVIKARMMEYGTTMVSY-547

208-DKPFLLPIEDVFSI-221
104-ERPTLAFLQDVMNI-117
```

iii- Formate dehydrogenase protein (FD- Band3) .

```
FD    198-ERVAELKTRGY-208    212-GLYDPAG-VGGTHVMYVLHHADKPNL-236
GAD65 317-RRILEVKQKGF-327    237-GIFSPGGAISNMYAMLIARYKMFPEV-262

221-GTHVMYVLHHADKPNLYHGLPENP-244    248-ETVKFWKGIWKPLAAVGFAA-267
541-GTTMVSYQPLGDKVNFFRMVISNP-565    451-DVFKLWL-MWRAKGTTGFEA-469
```

1- Phage integrase protein (PIP)

```
PIP    24-NGMHLLVHPNGSKYWRLQYRFGGKQKMLALGVYPDV-59
GAD65 419-NQMHASYLFQQDKHYDLSYDTG--DKALQCGRHVDV-452

379-IHKAEHLDERRLMLQW-394 106-HATNKKWSEEHSRRVLKSLED-126
444-LQCGRHVDVFKLWLMW-459  93-HATDLLPACEGERPTLAFLQD-113

100-QLAIEWHATNKKWSEEHSRRVLKSLEDNLFPAIGKR-135
454-KLWLMWRAKGTTGFEAHIDKCLE-LAEYLYNIIKNR-488
```

2- Bactriophage Baseplate (BB)

```
  2-RTIEAMQRQLLGLIGRAVVKSISAATK-28
105-RPTLAFLQDVMNILLQYVVKSFDRSTK-131
```

3- Hypothetical Proteins (HP)

```
69-EQGKVRPMYSLTKDGWIMVVMGFTG-93      67-IDEQGKVRP-75
14-EDGSGDPENPGTARAWCQVAQKFTG-38     304-CDERGKMIP-312

 40-DVLRKIEQVK-49      21-GEVVTTSRKIAKYFGKRHGDVLRKIEQVK-49
314-DLERRILEVK-324    551-GDKVNFFRMVISNPAATHQDIDFLIEEIE-579
```

Figure 8.5: Sequence homology between GAD65 and *E .coli* proteins of bands 1,2 & 3 by western blotting and identified by MS. The dark grey shadowed residues are identical and the faint grey ones are positive residues.

8.3.7 *E. coli* protein Superoxide Dismutase (SD) band4 shows linear epitopes on GAD65

The blast results between SD (band4) and GAD65 sequences showed 4 epitopes, The first epitope expressed homology with residues at 326-362, 529 - 540, 269-283, and 8-20 on GAD65, containing 10, 6, 5, and 3 identical and 16, 8, 8, and 8 positive residues. The analysis showed two 36 kDa proteins accession number gi/73854244 of *E. coli* transposase (TR), both of which showed homology to GAD65 occurring at residues 470-481 with 6 identical and 8 positive residues (Figure 8.6).

The results also showed homology with a 27 kDa small terminase subunit (ST) of *E. coli* accession number gi/293417396 expressing three epitopes at residues 204-210, 521-535 and 300-330 with 5, 7, 5 identical, 6, 9 and 15 positive residues, respectively.

The band 4 results also showed proteins with non-significant protein scores with MW 47, 50, 50.4, 51 and 52 kDa. Amongst these proteins a biotin carboxylase (BC), protein accession number gi / 9257125 laid epitopes with homology to GAD65 between residues 12-76 with 20 identical, 29 positive and two gaps. However, these proteins produce long strong epitopes rich glycine, alanine and aspartic acid residues. Furthermore, a protein of 47 kDa related to *E. coli* trigger factor (TF), protein ID/gi-91209509 showed two epitopes, one strong epitope occurred at residues 11-17 of GAD65 with 6 identical residues and the second epitope occurred at residues 293-343 with 14 identical and 19 positive residues (Figure 8.6).

iv- Superoxide Dismutase (SD- Band 4)

```
    SD 132-GKLAIVSTSNAGTPLTTDATPLLTV--------DVWEH-161  15-LAPHISAETIEY-26   150-ATPLLTVDVWEHAYY-164
GAD65 326-GFVPFLVSATAGTTVYGAFDPLLAVADICKKYKIWMH-362 529-VAPVIKARMMEY-540  269-AVPRLIAFTSEHSHF-283

  77-YWNCLAPNAGGEP-89
   8-FWSFGSEDGSGDP-20
```

1-Transposase (TR)

```
    TR 239-HEDKLMTIAERL-250
 GAD65 470-HIDKCLELAEYL-481
```

2- Small terminase subunit (ST)

```
   ST 125-MFTEEVA-131 207-ERLERELKPKPELKA-221  34-MLVKLAADQRTLKAIYSKELKAAKKRELLPF-64
GAD65 204-MFTYEIA-210 521-ERMSRLSKVAPVIKA-535 300-ILIKCDERGKMIPSDLERRILEVKQKGFVPF-330
```

3- Biotin carboxylase (BC)

```
   BC 136 GSDGPLGDDMDKNRAIAKRIGYPVIIKASGGGGGRGMRVVRGD----AELAQSISMTRAEAKAAFSND-199
GAD65  12 GSEDGSGDPENPGTA---RAWCQVAQKFTGGIGNKLCALLYGDSEKPAESGGSVTSRAATRKVACTCD-76
```

4-Triggers factor (TF)

```
  TF 262-FGVEDGS-269  210-GLGRRVTITIAADSIETAVKSELVNVAKKVRIDGFRKGKVPMNIVAQRYGA-260
GAD65 11- FGSEDGS-17   293-GIGTDSVILIKCDERGKMIPSDLERRILEVKQKGFVPFLVSATAGTTVYGA-343
```

Figure 8.6: Sequence homology between GAD65 and *E .coli* proteins produced by band 4 of western blotting and identified by MS. The bold shadowed residues are identical and the greys are positive residue.

8.3.8 *E. coli* DNA Starvation protection Protein (DspP) band5 shows linear epitopes on GAD65

The fifth protein band showed homology with the DNA starvation protection protein with 1 epitope having two homologous regions with GAD65 at residues 174-183 and 497-510 with 5 & 5 identical residues and 6 and 6 positive residues respectively (Figure 8.7). Interestingly, the band 5 results showed in addition to the DpsP protein, a 2 kDa, hypothetical protein (HP) of *E. coli* with 15 residues produced putative epitopes at residues 215-223 and 431-436 on GAD65, both with 4 identical, and 8 and 5 positive residues respectively. The HP protein has 15 residues of which 12 residues (80%) showed homology to the GAD65 sequences.

The results also detected a protein with the threshold protein score of 60. This protein is the 35 kDa L-arabinose transporter subunit (ATR) with protein ID/gi-194430431 of *E. coli*. It produced epitopes that covered extended regions of GAD65 at N, middle and C –terminal regions. A Blast of ATR against GAD65 detected two epitopes, one at residues 20-82 having 17 identical and 25 positives and another at residues 335-363 with 8 identical and 13 positives (Figure 8.7). The blast also showed 5 small potential neighbouring epitopes occurring at residues 500-509, 381-392, 364-381, 164-179, 138-152 and have shown 4, 3, 4, 7 and 5 identical and 5, 8, 8, 8 and 8 positive residues respectively.

v- DNA starvation protection protein (Band5 / DspP)

```
  DPS 223-GAPYYTNAVS-232  223-GAPYYTNAVSQVTP-236
GAD65 174-GHPRYFNQLS-183  497-GKPQHTNVCFWFVP-510
```

2- Hypothetical protein (HP)

```
     HP 3-LLQFIGMKK-11     10-KKYNLS-15
GAD65 215-LLEYVTLKK-223   431-KHYDLS-436
```

3- Arabinose transporter subunit (ATR)

```
  ATR  35-PEEPWFQTEW-KFADKAGKDLGFEVIKIAVPDGEKTLNAIDSLAASGAKGFVICTPDPKLGSA-96   197-TKSNDIPGAFDAANSMLVQHPEVKHWLIV-225
 GAD65 20-PENPGTARAWCQVAQKFTGGIGNKLCALLYGDSEKPAESGGSVTSRAATRKVACTCDQKPCSC-82   335-TAGTTVYGAFDPLLAVADICKKYKIWMHV-363

ATR   215-QHPEVKHWLI-224 253-INGVDAVSELS-264 229-DSTVLGGVRATEGQGFK-246   1-QTEWKFADKAGKDLGF-56   35-PEEPWFQTEWKFADK-49
GAD65 500-QHTNVCFWFV-509 381-LNGVERANSVT-392 364-DAAWGGGLLMSRKHKWK-381 164-QTTLKYAIKTGHPRYF-179 138-PNELLQEYNWELADQ-152
```

Figure 8.7: Sequence homology between GAD65 and *E .coli* proteins produced by band 5 of western blotting and identified by MS. The bold shadowed residues are identical and the greys are positive residues.

8.4 Discussion

GAD65 and insulin are the major pancreatic antigens which have been targeted by the autoimmune response in T1D, compared to other pancreatic antigens (Leslie *et al.*, 1999). T1D is currently associated with autoantibodies (Al-Bukhari *et al.*, 2002) and a T-cell autoimmune responses (Honeyman *et al.*, 1998), however, the GAD autoimmunity is attributed to autoantibodies created by environmental or non-genetic factors, besides the genetic predisposition on HLA genes which were classified for a long time as the main cause of this disease. Microorganisms, food protein toxins and viral infections (Stene *et al.*, 2010) are considered possible diabetogenic environmental factors (MacFarlane *et al.*, 2003; Goldberg and Krause, 2009). It would seem that both genetic and environmental factors contribute to the diabetic immunology response against particular pancreatic β-cell autoantigens.

Immunological studies have used sera from diabetes patients with GAD autoantibodies for determining epitopes which are targeted during development of T1D and whether they are aimed at the N-terminal, C-terminal or middle of the GAD65 back bone. Using various techniques, it's also possible to distinguish conformational and linear epitopes and which of them are more associated with T1D. For example, the phage display (PD) or peptide library techniques by which epitope fragments (9 -20 aa) of the GAD65 protein are produced and then screened against GAD65 antisera derived from the blood of T1D patients (Myers *et al.*, 2000). Linear epitopes were studied by producing GAD65 peptides (80-100 aa) as fusion proteins, which were purified and assayed for immune activity by ELISA or western blotting, using monoclonal antibodies specific to those regions (Fenalti and Rowley, 2008).

In the case of the present study the experiment was designed to use the full length GAD65 sequence to produce anti-serum instead of developing antibody against particular sequences, in order to make sure that all the GAD65 motifs (N, C and M) were involved. Moreover, the current study is the first to look specifically for GAD65 molecular mimicries in a range of microorganisms other than viruses by developing a polyclonal antiserum to search for molecular epitopes in bacteria which may be triggers for production of GAD65 autoantibodies in T1D.

The GAD65 antiserum was developed and used for screening total protein samples extracted from 45 strains of microorganisms during this study. The GAD65 serum was used in dot blots to find microorganisms whose protein could cross react with the GAD65 antibodies. The dot blot technique was used initially because this technique can quickly screen large numbers of microorganisms, identifying cross reacting of microorganisms which could then be analysed by western blotting to identify specific proteins which reacted with the GAD65 antibody.

The initial assay produced strong reactions with the GAD65 serum compared to the control pre-immune serum suggesting that the animal used had no previous immune response against any of the microbes tested. The GAD65 antiserum produced strong reactions against protein samples from the *Enterobacteriaceae* (*E. coli*, *Salmonella*, *Klebsiella*, *Citrobacter* and *Serratia*). Initially, it was thought that this result is might be attributed to the fact that these microbes have their own GAD enzymes which may share epitopes with human GAD65 such as the PLP binding domain (Myers *et al.*, 2000). However, this study has also looked for possible similarity between GAD65 from microbes and GAD65 from humans, using high similarly blast and identified many epitopes in *E. coli*, *Streptococcus,*

Protease and *Aspergillus niger* which only express a weak degree of similarity. Moreover, many studies have tried to identify sequence homology between pancreatic GAD65 and GAD65 from *E. coli* by testing diabetic and control sera with *E. coli* GAD65, using GAD65 solid phase ELISA and immunoblotting, which concluded no basis for cross-reactivity between the two antigens, and antibody reactivity to GAD65 in man, subsequently cannot arise from cross-reactivity to the *E. coli* GAD enzyme (Konidaris *et al.*, 2003).

However, the cross reaction of GAD65 antisera with proteins extracted from *Enterobacteriaceae* members is very interesting as many studies suggest that the autoimmune diabetes in T1D and in some cases of T2D, is linked extensively to the autoimmune response generated by gut invasive pathogenic bacteria and viral infection. Furthermore, the role of the bacterial microflora is also important in the induction of gut tolerance which protects against invading bacteria like *E. coli* by inducing systemic immunity (Dahlgren *et al.*, 1991; Delzenne and Cani, 2011; Giongo *et al.*, 2011). Some probiotics/ bacteria can stimulate antigen tolerance instead which reduces the diabetic autoimmunity via decrease intestinal inflammation (Majamaa and Isolauri, 1997; Vaarala, 2000; Yazdchi-Marandi *et al.*, 2000).

Studies have reported recently after screening data of T1D children that the collection of unhealthy microbial flora and pathogenic *Enterobacteriaceae* can cause disorders to the intestinal barrier, or a ‘leaky gut’, producing a specific immune response against GAD65 and other pancreatic antigens like insulin and PTP, which ultimately may result in pancreatic β-cell destruction (Neu *et al.*, 2010; Hasham and Tomer, 2011). Moreover, a study has shown that T1D in children results from losing the balance of digestion system bacteria while healthy children all had very similar microbial mixes. The diabetic children all

had erratic combinations with less overall variety which can lead to some entering the blood stream and induce the destructive, diabetic autoimmune response (Mshvildadze and Neu, 2010; Gebel, 2011).

The GAD65 western blotting results showed various patterns of reaction within *Enterobacteriaceae* members, however, *E. coli* produced the highest expressed and the highest number of bands (Figure.8.2) compared to the other species. However, the *Enterobacteriaceae* members pattern is very similar to the *E. coli,* this may be because these species are genetically and functionally similar. However, the western blotting against *V. anguillarum* and *A. hydrophila* produced different patterns and they belong to different families, *Vibrionaceae* (Dworkin and Falkow, 2006) and *Aeromonadaceae* (Aberoum and Jooyandeh 2010; Martino *et al.*, 2011) respectively.

The MS/MS was used to identify the *E. coli* protein bands that cross reacted with GAD65 antiserum. The results expressed high protein scores (up to 200) for all tested proteins which raised confidence of protein identification. The peptides which resulted from trypsin proteolysis were produced significant numbers and collectively their mass matched particular proteins of *E coli* mass as well as mass results (Bernot, 2004; Fagerquist *et al.*, 2009) the ion score of each protein significantly increased the probability of protein identity. Both ion score and peptide mass can exactly match peptide finger prints and subsequent sequences of individual peptides can confirm ID. The Mass spectra data were searched using Muscat software for identifying proteins in *E. coli* to confirm protein identity. The protein ID of the highest protein scores and an ion score of the top 20 proteins have been used to consider the individual protein bands identity.

The full length protein sequences extracted and the MW of each protein was confirmed to identify protein bands in western blotting. However, recently the MS protocol has been applied to protein separated in 2 D gel SDS-PAGE which involves the separation of the interested protein according to their PI values in horizontal electrophoresis followed by vertical electrophoresis into SDS-Page which produces proteins separated as dots which can be blotted separated from each other (Bernot, 2004; O'connor and Hames, 2008).

The full length of proteins identified from *E coli* which cross reacted with GAD65 serum were Outer membrane protein A (OmpA), Format Dehydrogenase (FD) Superoxide Dismutase (SD) and DNA starvation protection protein DspP (Figure 8.4) and these sequences were used to search for GAD65 molecular mimicries. The results identified epitope homologies mostly with middle and C terminal regions of GAD65. However, the epitopes with homology to the GAD65 C-terminal sequences were more spread compared to those that occurred in the middle region (Figure 8.5). All proteins that produced homology to the GAD65 C-terminal sequences occurred in within residues 419-565.

Some studies which used anti GAD65 antiserum from T1D patients against GAD65 regions presented by phage display technique reported that the autoimmune response against GAD65 in T1D is targeted at all regions on GAD65 (N, M, C-terminal), whereas, other studies particularly those that used GAD65 auto antibodies in most cases from T1D and during T2D mediating T1D and LADA diseases have targeted M, and C regions (Falorni *et al.*, 2000) of GAD65 & 67 and limited antibodies detected against the N-terminal (Hampe *et al.*, 2002; Maioli *et al.*, 2004).

Moreover, high affinity antibodies against epitopes located in the M, C regions occurring at aa sequences 96-444 and 445-585 respectively of GAD65 65 were

frequently found in multiple islet autoantibodies from children in early childhood (Bonifacio *et al.*, 2000; Mayr *et al.*, 2007). Studies have specified those GAD65 C-terminal sequences present at residues 404-585 and central or middle aa sequences 240-444 contain conformational epitopes that are targeted by antibodies, are frequently reported in individuals with high risk of developing in T1D (Daw and Powers, 1995; Falorni *et al.*, 1996; Syren *et al.*, 1996).

Whereas, the linear epitopes are also found on C & N –terminals occurring at aa on sequences 11-44 (Butler *et al.*, 1993; Kim *et al.*, 1994; Daw *et al.*, 1996).

Furthermore, studies which predicted the confirmation epitopes of GAD65 using fragments of GAD65 and immune-competition studies showed that the majority of GAD65 autoantibodies are directed against conformational epitopes and occurred on different regions of M & C terminals (Mauch *et al.*, 1993; Richter *et al.*, 1993). It was also found that a limited number of these autoantibodies can bind those discontinuous epitopes or the conformational epitopes after heating and SDS denaturation (Baekkeskov *et al.*, 1990; Tuomi *et al.*, 1994).

In the case of the current study the cross reacting proteins showed homology to GAD65 at the C terminal and M regions may be considered as inducers for antibodies against GAD65 during immune responses that results from *Enterobacteriaceae* or *E. coli* intestinal infection (Mulder, 2005). Antibodies against *E. coli* epitopes may cross react within GAD65 auto-antigens particularly in individuals suffering genetic predisposition of HLA gene (DR4-DQ8 & DR3-DQ2) in early childhood which then lead to subsequent autoimmune response against actual GAD65 antigens on pancreatic β-cells.

It is reported that autoimmune response inducers in T1D, in individuals with genetic disorders are still not known (Lernmark, 2011), and this study suggested that microbial epitopes might play an important role as inducers in

addition to many environmental factors that have been recently proposed to be autoimmune response creators or guides.

The current study results also showed that the MS /MS data of *E coli* bands 3, 4, 5 have matched proteins with significant ID in addition to the proteins which have been identified (FD, SD & DpsP proteins) of individual bands. However, proteins like PIP, HP, of band 3 and ST of band 4 and HP, ATR of band 5 have also expressed strong homology after blast of their sequences against GAD65, but they have different MW from the actual bands. All those secondary proteins have shown a strong similarity to the GAD65 mainly at the C terminal which agrees with what has been reported previously. Furthermore, some proteins have epitopes to the middle sequences, whereas, many of the proteins have N-terminal epitopes, in addition to epitopes seen at the C and M regions (Table 8.2). Some epitopes of these proteins hit more than one region on GAD65 for example protein HP, ATR and PIP (Figure 8.7). This result revealed that the MS/MS technique is a powerful technique whose data can be used in autoimmunity research to find the molecular mimicries between host antigens and the peptides from microbes. This study hypothesised for the first time a possible application for MS/MS in autoimmunity particularly in molecular mimicry field, in which MS/MS data of particular antigen can be used to search for molecular mimicries in microorganisms. In this case the homology will depend on charges and peptide mass instead of using the amino acid sequences as the only parameter in searching for homology.

The current study also reported that some proteins produced a new type of epitope in addition to the previously report homologies between *E. coli* proteins and GAD65 with up to 80% similarity (Table 8.2). Proteins like PIP has 4 linear epitopes within GAD65, and has 3 separate epitopes sharing homology to the

same sequence on GAD65. The PIP epitopes has homology to the GAD65 at residues 444-459 which shared homology with epitopes at residues 444-452 and 454-459 respectively (Figure 8.8 B). These types of homology may explain the increase in the number of antigen epitopes which are possessed by one microbial peptide in diminished immune tolerance to self-antigens.

On the other hand, blast results also showed a single epitope of a protein of *E. coli* showing the same degree of similarity or homology appeared in different positions on linear GAD65 protein sequences and this was seen consistently in all protein bands. All of them have shown a similarity to more than one region on the GAD65 (Figure 8.8 A). Those types of epitopes may play a role in bringing about an autoimmune response against large sequences of GAD65 antigen achieved by a single epitope of *E. coli* protein. Both types of microbial epitopes may explain the autoimmune response that is seen against GAD65 protein. Previous, studies on autoimmunity suggested a cryptic mechanism by which the autoimmune response is created in autoimmune disease and reasoned that microbial proteins do not have enough similarity to create response on the basis of molecular mimicry. But this might now change. These epitopes can be presented by the MHC-II molecules of macrophages or the dendritic cells to the T- cell CD4 initiating the B-lymphocytes to produce antibodies cross reacting with GAD65 and subsequently β-cells destruction.

Table 8.2: The homology between *E coli* protein bands identified by MS/MS and GAD65 sequences including the number of identical and positive residues and sequence position on GAD65 sequence.

Protein	Band	Epitopes No	Position on GAD65	Identical AA	Positive AA & Max Similarity %	
1-OmpA	**B1**	**1**	**C-512-542**	**10**	**16**	**53%**
2-OmpA	**B2**	**1**	**C-512-542**	**10**	**16**	**53%**
3-EF	B2	3	N-139-153	6	10	41%
			N-104-117	5	10	41%
			C-530-547	7	10	41%
4-FD	**B3**	**4**	**C-451-469**	**6**	**9**	**47%**
			M-317-327	**4**	**8**	**80%**
			C-541-565	**7**	**11**	**73%**
			M-237-262	**5**	**10**	**40%**
5-PIP	B3	4	C-444-459	5	8	53%
			C-454-488	10	16	67%
			C-419-452	12	16	48%
			N-93-113	8	11	55%
6-HP	B3	4	N-14-38	9	9	37%
			M-304-312	4	6	75%
			M-314-324	5	8	80%
			C-551-579	7	13	45%
7-BB	B3	1	N-105-131	8	15	58%
8-SD	**B4**	**4**	**M-326-362**	**10**	**16**	**44%**
			C-529-540	**6**	**8**	**72%**
			M-269-283	**5**	**8**	**57%**
			N-8-20	**3**	**8**	**67%**
9-TR	B4	1	C-470-481	6	8	72%
10-ST	B4	3	C-521-535	7	9	64%
			M-204-210	5	6	85%
			M-300-330	5	15	50%
11-BC	B4	1	N-12-76	20	29	45%
12-TF)	B4	2	N-1-17	6	6	35%
			M-293-343	14	19	38%
13-DspP	**B5**	**2**	**C-497-510**	**5**	**6**	**46%**
			N-174-183	**5**	**6**	**67%**
14-HP	B5	2	M-215-223	4	8	89%
			C-431-436	4	5	83%
15-ATR	B5	6	N-20-82	17	25	40%
			N-138-152	5	8	53%
			N-164-179	7	8	50%
			C-335-380	12	21	47%
			C-381-392	3	8	67%
			C-500-509	4	5	56%

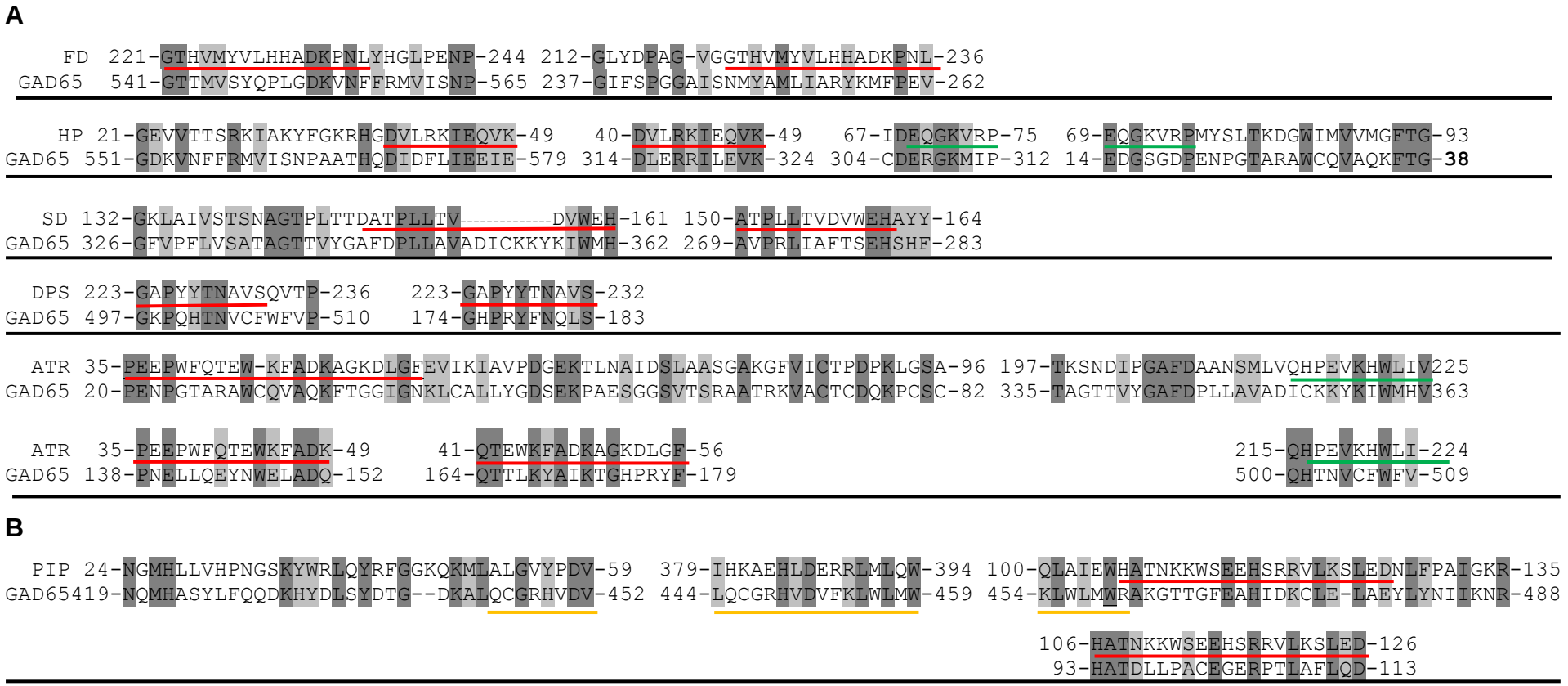

Figure 8.8: Sequences homology between GAD65 and *E. coli* proteins shows the homology between one single epitope (under line red and green) to multiple epitopes on GAD65 (A). The homology of multiple epitopes of *E. coli* protein to same and different epitopes on GAD65 (under line orange) sequences (B).

Chapter 9
General Discussion

General Discussion

The development of diabetes is a complex process which is dependent on genetic susceptibility and environmental factors. One of the possible environmental factors which contribute to the formation of diabetes is the exposure to certain microorganisms or their products (Tisch and McDevitt, 1996; MacFarlane *et al.*, 2003; Biros *et al.*, 2005).

This was the first study that was designed to look for and identify a number of possible direct interactions between microorganisms and the insulin pathway, (the production of insulin and interaction of insulin with host components) which could possibly contribute to the formation of diabetes.

In this study initially three lines of investigation which looked at the interaction of microbes with the insulin pathway were undertaken. Firstly, the toxicity of certain microbial products (secondary metabolites) to β-cells was tested. Secondly, the ability of microbes to bind insulin was surveyed with the view that any microbial insulin receptors which showed molecular mimicry with HIR may be able to induce an autoimmune response to HIR and / or to insulin bound to the microbial receptor. Thirdly, GAD has been recognised as a major pancreatic autoantigen, so a search was undertaken to find microbial proteins with molecular mimicry with mammalian GAD. Any of these 3 processes could possibly contribute to the formation of diabetes.

It was envisaged that at least one of these 3 lines of investigation would be fruitful and possibly form the main line of research for the thesis. However, each of the initial 3 area's of research proved productive and individually any of the 3 area's could have formed the basis for the thesis. A decision had to be made as to the direction of the rest of the thesis and it was decided to persist with each of the 3 lines of investigation, allowing the initial ground work to be done for

each of the 3 lines of research. Moreover, the remit before research was started was to investigate the interaction of microbes with the insulin pathway and this was seen to include all possible ways.

Furthermore, it became evident that the microbes that infect individuals with CF may be involved in the development of CFRD and possibly other forms of diabetes. It was known from the literature that certain microbial products (secondary metabolites) can specifically interact with the insulin pathway leading either to enhanced insulin production or diabetogenic toxicity to pancreatic beta cells. The first part of the research looked at the effect of secondary metabolites, phenazine & pyrrolnitrin, produced extensively by the major infectants of CF patients, *Burkholderi*a spp. and *Pseudomonas aeruginosa* for cytotoxicity to β-cells and modulation of the insulin pathway. Moreover, the extracellular products (supernatants) produced by both microorganisms were used to contribute to the cytotoxicity of the β-cells.

About 90% of CF suffers develop CFRD. CF patients are exposed to relatively high concentrations of phenazine and/or pyrrolnitrin during infection of the lungs causing toxicity to the lung epithelial cells. Both bacteria produce these compounds into the bloodstream which may contribute to pancreatic β-cell death. It would be useful in the future to measure the concentration of each compound in the blood and pancreas and determine whether these compounds are metabolized by the liver. Moreover, the nature by which INS-1 cell death by these compounds needs investigating as to whether it is by triggering apoptosis signals or more likely through necrosis caused by ROS.

This work also showed that these compounds interacted with beta cells to affect insulin transcription and secretion, modulating the insulin pathway. Patch clamping studies, investigating insulin gene expression and secretion,

transcription factors and Ca^{2+} concentration confirmed the direct regulation of the GSIS pathway by these compounds via specific regulation of glucose metabolism. But it would be better in the future to do a time course exposure for measuring Ca^{2+} content and electrophysiology to verify the time taken for whole GSIS induction.

In this study it was hypothesised that increased Ca^{2+} concentration, elevated insulin gene expression and secretion, but it will be useful to draw a link between calcium influx and insulin gene expression and secretion by blocking calcium influx with chelators or other reagents and by determining if calcium influx alone can mimic the effect of the compounds. To start to answer these questions the CamK4 & CaKK1 gene expression was studied because those genes products regulate insulin gene expression in response to increase intracellular Ca^{2+}.

Furthermore, monitoring transcription factors, GT-2, GK, CamK4, and CaKK1 gene expression requires confirmation with assays such as ELISA and western blotting to confirm the results at the protein expression level. However, the up regulation of those genes did indicate that the microbial compounds modulated signals of the GSIS pathway and glucose metabolism. In the future DNA microarray analysis of gene expression of the GSIS pathway in response to phenazine and pyrrolnitrin exposure could be done, to confirm whether these compounds can directly affect GSIS because of their redox activity. Alternatively, they may modulate via an as yet cryptic mechanism which might reveal a new way of regulating the insulin pathway and may provide a new target for treatment in future by using these compounds or derived compounds.

The second line of investigation revealed that insulin bound to *Burkholderia* sp and *A. salmonicida.* In the case of *Burkholderia* sp. it was hypothesised that the

molecular mimicry between IBPs and HIR might contribute to the development of CFRD by initiating antibody production against IBP during *Burkholderia* infection. These antibodies might cross-react with the HIR according to the homology of sequences within the IBP(s) and subsequently lead to insulin resistance or even the production of insulin antibody. A study could be done in the future to test all species of *Burkholderia* for insulin binding capacity.

This was the first time that an insulin binding activity was found for the fish pathogen *A. salmonicida.* The vast majority of insulin binding to this bacterium appears to be via the A layer, however, this study also detected insulin binding in the A-layer mutant strain MT004, revealing that more than protein or component mediated insulin binding. The ability of *A. salmonicida* to bind insulin requires more research to identify the components and mechanisms involved. Furthermore, the binding between insulin and the A-layer could be useful as an application in the purification of insulin, and for quantifying insulin.

The insulin that bound onto *Burkholderia* cells was confirmed as binding to a protein and not any other components by using western ligand blotting, in which many protocols were applied to optimise the protein preparation, blotting and binding conditions.

The construction of a gene library of *Burkholderia* facilitated the cloning and sequence analysis of genes for two types of insulin binding components, the siderophore receptor (IBP1) and the peptide transporter membrane and periplasmic components, IBP3 and IBP2 respectively. The IBP(s) genes require more functional studies to confirm the insulin binding mechanisms that have been proposed by this study. There are many techniques which would be useful such as PCR cloning to express them and confirm the binding, gene silencing using RNA interference (iRNA), gene knockouts or blocking the binding site

using specific antibodies, and in-vitro transcription and translation and MS/MS analysis.

The homology between the HIR and the *Burkholderia sp.* IBP(s) appeared at different epitopes, however, the sequence homology requires further immunological studies to confirm their immunogenicity in initiating an autoimmune response. For the antibodies to cross react, a phage display technique using HIR epitopes could be used to present those sequences and see if a cross - reaction does occur within antibodies raised against the IBP(s) of *Burkholderia spp*. In case of T-cells mediating immune responses it remains to be seen if it is possible to present the IBP(s) epitopes by the APC and macrophages (Martin and Mohr, 2000) to the immune system's cytotoxic T-cells because *B. multivorans* can be an intracellular pathogen, in addition to it's extracellular invasion mode. Therefore, *Burkholderia* bacteria can live inside the lung epithelial cells and APC like macrophages will present the IBP(s) epitopes via MHC-I to the cytotoxic T-cell possibly leading to pancreatic β-cell damage. Moreover, the macrophage could present those epitopes via MHC-II molecules to the CD4 helper T-cell, which plays a main role in immune response (Goldsby *et al.*, 2000; Kindt *et al.*, 2007). The second scenario hypothesised that may occur is that the insulin bound on the *Burkholderia* cell may be presented as a foreign antigen. Either scenario could produce a diabetic autoimmune response, particularly in immune compromise individuals like CF suffers. In order to verify this hypothesis, fluorescent microscopy and cytofluorometry could be used. Fluorescent labelled insulin hormone would first be bound to *Burkhoderia* bacteria and then the techniques would monitor the passing of the fluorescent labelled insulin signal to the macrophages, which will be produced inside or on

the cell membrane of the macrophages. For immunological confirmation animal models for CFRD may be useful to diabetes research.

The third line of investigation searched for pancreatic antigen GAD65 antigen homology in protein samples from a range of microorganisms using anti-GAD65 antibody. GAD sequence homology in microbial proteins may instigate antibodies which can cross react with the β-cell GAD65 causing β-cell destruction and subsequent development of T1D in genetically predisposed individuals, including children. Identification of the microbial proteins that can cross react with the anti-GAD65 antibody was the main aim of this research.

A number of microorganisms showed cross reaction with the anti-GAD65 antiserum and of these *E. coli* was chosen to investigate further. Molecular mimicry between GAD65 and *E. coli* proteins was detected. Strong sequence homology was found between microbial proteins and GAD65 particularly proteins like PIP and SD. However, the main finding which is unique to the present study is that all the *E. coli* proteins which cross-reacted with anti-GAD65 antiserum possessed single or multiple epitopes whose sequence homology could be detected within multiple epitopes on the GAD65 sequence. These results could explain how molecular mimicry works between the microorganisms and the pancreatic antigens. The microbial epitopes expressed a strong homology to the GAD65 epitopes; however, their immunogenicity and ability to create antibodies that can cross react needs further studies. *E coli* were studied amongst strains which showed strong reaction with GAD antiserum because *E coli* is a prevalent strain within the human gut microflora compared to other positive bacterial species tested. However, in the future all of these species should be analysed in order to extend the knowledge about the possible types of proteins which could be diabetogenic. The *E coli* proteins that

were hypothesised to create an autoimmune cross reaction require more confirmation and this might be achieved by creating a phage display assay of GAD65 epitopes (conformational & linear) and subjecting them to cross reaction with antibody created against microbial epitopes. Moreover, the GAD65 molecular mimicries need to be tested for immunogenicity presentation by T-cells from genetically susceptible T1D patients whose HLA genes are predisposed, and see if they possess the ability to direct the immune response against self-antigens. However, those epitopes must also be tested for antibody autoimmunity by immunizing the T1D model NOD mice and see whether they will initiate an autoantibody which reacts with their own GAD65.

This is the first study designed to look for the direct interaction between microorganisms and the insulin pathway and diabetes mellitus diseases. It tested three hypotheses affecting the insulin pathway and presenting a risk factor for pancreatic cell destruction. The role of microorganisms in CFRD was investigated by testing β-cell toxicity caused by secondary metabolites (pyrrolnitrin & phenazine) produced during long term infection. This part showed specific modulation of the β-cell pathway and GSIS (gene expression, insulin secretion, channel potential action).

This study suggests that these microbial molecular mimicries can induce a humoral autoimmune response producing antibodies which can cross react with the linear epitopes of HIR initiated by the *Burkholderia* IBPs epitopes or antibodies cross reacting with GAD65 initiated by GAD molecular mimicry of one of the *E. coli* bacterial proteins (OmpA, FD, SD or DpsP). These cross reacting antibodies are initiated by bacterial infection whose antigens are presented by the MHC-II molecules of macrophages or the dendritic cells to the T- cell CD4 initiating the B-lymphocytes to produce antibodies and stimulated

macrophages (Goldsby *et al.,* 2000). However, in the case of *Burkholderia* epitopes there is the possibility to stimulate the cytotoxic T-cell against the pancreatic beta cells in addition to the CD4 pathway. The T- cell cytotoxic pathway can also be stimulated because *B. multivorans* can be an intracellular pathogen in addition to their intercellular existence (Martin and Mohr, 2000). Therefore, *Burkholderia* can live inside lung epithelial cells and APC like macrophages, which will then present the IBP(s) epitopes via MHC-I to the T-Cell CD8 and subsequently induce a cytotoxic T-cell pathway leading to β-cell death. The second scenario hypothesised may occur by presenting the insulin bound to the *Burkholderia* membrane as a foreign antigen via both pathways, which is more possible to occur and produce a diabetic autoimmune response, particularly in immune- compromise individuals like CFRD suffers.

References

Aberoum, A., and Jooyandeh, H. (2010). A review on occurrence and characterization of the *Aeromonas* Species from marine fishes. *World J Fish & Marine Sc* 2, 519-523.

Abulafia-Lapid, R., Gillis, D., Yosef, O., Atlan, H., and Cohen, I. R. (2003). T cells and autoantibodies to human HSP70 in type 1 diabetes in children. *J Autoimmun* 20, 313-321.

Agnoli, K., Lowe, C. A., Farmer, K. L., Husnain, S. I., and Thomas, M. S. (2006). The ornibactin biosynthesis and transport genes of *Burkholderia cenocepacia* are regulated by an extracytoplasmic function σ factor which is a part of the fur regulon. *J Bacteriol* 188, 3631-3644.

Aguilar-Bryan, L., and Bryan, J. (2008). Neonatal diabetes mellitus. Endocr Rev 29, 265-291.

Akpan, J. O., Wright, P. H., and Dulin, W. (1987). The characterization of phenazine methosulfate stimulated insulin secretion. *Acta Diabetologica* 24, 56-78.

Al-Bukhari, T. A., Radford, P. M., Bouras, G., Davenport, C., Trigwell, S. M., Bottazzo, G. F., Lai, M., Schwartz, H. L., Tighe, P. J., and Todd, I. (2002). Distinct antigenic features of linear epitopes at the N-terminus and C-terminus of 65 kDa glutamic acid decarboxylase (GAD65): implications for autoantigen modification during pathogenesis. *Clin Exp Immunol* 130, 131-139.

Albert, L. J., and Inman, R. D. (1999). Molecular mimicry and autoimmunity. *N Engl J Med* 341, 2068-2074.

Alberti, K., and Zimmet, K. P. (1998). Definition, diagnosis and classification of diabetes mellitus and its complications part 1: diagnosis and classification of diabetes mellitus - provisional report of a WHO consultation. *Diabetic Med* 15, 539-553.

Alice, A. F., Lopez, C. S., Lowe, C. A., Ledesma, M. A., and Crosa, J. H. (2006). Genetic and transcriptional analysis of the siderophore malleobactin biosynthesis and transport genes in the human pathogen *Burkholderia pseudomallei* K96243. *J. Bacteriol* 188, 1551-1566.

Allen, L., Dockrell, D. H., Pattery, T., Lee, D. G., Cornelis, P., Hellewell, P. G., and Whyte, M. K. B. (2005). Pyocyanin production by *Pseudomonas aeruginosa* induces neutrophil apoptosis and impairs neutrophil-mediated host defenses *in vivo*. *J Immunol* 174, 3643-3649.

Allice, T. T., Scutera, T. S., Chirillo, T. M., and Savoia, T. D. (2006). *Burkholderia* respiratory tract infections in Italian patients with cystic fibrosis: molecular characterization. *J Infection* 53, 159-165.

Amin, R., Dupuis, A., Aaron, S. D., and Ratjen, F. (2010). The effect of chronic infection with *Aspergillus fumigatus* on lung function and hospitalization in patients with cystic fibrosis. *Chest* 137, 171-176.

Andrali, S. S., Sampley, M. L., Vanderford, N. L., and Ozcan, S. (2008). Glucose regulation of insulin gene expression in pancreatic beta-cells. *Biochem J* 415, 1-10.

Angermayr, M., Strobel, G., Müller, G., and Bandlow, W. (2000). Stable plasma membrane expression of the soluble domain of the human insulin receptor in yeast. *FEBS Lett* 481, 8-12.

Arnesen, K. R., Mikkelsen, H., Schroder, M. B., and Lund, V. (2010). Impact of reattaching various *Aeromonas salmonicida* A-layer proteins on vaccine efficacy in atlantic cod (*Gadus morhua*). *Vaccine* 28, 4703-4708.

Artigot, M. P., Loiseau, N., Laffitte, J., Mas-Reguieg, L., Tadrist, S., Oswald, I. P., and Puel, O. (2009). Molecular cloning and functional characterization of two CYP619 cytochrome P450s involved in biosynthesis of patulin in *Aspergillus clavatus*. *Microbiology* 155, 1738-1747.

Artner, I., Hang, Y., Guo, M., Gu, G., and Stein, R. (2008). MafA is a dedicated activator of the insulin gene in vivo. *J Endocrinol* 198, 271-279.

Arumugam, R., Horowitz, E., Lu, D., Collier, J. J., Ronnebaum, S., Fleenor, D., and Freemark, M. (2008). The interplay of prolactin and the glucocorticoids in the regulation of beta-cell gene expression, fatty acid oxidation, and glucose-stimulated insulin secretion: implications for carbohydrate metabolism in pregnancy. *Endocrinology* 149, 5401-5414.

Asfari, M., Janjic, D., Meda, P., Li, G., Halban, P. A., and Wollheim, C. B. (1992). Establishment of 2-mercaptoethanol-dependent differentiated insulin- secreting cell lines. *Endocrinology* 130, 167-178.

Ashcroft, F. M. (1999). ATP-sensitive K^+ channels and insulin secretion: their role in health and disease. *Diabetologia* 42, 903-919.

Ashcroft, F. M. (2000). The yin and yang of the K(ATP) channel. *J Physiol* 528, 405.

Ashcroft, F. M., and Gribble, F. M. (2000). Tissue-specific effects of sulfonylureas: lessons from studies of cloned K(ATP) channels. *J Diabetes Complicat* 14, 192-196.

Atkinson, M. A., and Maclaren, N. K. (1994). The pathogenesis of insulin-dependent diabetes mellitus. *N Engl J Med* 331, 1428-1436.

Atkinson, M. A., Maclaren, N. K., Scharp, D. W., Lacy, P. E., and Riley, W. J. (1990). 64,000 Mr autoantibodies as predictors of insulin-dependent diabetes. *Lancet* 335, 1357-1360.

Baekkeskov, S., Aanstoot, H. J., Christgau, S., Reetz, A., Solimena, M., Cascalho, M., Folli, F., Richter-Olesen, H., and De camilli, P. (1990). Identification of the 64K autoantigen in insulin-dependent diabetes as the GABA-synthesizing enzyme glutamic acid decarboxylase. *Nature* 347, 151-156.

Baldwin, A., Mahenthiralingam, E., Thickett, K. M., Honeybourne, D., Maiden, M. C. J., Govan, J. R., Speert, D. P., LiPuma, J. J., Vandamme, P., and Dowson, C. G. (2005). Multilocus sequence typing scheme that provides both species and strain differentiation for the *Burkholderia cepacia* complex. *J. Clin. Microbiol* 43, 4665-4673.

Barkai-Golan, R., and Paster, N. (2008). Mycotoxins in fruits and vegetables Elsevier, San Diego, CA. USA.

Baydas, G., Sonkaya, E., Tuzcu, M., Yasar, A., and Donder, E. (2005). Novel role for gabapentin in neuroprotection of central nervous system in streptozotocine-induced diabetic rats. *Acta Pharmacol Sin* 26, 417-422.

Bernot, A. (2004). Genome transcriptome and proteome analysis. Wiley, Chichester, West Sussex, England.

Beta cell Biology consortium (2004). Insulin-mediated glucose uptake. In Panel 3.http://www.betacell.org/content/articlepanelview/article_id/1/panel_id/3.

Betley, S., Alberti, K. G., and Agius, L. (1989). Regulation of fatty acid and carbohydrate metabolism by insulin, growth hormone and tri-iodothyronine in hepatocyte cultures from normal and hypophysectomized rats. *Biochem J* 258, 547-552.

Bhattacharjee, A., Whitehurst, R. M., Jr., Zhang, M., Wang, L., and Li, M. (1997). T-type calcium channels facilitate insulin secretion by enhancing general excitability in the insulin-secreting beta-cell line, INS-1. *Endocrinology* 138, 3735-3740.

Birnboim, H. C., and Doly, J. (1979). A rapid alkaline extraction procedure for screening recombinant plasmid DNA. *Nucl. Acids Res* 7, 1513-1523.

Bioinformatics resource center (2008). Pathema Burkholderia. http://pathema.jcvi.org/cgi-bin/Burkholderia/PathemaHomePage.cgi.

Biros, E. E., Jordan, M. M., and Baxter, A. A. (2005). Genes mediating environment interactions in type 1 diabetes.*Rev of diabetic studies* 2, 192-207.

Bkaily, G., Naik, R., Jaalouk, D., Jacques, D., Economos, D., D'Orleans-Juste, P., and Pothier, P. (1998). Endothelin-1 and insulin activate the steady-state voltage dependent R-type Ca^{2+} channel in aortic smooth muscle cells via a pertussis toxin and cholera toxin sensitive G-protein. *Mol Cell Biochem* 183, 39-47.

Bonifacio, E., Lampasona, V., Bernasconi, L., and Ziegler, A. G. (2000). Maturation of the humoral autoimmune response to epitopes of GAD in preclinical childhood type 1 diabetes. *Diabetes* 49, 202-208.

Bonifacio, E., Lampasona, V., and Bingley, P. J. (1998). IA-2 (Islet cell antigen 512) is the primary target of humoral autoimmunity against type 1 diabetes-associated tyrosine phosphatase autoantigens. *J Immunol* 161, 2648-2654.

Bouskila, M., Hirshman, M. F., Jensen, J., Goodyear, L. J., and Sakamoto, K. (2008). Insulin promotes glycogen synthesis in the absence of GSK3 phosphorylation in skeletal muscle. *Am J Physiol Endocrinol Metab* 294, E28-35.

Bowen, R. (2004). Pathophisiology of endocrine system. In physiologic effects of insulin, http:// www vivo colostate.edu /hbook /pathphys /endocrine / pancreas/insulin_phys.html.

Bradford, M. M. (1976). A rapid and sensitive method for the quantitation of microgram quantities of protein utilizing the principle of protein-dye binding. *Anal Biochem* 72, 248-254.

Brown, J. T., Kant, A., and Mailman, R. B. (2009). Rapid, semi-automated, and inexpensive radioimmunoassay of cAMP: application in GPCR-mediated adenylate cyclase assays. *J Neurosci Meth* 177, 261-266.

Brunner, Y., Schvartz, D., Priego-Capote, F., Couté, Y., and Sanchez, J. C. (2009). Glucotoxicity and pancreatic proteomics. *J Proteomics* 71, 576-591.

Bruns, D., and Jahn, R. (2002). Molecular determinants of exocytosis. *Pflugers Arch* 443, 333-338.

Buchanan, T. A., and Xiang, A. H. (2005). Gestational diabetes mellitus. *J Clin Invest* 115, 485-491

Burke, J., and Handy, R. D. (2005). Sodium-sensitive and -insensitive copper accumulation by isolated intestinal cells of rainbow trout *Oncorhynchus mykiss*. *J Exp Biol* 208, 391-407.

Burnie, J. J. P., Al-Wardi, E. E. J., Williamson, P. P., Matthews, R. R. C., Webb, K. K., and David, T. T. (1995). Defining potential targets for immunotherapy in *Burkholderia cepacia* infection. *FEMS Immunol Med Mic* 10, 157.

Burns, D. L. (1988). Subunit structure and enzymic activity of pertussis toxin. *Microbiol Sci* 5, 285-287.

Buteau, J., Roduit, R., Susini, S., and Prentki, M. (1999). Glucagon-like peptide-1 promotes DNA synthesis, activates phosphatidylinositol 3-kinase and increases transcription factor pancreatic and duodenal homeobox gene 1 (PDX-1) DNA binding activity in beta (INS-1)-cells. *Diabetologia* 42, 856-864.

Butler, M. H., Solimena, M., Dirkx, R., Jr., Hayday, A., and De Camilli, P. (1993). Identification of a dominant epitope of glutamic acid decarboxylase (GAD65) recognized by autoantibodies in stiff-man syndrome. *J Exp Med* 178, 2097-2106.

Campanile, A., and Iaccarino, G. (2009). G-protein-coupled receptor kinases in cardiovascular conditions: focus on G-protein-coupled receptor kinase 2, a gain in translational medicine. *Biomark Med* 3, 525-540.

Carbonetti, N. H. (2010). Pertussis toxin and adenylate cyclase toxin: key virulence factors of *Bordetella pertussis* and cell biology tools. *Future Microbiol* 5, 455-469.

CAST (2003). Mycotoxins: risks in plant, animal, and human systems - new report.Council for Agricultural Science and Technology. *Task Force Report*.

CDCP, (2011). National Diabetes Fact Sheet: national estimates and general information on diabetes and prediabetes in the united states,. Atlanta, GA: U.S. Department of Health and Human Services, Centers for Disease Control and Prevention.

Cerf, M. E., Muller, C. J. F., Du Toit, D. F., Louw, J., and Wolfe-Coote, S. A. (2005). Transcription factors, pancreatic development, and beta-cell maintenance. *Biochem Bioph Res Co* 326, 699-702.

Chan, S. L., Pallett, A. L., and Morgan, N. G. (1997). Clotrimazole and efaroxan stimulate insulin secretion by different mechanisms in rat pancreatic islets. *N-S Arch Pharmacol* 356, 763-768.

Chan, S. L. F., Mourtada, M., and Morgan, N. G. (2001). Characterization of a K_{ATP} channel–independent pathway involved in potentiation of insulin secretion by efaroxan. *Diabetes* 50, 340-347.

Chiang, C. S., Stacey, G., and Tsay, Y. F. (2004). Mechanisms and functional properties of two peptide transporters, AtPTR2 and fPTR2. *J Biol Chem* 279, 30150-30157.

Christopher, G. K., and Sundermann, C. A. (1996). Intracellular insulin binding in *Tetrahymena pyriformis*. *Tissue & Cell* 28, 427-437.

Chu, C., Gui, Y. H., Ren, Y. Y., and Shi, L. Y. (2012). The impacts of maternal gestational diabetes mellitus (GDM) on fetal hearts. *Biomed Environ Sci* 25, 15-22.

Clarke, L., and Carbon, J. (1976). A colony bank containing synthetic CoI EI hybrid plasmids representative of the entire *E. coli* genome. *Cell* 9, 91-99.

Collier, E., Watkinson, A., Cleland, C. F., and Roth, J. (1987). Partial purification and characterization of an insulin-like material from spinach and Lemna gibba G3. *J Biol Chem* 262, 6238-6247.

Coulton, J. W., Mason, P., Cameron, D. R., Carmel, G., Jean, R., and Rode, H. N. (1986). Protein fusions of 3-galactosidase to the ferrichrome-iron receptor of *E coli* K-12. *J Bacteriol* 165, 181-192.

Coutinho, H. D. (2007). *Burkholderia cepacia* complex: virulence characteristics, importance and relationship with cystic fibrosis. *Indian J Med Sci* 61, 422-429.

Cozzone, A. J. (2005). Role of protein phosphorylation on serine /threonine and tyrosine in the virulance of bacterial pathogens. *J Mol Microbiol Biotechnol* 9, 198-213.

Cozzone, A. J., Christophe, G., Patricia, D., and Bertrand, D. (2004). Protein phosphorylation on tyrosine in bacteria. *Arch Microbiol* 181, 171-181.

Crosa, J. H. (1989). Genetics and molecular biology of siderophore-mediated iron transport in bacteria. *Microbiol Mol Biol Rev* 53, 517-530.

Cui, L., Yu, W.-P., De Aizpurua, H. J., Schmidli, R. S., and Pallen, C. J. (1996). Cloning and characterization of islet cell antigen-related protein tyrosine phosphatase (PTP), a novel receptor-like PTP and autoantigen in insulin-dependent Diabetes. *J. Biol Chem* 271, 24817-24823.

Dahlgren, U. I., Wold, A. E., Hanson, L. A., and Midtvedt, T. (1991). Expression of a dietary protein in *E. coli* renders it strongly antigenic to gut lymphoid tissue. *Immunology* 73, 394-397.

Dalluge, J. J. (2000). Mass spectrometry for direct determination of proteins in cells: applications in biotechnology and microbiology. *Fresenius J Anal Chem* 366, 701-711.

Damanhouri, L. H. L. H., Dromey, J. A. J. A., Christie, M. R. M. R., Nasrat, H. A. H. A., Ardawi, M. S. M. S. M., Robins, R. A. R. A., and Todd, I. I. (2005). Autoantibodies to GAD and IA-2 in saudi arabian diabetic patients. *Diabetic medicine* 22, 448.

Daniel, H., Spanier, B., Kottra, G., and Weitz, D. (2006). From bacteria to man: archaic proton-dependent peptide transporters at work. *Physiology* 21, 93-102.

Davies, J. J. (1997). Molecular mimicry: Can epitope mimicry induce autoimmune disease? *Immunol Cell Biol* 75, 113-126.

Daw, K., and Powers, A. C. (1995). Two distinct glutamic acid decarboxylase auto-antibody specificities in IDDM target different epitopes. *Diabetes* 44, 216-220.

Daw, K., Ujihara, N., Atkinson, M., and Powers, A. C. (1996). Glutamic acid decarboxylase autoantibodies in stiff-man syndrome and insulin-dependent diabetes mellitus exhibit similarities and differences in epitope recognition. *J Immunol* 156, 818-825.

Delzenne, N., and Cani, P. (2011). Can we change metabolism by changing the gut flora In *4th international congress on prediabetes and metabolic syndrome* pp. 6-7, Madrid, Spain.

Demain, A. L. (1999). Pharmaceutically active secondary metabolites of microorganisms. *Appl. Microbiol. Biotechnol* 52, 455-463.

Denning, G. M., Iyer, S. S., Reszka, K. J., O'Malley, Y., Rasmussen, G. T., and Britigan, B. E. (2003). Phenazine-1-carboxylic acid, a secondary metabolite of *Pseudomonas aeruginosa*, alters expression of immunomodulatory proteins by human airway epithelial cells. *Am J Physiol-Lung Cell Mol Physiol* 285, L584-L592.

Devaraj, H., Shanmugasundaram, K. R., and Shanmugasundaram, E. R. (1986). Role of patulin as a diabetogenic lactone. *Indian J Exp Biol* 24, 458-459.

Diabetes UK, (2012). Gestational diabetes, *http://www.nhs.uk/conditions/gestational-iabetes/Pages/Introduction.aspx#close*.

Dietz, E.E., Uhlenbruck, G., and Lutticken, R. (1989). An insulin-receptor in microorganisms-fact or fiction. *Die Naturwissenschaften* 76, 269-270.

Docherty, K., and Clark, A. R. (1994). Nutrient regulation of insulin gene expression. *FASEB J* 8, 20-27.

Docherty, L. E., Poole, R. L., Mattocks, C. J., Lehmann, A., Temple, I. K., and Mackay, D. J. (2010). Further refinement of the critical minimal genetic region for the imprinting disorder 6q24 transient neonatal diabetes. *Diabetologia* 53, 2347-2351.

Doig, P., Emody, S. L., and Trus, t. J. (1992). Binding of laminin and fibronectin by the trypsin-resistant major structural domain of the crystalline virulence surface array protein of *Aeromonas salmonicid*. *J Biol Chemi* 2671 43-49.

Dong, X., Stothard, P., Forsythe, I. J., and Wishart, D. S. (2004). PlasMapper: a web server for drawing and auto-annotating plasmid maps. *Nucl. Acids Res* 32, W660-664.

Doyle, M. E., and Egan, J. M. (2003). Pharmacological agents that directly modulate insulin secretion. *Pharmacol Rev* 55, 105-131.

Dufer, M., Haspel, D., Krippeit-Drews, P., Kelm, M., Ranta, F., Nitschke, R., Ullrich, S., Aguilar-Bryan, L., Bryan, J., and Drews, G. (2007). The KATP channel is critical for calcium sequestration into non-ER compartments in mouse pancreatic beta cells. *Cell Physiol Biochem* 20, 65-74.

Dworkin, M., and Falkow, S. (2006). The prokaryotes : A handbook on the biology of bacteria. Springer, New York ; London.

Eisenberg, M. L., Maker, A. V., Slezak, L. A., Nathan, J. D., Sritharan, K. C., Jena, B. P., Geibel, J. P., and Andersen, D. K. (2005). Insulin receptor (IR) and glucose transporter 2 (GLUT2) proteins form a complex on the rat hepatocyte membrane. *Cell Physiol Biochem* 15, 051-058.

El-Banna, N., and Winkelmann, G. (1998). Pyrrolnitrin from *Burkholderia cepacia*: antibiotic activity against fungi and novel activities against streptomycetes. *J Appl Microbiol* 85, 69-78.

Elias, D. D., Markovits, D., Reshef, T., Vanderzee, R., and Cohen, I. R. (1990). Induction and therapy of autoimmune diabetes in the non -obese diabetic (NOD/LT) mouse by A 65-KDA heat- shock protein. *P Natl Acad Sci USA* 87, 1576-1580.

Ellis, A. E. (1988). Lack of relatioship between virulance of *Aeromonas salmonicida* and the putative virulance factors A-layer, extracellular proteases and and extracellular hemolysins. *J Fish Dis* 11, 309-323.

Ellis, L., Morgan, D. O., Clauser, E., Roth, R. A., and Rutter, W. J. (1987). A membrane-anchored cytoplasmic domain of the human insulin receptor mediates a constitutively elevated insulin-independent uptake of 2-deoxyglucose. *Mol Endocrinol* 1, 15-24.

Elsner, M., Guldbakke, B., Tiedge, M., Munday, R., and Lenzen, S. (2000). Relative importance of transport and alkylation for pancreatic beta-cell toxicity of streptozotocin. *Diabetologia* 43, 1528-1533.

Erecinska, M., Bryla, J., Michalik, M., Meglasson, M. D., and Nelson, D. (1992). Energy metabolism in islets of langerhans. *Biochim Biophys Acta* 1101, 273-295.

Eto, K., Tsubamoto, Y., Terauchi, Y., Sugiyama, T., Kishimoto, T., Takahashi, N., Yamauchi, N., Kubota, N., Murayama, S., Aizawa, T., Akanuma, Y., Aizawa, S., Kasai, H., Yazaki, Y., and Kadowaki, T. (1999). Role of NADH shuttle system in glucose-induced activation of mitochondrial metabolism and insulin secretion. *Science* 283, 981-985.

Evans-Molina, C., Garmey, J. C., Ketchum, R., Brayman, K. L., Deng, S., and Mirmira, R. G. (2007). Glucose regulation of insulin gene transcription and pre-mRNA processing in human islets. *Diabetes* 56, 827-835.

Fagerquist, C. K., Garbus, B. R., Williams, K. E., Bates, A. H., Boyle, S., and Harden, L. A. (2009). Web-based software for rapid top-down proteomic identification of protein biomarkers, with implications for bacterial identification. *Appl Environ Microbiol* 75, 4341-4353.

Fajans, S. S., Bell, G. I., and Polonsky, K. S. (2001). Molecular mechanisms and clinical pathophysiology of maturity-onset diabetes of the young. *New Engl J Med* 345, 971-980.

Falorni, A., Ackefors, M., Carlberg, C., Daniels, T., Persson, B., Robertson, J., and Lernmark, å. (1996). Diagnostic sensitivity of immunodominant epitopes of glutamic acid decarboxylase (GAD65) autoantibodies in childhood IDDM. *Diabetologia* 39, 1091-1098.

Falorni, A., Gambelunghe, G., Forini, F., Kassi, G., Cosentino, A., Candeloro, P., Bolli, G. B., Brunetti, P., and Calcinaro, F. (2000). Autoantibody recognition of COOH-terminal epitopes of GAD65 marks the risk for insulin requirement in adult-onset diabetes mellitus. *J Clin Endocrinol Metab* 85, 309-316.

Farra, C., Menassa, R., Awwad, J., Morel, Y., Salameh, P., Yazbeck, N., Majdalani, M., Wakim, R., Yunis, K., Mroueh, S., and Cabet, F. (2010). Mutational spectrum of cystic fibrosis in the Lebanese population. *J Cyst Fibros* 9, 406-410.

Fast, M. D., Tse, B., Boyd, J. M., and Johnson, S. C. (2009). Mutations in the *Aeromonas salmonicida* subsp. salmonicida type III secretion system affect atlantic salmon leucocyte activation and downstream immune responses. *Fish Shellfish Immun* 27, 721-728.

Fawell, S. E., McKenzie, M. A., Greenfield, N. J., Adebodun, F., Jordan, F., and Lenard, J. (1988). Stimulation by mammalian insulin of glycogen metabolism in a wall-less strain of *Neurospora crassa*. *Endocrinology* 122, 518-523.

Fenalti, G., and Rowley, M. J. (2008). GAD65 as a prototypic autoantigen. *J Autoimmun* 31, 228-232.

Fernandez, A. I., Fernandez, A. F., Perez, M. J., Nieto, T. P., and Ellis, A. E. (1998). Siderophore production by *Aeromonas salmonicida* subsp. salmonicida. Lack of strain specificity. *Dis Aquat Organ* 33, 87-92.

Fridlyand, L. E., Tamarina, N., and Philipson, L. H. (2003). Modeling of Ca^{2+} flux in pancreatic beta-cells: role of the plasma membrane and intracellular stores. *Am J Physiol Endocrinol Metab* 285, E138-154.

Fujinami, R. S., von Herrath, M. G., Christen, U., and Whitton, J. L. (2006). Molecular mimicry, bystander activation, or viral persistence: Infections and autoimmune disease. *Clin. Microbiol. Rev* 19, 80-94.

Gebel, E. (2011). The host with the most. A human body's bacteria may offer clues to why diabetes develops. *Diabetes Forecast* 64, 36-39.

Gerber, S. H., and Sudhof, T. C. (2002). Molecular determinants of regulated exocytosis. *Diabetes* 51 Suppl 1, S3-11.

Gey, G. O., and Gey, M. K. (1936). Maintenance of human normal cells in continuous culture: preliminary report; cultivation of mesoblastic tumors and normal cells and notes on methods of culture. *Am J Cancer* 27, 45-76.

Gilliland, B. C. (1989). Rheumatoid arthritis: a model of chronic inflammation. *Arzneimittelforschung* 39, 952-955; discussion 955-956.

Giongo, A., Gano, K. A., Crabb, D. B., Mukherjee, N., Novelo, L. L., Casella, G., Drew, J. C., Ilonen, J., Knip, M., Hyoty, H., Veijola, R., Simell, T., Simell, O., Neu, J., Wasserfall, C. H., Schatz, D., Atkinson, M. A., and Triplett, E. W. (2011). Toward defining the autoimmune microbiome for type 1 diabetes. *ISME J* 5, 82-91.

Goldberg, E., and Krause, I. (2009). Infection and type 1 diabetes mellitus - A two edged sword? *Autoimmun Rev* 8, 682-686.

Goldsby, R. A., Kindt, T. J., Osborne, B. A., and Kuby, J. (2000). Kuby immunology. W.H. Freeman, New York.

Govan, J. R., and Deretic, V. (1996). Microbial pathogenesis in cystic fibrosis: mucoid *Pseudomonas aeruginosa* and *Burkholderia cepacia*. *Microbiol Rev.* 60, 539-574.

Gravel, P. (2007). Protein Blotting, pp. 365-375. Triskel Integrated Services SA, Geneva, Switzerland.

Graves, T. K., and Hinkle, P. M. (2003). Ca^{2+}-induced Ca^{2+} release in the pancreatic beta-cell: direct evidence of endoplasmic reticulum Ca^{2+} release. *Endocrinology* 144, 3565-3574.

Gray, E., Muller, D., Squires, P. E., Asare-Anane, H., Huang, G.-C., Amiel, S., Persaud, S. J., and Jones, P. M. (2006). Activation of the extracellular calcium-sensing receptor initiates insulin secretion from human islets of Langerhans: involvement of protein kinases. *J Endocrinol* 190, 703-710.

Gu, C., Stein, G. H., Pan, N., Goebbels, S., Hornberg, H., Nave, K. A., Herrera, P., White, P., Kaestner, K. H., Sussel, L., and Lee, J. E. (2010). Pancreatic beta cells require NeuroD to achieve and maintain functional maturity. *Cell Metab* 11, 298-310.

Habener, J. F., Kemp, D. M., and Thomas, M. K. (2005). Transcriptional regulation in pancreatic development. *Endocrinology* 146, 1025-1034.

Hadjiliadis, D., Madill, J., Chaparro, C., Tsang, A., Waddell, T. K., Singer, L. G., Hutcheon, M. A., Keshavjee, S., and Elizabeth Tullis, D. (2005). Incidence and prevalence of diabetes mellitus in patients with cystic fibrosis undergoing lung transplantation before and after lung transplantation. *Clin Transplant* 19, 773-778.

Hagopian, W. A., Karlsen, A. E., Gottsater, A., Landin-Olsson, M., Grubin, C. E., Sundkvist, G., Petersen, J. S., Boel, E., Dyrberg, T., and Lernmark, A. (1993a). Quantitative assay using recombinant human islet glutamic acid decarboxylase (GAD65) shows that 64 K autoantibody positivity at onset predicts diabetes type. *J Clin Invest* 91, 368-374.

Hagopian, W. A., Michelsen, B., Karlsen, A. E., Larsen, F., Moody, A., Grubin, C. E., Rowe, R., Petersen, J., McEvoy, R., and Lernmark, A. (1993b). Autoantibodies in IDDM primarily recognize the 65,000-M(r) rather than the 67,000-M(r) isoform of glutamic acid decarboxylase. *Diabetes* 42, 631-636.

Hamill, O. P., Marty, A., Neher, E., Sakmann, B., and Sigworth, F. J. (1981). Improved patch-clamp techniques for high-resolution current recording from cells and cell-free membrane patches. *Pflüg Arch Eur J Phy* 391, 85-100.

Hammar, N., Farahmand, B., Gran, M., Joelson, S., and Andersson, S. W. (2010). Incidence of urinary tract infection in patients with type 2 diabetes. Experience from adverse event reporting in clinical trials. *Pharmacoepidemiol Drug Saf* 19, 1287-1292.

Hampe, C. S., Kockum, I., Landin-Olsson, M., Torn, C., Ortqvist, E., Persson, B., Rolandsson, O., Palmer, J., and Lernmark, A. (2002). GAD65 antibody epitope patterns of type 1.5 diabetic patients are consistent with slow-onset autoimmune diabetes. *Diabetes Care* 25, 1481-1482.

Hancock, J. T. (2005). Cell signalling. Oxford University Press, Oxford; New York.

Hans, K. Å., Outi, V., Heikki, H., Jorma, I., and Mikael, K. (2002). Environmental factors in the etiology of type 1 diabetes. *Am J Med Genet* 115, 18-29.

Harati, H., Hadaegh, F., Saadat, N., and Azizi, F. (2009). Population-based incidence of type 2 diabetes and its associated risk factors: results from a six-year cohort study in Iran. *BMC Public Health* 9, 186.

Hardin, D. S., Leblanc, A., Marshall, G., and Seilheimer, D. K. (2001). Mechanisms of insulin resistance in cystic fibrosis. *Am J Physiol Endocrinol Metab* 281, E1022-1028.

Hasham, A., and Tomer, Y. (2011). The recent rise in the frequency of type 1 diabetes: Who pulled the trigger? *J Autoimmun* 37, 1-2.

Hay, C. W., and Docherty, K. (2006). Comparative analysis of insulin gene promoters: implications for diabetes research. *Diabetes* 55, 3201–3213.

Hedeskov, C. J., Capito, K., and Thams, P. (1987). Cytosolic ratios of free NADPH/$NADP^+$ and NADH/NAD^+ in mouse pancreatic islets, and nutrient-induced insulin secretion. *Biochem J* 241, 161-167.

Henderson, N. S., Nijtmans, L. G. J., Lindsay, J. G., Lamantea, E., Zeviani, M., and Holt, I. J. (2000). Separation of intact pyruvate dehydrogenase complex using blue native agarose gel electrophoresis. *Electrophoresis* 21, 2925-2931.

Hesketh, J. E., and Campbell, G. P. (1987). Effects of insulin, pertussis toxin and cholera toxin on protein synthesis and diacylglycerol production in 3T3 fibroblasts: evidence for a G-protein mediated activation of phospholipase C in the insulin signal mechanism. *Biosci Rep* 7, 533-541.

Hettiarachchi, K. D., Zimmet, P. Z., and Myers, M. A. (2004). Transplacental exposure to bafilomycin disrupts pancreatic islet organogenesis and accelerates diabetes onset in NOD mice. *J Autoimmun* 22, 287-296.

Hettiarachchi, K. D., Zimmet, P. Z., and Myers, M. A. (2006). The effects of repeated exposure to sub-toxic doses of plecomacrolide antibiotics on the endocrine pancreas. *Food ChemToxicol* 44, 1966-1977.

Hirst, I. D., Hastings, T. S., and Ellis, A. E. (1991). Siderophore production by *Aeromonas salmonicida*. *J Gen Microbiol* 137, 1185-1192.

Holland, A. M., Góñez, L. J., Naselli, G., MacDonald, R. J., and Harrison, L. C. (2005). Conditional expression demonstrates the role of the homeodomain transcription factor Pdx-1 in maintenance and regeneration of β-cells in the adult pancreas. *Diabetes* 54, 2586-2595.

Honeyman, M. C., Stone, N. L., and Harrison, L. C. (1998). T-cell epitopes in type 1 diabetes autoantigen tyrosine phosphatase IA-2: potential for mimicry with rotavirus and other environmental agents. *Mol Med* 4, 231-239.

Horváth, L., Cervenak, L., Oroszlán, M., Prohászka, Z., Uray, K., Hudecz, F., Baranyi, É., Madácsy, L., Singh, M., Romics, L., Füst, G., and Pánczél, P. (2002). Antibodies against different epitopes of heat-shock protein 60 in children with type 1 diabetes mellitus. *Immun Lett* 80, 155-162.

Horwitz, M. S., Ilic, A., Fine, C., Rodriguez, E., and Sarvetnick, N. (2002). Presented antigen from damaged pancreatic β cells activates autoreactive T cells in virus-mediated autoimmune diabetes. *J Clin Invest* 109, 79-87.

Hou, J. C., Min, L., and Pessin, J. E. (2009). Insulin granule biogenesis, trafficking and exocytosis. *Vitam Horm* 80, 473-506.

Hu, S., Jiang, J., and Wong, D. T. (2010). Proteomic analysis of saliva: 2D gel electrophoresis, LC-MS/MS, and Western blotting. *Methods Mol Biol* 666, 31-41.

Huang, W.-M., Fourquet, R. L., Wu, E., and Wu, J.-Y. (1990). Molecular cloning and amino acid sequnces of brain L-glutamate decarboxylase. *Proc Natl Acad Sci* 87, 8491-8495.

Hwang, J., Chilton, W. S., and Benson, D. M. (2002). Pyrrolnitrin production by *Burkholderia cepacia* and biocontrol of *Rhizoctonia* stem rot of poinsettia. *Biol Control* 25, 56-63.

Idevall-Hagren, O., Barg, S., Gylfe, E., and Tengholm, A. (2010). cAMP mediators of pulsatile insulin secretion from glucose-stimulated single beta-cells. *J Biol Chem* 285, 23007-23018.

Iype, T., Francis, J., Garmey, J. C., Schisler, J. C., Nesher, R., Weir, G. C., Becker, T. C., Newgard, C. B., Griffen, S. C., and Mirmira, R. G. (2005). Mechanism of insulin gene regulation by the pancreatic transcription factor Pdx-1 - application of pre-mRNA analysis and chromatin immunoprecipitation to assess formation of functional transcriptional complexes. *J Biol Chem* 280, 16798-16807.

Jensen, P., Johansen, H. K., Carmi, P., Høiby, N., and Cohen, I. R. (2001). Autoantibodies to pancreatic hsp60 precede the development of glucose intolerance in patients with cystic fibrosis. *J Autoimmun* 17, 165-172.

Jeromson, S., Keig, P., and Kerr, K. (1999). Concise communication - Interaction of insulin and *Burkholderia cepacia*. *Clin Microbiol Infec* 5, 439-442.

Jijakli, H., Rasschaert, J., Nadi, A. B., Leclercq-Meyer, V., Sener, A., and Malaisse, W. J. (1996). Relevance of lactate dehydrogenase activity to the control of oxidative glycolysis in pancreatic islet β-cells. *Arch Biochem Biophys* 327, 260-264.

Jilly, B. B., Schreckenberger, P. C., and Lebeau, L. J. (1984). Rapid glutamic acid decarboxylase test for identification of bacteroides and *Closterdium* spp. *J Clin Microbiol* 19, 592-593.

Johnston, J. A., and Van Horn, E. R. (2011). The effects of correction insulin and basal insulin on inpatient glycemic control. Medsurg Nurs 20, 187-193.

Jones, A. M., Dodd, M. E., and Webb, A. K. (2001). *Burkholderia cepacia*: current clinical issues, environmental controversies and ethical dilemmas. *Eur Respir J* 17, 295-301.

Jurgen Schrezenmeir, a. A. J. (2000). Milk and Diabetes. *J Am Coll Nutr* 19, 176s.

Judkowski, V. A., Allicotti, G. M., Sarvetnick, N., and Pinilla, C. (2004). Peptides from common viral and bacterial pathogens can efficiently activate diabetogenic T-cells. *Diabetes* 53, 2301-2309.

Kahn, S. E., Hull, R. L., and Utzschneider, K. M. (2006). Mechanisms linking obesity to insulin resistance and type 2 diabetes. *Nature* 444, 840-846.

Kanai, K. K., Kondo, E. E., and Kurata, T. T. (1996). Affinity and response of *Burkholderia pseudomallei* and *Burkholderia cepacia* to insulin. *Se Asian J Trop Med* 27, 584-591.

Kaneto, H., Miyatsuka, T., Kawamori, D., Yamamoto, K., Kato, K., Shiraiwa, T., Katakami, N., Yamasaki, Y., Matsuhisa, M., and Matsuoka, T. A. (2008). PDX-1 and MafA play a crucial role in pancreatic beta-cell differentiation and maintenance of mature beta-cell function. *Endocr J* 55, 235-252.

Kaneto, H., Miyatsuka, T., Nakatani, Y., and Matsuoka, T.-a. (2005). PDX-1 and MafA: key transcription factors in pancreas. *Am J Bioch Biotech* 1, 54-63.

Kanthakumar, K., Taylor, G., Tsang, K. W. T., Cundell, D. R., Rutman, A., Smith, S., Jeffery, P. K., Cole, P. J., and Wilson, R. (1993). Mechanisms of action of *Pseudomonase aeruginosa* pyocyanin on humman ciliary beta in -vitro. *Infect. Immun* 61, 2848-2853.

Kaplin, A. I., Snyder, S. H., and Linden, D. J. (1996). Reduced nicotinamide adenine dinucleotide-selective stimulation of inositol 1,4,5-trisphosphate receptors mediates hypoxic mobilization of calcium. *J Neurosci* 16, 2002-2011.

Karnieli, E., and Armoni, M. (2008). Transcriptional regulation of the insulin-responsive glucose transporter GLUT4 gene: from physiology to pathology. *Am J Physiol Endocrinol Metab* 295, E38-45.

Kataoka, K., Han, S.-i., Shioda, S., Hirai, M., Nishizawa, M., and Handa, a. H. (2002). MafA Is a glucose-regulated and pancreatic β-cell-specific transcriptional activator for the insulin gene. *J Biol Chem* 277 49903–49910.

Kataoka, K., Shioda, S., Ando, K., Sakagami, K., Handa, H., and Yasuda, K. (2004). Differentially expressed Maf family transcription factors, c-Maf and MafA, activate glucagon and insulin gene expression in pancreatic islet alpha- and beta-cells. *J Mol Endocrinol* 32, 9-20.

Kay, W. W., Phipps, B. M., Ishiguro, E. E., and TrustT, T. J. (1985). Porphyrin binding by the surface array virulence protein of *Aeromonas salmonicida*. *J Bacterial* 164 .

Kazlauskaite, R., and Fogelfeld, L. (2003). Insulin therapy in type 2 diabetes. *Disease-a-Month* 49, 377-420.

Keller, D. M., McWeeney, S., Arsenlis, A., Drouin, J., Wright, C. V. E., Wang, H., Wollheim, C. B., White, P., Kaestner, K. H., and Goodman, R. H. (2007). Characterization of pancreatic transcription factor Pdx-1 binding sites using promoter microarray and serial analysis of chromatin occupancy. *J Biol Chem* 282, 32084-32092.

Kenna, D. T., Barcus , V. A., Langley , R. J., Vandamme , P., and Govan, J. R. W. (2003). Lack of correllation between O-Serotype, baceriophage susceptibility and genomovar status in *Bulkhoderia cepacia* complex. *FEMS Immun Med Mic* 35, 87-92.

Keppetipola, N., and Shuman, S. (2008). A Phosphate-binding histidine of binuclear metallophosphodiesterase enzymes is a determinant of 2',3'-cyclic nucleotide phosphodiesterase activity. *J Biol Chem* 283, 30942-30949.

Khalaf, L. J., and Taylor, K. W. (1988). Pertussis toxin reverses the inhibition of insulin secretion caused by Arg8 vasopressin in rat pancreatic islets. *FEBS Lett* 231, 148-150.

Kieffer, T. J., and Francis, H. J. (1999). The glucagon-like peptides. *Endocr Rev* 20, 876-913.

Kim, J.-W., Seghers, V., Cho, J.-H., Kang, Y., Kim, S., Ryu, Y., Baek, K., Aguilar-Bryan, L., Lee, Y.-D., Bryan, J., and Suh-Kim, H. (2002). Transactivation of the mouse sulfonylurea receptor I gene by Beta2/NeuroD. *Mol Endocrinol* 16, 1097-1107.

Kim, J., Namchuk, M., Bugawan, T., Fu, Q., Jaffe, M., Shi, Y., Aanstoot, H. J., Turck, C. W., Erlich, H., Lennon, V., and Baekkeskov, S. (1994). Higher autoantibody levels and recognition of a linear NH2-terminal epitope in the autoantigen GAD65, distinguish stiff-man syndrome from insulin-dependent diabetes mellitus. *J Exp Med* 180, 595-606.

Kim, R., Yokota, H., and Kim, S.-H. (2000). Electrophoresis of proteins and protein-protein complexes in a native agarose gel. *Anal Biochem* 282, 147-149.

Kim, S. H., Shin, B. H., Kim, Y. H., Nam, S. W., and Jeon, S. J. (2007). Cloning and expression of a full-length glutamate decarboxylase gene from *Lactobacillus brevis* BH2. In *Biotechnol Bioproc* E, pp. 707-712.

Kindt, T. J., Goldsby, R. A., Osborne, B. A., and Kuby, J. (2007). Kuby immunology. W.H. Freeman, New York.

Kole, H. K., Muthukumar, G., and Lenard, J. (1991). Purification and properties of a membrane-bond-isulin binding-protein , a putative receptor,from *Neurospora crassa*. *Biochemistry* 30, 682-688.

Konidaris, C., Mitlianga, P. G., and Papadopoulos, G. K. (2003). No specific reactivity to *E. coli* glutamic acid decarboxylase from sera of newly-diagnosed insulin dependent diabetic patients. *Int J Immunopathol Pharmacol* 16, 129-138.

Konrad, R. J., Major, C. D., and Wolf, B. A. (1994). Diacylglycerol hydrolysis to arachidonic acid is necessary for insulin secretion from isolated pancreatic islets: sequential actions of diacylglycerol and monoacylglycerol lipases. *Biochemistry* 33, 13284-13294.

Kornreich, B. G. (2007). The patch clamp technique: Principles and technical considerations. *J Vet Cardiol* 9, 25-37.

Koulmanda, M., Qipo, A., Auchincloss, H., and Smith, R. N. (2003). Effects of streptozotocin on autoimmune diabetes in NOD mice. *Clin Exp Immunol* 134, 210-216.

Kukreja, A., and Maclaren, N. K. (2000). Current cases in which epitope mimicry is considered as a component cause of autoimmune disease: immune-mediated (type 1) diabetes. *Cell Mol Life Sci* 57, 534-541.

Kuti, J. L., Moss, K. M., Nicolau, D. P., and Knauft, R. F. (2004). Empiric treatment of multidrug-resistant *Burkholderia cepacia* lung exacerbation in a patient with cystic fibrosis: application of pharmacodynamic concepts to meropenem therapy. *Pharmacotherapy* 24, 1641-1645.

Laemmli, U. K. (1970). Cleavage of structural proteins during the assembly of the head of bacteriophage T4. *Nature* 227, 680-685.

Lammi, N., Marjatta , K., and Tuomilehto , J. (2005). Do microbes have a causal role in type 1 diabetes? *Med Sci Monit* 11, RA63-69.

Lawrence, M. C., Bhatt, H. S., Watterson, J. M., and Easom, R. A. (2001). Regulation of insulin gene transcription by a Ca^{2+}-responsive pathway involving calcineurin and nuclear factor of activated T-cells. *Mol Endocrinol* 15, 1758-1767.

Le Lay, J., and Stein, R. (2006). Involvement of PDX-1 in activation of human insulin gene transcription. *J Endocrinol* 188, 287-294.

Leech, S. (1998). Molecular mimcry in autoimmune disease. *Arch.Dis.child* 79, 448.

Leibiger, B., Moede, T., Uhles, S., Berggren, P. O., and Leibiger, I. B. (2002). Short-term regulation of insulin gene transcription. *Biochem Soc Trans* 30, 312-317.

Lenard, J. (1992). Mammalian hormones in microbial cells. *Trends Biochem Sci* 17, 147-150.

Lernmark, A. (2011). Is there a role for immune therapy in type 2 diabetes. In *4th international congress on prediabetes and metabolic syndrome* pp. 21, Madrid, Spain.

Leroith, D., Shiloach, J., Heffron, R., Rubinovitz, C., Tanenbaum, R., and Roth, J. (1985). Insulin -related material in microbes-simillaraty and diffrences from mammalian insulin I. *Can J Biochem Cell B* 63, 839-849.

Leroith, D., Shiloach, J., Roth, J., and Lesniak, M. A. (1981). Insulin or a closely related molecule is native to *E coli*. *J Biol Chem* 256, 6533-6536.

Leslie, R. D., Atkinson, M. A., and Notkins, A. L. (1999). Autoantigens IA-2 and GAD in Type I (insulin-dependent) diabetes. *Diabetologia* 42, 3-14.

Li, c., and zang, B. (2007). Insulin signaling and action: glucose, lipids, protein http://www.endotext.org/diabetes/index.htm.

Li, F., and Zhang, Z. M. (2009). Comparative identification of Ca^{2+} channel expression in INS-1 and rat pancreatic beta cells. *World J Gastroenterol* 15, 3046-3050.

Li, X., Quan, C. S., Yu, H. Y., and Fan, S. D. (2008). Multiple effects of a novel compound from *Burkholderia cepacia* against Candida albicans. *FEMS Microbiol lett* 285, 250-256.

Lim, A., Park, S. H., Sohn, J. W., Jeon, J. H., Park, J. H., Song, D. K., Lee, S. H., and Ho, W. K. (2009). Glucose deprivation regulates K_{ATP} channel trafficking via AMP-activated protein kinase in pancreatic beta-cells. *Diabetes* 58, 2813-2819.

Lipson, K. L., Fonseca, S. G., Ishigaki, S., Nguyen, L. X., Foss, E., Bortell, R., Rossini, A. A., and Urano, F. (2006). Regulation of insulin biosynthesis in pancreatic beta cells by an endoplasmic reticulum-resident protein kinase IRE1. *Cell Metab* 4, 245-254.

LiPuma, J. J., Rathinavelu, S., Foster, B. K., Keoleian, J. C., Makidon, P. E., Kalikin, L. M., and Baker, J. R., Jr. (2009). In vitro activities of a novel nanoemulsion against *Burkholderia* and other multidrug-resistant cystic fibrosis-associated bacterial species. *Antimicrob Agents Ch* 53, 249-255.

Liu, G. Y., and Nizet, V. (2009). Color me bad: microbial pigments as virulence factors. *Trends Microbiol* 17, 406-413.

Lodge, J., Lund, P. A., and Minchin, S. (2007). Gene cloning : principles and applications. Taylor & Francis Group, New York.

Look, D. C., Stoll, L. L., Romig, S. A., Humlicek, A., Britigan, B. E., and Denning, G. M. (2005). Pyocyanin and its precursor phenazine-1-carboxylic acid increase IL-8 and intercellular adhesion molecule-1 expression in human airway epithelial cells by oxidant-dependent mechanisms. *J Immunol* 175, 4017-4023.

Luzardo, Y., and Mathews, C. E. (2010). Attacking the source: anti-PDX-1 responses in type 1 diabetes. *Lab Invest* 90, 6-8.

Ma, J., Rayner, C. K., Jones, K. L., and Horowitz, M. (2009). Insulin secretion in healthy subjects and patients with type 2 diabetes--role of the gastrointestinal tract. *Best Pract Res Clin Endocrinol Metab* 23, 413-424.

MacDonald, M. J., Fahien, L. A., Brown, L. J., Hasan, N. M., Buss, J. D., and Kendrick, M. A. (2005a). Perspective: emerging evidence for signaling roles of mitochondrial anaplerotic products in insulin secretion. *Am J Physiol Endocrinol Metab* 288, E1-15.

MacDonald, P., Joseph, J., and Rorsman, P. (2005b). Glucose-sensing mechanisms in pancreatic β-cells. *Phil Trans R Soc B* 360, 2211-2225.

MacFarlane, A., Amanda, J., and Scott, F. W. (2003). Environmental agents and type 1 diabetes In *Textbook of Diabetes*, pp. 17.11-17.16.

Macfarlane, W. M., O'Brien, R. E., Barnes, P. D., Shepherd, R. M., Cosgrove, K. E., Lindley, K. J., Aynsley-Green, A., James, R. F., Docherty, K., and Dunne, M. J. (2000). Sulfonylurea receptor 1 and Kir6.2 expression in the novel human insulin-secreting cell line NES2Y. *Diabetes* 49, 953-960.

Mackay, I. R., Rosen, F. S., Davidson, A., and Diamond, B. (2001). Autoimmune diseases. *New Engl J Med* 345, 340-350.

Maclaren, N.N., and Atkinson, M.A. (1993). Islet cell autoantigens in insulin-dependent diabetes. *J clin invest* 92, 1608-1616.

Maclaren, N. N., and Atkinson, M. A. (1997). Insulin-dependent diabetes mellitus: The hypothesis of molecular mimicry between islet cell antigens and microorganisms. *Mol Med Today* 3, 76-83.

Madiyalakan, R., and Shanmugasundaram, E. R. (1978). Effect of patulin on mouse liver glycogen phosphorylase. *Indian J Exp Biol* 16, 1084-1085.

Maechler, P., Carobbio, S., and Rubi, B. (2006). In beta-cells, mitochondria integrate and generate metabolic signals controlling insulin secretion. *Int J Biochem Cell B* 38, 696-709.

Maeda, N., Tamagawa, T., Niki, I., Miura, H., Ozawa, K., Watanabe, G., Nonogaki, K., Uemura, K., and Iguchi, A. (1996). Increase in insulin release from rat pancreatic islets by quinolone antibiotics. *Br J Pharmacol* 117, 372-376.

Mahendrarajah, K., Dalby, P. A., Wilkinson, B., Jackson, S. E., and Main, E. R. (2011). A high-throughput fluorescence chemical denaturation assay as a general screen for protein-ligand binding. *Anal Biochem* 411, 155-157.

Mahenthiralingam, E., Baldwin, A., and Vandamme, P. (2002). *Burkholderia cepacia* complex infection in patients with cystic fibrosis. *J Med Microbiol* 51, 533-538.

Maioli, M., Alejandro, E., Tonolo, G., Gilliam, L. K., Bekris, L., Hampe, C. S., Obinu, D. A., Manconi, A., Puddu, L., Lynch, K., Lernmark, A. (2004). Epitope-restricted 65-Kilodalton glutamic acid decarboxylase autoantibodies among new-onset sardinian type 2 diabetes patients define phenotypes of autoimmune diabetes. *J Clin Endocrinol Metab* 89, 5675-5682.

Majamaa, H., and Isolauri, E. (1997). Probiotics: a novel approach in the management of food allergy. *J Allergy Clin Immunol* 99, 179-185.

Major, T. A., Panmanee, W., Mortensen, J. E., Gray, L. D., Hoglen, N., and Hassett, D. J. (2010). Sodium nitrite-mediated killing of the major cystic fibrosis pathogens *Pseudomonas aeruginosa*, *Staphylococcus aureus*, and *Burkholderia cepacia* under anaerobic planktonic and biofilm conditions. *Antimicrob agents Ch* 54, 4671-4677.

Mannhold, R. (2004). K_{ATP} channel openers: structure-activity relationships and therapeutic potential. *Chem Inform* 35, 213-266.

Marsden, M. J., Vaughan, L. M., Foster, T. J., and secombes, C. J. (1996). A live (DaroA) *Aeromonas salmonicida* vaccine for furunculosis preferentially stimulates T-cell responses relative to B-cell responses in rainbow Trout (*Oncorhynchus mykiss*). *Infect Immun* 64, 3863–3869.

Martin, D. W., and Mohr, C. D. (2000). Invasion and intracellular survival of *Burkholderia cepacia*. Infect Immun 68, 24-29.

Martino, M. E., Fasolato, L., Montemurro, F., Rosteghin, M., Manfrin, A., Patarnello, T., Novelli, E., and Cardazzo, B. (2011). Determination of microbial diversity of *Aeromonas* strains on the basis of multilocus sequence typing, phenotype, and presence of putative virulence genes. *Appl Environ Microbiol* 77, 4986-5000.

Mauch, L., Abney, C. C., Berg, H., Scherbaum, W. A., Liedvogel, B., and Northemann, W. (1993). Characterization of a linear epitope within the human pancreatic 64-kDa glutamic acid decarboxylase and its autoimmune recognition by sera from insulin-dependent diabetes mellitus patients. *Eur J Biochem* 212, 597-603.

Mayr, A., Schlosser, M., Grober, N., Kenk, H., Ziegler, A. G., Bonifacio, E., and Achenbach, P. (2007). GAD autoantibody affinity and epitope specificity identify distinct immunization profiles in children at risk for type 1 diabetes. *Diabetes* 56, 1527-1533.

McCance, K. L., and Huether, S. E. (2002). *Pathophysiology,* the biologic basis for disease in adults & children. Mosby, St. Louis, Missouri, USA.

Mc Manus, T. E., Moore, J. E., Crowe, M., Dunbar, K., and Elborn, J. S. (2003). A comparison of pulmonary exacerbations with single and multiple organisms in patients with cystic fibrosis and chronic *Burkholderia cepacia* infection. *J Infect* 46, 56-59.

Mercado, F., Vega, R., and Soto, E. (2005). Ion channels that are sensitive to the extracellular concentration of protons: their structure, function, pharmacology and pathophysiology. *Rev Neurol* 41, 667-675.

Mercan, D., Delville, J. P., Leclercq-Meyer, V., and Malaisse, W. J. (1993). Preferential stimulation by D-glucose of oxidative glycolysis in pancreatic islets: comparison between β and non-β cells. *Biochem Mol Biol Int* 29, 475-481.

Misler, S., Zhou, Z., Dickey, A. S., Silva, A. M., Pressel, D. M., and Barnett, D. W. (2009). Electrical activity and exocytotic correlates of biphasic insulin secretion from beta-cells of canine islets of langerhans: contribution of tuning two modes of Ca^{2+} entry-dependent exocytosis to two modes of glucose-induced electrical activity. *Channels (Austin)* 3, 181-193.

Moeck, G. S., and Coulton, J. W. (1998). TonB-dependent iron acquisition: mechanisms of siderophore-mediated active transport. *Mol Microbiol* 28, 675-681.

Momany, C., Ghosh, R., and Hackert, M. L. (1995). Structural motifs for pyridoxal-5'-phosphate binding in decarboxylases: an analysis based on the crystal structure of the *Lactobacillus* 30a ornithine decarboxylase. *Protein Sci* 4, 849-854.

Moore, J. E., and Elborn, J. S. (2001). *Burkholderia cepacia* and cystic fibrosis --50 years on *Commun Dis Public Health*.4,114-116.

Moskalew, S., Sochansk, K., and Wiwatows, T. (1974). Presence of a factor toxic to pancreatic Beta cells in some collagenaes preparations. *Bulletin de l'Académie polonaise des sciences. Série des sciences biologiques* 22, 127-130.

Moskowitz, S. M., Emerson, J. C., McNamara, S., Shell, R. D., Orenstein, D. M., Rosenbluth, D., Katz, M. F., Ahrens, R., Hornick, D., Joseph, P. M., Gibson, R. L., Aitken, M. L., Benton, W. W., and Burns, J. L. (2010). Randomized trial of biofilm testing to select antibiotics for cystic fibrosis airway infection. *Pediatr Pulmonol*,10, 184-192.

Mourtada, M., Brown, C. A., Smith, S. A., Piercy, V., Chan, S. L. F., and Morgan, N. G. (1997). Interactions between imidazoline compounds and sulphonylureas in the regulation of insulin secretion. *Br J Pharmacol* 121, 799–805.

Mshvildadze, M., and Neu, J. (2010). The infant intestinal microbiome: friend or foe? *Early Hum Dev* 86, 67-71.

Muirhead, R. P., and Hothersall, J. S. (1995). The effect of phenazine methosulphate on intermediary pathways of glucose metabolism in the lens at different glycaemic levels. *Exp Eye Res* 61, 619-627.

Mulder, S. J. S. J. (2005). Bacteria of food and human intestine are the most possible sources of the gad-trigger of type 1 diabetes. *Med Hypotheses* 65, 308-311.

Müller-Wieland, D., White, M. F., Behnke, B., Gebhardt, A., Neumann, S., Krone, W., and Kahn, C. R. (1991). Pertussis toxin inhibits autophosphorylation and activation of the insulin receptor kinase. *Biocheml Biop Res Co* 181, 1479-1485.

Muretta, J. M., and Mastick, C. C. (2009). Chapter 10: How insulin regulates glucose transport in adipocytes. In vitamins & hormones (L. Gerald, Ed.), pp. 245-286. Academic Press.

Myers, M., Mackay, I., and Zimmet, P. (2002). Digging up the dirt on vegetables. *Diabetes Voice* 47, 35-37.

Myers, M. A., Davies, J. M., Tong, J. C., Whisstock, J., Scealy, M., Mackay, I. R., and Rowley, M. J. (2000). Conformational epitopes on the diabetes autoantigen GAD65 identified by peptide phage display and molecular modeling. *J Immunol* 165, 3830-3838.

Myers, M. A., Hettiarachchi, K. D., Ludeman, J., Wilson, A., Wilson, C., and Zimmet, P. (2003). Dietary microbial toxins and type 1 diabetes. *Ann NY Acad Sci* 1005, 418-422.

Myers, M. A., Mackay, I. R., Rowley, M. J., and Zimmet, P. Z. (2001). Dietary microbial toxins and type 1 diabetes--a new meaning for seed and soil. *Diabetologia* 44, 1199-1200.

Narendran, P., Mannering, S. I., and Harrison, L. C. (2003). Proinsulin a pathogenic autoantigen in type 1 diabetes. *Autoimmun Rev* 2, 204-210.

Naya, F. J., M.M., C., and Tsai, M.-J. (1995). Tissue-specific regulation of the insulin gene by a novel basic helix-loop-helix transcription factor. *Genes Dev* 9 1009-1019.

NDIC (National Diabetes Information). (2012). Monogenic forms of diabetes: neonatal diabetes mellitus and maturity-onset diabetes of the young . US Department of Health and Human Service.

Nelson, J. (2008). Structure and function in cell signalling. John Wiley & Sons, Chichester, England ; Hoboken, NJ.

Neu, J., Lorca, G., Kingma, S. D., and Triplett, E. W. (2010). The intestinal microbiome: relationship to type 1 diabetes. *Endocrinol Metab Clin North Am* 39, 563-571.

Nijtmans, L. G. J., Henderson, N. S., and Holt, I. J. (2002). Blue native electrophoresis to study mitochondrial and other protein complexes. *Methods* 26, 327-334.

Nikoskelainen, S., Verho, S., Airas, K., and Lilius, E.-M. (2005). Adhesion and ingestion activities of fish phagocytes induced by bacterium *Aeromonas salmonicida* can be distinguished and directly measured from highly diluted whole blood of fish. *Dev Comp Immunol* 29, 525-537.

Notkins, A. L., and Lernmark, A. (2001). Autoimmune type 1 diabetes: resolved and unresolved issues. *J Clin Invest* 108, 1247-1252.

O'connor, c. d., and Hames, B. D. (2008). Proteomics. Bloxham, Oxfordshire : Scion, UK.

Ohneda, K., Ee, H., and German, M. (2000). Regulation of insulin gene transcription. *Semin Cell Dev Biol* 11, 227-233.

Olbrot, M., Rud, J., Moss, L. G., and Sharma, A. (2002). Identification of beta-cell-specific insulin gene transcription factor RIPE3b1 as mammalian MafA. *Proc Natl Acad Sci USA* 99, 6737-6742.

Oldstone, M. B. A. (1998). Molecular mimicry and immune-mediated diseases. *FASEB J.* 12, 1255-1265.

Osbak, K. K., Colclough, K., Saint-Martin, C., Beer, N. L., Bellanné-Chantelot, C., Ellard, S., and Gloyn, A. L. (2009). Update on mutations in glucokinase (GCK), which cause maturity-onset diabetes of the young, permanent neonatal diabetes, and hyperinsulinemic hypoglycemia. *Hum Mutat* 30, 1512-1526.

Panten, U., and Rustenbeck, I. (2008). Fuel-induced amplification of insulin secretion in mouse pancreatic islets exposed to a high sulfonylurea concentration: role of the NADPH/$NADP^+$ ratio. *Diabetologia* 51, 101-109.

Papakonstantinou, T., Law, R. H. P., Gardiner, P., Rowley, M. J., and Mackay, I. R. (2000). Comparative expression and purification of human glutamic acid decarboxylase from *Saccharomyces cerevisiae* and Pichia pastoris. *Enzyme Microb Tech* 26, 645-652.

Papouchado, M. L., Ermácora, M. R., and Poskus, E. (1996). Detection of glutamic acid decarboxylase (GAD) autoantibodies by indirect immunofluorescence using CHO cells expressing recombinant human GAD65. *J Autoimmun* 9, 689-697.

Park, K. B., and Oh, S.-H. (2007). Cloning, sequencing and expression of a novel glutamate decarboxylase gene from a newly isolated lactic acid bacterium, *Lactobacillus brevis* OPK-3. *Bioresource Technol* 98, 312-319.

Paulsen, I. T., Park, J. H., Choi, P. S., and Saier, M. H. (1997). A family of Gram-negative bacterial outer membrane factors that function in the export of proteins, carbohydrates, drugs and heavy metals from Gram-negative bacteria. *FEMS Microbio lett* 156, 1-8.

Peckham, D. D., Leonard, C. C., Range, S. S., and Knox, A. A. (1996). Nutritional status and pulmonary function in patients with cystic fibrosis with and without *Burkholderia cepacia* colonization: role of specialist dietetic support. *J Hum Nutr Diet* 9, 173.

Peng, H., and Hagopian, W. (2006). Environmental factors in the development of type 1 diabetes. *Rev Endocr Metab Disord* 7, 149-162.

Peschke, E. (2008). Melatonin, endocrine pancreas and diabetes. *J Pineal Res* 44, 26-40.

Petersen, J. S., Kulmala, P., Clausen, J. T., Knip, M., and Dyrberg, T. (1999). Progression to type 1 diabetes is associated with a change in the immunoglobulin isotype profile of autoantibodies to glutamic acid decarboxylase (GAD65). Childhood diabetes in finland study group. *Clin Immunol* 90, 276-281.

Pi, J., Bai, Y., Zhang, Q., Wong, V., Floering, L. M., Daniel, K., Reece, J. M., Deeney, J. T., Andersen, M. E., Corkey, B. E., and Collins, S. (2007). Reactive oxygen species as a signal in glucose-stimulated insulin secretion. *Diabetes* 56, 1783-1791.

Pierce, K. L., Premont, R. T., and Lefkowitz, R. J. (2002). Seven-transmembrane receptors. *Nat Rev Mol Cell Biol* 3, 639-650.

Pihoker, C., Gilliam, L. K., Hampe, C. S., and Lernmark, A. (2005). Autoantibodies in diabetes. *Diabetes* 54, S52-61.

Pittman, I., Philipson, L. H., and .Steiner, D. F. (2004). Diabetes and carbohydrate metabolism in insulin biosynthesis, secreton, structure and structure activity relationship, http:// www. endotext. org/ diabetes/ diabetes1/diabetesframe1.html.

Poitout, V., Hagman, D., Stein, R., Artner, I., Robertson, R. P., and Harmon, J. S. (2006). Regulation of the insulin gene by glucose and fatty acids. *J. Nutr* 136, 873-876.

Porte, D., Sherwin, R. S., Baron, A., Ellenberg, M., and Rifkin, H. (2003). *Ellenberg and Rifkin's diabetes mellitus :* theory and practice. McGraw-Hill, Health Professions Division, New York.

Poulin, G., Turgeon, B., and Drouin, J. (1997). NeuroD1/beta2 contributes to cell-specific transcription of the proopiomelanocortin gene. *Mol Cell Biol* 17, 6673-6682.

Prentki, M., Vischer, S., Glennon, M. C., Regazzi, R., Deeney, J. T., and Corkey, B. E. (1992). Malonyl-CoA and long chain acyl-CoA esters as metabolic coupling factors in nutrient-induced insulin secretion. *J Biol Chem* 267, 5802-5810.

Preveral, S., Gayet, L., Moldes, C., Hoffmann, J., Mounicou, S., Gruet, A., Reynaud, F., Lobinski, R., Verbavatz, J. M., Vavasseur, A., and Forestier, C. (2009). A common highly conserved cadmium detoxification mechanism from bacteria to humans: heavy metal tolerance conferred by the ATP-binding cassette (ABC) transporter SpHMT1 requires glutathione but not metal-chelating phytochelatin peptides. *J Biol Chem* 284, 4936-4943.

Punj, V., Sharma, R., Zaborina, O., and Chakrabarty, A. M. (2003). Energy-generating enzymes of *Burkholderia cepacia* and their interactions with macrophages. *J. Bacteriol* 185, 3167-3178.

Qu, K., Martin, D. L., and Lawrence, C. E. (1998). Motifs and structural fold of the cofactor binding site of human glutamate decarboxylase. *Protein Sci* 7, 1092-1105.

Rabinovitch, A., and Suarez-Pinzon, W. L. (1998). Cytokines and their roles in pancreatic islet beta cell destruction and insulin dependent diabetes mellitus. *Biochem Pharmacol* 55, 1139-1149.

Ran, H. M., Hassett, D. J., and Lau, G. W. (2003). Human targets of *Pseudomonas aeruginosa* pyocyanin. *P Nat Acad Sci USA* 100, 14315-14320.

Reinbothe, T. M., Ivarsson, R., Li, D. Q., Niazi, O., Jing, X., Zhang, E., Stenson, L., Bryborn, U., and Renstrom, E. (2009). Glutaredoxin-1 mediates NADPH-dependent stimulation of calcium-dependent insulin secretion. *Mol Endocrinol* 23, 893-900.

Renstrom, E., Ivarsson, R., and Shears, S. B. (2002). Inositol 3,4,5,6-tetrakisphosphate inhibits insulin granule acidification and fusogenic potential. *J Biol Chem* 277, 26717-26720.

Reszka, K. J., O'Malley, Y., McCormick, M. L., Denning, G. M., and Britigan, B. E. (2004). Oxidation of pyocyanin, a cytotoxic product from *Pseudomonas aeruginosa*, by microperoxidase 11 and hydrogen peroxide. *Free Radical Bio Med* 36, 1448-1459.

Richer, M. J., and Horwitz, M. S. (2009). Coxsackievirus infection as an environmental factor in the etiology of type 1 diabetes. *Autoimmun Rev* 8, 611-615.

Richter, W., Shi, Y., and Baekkeskov, S. (1993). Autoreactive epitopes defined by diabetes-associated human monoclonal antibodies are localized in the middle and C-terminal domains of the smaller form of glutamate decarboxylase. *Proc Natl Acad Sci USA* 90, 2832-2836.

Roep, B. O., Hiemstra, H. S., Schloot, N. C., De Vries, R. R., Chaudhuri, A., Behan, P. O., and Drijfhout, J. W. (2002). Molecular mimicry in type 1 diabetes: immune cross-reactivity between islet autoantigen and human cytomegalovirus but not Coxsackie virus. *Ann N Y Acad Sci* 958, 163-165.

Ronnestad, I., Gavaia, P. J., Viegas, C. S., Verri, T., Romano, A., Nilsen, T. O., Jordal, A. E., Kamisaka, Y., and Cancela, M. L. (2007). Oligopeptide transporter pepT1 in atlantic cod (*Gadus morhua*): cloning, tissue expression and comparative aspects. *J Exp Biol* 210, 3883-3896.

Rorsman, P., and Renstrom, E. (2003). Insulin granule dynamics in pancreatic beta cells. *Diabetologia* 46, 1029-1045.

Rubi, B., del Arco, A., Bartley, C., Satrustegui, J., and Maechler, P. (2004). The malate-aspartate NADH shuttle member aralar1 determines glucose metabolic fate, mitochondrial activity, and insulin secretion in beta cells. *J Biol Chem* 279, 55659-55666.

Rudek, M. A., Zhao, M., He, P., Zabelina, Y., Jin, R., Messersmith, W. A., Wolff, A. C., and Baker, S. D. (2005). Validation and implementation of a liquid chromatography/tandem mass spectrometry assay to quantitate dimethyl benzoylphenylurea (BPU) and its five metabolites in human plasma and urine for clinical pharmacology studies. *J Chromatogr B Analyt Technol Biomed Life Sci* 828, 41-54.

Sabbah, E., Kulmala, P., Veijola, R., Vahasalo, P., Karjalainen, J., Tuomilehto-Wolf, E., Akerblom, H. K., and Knip, M. (1996). Glutamic acid decarboxylase antibodies in relation to other autoantibodies and genetic risk markers in children with newly diagnosed insulin-dependent diabetes. childhood diabetes in finland study group. *J Clin Endocrinol Metab* 81, 2455-2459.

Saier, M. H., Jr (2000). Families of transmembrane transporters selective for amino acids and their derivatives. *Microbiology* 146, 1775-1795.

Saif-Ali, R., Harun, R., Kamaruddin, N., Al-Jassabi, S., and Ngah, W. (2012). Association of hepatocyte nuclear factor 4 alpha polymorphisms with type 2 diabetes with or without metabolic syndrome in malaysia. *Biochem Genet* 50, 298-308.

Salituro, G. M., Pelaez, F., and Zhang, B. B. (2001). Discovery of a small molecule insulin receptor activator. In recent progress in hormone research*, Vol 56*, pp. 107-126. *Endocrine Soc*, Bethesda.

Sambrook, J., and Russell, D. W. (2001). Molecular cloning : a laboratory manual. Cold Spring Harbor Laboratory Press, Cold Spring Harbor, N.Y.

Satin, L. S., Tavalin, S. J., Kinard, T. A., and Teague, J. (1995). Contribution of L- and non-L-type calcium channels to voltage-gated calcium current and glucose-dependent insulin secretion in HIT-T15 cells. *Endocrinology* 136, 4589-4601.

Schütt, C., Fürll, B., Stelter, F., Jack, R. S., and Witt, S. (1997). CHO transfectants produce large amounts of recombinant protein in suspension culture. *J Immunol Methods* 204, 99-102.

Seino, S., Takahashi, H., Fujimoto, W., and Shibasaki, T. (2009). Roles of cAMP signalling in insulin granule exocytosis. *Diabetes Obes Metab* 11 Suppl 4, 180-188.

Semiz, S., Park, J. G., Nicoloro, S. M., Furcinitti, P., Zhang, C., Chawla, A., Leszyk, J., and Czech, M. P. (2003). Conventional kinesin KIF5B mediates insulin-stimulated GLUT4 movements on microtubules. *EMBO J* 22, 2387-2399.

Seng, P., Rolain, J. M., Fournier, P. E., La Scola, B., Drancourt, M., and Raoult, D. (2010). MALDI-TOF-mass spectrometry applications in clinical microbiology. *Future Microbiol* 5, 1733-1754.

Shao, J., Catalano, P. M., Yamashita, H., Ruyter, I., Smith, S., Youngren, J., and Friedman, J. E. (2000). Decreased insulin receptor tyrosine kinase activity and plasma cell membrane glycoprotein-1 overexpression in skeletal muscle from obese women with gestational diabetes mellitus (GDM): evidence for increased serine/threonine phosphorylation in pregnancy and GDM. *Diabetes* 49, 603-610.

Sharp, D. (2009). Environmental toxins, a potential risk factor for diabetes among Canadian Aaboriginals. *Int J Circumpolar Health* 68, 316-326.

Sheldon, K. (2004). Cell signalling pathways : productive sources of pharmaceutical targets. D & MD Publications, Westborough, MA.

Shushan, E. B., Cerasi, E., and Melloul, D. (1999). Regulation of the insulin gene by glucose: stimulation of trans-activation potency of human PDX-1 N-terminal domain. *DNA Cell Biol* 18, 471-479.

Siljander, H., Harkonen, T., Hermann, R., Simell, S., Hekkala, A., Salonsaari, R. T., Simell, T., Simell, O., Ilonen, J., Veijola, R., and Knip, M. (2009). Role of insulin autoantibody affinity as a predictive marker for type 1 diabetes in young children with HLA-conferred disease susceptibility. *Diabetes Metab Res Rev* 25, 615-622.

Silva, L. B., Santos, S. S. S., Azevedo, C. R., Cruz, M. A. L., Venâncio, T. M., Cavalcante, C. P., Uchôa, A. F., Astolfi Filho, S., Oliveira, A. E. A., Fernandes, K. V. S., and Xavier-Filho, J. (2002). The leaves of green plants as well as a cyanobacterium, a red alga, and fungi contain insulin-like antigens. *Braz J Med Biol Res* 35, 297-303.

Silva, S. J. N. d., Schuch, P. Z., Bernardi, C. R., Vainstein, M. H., Jablonski, A., and Bender, R. J. (2007). Patulin in food: state of the art and analytical trends. *Revista Brasileira de Fruticultura* 29, 406-413.

Simpson, A. A., and Wuthiekanun, A. V. (2000). Interaction of insulin with *Burkholderia pseudomallei* may be caused by a preservative. *J Clin pathol* 53, 159-160.

Singaram, S. S., Lawrence, R. S., and Hornemann, U. (1979). Studies on the biosynthesis of the antibiotic streptozocin by *Streptomyces achromogenes* var streptozoticus feeding experiments with C-14 and tritium labeled precursors. *J Antibiot* 32, 379-385.

Siuzdak, G. (1994). The emergence of mass spectrometry in biochemical research. *Proc Natl Acad Sci USA* 91, 11290-11297.

Skretas, G., and Georgiou, G. (2008). Engineering G protein-coupled receptor expression in bacteria. *P Nat Acad Sci USA* 105, 14747-14748.

Smalley, J. W., Charalabous, P., Birss, A. J., and Hart, C. A. (2001). Detection of heme-binding proteins in epidemic strains of *Burkholderia cepacia*. *Clin Diagn lab immun* 8, 509-514.

Smith, A. J., Taneja, T. K., Mankouri, J., and Sivaprasadarao, A. (2007). Molecular cell biology of KATP channels: implications for neonatal diabetes. *Expert Rev Mol Med* 9, 1-17.

Smith, D. K., Kassam, T., Singh, B., and Elliott, J. F. (1992). *E. coli* has two homologous glutamate decarboxylase genes that map to distinct loci. *J. Bacteriol* 174, 5820-5826.

Soares, M. B., Schon, E., Henderson, A., Karathanasis, S. K., Cate, R., Zeitlin, S., Chirgwin, J., and Efstratiadis, A. (1985). RNA-mediated gene duplication: the rat preproinsulin I gene is a functional retroposon. *Mol Cell Biol* 5, 2090-2103.

Sokol, P. A., Darling, P., Lewenza, S., Corbett, C. R., and Kooi, C. D. (2000). Identification of a siderophore receptor required for ferric ornibactin uptake in *Burkholderia cepacia*. *Infect Immun* 68, 6554-6560.

Souza, A. M. F. d., and López, J. A. (2004). Insulin or insulin-like studies on unicellular organisms: a review. *Braz Arch Biol Tech* 47, 973-981.

Sparkman, O. D. (2000). Mass spectrometry desk reference. Global View Pub., Pittsburgh, Pa. Cincinnati, Ohio,USA.

Stayoussef, M., Benmansour, J., Al-Jenaidi, F. A., Said, H. B., Rayana, C. B., Mahjoub, T., and Almawi, W. Y. (2011). GAD65 and IA-2 autoantibodies in relation to HLA Class II DR and DQ alleles and haplotypes in type 1 diabetes mellitus. *Clin Vaccine Immunol*.

Stefaan, W., and Brian, A. H. (1995). Serine/threonine protein phosphatases. *Biochem. J* 311, 17-29.

Steiner, D. F., Chan, S. J., Welsh, J. M., and Kwok, S. C. (1985). Structure and evolution of the insulin gene. *Annu Rev Genet* 19, 463-484.

Steiner, H.-Y., Naider, F., and Becker, J. M. (1995). The PTR family: a new group of peptide transporters. *Mol Microbiol* 16, 825-834.

Stene, L. C., Oikarinen, S., Hyöty, H., Barriga, K. J., Norris, J. M., Klingensmith, G., Hutton, J. C., Erlich, H. A., Eisenbarth, G. S., and Rewers, M. (2010). Enterovirus infection and progression from islet autoimmunity to type 1 diabetes. *Diabetes* 59, 3174-3180.

Stephan, H., Freund, S., Beck, W., Jung, G., Meyer, J. M., and Winkelmann, G. (1993). Ornibactins a new family of sidrophores from *Pseudomonas.* Biometals 6, 93-100.

Stoyanova, M., Pavlina, I., Moncheva, P., and Bogatzevska, N. (2007). Biodiversity and incidence of *Burkholderia* species. *Biotechnol Biotec. Eq.* 21, 306-310.

Straub, S. G., and Sharp, G. W. (2002). Glucose-stimulated signaling pathways in biphasic insulin secretion. *Diabetes Metab Res Rev* 18, 451-463.

Syren, K., Lindsay, L., Stoehrer, B., Jury, K., Luhder, F., Baekkeskov, S., and Richter, W. (1996). Immune reactivity of diabetes-associated human monoclonal autoantibodies defines multiple epitopes and detects two domain boundaries in glutamate decarboxylase. *J Immunol* 157, 5208-5214.

Tanaka, S., Maeda, S., Hashimoto, M., Fujimori, C., Ito, Y., Teradaira, S., Hirota, K., Yoshitomi, H., Katakai, T., Shimizu, A., Nomura, T., Sakaguchi, N., and Sakaguchi, S. (2010). Graded attenuation of TCR signaling elicits distinct autoimmune diseases by altering thymic T cell selection and regulatory T cell function. *J Immunol* 185, 2295-2305.

Thams, P., and Capito, K. (1997). Inhibition of glucose-induced insulin secretion by the diacylglycerol lipase inhibitor RHC 80267 and the phospholipase A2 inhibitor ACA through stimulation of K^+ permeability without diminution by exogenous arachidonic acid. *Biochem Pharmacol* 53, 1077-1086.

Thomas, M. (2007). Iron acquisition mechanisms of the;Burkholderia cepacia complex. *Biometals* 20, 431-452.

Tisch, R., and McDevitt, H. (1996). Insulin-dependent diabetes mellitus. *Cell* 85, 291-297.

Tiwari, S., Pratyush, D. D., Dwivedi, A., Gupta, S. K., Rai, M., and Singh, S. K. (2012). Microbiological and clinical characteristics of diabetic foot infections in northern India. *J Infect Dev Ctries* 6, 329-332.

Tomii, K., and Kanehisa, M. (1998). A comparative analysis of ABC transporters in complete microbial genomes. *Genome Res* 8, 1048-1059.

Towbin, H., Staehelin, T., and Gordon, J. (1979). Electrophoretic transfeer of proteins frome polyacrylamide gels to nitrocellulose sheets-proceduer and some applications . *P Natl Acad Sci USA* 76, 4350-4354.

Tridgell, D. M., Spiekerman, C., Wang, R. S., and Greenbaum, C. J. (2011). Interaction of onset and duration of diabetes on the percent of GAD and IA-2 antibody-positive subjects in the type 1 diabetes genetics consortium database. *Diabetes Care* 34, 988-993.

Tripathy, D., and Chavez, A. O. (2010). Defects in insulin secretion and action in the pathogenesis of type 2 diabetes mellitus. *Curr Diab Rep* 10, 184-191.

Trust, T. J., Kostrzynska, M., Emody, L., and Wadstrom, T. (1993). High-affinity binding of the basement membrane protein collagen type IV to the crystalline virulence surface protein array of *Aeromonas salmonicida*. *Mol Microbiol* 7, 593-600.

Tuomi, T., Rowley, M. J., Knowles, W. J., Chen, Q. Y., McAnally, T., Zimmet, P. Z., and Mackay, I. R. (1994). Autoantigenic properties of native and denatured glutamic acid decarboxylase: evidence for a conformational epitope. *Clin Immunol Immunopathol* 71, 53-59.

Tuomilehto, J., Vidgren, G., Toivanen, L., Tuomilehto-Wolf, E., Kohtamaki, K., Stengård, J., Zimmet, P., Mackay, I. R., Rowley, M., and Koskela, P. (1994). Antibodies to glutamic acid decarboxylase as predictors of insulin-dependent diabetes mellitus before clinical onset of disease. *Lancet* 343, 1383-1385.

Turk, J., Corbett, J. A., Ramanadham, S., Bohrer, A., and McDaniel, M. L. (1993). Biochemical evidence for nitric oxide formation from Streptozotocin in isolated pancreatic islets. *Biochem Bioph Res Co* 197, 1458-1464.

Vaarala, O. O. (2000). The role of the gut in -cell autoimmunity and type 1 diabetes: a hypothesis. *Pediatric diabetes* 1, 217.

Van Lummel, M., van Veelen, P. A., Zaldumbide, A., de Ru, A., Janssen, G. M. C., Moustakas, A. K., Papadopoulos, G. K., Drijfhout, J., Roep, B. O., and Koning, F. (2012). The type 1 diabetes associated HLA-DQ8-trans dimer accomodates a unique peptide repertoire. *J Biol Chem* 16, 9514-24.

Vercelli, D. (2006). Mechanisms of the hygiene hypothesis - molecular and otherwise. *Curr Opin Immunol* 18, 733-737.

Vikman, J., Svensson, H., Huang, Y. C., Kang, Y., Andersson, S. A., Gaisano, H. Y., and Eliasson, L. (2009). Truncation of SNAP-25 reduces the stimulatory action of cAMP on rapid exocytosis in insulin-secreting cells. *Am J Physiol Endocrinol Metab* 297, E452-461.

Virtanen, S. M., Roivainen, M., Andersson, M. A., Ylipaasto, P., Hoornstra, D., Mikkola, R., and Salkinoja-Salonen, M. S. (2008). *In vitro* toxicity of cereulide on porcine pancreatic langerhans islets. *Toxicon* 51, 1029-1037.

Walker, M. D. (2004). Pancreatic transcription factors: Implications for diabetes therapy. *Israel Med Assoc J* 6, 262-264.

Wang, D. S., Dickson, D. W., and Malter, J. S. (2006). beta-amyloid degradation and Alzheimer's disease. *J Biomed Biotechnol* 2006, 58406.

Wang, Z., and Thurmond, D. C. (2009). Mechanisms of biphasic insulin-granule exocytosis - roles of the cytoskeleton, small GTPases and SNARE proteins. *J Cell Sci* 122, 893-903.

Watada, H., Kajimoto, Y., Umayahara, Y., Matsuoka, T., Kaneto, H., Fujitani, Y., Kamada, T., Kawamori, R., and Yamasaki, Y. (1996). The human glucokinase gene beta-cell-type promoter: an essential role of insulin promoter factor 1/PDX-1 in its activation in HIT-T15 cells. *Diabetes* 45, 1478-1488.

Welker, M., and Moore, E. R. (2011). Applications of whole-cell matrix-assisted laser-desorption/ionization time-of-flight mass spectrometry in systematic microbiology. *Syst Appl Microbiol* 34, 2-11.

Westall, F. C. (2006). Molecular mimicry revisited: gut bacteria and multiple sclerosis. *J Clin Microbiol* 44, 2099-2104.

Wheeler, A., Wang, C., Yang, K., Fang, K., Davis, K., Styer, A. M., Mirshahi, U., Moreau, C., Revilloud, J., Vivaudou, M., Liu, S., Mirshahi, T., and Chan, K. W. (2008). Coassembly of different sulfonylurea receptor subtypes extends the phenotypic diversity of ATP-sensitive potassium (K_{ATP}) channels. *Mol Pharmacol* 74, 1333-1344.

Whitby, p. W., Carter, K. B., Hatter, K. l., Lpuma, J. j., and Stull, T. L. (2000). Identification of members of the *Bulkholderia cepatia* complex by species specific PCR. *J Clin Microbiol* 38, 2962-2965.

White, I. N., and Brown, K. (2004). Techniques: the application of accelerator mass spectrometry to pharmacology and toxicology. *Trends Pharmacol Sci* 25, 442-447.

Williams, G. G., and Pickup, J. C. J. C. (2004). Handbook of diabetes. Blackwell Publishing Ltd, UK.

Wilson, K., and Walker, J. M. (2005). Principles and techniques of biochemistry and molecular biology. Cambridge University Press, Cambridge; New York.

Wilson, M. E., Scheel, D., and German, M. S. (2003). Gene expression cascades in pancreatic development. *Mech Develop* 120, 65-80.

Wilson, R., Sykes, D. A., Watson, D., Rutman, A., Taylor, G. W., and Cole, P. J. (1988). Measurement of *Pseudomonas aeruginosa* phenazine pigments in sputum and assessment of their contribution to sputum sol toxicity for respiratory epithelium. *Infect Immun.* 56, 2515-2517.

Wollheim, C. B., Blondel, B., and Sharp, G. W. G. (1974). Effect of cholera toxin on insulin release in monolayer cultures of the endocrine pancreas. *Diabetologia* 10, 783-787.

Wong, D. W. S. (2006). The ABCs of gene cloning. Springer, New York, NY.

Wood, C., Williams, C., and Waldron, G. J. (2004). Patch clamping by numbers. *Drug Discov Today* 9, 434-441.

Woods, D. E., Jones, A. L., and Hill, P. J. (1993). Interaction of insulin with *Pseudomonas pseudomallei. Infect Immun.* 61, 4045-4050.

Wouters, M. F. A., and Speijers, G. J. A. (1995). Toxicological evaluations of certain food additives and contaminants in food: Patulin. *WHO Food Addit* 35, 377–402.

Yamashita, K., Cram, D. S., and Harrison, L. C. (1993). Molecular cloning of full-length glutamic acid decarboxylase 67 from human pancreas and islets. *Biochem Bioph Res Co* 192, 1347-1352.

Yazdchi-Marandi, L., Yazdanparast, R., and Rafieii, S. (2000). Oral administration of *E. coli* glutamic acid decarboxylase has immunomodulatory effects in streptozotocin-induced diabetes. *Microbios* 102, 135-145.

Yen, M.-R., Peabody, C. R., Partovi, S. M., Zhai, Y., Tseng, Y.-H., and Saier, M. H. (2002). Protein-translocating outer membrane porins of Gram-negative bacteria. *BBA -Biomembranes* 1562, 6-31.

Youngren, J. F. (2007). Regulation of insulin receptor function. *Cell Mol Life Sci* 64, 873-891.

Yu, X., Murao, K., Sayo, Y., Imachi, H., Cao, W. M., Ohtsuka, S., Niimi, M., Tokumitsu, H., Inuzuka, H., Wong, N. C., Kobayashi, R., and Ishida, T. (2004). The role of calcium/calmodulin-dependent protein kinase cascade in glucose upregulation of insulin gene expression. *Diabetes* 53, 1475-1481.

Yuhara, S., Komatsu, H., Goto, H., Ohtsubo, Y., Nagata, Y., and Tsuda, M. (2008). Pleiotropic roles of iron-responsive transcriptional regulator Fur in *Burkholderia multivorans*. *Microbiology* 154, 1763-1774.

Zechel, M. A., Elliott, J. F., Atkinson, M. A., and Singh, B. (1998). Characterization of novel T-cell epitopes on 65 kDa and 67 kDa glutamic acid decarboxylase relevant in autoimmune responses in NOD Mice. *J Autoimmun* 11, 83-95.

Zhai, Y. F., Heijne, W., and Saier, M. H. (2003). Molecular modeling of the bacterial outer membrane receptor energizer, ExbBD/TonB, based on homology with the flagellar motor, MotAB. *BBA- Biomembranes* 1614, 201-210.

Zhang, C., Moriguchi, T., Kajihara, M., Esaki, R., Harada, A., Shimohata, H., Oishi, H., Hamada, M., Morito, N., Hasegawa, K., Kudo, T., Engel, J. D., Yamamoto, M., and Takahashi, S. (2005). MafA is a key regulator of glucose-stimulated insulin secretion. *Mol Cell Biol* 25, 4969-4976.

Zhao, Z. S., Granucci, F., Yeh, L., Schaffer, P. A., and Cantor, H. (1998). Molecular mimicry by herpes simplex virus-type 1: autoimmune disease after viral infection. *Science* 279, 1344-1347.

Zhou, S. M., Jiang, L. P., Geng, C. Y., Cao, J., and Zhong, L. F. (2010). Patulin-induced oxidative DNA damage and p53 modulation in HepG2 cells. *Toxicon* 55, 390-395.

Zimmet, P. (1996). Antibodies to glutamic acid decarboxylase in the prediction of insulin dependency. *Diabetes Res Clin Pract 34 Suppl, S12*5-131.

Zirbes, J., and Milla, C. E. (2009). Cystic fibrosis related diabetes. *Paediatr Respir Rev* 10, 118-123.

Zünkler, B. J., and Wos, M. (2003). Effects of lomefloxacin and norfloxacin on pancreatic beta-cell ATP-sensitive K^+ channels. *Life Sci* 73, 429-435.

Appendix 1

Media preparation and formulation of reagents

SDS-PAGE reagent

Buffer A

Tris-HCL	0.75 M
SDS	0.05 %

The pH adjusted to 8.8 with NaOH .

Buffer B

Tris-HCl	0.025 M
SDS	0.2 %

The pH adjusted to 6.8 with HCI.

Electrophoresis buffer

Tris-HCl	25 mM
Glycine	250 mM
SDS	0.2 %

The pH adjusted to 8.3 with NaOH.

SDS-PAGE loading buffer (2X)

Tris-HCL (0.5M)	2.5 ml
SDS (10%) 0.2 ml	
B-mercaptoethanol	0.5 ml
Bromophenol Blue (0.1%)	0.5 ml
Glycerol	2 ml
dd H_2O	6.3 ml

SDS -Solution (10%)

SDS stock (10%) made in 100 ml volumes, filtrated using Whatman paper filter and stored at ambient temperature for no more than 1week.

Ammonium persulphates (APS)

10%W/V, solution in dd H_2o was prepared immediately prior to use.

Resolving gel 12.5%

Buffer A	5.2 ml
dd H_2O	1.4 ml
Acryl Mix (30:1)	4.4 ml
APS	100 µl
TEMED	30 µl

Stacking gel (5%)

Buffer B	2 ml
dd H_2O	1.3 ml
Acryl Mix (30:1)	0.7 ml
APS	100 µl
TEMED	15 µl

Polyacrylamide gels staining buffer1/1L

Coomassie brilliant Blue –R	1.25 gm
Methanol	400 ml
Glacial Acetic Acid	70 ml
dd H_2O	530 ml

The staining solution was filtered by whatman No.1 filter paper.

Distaining solution/1L

Methanol	400 ml
Glacial Acetic Acid	70 ml
dd H_2O	530 ml

Blue native electrophoresis-PAGE (BN-PAGE)

Sample buffer solutions

Mopes /sucrose	440 mM sucrose, 20 mM mopes, 1 mM EDTA, 0.2 mM PMSF
Aminocaproic acid	1ml in 50 mM Tris-HCl (pH7.0)
Dodcylmaltoside	5% (W/V)
Coomassie Blue G250	5% (W/V)

Sample Buffer

Mopes sucrose buffer	250µl
Aminocaproic acid	40µl
Dodecyl maltoside	20µl
Comassi blue G250	10µl

Gel Buffer PH 7.0 at 4 °C

Acrylamide (Acryl Mix (30:1)

Gel buffer (3X)	150 mM bis –Tris, 1.5mM Aminocaproic acid
Anode Buffer	50 mM bis-tris –HCl
Cathode Buffer A	50mM Tricine ,15mMbis tris – HCl
Cathode Buffer B	Cathode Buffer A = 0.02% Coomassie Blue G250

Casting the Gel Buffer

Acrylamide	2.6 ml
Gel buffer (3X)	3.33 ml
Glycerol	2 ml
H_2O	1.98 ml
APS (10%) 30 µl	
TEMED	3 µl

Stacking Gel

Acrylamide	0.4 ml
Gel buffer (3X)	1.67 ml
dd H_2O	2.87 ml
APS (10%)	5.5 µl

TEMED	3µl

Protein agrose gel electrophorsis

Buffer A

Tris-HCl	25 mM (PH- 8.5)
Glycine	19.2 mM

Sample Buffer

Glycerol	20 %
Bromophenole blue	0.2 %
Tris-base	0.12 M

Horizontal agarose gel

0.8 % W/V agrose gel dissolved in buffer A.

Western ligand blotting reagents

Transfer buffer / 2L

Tris –HCl	6.1 gm
Glycine	28.8 gm
Methanol	400 ml
dd H_2O	1600 ml

The pH adjusted to 8.3

PBS dulbecco's

One tablet (Oxoid) dissolved in 100 ml dd H_2O .Sterilised by autoclaving for 15 min at 151b/in^2.

Blocking reagent for ligand blotting

3% W/V bovine serum albumin (BSA) in 10mM of MOPS buffer.

Blocking reagent for western blotting

3% W/V bovine serum albumin (BSA) prepared in washing buffer.

Blocking Buffer

PBS	0.1M
Tween 20	0.1%
BSA	3%

Washing Buffer

PBS	0.1 M
Tween20	0.1 %

DAB/Nickel chloride development solution

PBS	100 ml
DAB	0.06 gm
$NiCl_2$	0.03 gm

Solution made freshly immediately prior to use in ligand blot development and the chromogenic reaction initiated by addition of 100 µl H_2o_2 solution.

Ponceau S staining buffer
Prepared by dissolving 1 gm of Ponceau S in 100 ml of 10 % acetic acid.

Culture medias

LB Agar (1L)

NaCl	10 g
Tryptone	10 g
Yeast extracts	5 g
Agar	20 g

H_2O dye was added to a final volume of 1 litre, pH Adjusted to 7 with 5 N NaOH, Sterilised by autoclaving for 15 min at 15 lbs/in^2.

Bacteroides Bile Esculin Agar (BBE) /1L

Oxgall	20 gm
Pancreatic Digested Casein	15 gm
Peptic digest of soybean meal	5 gm
NaCl	5 gm
Esculin	1 gm
Ferric ammonium citrate	0.5 gm
Gentamicin	0.1 gm
Hemin	1 2.5 mg
Vitamin K solution (10mM)	1 ml
Agar	15 gm

H_2O dd was added to a final volume of 1 litre, pH Adjusted to 7.0 with 5 N NaOH, Sterilised by autoclaving for 15 min at 15 lbs/in^2.

LB Broth (1L)

NaCl	10 g
Tryptone	10 g
Yeast extracts	5 g

H_2O dd was to a final volume of 1 litre, pH was adjusted to 7.0 with 5 N NaOH, Sterilised by autoclaving for 15 min at 15 lbs/in^2.

LB Broth with Supplements
LB broth (1 litre)' the following filter-sterilized supplements ($MgSO_4$ and Maltose) to final concentration 10 and 2 mM respectively, were added prior to use.

LB–Kanamycin Agar (1L)
LB agar (1 liter) was prepared, cooled to 55 °C and 4 ml of 12.5 mg/ml Kanamycin (filter sterilized) was added.

LB– Kanamycin Broth (1L)
LB broth (1 litre) was prepared, pH was adjusted to 7.0 with 5 N NaOH, Sterilised by autoclaving for 15 min at 15 lbs/in^2 . Cool to 55 °C and 4 ml of 12.5 mg/ml Kanamycin was added (filter sterilized).

NZY Agar (1L)

NaCl	5 gm
MgSO4 **.**7H_2O	2 gm
Yeast Extract	5 gm
Casein hydrolysate	10 gm
Agar	15 gm

H_2O dd was added to a final volume of 1 litre, pH adjusted to 7.0 with 5 N NaOH, Sterilised by autoclaving for 15 min at 15 lbs/in^2.

NZY Broth (1L)

NaCl	5 gm
MgSO4 .7H2O	2 gm
Yeast Extracts	5 gm
Casein hydrolysate	10 gm

H2O dd was added to a final volume of 1 litre, pH adjusted to 7.0 with 5 N NaOH, sterilised by autoclaving for 15 min at 15 lbs/in^2.

NZY Top Agar (1L)

NZY broth	1 litre
Agrose	0.7% (w/v)

Sterilised by autoclaving for 15 min at 15 lbs/in^2.

Miniprep plasmid DNA extraction reagents

Solution B&D I

Tris-base	25 mM
EDTA	10 mM
Glucose	50 mM

The pH Adjusted to 8.0 with 5 N NaOH, sterilised by autoclaving for 15 min at 15 lbs/in^2.

Solution B&D II

SDS	1%
NaOH	0.2 M

Solution B&D III

Sodium Acetate	3M

pH Adjusted to 4.8 with 5 N NaOH, sterilised by autoclaving for 15 min at 15 lbs/in^2.

Solution B&D IV

Tris-HCl	0.05 M
Sodium Acetate	0.1 M

The pH Adjusted to 8.0 with 5 N NaOH, Sterilised by autoclaving for 15 min at 15 lbs/in^2.

TE Buffer

Tris-base	10 mM
EDTA	1 mM

pH Adjusted to 8.0 with 5 N NaOH, sterilised by autoclaving for 15 min at 15 lbs/in^2.

DNA loading buffer (5X)

TE Buffer	10 ml
Ficoll	15 %
Bromophenole blue	0.25%

TBE buffer (5X)

Tris-base	54 gm
EDTA	20ml (EDTA 0.5 M, PH 8)
Boric Acid	27.5 gm

H_2O dd was added to a final volume of 1 litre, pH Adjusted to 8.0 with 5 N NaOH, sterilised by autoclaving for 15 min at 15 lbs/in^2.

SM Buffer /1L

NaCl	5.8 gm
MgSO4 ·7H_2O	2.0 gm
Tris-HCl	50.0 ml (1 M, pH 7.5)
Gelatine	5.0 ml (2% (w/v)

H_2O dd was added to a final volume of 1 litre, pH Adjusted to 7.5 with 5 N NaOH, sterilised by autoclaving for 15 min at 15 lbs/in^2.

Blue /white screening

X-gal solution

5-bromo-4-chloro-3-indolyl-β—D-galactoside (X-gal) made up as stock solution 250mg/ml indimethylformamide (DMF). Filters sterilised and store at 4°C.

IPTG solution

Isopropyl-β-thiogalctopyranoside (IPTG) made up as stock solution 0.5M in molecular biology water. Filter sterilised and stored at 4 °C.

Southern blotting reagents

SSc (20x)

$Na_3C_6H_5O_7$	88 gm
NaCl	175.32 gm

H_2O dd was added to a final volume of 1 litre, pH Adjusted to 7.0 with 5 N NaOH, Sterilised by autoclaving for 15 min at 15 lbs/in^2.

Denaturation solution

NaCl	1.5 M
NaOH	0.5 M

Neutralization solution

NaCl	1.5 M
Tris-HCl	1 M

H_2O dd was added to a final volume of 1 litre, pH Adjusted to 8.0 with 5 N NaOH, Sterilised by autoclaving for 15 min .at 15 lbs/in^2.

Washing Buffer

Maleic acid	0.1 M
NaCl	0.15 M
Tween-20	3% (v/v) added after autoclaving

H_2O dd was added to a final volume of 1 litre, pH adjusted to 7.5 with 5 N NaOH, sterilised by autoclaving for 15 min at 15 lbs/in^2.

Prehybrdisation buffer

Dissolve 50 gm in 100 ml of detection buffer.

Maleic acid buffer

Maleic acid	0.1 M
NaCl	0.15 M

H_2O dd was added to a final volume of 1 litre, pH adjusted to 7.5 with 5 N NaOH, Sterilised by autoclaving for 15 min at 15 lbs/in^2.

Detection buffer

Tris-HCl	0.1 M
NaCl	0.1 M

H_2O dd was added to a final volume of 1 litre, pH adjusted to 7.5 with 5 N NaOH, Sterilised by autoclaving for 15 min at 15 lbs/in^2.

Stringency buffer -1

SSc	2 X
SDS	0.1 %

H_2O dd was added to a final volume of 1 litre, pH adjusted to 7 with 5 N NaOH, Sterilised by autoclaving for 15 min at 15 lbs/in^2.

Stringency buffer -2

SSc	0.5 X
SDS	0.1 %

Add dd H2O to a final volume of 1 litre, adjusted pH to 7.0 with 5 N NaOH, Sterilised by autoclaving for 15 min at 15 lbs/in^2.

<u>Cytotoxicity effect of Microbial compounds on pancreatic (INS-1)</u>

Cell Culture of INS-1 cells

RPMI 1640	
Glucose	11mM
Glutamine	2mM

Foetal Bovine serum (FBS)	10%
Penicillin	100 unit/ml
Streptomycin	100 µg/ml
Sodium Pyruvate	1 mM
β-Mercaptoethanol	50 µM

Cytotoxic agents stocks

Pyrrolnitrin	10 mg/ml ethanol
Phenazine	10 mg/ml acetone
Patulin	10 mg/ml MBW

Serial diluted stock solutions prepared from each compounds.

Insulin Secretion Assay

Insulin assay Buffer (IAB)/1L

Na_2HPO_4	2.85 gm
KH_2PO_4	0.675 gm
NaCl	4.5 gm
EDTA	1.86 gm
BSA	2.5 gm (added last)

Dissolved in 500ml MBW and buffer was adjusted to pH 7.4.

Gey & Gey Buffer (10X) /L

NaCl	1 M
$NaHCO_3$	250 mM
KCl	3.7 gm

M reagent

$MgCl_2$ .6 H_2O	10.15 gm
$MgSO_4$ .7 H_2O	3.7 gm

Dissolved in 100 ml MBW and the buffer was adjusted to pH 7.4.

P reagent

Na_2HPO_4	7.1 gm
KH_2PO_4	2 gm

Dissolved in 100 ml MBW and the buffer was adjusted to pH 7.4.

Gey & Gey (1x)

Gey & Gey(10x)	100 ml
ddH_2O	900 ml
M+P	2 ml aliquots
$CaCl_2$ (1M)	1 ml

Buffer was adjusted to pH 7.4

Gey & Gey-A

Gey & Gey (1x)	100 ml
Glucose	0.2 mM
BSA	0.1%

Gey & Gey-B

Gey & Gey (1x)	100 ml
Glucose	20 mM
BSA	0.1%

Gey & Gey-C

Gey & Gey (1x)	100 ml
KCl	25 mM
BSA	0.1 %

Radioimmunoassay

Crystalline human insulin

Human insulin stock prepared as stock 8ng/ml in insulin assay buffer used to prepare one fold dilutions 8 ng-0.25 ng /ml to perform the standard curve.

Hot Insulin

^{125}I insulin was prepared as stock (0.5 µCi/8ml IAB).

Guinea Pig anti-bovine insulin antibody (ICN)

ICN prepared as 1 in 20000 IAB.

Gamma globulins reagents

Gamma globulins	2 mg/ml PBS
PEG 6000	30 % IAB
Tween 20	0.05 %

Gamma globulins prepared freshly in PBS and mixed with PEG reagents 1:1 prior RIA assay and supplemented with 0.05% Tween 20.

Protein extraction buffer

Hepes	50 mM
NaCl	150 mM
DTT	1 mM
EDTA	0.5 mM

The buffer was prepared in dd H_2O and the buffer was adjusted to pH=7.5.

Cleavage Solution

TEV Protease	66 µl
Protein extraction buffer	1.1ml

DNase Solution: 0.5mg/ml halotag buffer

Lysozyme Stock: Lysozyme 10mg/ml halotag buffer

ATP Solution: 1M

Alkaline Phosphatase Detection Buffer

NaCl	0.1M
Tris-OH	0.1M
$MgCl_2$	5 mM

The buffer was prepared in dd H_2O and the buffer was adjusted to pH=9.5, 5-bromo-4-chloro-3-indolyl phosphate (BCIP) 0.02 % and p-nitro blue tetrazolium (NBT) 0.03% dissolved in DMF was added.

Appendix 2

Data relevant for this study

Data relevant for chapter (3 & 4) pancreatic β-cells toxicity and insulin pathway modulation by microbial compounds

Figure 1 Sequencing results of insulin pathway amplicons confirming the ID of the insulin pathway genes that assessed by qRT-PCR during this study.

Rattus norvegicus, insulin, mRNA NM_019129.2, the blue highlighted sequences is INS-1M primer binding sites and INS-1 primers are highlighted in red.

```
          78 gcc ctgctcgtcc tctgggagcc caagcctgcc caggcttttg
121 tcaaacagca cctttgtggt cctcacctgg tggaggctct gtacctggtg tgtggggaac
181 gtggtttctt ctacacaccc aagtcccgtc gtgaagtgga ggacccgcaa gtgccacaac
241 tggagctggg tggaggcccg gaggccgggg atcttcagac cttggcactg gaggttgccc
301 ggcagaagcg tggcattgtg gatcagtgct gcaccagcat ctgctccctc taccaactgg
361 agaactactg caactgagtc caccactccc cgcccacccc tctgcaatg 409
```

Rattus norvegicus, mRNA NM_019130, the blue highlighted sequences is INS-2M primer binding sites and INS-2 primers are highlighted in red.

```
12 gatccgctt cctgcccctg ctggccctgc tcatcctctg ggagccccgc
 61 cctgcccagg cttttgtcaa acagcacctt tgtggttctc acttggtgga agctctctac
121 ctggtgtgtg gggagcgtgg attcttctac acacccatgt cccgccgcga agtggaggac
181 ccacaagtgg cacaactgga gctgggtgga ggcc 214
```

Rattus norvegicus, β-actin, mRNA NM_031144.2 primers binding sites are highlighted in red.

```
   251 aggcccaaga gcaagagagg catcctgaccc tgaagtaccc cattgaacac
301 ggcattgtca ccaactggga cgatatggag aagatttggc accacacttt ctacaatgag
361 ctgcgtgtgg cccctgagga gcaccctgtg ctgctcaccg aggccctct gaaccctaag
421 gccaaccgtg aaaagatgac ccagatcatg tttgagacct tcaacacccc agccatgtac
481 gtagccatcc aggctgtgtt gtccctgtat gcctctggtc gtaccactgg cattgtgatg
541 gactccggag acggggtcac ccacactgtg cccatctatg agg 583
```

Rattus norvegicus, Pdx1, mRNA NM_022852.3 primers binding sites are highlighted in red.

```
163 gaggggtc cggtgccaga
181 gttcagtgct aatccccctg cgtgcctgta catgggccgc cagcccccac ctccgccgac
241 accccagttt gcaggctcgc tgggaacgct ggaacaggga agtcccccgg acatctcccc
301 atacgaagtg cccccgc 183
```

Rattus norvegicus, RIPE3b1/MafA , mRNA XR_008949.1 primers binding sites are highlighted in red.

```
446 agctc cgcggcttca gcaaggagga ggtcatccga
481 ctgaaacaga agcggcgcac gctcaagaac cgcggctacg cgcagtcgtg ccgcttcaag
541 cgggtgcagc agcggcacat tctggagagc gagaagtgcc agctccagag ccaggtggag
601 cagctgaagc tggaggtggg gcgt 624
```

Rattus norvegicus, Beta2 /NeuroD, mRNA AF107728 primers binding sites are highlighted in red.

```
629 cc agcgcttcct tcccggtgca tccctactcc
661 taccagtccc ctggactgcc cagcccgccc tacggcacca tggacagctc ccatgtcttc
721 cacgtcaagc cgccgccaca cgcctacagc gcagccctgg agcccttctt tgaaagcccc
781 ctaactgatt gcaccagccc ttcctttgac ggacccctca gcccgccgct cagcatcaat
841 ggc 843
```

Figure 1: Continued

Rattus norvegicus, GK mRNA M25807.1 primers binding sites are highlighted in red.

```
583 tcctgcta   ctatgaagac
601 cgccaatgtg aggtcggcat gattgtgggc actggctgca atgcctgcta catggaggaa
661 atgcagaatg tggagctggt ggaaggggat gagggacgca tgtgcgtcaa cacggagtgg
721 ggcgccttcg gggactcggg cgagctggat gagttcctac tggagtatga ccggatggtg
781 gatgaaagct cagcg 795
```

Rattus norvegicus, Glut-2 mRNA NM_012879.2 primers binding sites are highlighted in red.

```
194 acacccc actcatagtc acaccagcac atacgacacc agacgcctgg
241 gaagaagaga ctgaaggatc tgctcacata gtcactatgc tctggtctct gtctgtgtcc
301 agctttgcag taggcggaat ggtcgcctcg ttctttggtg ggtggctt 348
```

Rattus norvegicus, Camk4, mRNA NM_0127272 sequences in red are primer binding sites to amplify Glut-2.

```
859 ac attccaagcc ctccaacacc cgtgggtcac aggaaaagca gccaactttg
1001 tccacatgga taccgctcag aaaaagcttc aagaattcaa tgctaggcgc aagcttaagg
1061 cggcagtgaa ggctgtggtg gcctcttctc ggctgggaag tgccagcagc agtcacacca
1121 acatccaaga aagcaacaaa gccagctcgg aggcacagcc cgcccaagac ggcaaggaca
1181 agacagatc 1099
```

Rattus norvegicus Camkk1, mRNA NM_031662 sequences in red are primer binding sites to amplify Glut-2.

```
825 catcaa gccgtccaat
841 ctgctccttg gggacgatgg gcacgtgaag atcgccgact ttggtgtcag caaccagttt
901 gaggggaatg atgctcagct gtccagtacg gcagggaccc cagcattcat ggccccggag
961 gccatctctg acaccggcca gagcttcagt gggaaggcct tggatgtatg ggccactggg
1021 gtta 1024
```

Data relevant for chapter 3 & 4 (Insulin Binding)

Figure 2: Insulin binding assay with whole cell microbe using peroxidase labelled insulin Row A is control without insulin peroxidase and Row B treated with insulin Peroxidase and screening binding *A salmonicida* binding to FITC insulin binding.

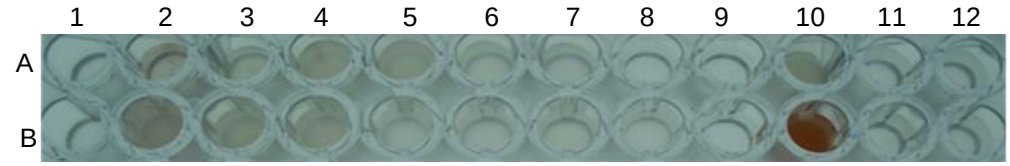

1-Ps aeruginosa 2- Ps fluorescence 3- Ps putida 4- Rhizobium sp 5 - E coli 6- Citerobacter freundii 7- Klebsiella aerogenes 8-Acinetobacter acetii 9- Alcaligens viscosus 10- Burkholderia cepacia II 11-Salmonella typhimurium 12- Erwinia caratovora.

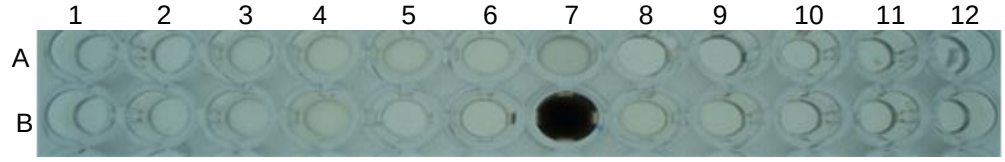

1-Serratia marcescen 2-Hafnia alvei 3-Vibrio anguillarum 4-Bacteroides fragilis 5-Chromobacterium violaceum 6- Proteus valgaris 7- Aeromonas salmonicida 8- Sarcina lutea 9- Streptococcus pyogenes 10-Staphylococcus aureus 11- Micrococcus luteus 12-Bacillus subtillus.

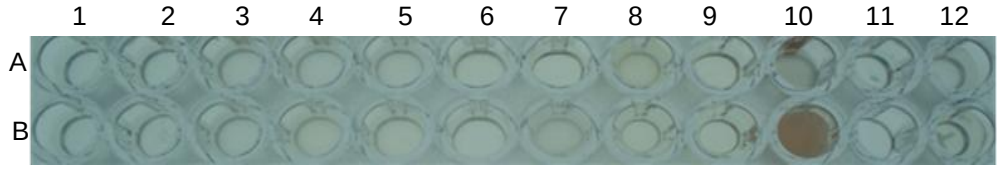

1-Clostridium frundii 2-Lactobacillus casei 3-Listeria monocytogenes 4-Corynebacterium aqutica 5-Brivibacterium linens 6-Microbacterium lacticum 7-Cellulomonase flavigena 8-Yersinia ruckri 9-Mycobacterium phlei 10- Burkholderia cepacia III 11- Rhodococcus equi 12-Acetobacterium acetii.

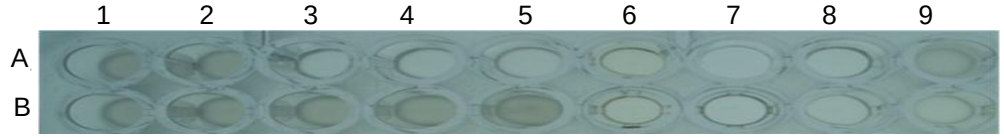

1-Zygosaccharomyces rouxii 2-Schizosaccharomyces pombe 3-Saccharomyces cerevisiae 4-Schizosaccharomyces octosporus 5-Saccharomyces certsbergesis 6- Nocardia cellulans 7-Agrobacterium rhizogenes 8-Burkholderia thailendensis 9- Burkholderia cocoverenans.

Figure 3: continued

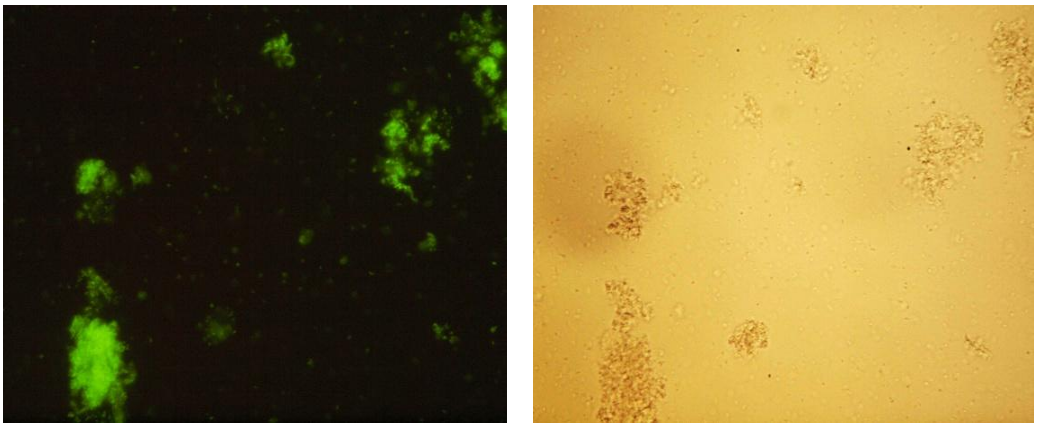

A salmonicida CM30 (bright field view)

Figure 4: Western ligand of IBP(s) of *E coli* lyaset infected by phagemid p1 (lane 1 & 2) & E coli lysat infected by phagemid p2 (lane 3, 4, 5,6) expressing multiple bands compare to *Burkhoderia cepacia II* (lane 7&8).

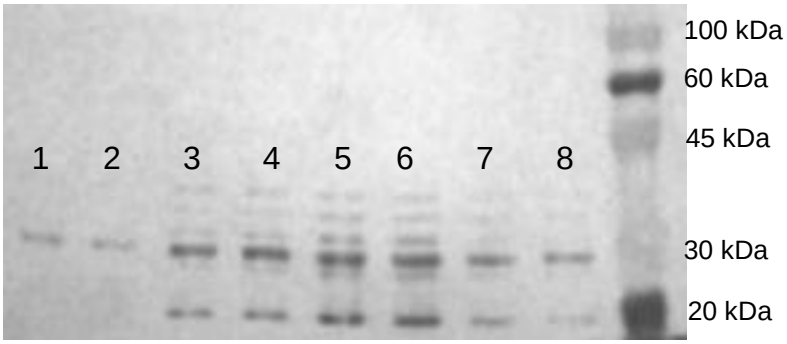

Figure 5: Full length DNA sequences of the insert of the phagemid p1.

```
   1 GTACCCACCC GGGTGGAAAT CGATGGGCCC GCGGCCGCTC TAGAAGTACT CTCGAGAAGC
  61 TTTTTGAATT CTTTGCGCAT CGCCAACATT CATCCGGGCA TCACGGCCGA CGGTTCGCCG
 121 TACCAGCGGC GCGGCGCATG GGCGACGCTC GATGCGCTGC ACGGCGCGCG CGGCGAGCGC
 181 GTCGACTGGG CGACCGGCAC GACGACGCCG GTCGCGCCCG TGACGATGAC GGGCGCCTCG
 241 TTCCACTATG TCGACAACGG CATCGATTCC GGCGAGGTGA TCTGCGACGT GCTCGACACG
 301 CCGATCGCGC CGGACGACAC GATCCTCGAA CTGCGCTGGA ACAACTTCCA GCGCAGCCTG
 361 TTTCCGGCGC TCGAGCGCGG GCTGCATCTC CTCGCCGATC GCCACGACGC GGGAGCACTG
 421 TGATGGCACC GACGCTGACG CAACCCGAAG AAGCGATCGA GACGGCCGAC GGCAACGTCG
 481 CCGCCTGGCG CGATCACGGC GCCGATACGG CGCCCGCCGT CGACCGCGTG CTCGACGCAT
 541 GGCGGCCCGA CGATCCGCCG GGCGCGCTGC TCGCCGAGCT CGTCGCGCTG TTCAATACCG
 601 ACGCACGGCG CGATGCCGCG ACGATCGCGC TGCCGATCGC AGGCACCGAC CCGGACGCCG
 661 TCGCGGCGTA CGTCGCGCGC GCGGTGCGCG AAGGCGTGAT CGACGCGGCG CAACGCGCGG
 721 GCGACCGCCT TGACGTGACC ACGTCGCGCG CGACGTTCTG GCAGCATCCG CAGCCGTGGC
 781 TGAAGGCGCC CGCGTCGGGC GGGATGCCGC TGCGCTACAC GATCACGAAC GGGCACCGTC
 841 ATCCGGTGCG GCCGCCGACG CCGGCCGGCG AGATCTATGC GCGCTACATG CCGCAGGTCG
 901 GGATGACGTT CAGCCTGCGC ACCGTCGACG TCGACGCGCA TGCGGACCTG TTCAGCGGCT
 961 GGATGAATCT CGATCGCGTC GCGCATTTCT GGGATCAGCG CGGCACGCGC GATGAGCATG
1021 CCGCGTATCT CGCGGAGCGG CTCGCCGATC CGCACATGCA TCCGATGATC TCGCGCGCCT
1081 GCAGGTCGAC ACTAGTGGAT CACGAAGGAC ATTTTAGGAG GCGACGGCAA CTTCAACTAT
1141 TACCGGAAGA AGGAGTGGTC GCTCGGCTAT CAGTTCGAGC ACAACCTGAA CTCGATGTGG
1201 ACGTTCCGGC AGAACACGCG ATGGATGCAT CTGTCGCTCG ACAACGGCTC GGTGTGGGGA
1261 GCGGGCTTCG CCGACGAAAC GCTGACCGAA ATCAACCGCT GGGCCGGCGT GTTCCAGATG
1321 AACTACAGCC GCTTCGACAT CGACAACAAC CTCGAGGGCC GTTTTGCGAC GGGTCCGCTC
1381 CAGCACACGC TGCTGCTCGG CTTCCAGTAC AACCGCCAGA CGGCGACCGA TAGCGAATGG
1441 CTCGCCGCCG CGCCGACGCT GAACCTCTAC AACCCGGTGT ACACGCCGGT CACGACGGCC
1501 GTGTTTTCCG ATCCGGACAC CACGTACCGC ACCAACACGT ACACGACGAT GAACACGTTC
1561 GGCCTGTACG CGCAGGACCA GATCAAGTGG AACCGCTGGA CGCTGACGCT CGGCGGCCGC
1621 GAGGACTGGG TCAACATGCG GATGGACGAT CGCGCGGCCG GCACGCAGTC GAAGGCCGAC
1681 GTGTCGGCGT TTACGGGCCG CGTCGGCCTC ACGTATCAGG CCGGCTACGG GCTGTCGCCG
1741 TATATCAGCT ATTCGACGTC GTTCAATCCG ATCATCGGCG TGAGCTTGCT CGACGGCGGG
1801 GTGCCGAAGC CGACGCGCGG CAGACAGATC GAAGCGGGCC TGCGCTGGCA GCCGCCCGGC
1861 AAGAACCTGA TGCTGAATGC CGCGATCTAT CAGATCAACC AGACCAACGG CGTTACGCCG
1921 GCGCTGCTGA CGCACGATCC GAGCGGCACG AAATCCGTGC AGACCGGGGA AGTGCGCGCG
1981 CGCGGGATCG AGCTGAGCGC AACCGGCAAG GTCACGCCGA ACCTGTCGCT GATCGCGTCG
2041 TACGCGTATC AGACGGCGCG ATATCGGGAT AGCTGAGCGC AACGGCAAGG TCCACCCGGG
2101 TGGAAATCGA TGGGCCCGCG GCCGCTCTAG AAGTACTCTC GAGAAGCTTT TTGAATTCTT
2161 GGATCATCGG ATGCATGTGC GATCGGCGAG CCGCTCCGCG AGATACGCGC ATGCTCATCG
2221 CGCGTGCCGC GCTGATCCCA GAAATGCGCG ACGCGATCGA GATTCATCCA GCCGCTGAAC
2281 AGGTCCGCAT GCGCGTCGAC GTCGACGGTG CGCAGGCTGA ACGTCATCCC GACCTGCGGC
2341 ATGTAGCGCG CATAGATCTC GCCGGCCGGA GTCGGCGGAC GCACCGGA
```

Figure 6: Full length DNA sequence of the insert of the phagemid p2.

```
   1 TGGTACCCAC CCGGGTGGAG ATCGATGGGC CCGCGGCCGC TCTAGAAGTA CTCTCGAGAA
  61 GCTTTTTGAA TTCTTTGGAC TCGCTCGTGT TTCAACTGCC GGTCAGCTAC GAGAACCGAT
 121 GAAAACCGAC AAGCAGTTGA AGCAGGATGT CCAGGACGAA CTGGAGTCAG ACCCGTCGAT
 181 CGATTCGACC CGTATCGGTG TCGAGGTGGC TGACCGGATC GTGACGCTTT CGGGGCACCC
 241 GCCGAGCTAC GCGGAGAAGC TGGCGATCGA GCGCGCGGCG AACCGCGTGG CCGGTGTCAA
 301 GGCGCTCGTC GTGGACATGA CCGTGCATCT GCCGGACGAC GACGTGCGCA CCGACGAGGA
 361 CATCGCGAAG GCGGTACGCT CGGTGCTGCA CTGGACGGTC GGTCTACATG ACGACGCGGT
 421 CAAGGTGCAG GTCGAACGCG GCTGGATCAC GTTGTCCGGC AAGGTCGACT GGGCATACCA
 481 GAGCCACCTG GCCGTGCGCG CGATCTCGCA GATGCGCAGC GTGACGGGCG TGACCGACCA
 541 CATCACGGTA CAGGGGACGG TCGGTTCGGA CGACATCGGC GGAAACATCA AACGCGCGAT
 601 CATGCGCCAC GCGGAGCGCG AGGCTAAGCA TATCGCGATC GAAGTGCACG ACGGCACCGT
 661 GCGGCTGTCC GGAAAAGTCG GCTCGTTCTC CGAACGCAAG GCCGTGCGCG GGGCCGCGTG
 721 GTCCGCGCGC GGCGTGCGCG CCGTCGTCGA CGATCTGGTG GTCGAGTAAG GTCGGTAGCC
 781 GGATGAGCAG TCCACGGAGA TCAAGGAGGG CAGTCAAATG ACACTTTCGG GTGAACTTCA
 841 CGAAGCGGAC TGGTCGGTCA TGATCACGCC GAGCGACGCA TACATATAGG CGAGCGCGTC
 901 GTTTCGGAAT CGACAGCATC AGGTAGCCGG CGCACAGCAC GGCCGCGCCT GAGGATCCCC
 961 GATGCGATGG CGTTTGCTGT CAAGGCTCTG TTGCACGAGA ATTTCATGAG CTGTGGGAAC
1021 GACGCGGCTT TCGCGTTAGC TGCGTGAAGC CACTATGACC ACAACTGACC GCGCTCACGG
1081 CACCAAAGCT ACGGAAGACA ACAAACCGTA TCCGCTTCAT GCAATTCAGC TGGCCGACCT
1141 CCGAGTGGTG GAGGTCAGCT TGCGTGCAAA TATGGATGTG GCAAAGAGCG ATCCGCCTGG
1201 AACGTTTGAG CTTACTACCG GCCACGGCGT CTATGACGCC GAGCACAAGC GCATCCAGGT
1261 GAAAGTTGCG GCCACAATGG GGCATCAAGA CGATGGAAAG TCACCGTTTG CGCTCAAGGT
1321 CGAATCGCGC GCCTGCAGGT CGACACTAGT GGATCCGTCG CGCATCGTCG TGTTCCAGGA
1381 TCGCGGCGCT CTATGCGGCC GCCATCGATC GTGTCGGGGC TCGCGGCCGC CGCGCGGCGC
1441 GGATGAGCGC TTCCGCCCTC CTCCATCGTC ATCCGGCCAA CGTCGCGGGC CGCGACTTCG
1501 TCGTCGGCGA TCTGCACGGC TGCGTCGATG CGCTGCGCGC ACTGCTGCGC GAGGTGCGCT
1561 TCGATCCGGC GCGCGACCGG CTGTTCTCGG TCGGCGATCT CGTCGACCGC GGGCCGGCAT
1621 CCGAAACCGC GCTCGAGCTG CTCGATCGCC CGTGGTGTCA CGTCGTGCGC GGCAATCACG
1681 AAGAAGTGCT GAGCCTCGTC GCGCGCGGCA AGCTGCCGGC CGACGCATGG CGCGGCATCG
1741 GCGGCGACTG GGGCGCCGAT CTGCCGCCCG AGCGGCTGCG CGCGTACGCG GCGCGCGTCG
1801 AAGCGCTGCC GCTCGTGCGC GTGATCGGCG AAGGCGCGAC GCGCTTCAAC GTGCTGCATG
1861 CGGAATTCTT CGGCTCGGAC GCCGATCTAG ATACCGGCGA CTATCCGCCC GACGTGCGCG
1921 AGCGGCTGAT CTGGGGCCGC GATCTCGTGC AGGGACTCGT CGATCCGGGC TGGCAGGCCG
1981 GCCTCTCGCT GACCTGCAGC GGCCATACGC CGGTGCGCGT GCCGCAGCGG ATCGGCGCGC
2041 AATGGTTCAT CGATACGGGT GCGTTCGCAC CGGCCGGCCG GCTGACGCTC GCCGAGCCGC
2101 GCACGGGACA GACGTGGTCG ATCACGCAGG CCGCCGCACG CGAACGCGGA GCGGCCGCGT
2161 GGCCGCTGCC GTGACGCCCG CACGACTGTC CGGCCGGACA CCGCGACACA CATACCGCCT
2221 CGAATGCACG GGCAGCGCAA CGCCCGCATG CGCACCTACC CGACCTGATT CAGCRSTCGA
2281 ACACCGCGTC GATCGCGGAG CCGTTCCAGT TGTACTCGAG ATACGCCGCG TGATGGCAGT
2341 CGCGCAGCAG CGTCGTGCGA AACGCCGCGA GGCATTCGCC GTGCGGATCG CGCACCGACG
2401 GATAGACGAT CGCTGCGTCC GCTCCACGTG TGACGCTCGG GCGACACGCC TATGGAGCGC
2461 TCGCAGATCA ATCGCGAGAT GCCGCGCCAC ACCCACCTTG TCCCCGTCGA ATCGCTCGAA
2521 TGTCCGCAGG TACGCGACTG CTTCGGAAAA CCGCTCCCCG ATTATGCGCG CTGCAGCGGC
2581 TGCTTCCTCG CGCATCTCGA GCGACGCCAG CGGTTCGTAT TTCTCGGGAG CCGAGAGCCG
2641 GGCGGCAATG GCGTTTGGCA TGAAGTCGCC GTCATCGTCG ACATCATCTC GGTCGATACG
2701 TGTGGCGAAG CGCTCCTGAC GGTTGACGAA CCTGCCGAAC TCTCGCTGCA GGCG
```

Figure 7: Full length protein sequences of human insulin receptor which was used to search the homology within *B. multivorans* IBP(s).

Insulin receptor Homo sapiens

```
   1 mgtggrrgaa aapllvavaa lllgaaghly pgevcpgmdi rnnltrlhel encsvieghl
  61 qillmfktrp edfrdlsfpk limitdylll frvygleslk dlfpnltvir gsrlffnyal
 121 vifemvhlke lglynlmnit rgsvrieknn elcylatidw srildsvedn yivlnkddne
 181 ecgdicpgta kgktncpatv ingqfvercw thshcqkvcp tickshgcta eglcchsecl
 241 gncsqpddpt kcvacrnfyl dgrcvetcpp pyyhfqdwrc vnfsfcqdlh hkcknsrrqg
 301 chqyvihnnk cipecpsgyt mnssnllctp clgpcpkvch llegektids vtsaqelrgc
 361 tvingsliin irggnnlaae leanlgliee isgylkirrs yalvslsffr klrlirgetl
 421 eignysfyal dnqnlrqlwd wskhnltitq gklffhynpk lclseihkme evsgtkgrqe
 481 rndialktng dqascenell kfsyirtsfd killrwepyw ppdfrdllgf mlfykeapyq
 541 nvtefdgqda cgsnswtvvd idpplrsndp ksqnhpgwlm rglkpwtqya ifvktlvtfs
 601 derrtygaks diiyvqtdat npsvpldpis vsnsssqiil kwkppsdpng nithylvfwe
 661 rqaedselfe ldyclkglkl psrtwsppfe sedsqkhnqs eyedsagecc scpktdsqil
 721 keleessfrk tfedylhnvv fvprpsrkrr slgdvgnvtv avptvaafpn tsstsvptsp
 781 eehrpfekvv nkeslvisgl rhftgyriel qacnqdtpee rcsvaayvsa rtmpeakadd
 841 ivgpvtheif ennvvhlmwq epkepngliv lyevsyrryg deelhlcvsr khfalergcr
 901 lrglspgnys vriratslag ngswteptyf yvtdyldvps niakiiigpl ifvflfsvvi
 961 gsiylflrkr qpdgplgply assnpeylsa sdvfpcsvyv pdewevsrek itllrelgqg
1021 sfgmvyegna rdiikgeaet rvavktvnes aslreriefl neasvmkgft chhvvrllgv
1081 vskgqptlvv melmahgdlk sylrslrpea ennpgrpppt lqemiqmaae iadgmaylna
1141 kkfvhrdlaa rncmvahdft vkigdfgmtr diyetdyyrk ggkgllpvrw mapeslkdgv
1201 fttssdmwsf gvvlweitsl aeqpyqglsn eqvlkfvmdg gyldqpdncp ervtdlmrmc
1261 wqfnpkmrpt fleivnllkd dlhpsfpevs ffhseenkap eseelemefe dmenvpldrs
1321 shcqreeagg rdggsslgfk rsyeehipyt hmnggkkngr iltlprsnps
```

Figure 8: Translated sequences of the putative ORF(s) detected on the insert of recombinant phagemid p1.

Ornibactin synthatase

```
  1 RIANIHPGIT ADGSPYQRRG AWATLDALHG ARGERVDWAT GTTTPVAPVT MTGASFHYVD
 61 NGIDSGEVIC DVLDTPIAPD DTILELRWNN FQRSLFPALE RGLHLLADRH DAGAL
```

Acetyl CoA:N6-hydroxylysine acetyl transferase

```
  1 MAPTLTQPEE AIETADGDVA ALRDHGADTA PAADRVLDAW RPDDPPGALL AELVALFNTD
 61 ARRDAATIAL PIAGTDPDAV AAYVARAVRE GVIDAAQRAG DRDVTTSRAT FWQHPQPWLK
121 APASGGMPLR YTITNGHLRH PVRPPTPAGE IYARYMPQVG MTFSLRTVDV DAHADLFSGW
181 MNLDRVAHFW DQRGTRDEHA AYLAERLADP HM
```

Ornibactin

```
  1 VVARLSVRAQ PELDVDVPAE HAMDASVARQ RLGVGSGLRR RNADRNQPLG RRVPDELQPL
 61 RHRQQPRGPF CDGSAPAHAA ARFQYNRQTA TDSEWLAAAP TLNLYNPVYT PVTTAVFSDP
121 DTTYRTNTYT TMNTFGLYAQ DQIKWNRWTL TLGGREDWVN MRMDDRAAGT QSKADVSAFT
181 GRVGLTYQAG YGLSPYISYS TSFNPIIGVS LLDGGVPKPT RGRQIEAGLR WQPPGKNLML
241 NAAIYQINQT NGVTPALLTH DPSGTKSVQT GEVRARGIEL SATGKVTPNL SLIASYAYQ
```

Figure 9: Translated sequences of the putative ORF(s) detected on the insert of recombinant phagemid p2

Transporter periplasmic

```
  1 MKTDKQLKQD VQDELESDPS IDSTRIGVEV ADRIVTLSGH PPSYAEKLAI ERAANRVAGV
 61 KALVVDMTVH LPDDDVRTDE DIAKAVRSVL HWTVGLHDDA VKVQVERGWI TLSGKVDWAY
121 QSHLAVRAIS QMRSVTGVTD HITVQGTVGS DDIGGNIKRA IMRHAEREAK HIAIEVHDGT
181 VRLSGKVGSF SERKAVRGAA WSARGVRAVV DDLVVE
```

Transmembrane transporter

```
  1 MMHAPVSQTR SFTTVFLIEM WERFGYYGMA ALLVLFMVDR LGFTDSHANL TWGAFTALVY
 61 ASPSIGGWIG DKVLGARRTM ILGAAVLCAG YLMLAVPNDA LAYMYASLGV IVVGNGLFKA
121 NAANLVRRIY EGDDARIDSA FTIYYMAVNI GSTVSMLATP WIKDHWGWHT AFAVCCGGML
181 LAILNFMLMH RTLAHIGSQP DDEPIRWKRl gavaaggval alVTLYVLQH KQLAVASVWT
241 AAVAILAIFA YMIAKSERSE RAGLIAALVL IAQVILFFIF YVQMSTSLTL FALRNVDPRF
301 ILFGTTL
```

Serine threonine phosphatase

```
  1 MSASALLHRH PANVAGRDFV VGDLHGCVDA LRALLREVRF DPARDRLFSV GDLVDRGPAS
 61 ETALELLDRP WCHVVRGNHE EVLSLVARGK LPADAWRGIG GDWGADLPPE RLRAYAARVD
121 ALPLVRVIGE GATRFNVLHA EFFGSDADLD TGDYPPDVRE RLIWGRDLVQ GLVDPGWQAG
181 LSLTCSGHTP VRVPQRIGAQ WFIDTGAFAP AGRLTLAEPR TGQTWSITQA AARERGAAAW
241 PLP
```

Hypothetical protein

```
1 GLGIVYPSVR DPHGECLAAF RTTLLRDCHH AAYLEYNWNG SAIDAVFELN QVG
```

Data relevant for chapter 7&8 (GAD molecular mimicry

Figure 10: Extraction and purification of PG1 plasmids (lane 8) amongst non-recombinant or fault recombinant plasmids compared to the pFN22A plasmids (lane 1).

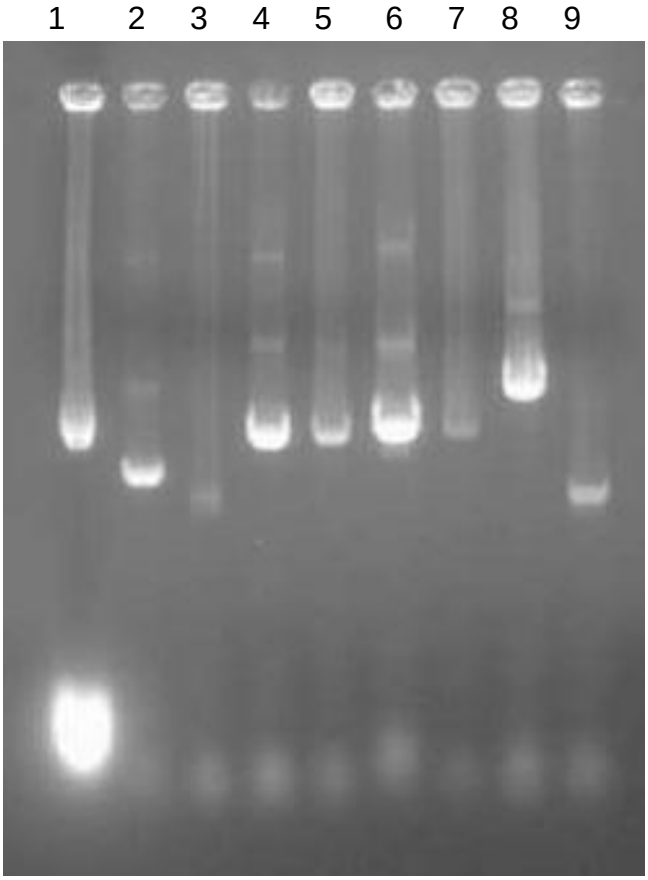

Figure 11: Full length sequences of pancreatic antigen protein GAD65

```
1 MASPGSGFWS FGSEDGSGDP ENPGTARAWC QVAQKFTGGI GNKLCALLYG
 51 DSEKPAESGG SVTSRAATRK VACTCDQKPC SCPKGDVNYA LLHATDLLPA
101 CEGERPTLAF LQDVMNILLQ YVVKSFDRST KVIDFHYPNE LLQEYNWELA
151 DQPQNLEEIL THCQTTLKYA IKTGHPRYFN QLSTGLDMVG LAADWLTSTA
201 NTNMFTYEIA PVFVLLEYVT LKKMREIIGW PGGSGDGIFS PGGAISNMYA
251 MLIARYKMFP EVKEKGMAAV PRLIAFTSEH SHFSLKKGAA ALGIGTDSVI
301 LIKCDERGKM IPSDLERRIL EVKQKGFVPF LVSATAGTTV YGAFDPLLAV
351 ADICKKYKIW MHVDAAWGGG LLMSRKHKWK LNGVERANSV TWNPHKMMGV
401 PLQCSALLVR EEGLMQSCNQ MHASYLFQQD KHYDLSYDTG DKALQCGRHV
451 DVFKLWLMWR AKGTTGFEAH IDKCLELAEY LYNIIKNREG YEMVFDGKPQ
501 HTNVCFWFVP PSLRVLEDNE ERMSRLSKVA PVIKARMMEY GTTMVSYQPL
      551 GDKVNFFRMV ISNPAATHQD IDFLIEEIER LGQDL
```

Figure 12: Spectrum report generated from MS/MS analysis of *E coli* protein band 1 cross reacting with GAD65 antiserum.

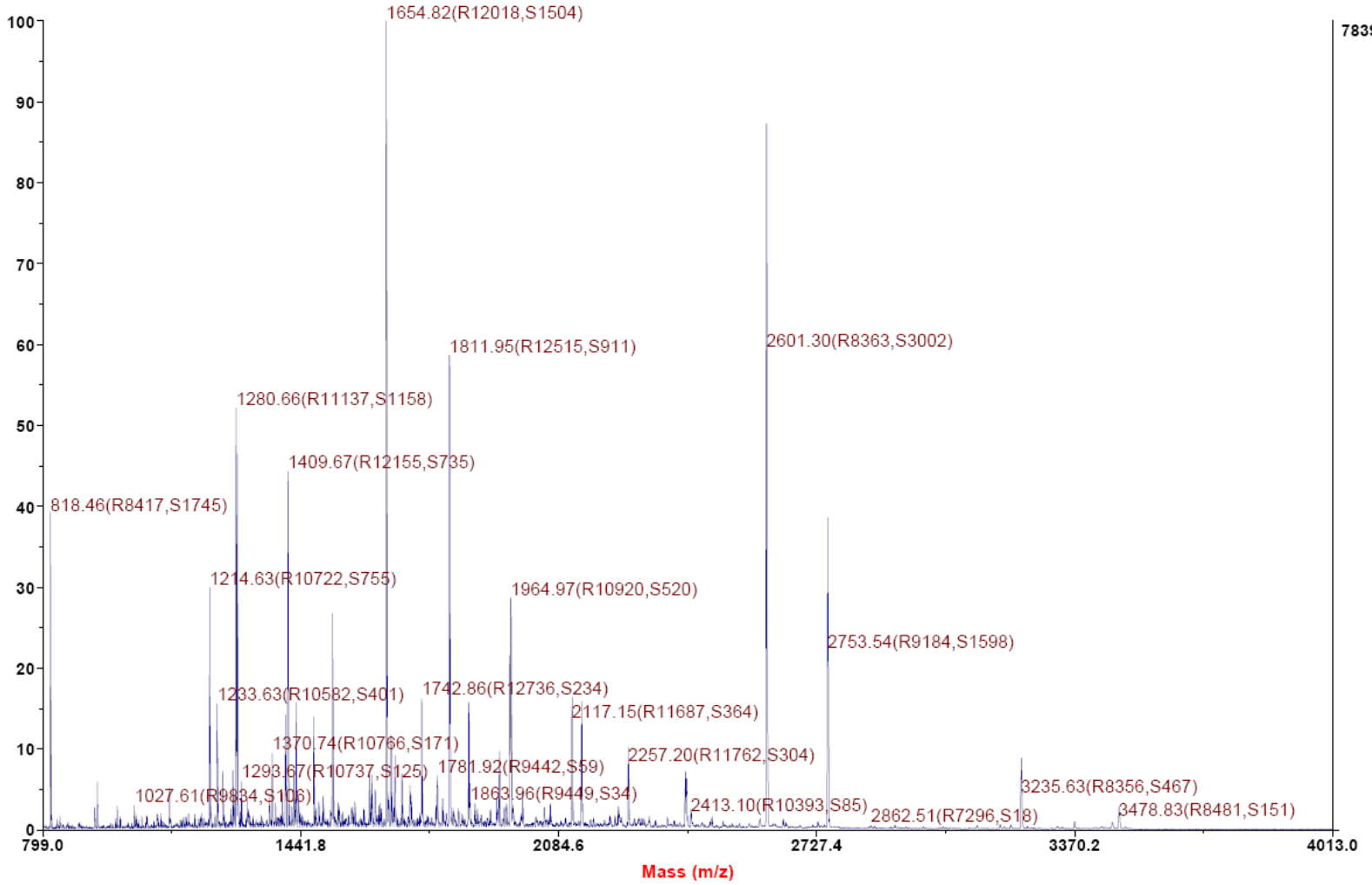

Figure 13: Spectrum report generated from MS/MS analysis of *E coli* protein band 2 cross reacting with GAD65 antiserum.

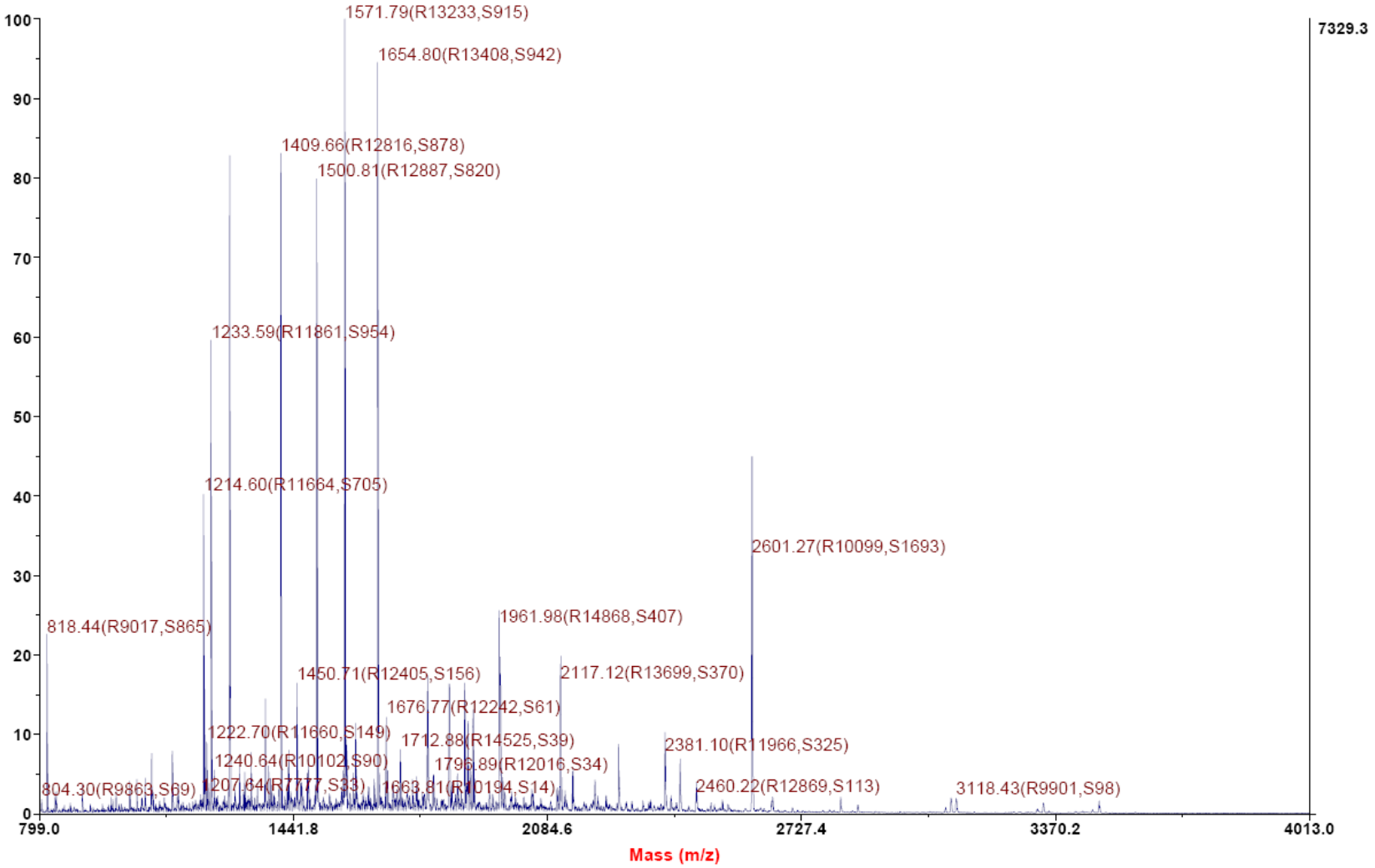

Figure 14: Spectrum report generated from MS/MS analysis of *E coli* protein band 3 cross reacting with GAD65 antiserum.

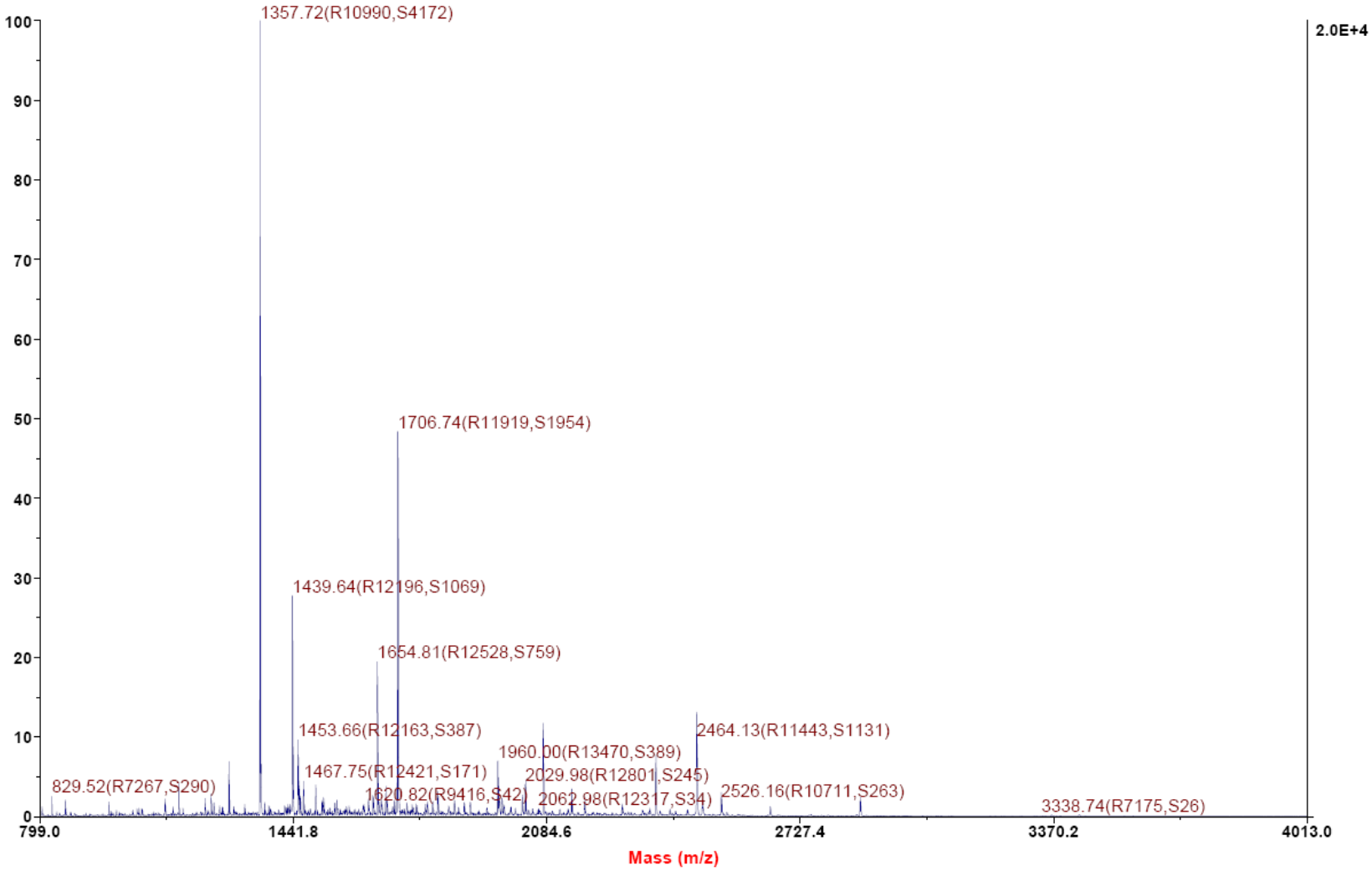

Figure 15: Spectrum report generated from MS/MS analysis of *E coli* protein band 4 cross reacting with GAD65 antiserum.

Figure 16: Spectrum report generated from MS/MS analysis of *E coli* protein band 5 cross reacting with GAD65 antiserum.

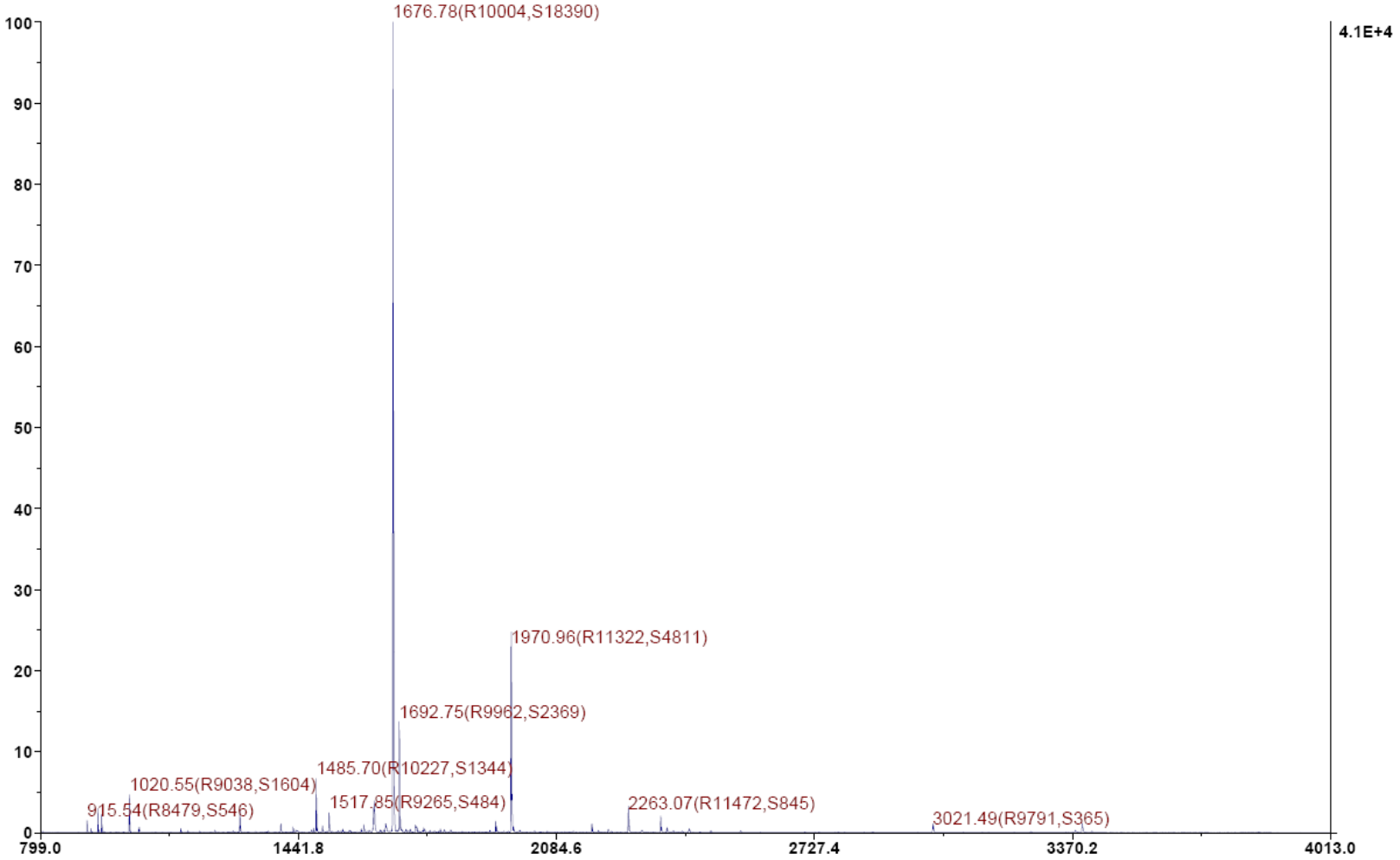

Appendix 3

Publications of this study